

Faculty of Computing, Engineering and the Built Environment
Belfast School of Architecture and the Built Environment
Ulster University



The development of fibre reinforced geopolymer cladding systems with integral foamed insulation

Luke Oakes

BSc (Hons)

Thesis submitted for the degree of
Doctor of Philosophy
August 2023

This report is less than 100,000 words

Acknowledgements

Without the tireless work and support provided by my primary supervisor Dr Bryan Magee this project would simply not have been possible. While still an undergraduate Bryan's advice to apply for this project funding was paramount to my decision to begin my research career and I will always be extremely thankful for the influence Bryan has had on not just my career, but my life as a result. I can honestly say I have become a completely different, much more confident person through the wide range of experiences and challenges this doctoral study has afforded me. Bryan helped to instil a consistent core vision for the project, inspiration for novel data presentation and his help with document editing and academic writing has been central to my development as a researcher. I would also like to thank my supporting supervisors, Dr Phillip Millar and Dr Allistair McIlhagger, for their help liaising with companies to provide novel materials required for the project and advice on data analysis/test procedures.

Outside of Ulster University the personal support received from my loved ones, especially my partner Zara and my mother Jean were irreplaceable, and they both have put up with so much to help me see the process through. The emotional and often financial support they provided was perhaps the single most important factor that kept driving me towards completion. The constant encouragement, love and understanding both have shown to me throughout the process has helped immensely when the pressures mounted, and I simply could not have gotten this far without them. My partner Zara also gave birth to our first child Ruben during the project, who has provided so much motivation in tough times and I will be forever thankful for all she has done for us to get him here.

Abstract

This research aimed to develop the next generation of building cladding, which can reduce the environmental impact civil engineers have on our planet, create the unique, architectural styles of the future, and provide increased safety to people in buildings, while eliminating fire tragedies like Grenfell tower.

Global warming is the most pressing issue currently faced by society. Carbon dioxide levels are the highest in human history and without major changes by 2100, temperatures are predicted to rise by up to 6⁰C. There is no longer any real scientific debate, 97% of researchers confirm this, yet we so far governments and industry have failed to enact the changes required to meet climate change targets such as achieving net zero by 2050 (Skidmore, 2023). Full decarbonisation of the construction industry by 2050 will require widespread rapid change, which will need to be implemented by 2030. One vital area to change is how buildings are constructed. Buildings account for around 40% of the energy used and a third of the greenhouse gases emitted worldwide, with their component materials making up a further 10% (World Green Building Council , 2019). The EU recognise the scale of change required to achieve net zero and plan to invest £84 billion through Horizon Europe by 2027 to address these challenges and aim to make all new builds require no energy from the grid by 2030 (European Commission, 2020). Lightweight, non-structural cladding can create energy efficient buildings. However, achieving high levels of insulation, fire safety and surface finish whilst using minimal amounts of energy, time and money whilst emitting minimal greenhouse gases is becoming increasingly challenging. Materials commonly used for building cladding include Glass reinforced concrete, sheet glass walling and aluminium plastic composites, which were unfortunately set alight on Grenfell tower. While these all excel in providing an aesthetically pleasing and low maintenance finish, they have high embodied energy and CO₂; whereby they use cavities and separate flammable insulation materials for their

thermal protection. This is no longer acceptable from environmental and safety perspectives; hence new material solutions must be developed.

Geopolymers are considered to be serious contenders as stronger alternatives to Portland cement-based concretes and mortars. They have similar mechanic strength properties and are equally fire-proof, but are formed from recycled waste and have significantly smaller carbon footprints. Geopolymers with fibre reinforcement and chemical foaming additives can produce a fireproof high strength material for cladding applications, with huge design flexibility. Furthermore, geopolymer mixtures can be tailored such that their mechanical and thermal performances exceed existing standard materials, with added benefits such as being lightweight (due to reduced thickness) and no cavities for fire to spread.

This research developed novel mix design methods suitable for a wide range of geopolymer mix designs and source materials, including MK, GGBS, SF and IS precursors with potassium silicate activation. Optimised empirical equations accurately predicted strength, flowability and carbon embodiment, which informed a user-friendly contour-based mix design procedure. Fibre composites created with 2% volume of 13 μ m, concrete-sized, basalt fibres in a GGBS/MK mortar achieved 84% the MOR of a GRC control and concrete. Specific sizing was proven effective and necessary for basalt fibres in high performance geopolymer composites. Industrial surfactant-based geopolymer foam insulation was created with density > 607 kg/m³ and TC >0.0933 W/mk. This thereby presents a new range of novel, ‘greener’ cladding materials that comply with UK building regulation U-values. Furthermore, a carbon embodiment of 0.228 kgCO₂/kg was achieved, which represented a 62% reduction compared with the average GRC studied.

Table of Contents

Acknowledgements	ii
Abstract	iii
Table of Contents	v
List of Figures	xiii
List of Tables.....	xvii
List of Abbreviations and Symbols.....	xx
Chapter 1 – Introduction	1
1.1 Background	1
1.2 Aim.....	3
1.3 Objectives	3
1.4 Thesis structure.....	3
Chapter 2 – Literature Review	6
2.1 Introduction	6
2.2 Requirements of modern building cladding	6
2.2.1 Thermal performance of structures	7
2.2.2 Fire resistance.....	8
2.2.3 Structural safety	9
2.2.4 The future of the cladding industry.....	13
2.3 Cementitious cladding systems	14
2.3.1 Environmental impact of GRC	16
2.4 Geopolymers	18

2.4.1	Geopolymer definition and chemistry.....	19
2.4.2	Binder material options for geopolymers.....	23
2.4.3	MK precursor	24
2.4.4	Fly ash precursor	25
2.4.5	GGBS precursor	26
2.4.6	Silica fume precursor	27
2.4.7	Novel geopolymer precursors from waste materials.....	28
2.4.8	Alkali activators for geopolymers.....	30
2.5	Mixture proportioning of Geopolymers	31
2.6	Geopolymer matrix fibre composites	40
2.6.1	Fibre / matrix interface bond and sizing technologies	47
2.7	Foamed geopolymers for insulation	52
2.8	Environmental impact of Geopolymers	55
2.9	Summary and knowledge gaps.....	59
Chapter 3 – Materials and testing methodologies		61
3.1	Introduction	61
3.2	Materials.....	61
3.2.1	Geopolymer precursors	61
3.2.2	Filler material	64
3.2.3	Activators and additives.....	64
3.2.4	Fibres.....	65
3.2.5	Foaming agents	66

3.3	Preparation of geopolymer mortars and pastes	67
3.3.1	Structural mortar preparation	67
3.3.2	Mortar/paste preparation for foaming	75
3.4	Casting and curing of samples.....	75
3.4.1	Cubes for compressive strength tests	75
3.4.2	Fibre reinforced panels.....	76
3.4.3	Foamed mortars and pastes	77
3.5	Test procedures.....	78
3.5.1	Fresh properties	78
3.5.2	Uniaxial compressive strength	78
3.5.3	Flexural strength.....	79
3.5.4	Foamed materials	81
Chapter 4 – Geopolymer mortar development.....		85
4.1	Introduction	85
4.2	Phase A: Geopolymer mortars created from single source materials.....	85
4.2.1	MK based geopolymer mortars	85
4.3	Phase B: Single replacement of metakaolin geopolymers with industrial waste materials	89
4.3.1	MK replacement with GGBS	90
4.3.2	MK replacement with FA.....	93
4.3.3	MK replacement with SF	94
4.3.4	MK replacement with IS	94

4.3.5	Summary	94
4.4	Phase C: Replacement of MK with multiple industrial waste materials	95
4.5	Phase D: Influence of singular mixture proportioning ratios	100
4.5.1	Mix designs.....	100
4.5.2	Compressive strength.....	101
4.5.3	Relationships between singular mixture proportioning ratios and strength	102
4.6	Phase E: Simplified preliminary mix design methodology.....	105
4.7	Phase F: Synergistic influence of multiple mixture proportioning ratios	106
4.7.1	Compressive strength.....	109
4.7.2	Flowability.....	109
4.7.3	Embodied carbon.....	109
4.8	Contour based mix design methodology	113
4.9	Chapter summary	114
Chapter 5 – Assessment of fibre reinforced geopolymer mortar panels.....		136
5.1	Introduction	136
5.2	Phase 1: 4-point bending testing of GRC vs glass, basalt and steel fibre geopolymer composites to GRCA standard.....	137
5.2.1	Introduction.....	137
5.2.2	Composites.....	138
5.2.3	Load/displacement curves.....	139
5.2.4	LOP and MOR results.....	144

5.2.5	Summary	146
5.3	Phase 2: 4-point bending testing of GRC vs basalt fibre geopolymer composites to ASTM C974-03	147
5.3.1	Introduction.....	147
5.3.2	Load/displacement curves.....	148
5.3.3	LOP and MOR results.....	150
5.3.4	Summary	151
Chapter 6 – Development of foamed geopolymer insulation materials.....		152
6.1	Introduction	152
6.2	Results of research phases	152
6.2.1	Phase 1 - Investigation of foamed MK-based mortars.....	152
6.2.2	Phase 2 - Investigation of foamed MK pastes.....	154
6.2.3	Phase 3 - Thermal conductivity testing and proposed cladding panels ..	160
6.2.4	Phase 4 - Proposed claddings panels.....	161
6.3	Summary	166
Chapter 7 – Discussion		167
7.1	Engineering performance	167
7.1.1	Mortar performance	167
7.1.1.1	L/S ratio.....	167
7.1.1.2	A/B ratio.....	169
7.1.1.3	S/A ratio.....	171
7.1.1.4	Strength prediction equations.....	173

7.1.2	Basalt fibre geopolymer composite performance	178
7.1.3	Foamed geopolymer insulation performance.....	180
7.2	Engineering practicality	181
7.2.1	Availability of pozzolanic precursor supply	182
7.2.2	Availability of activating mediums.....	186
7.2.3	Availability of basalt fibre reinforcement.....	188
7.2.4	Geopolymer production facilities.....	188
7.3	Sustainability	190
7.3.1	LCA methodologies	191
7.3.2	Relative carbon embodiment of geopolymer/basalt fibre cladding materials	192
7.4	Financial analysis	194
7.5	The future	196
Chapter 8 – Conclusions and recommendations		201
8.1	Conclusions	201
8.2	Recommendations for further work	203
References.....		206
Appendices		
Appendix 1: Conference paper from ICCAC 2018 in Florida.....		235
Appendix 2: Conference paper from YRF 2018 in Newcastle		246
Appendix 3: Conference paper from CERI 2018 in Dublin, Ireland.....		248

Appendix 4: Journal paper in JSIM 2018	251
Appendix 5: Declaration	262

List of Figures

Chapter 2

Figure 2.1. Typical stress/strain curve for GRC materials (White, 2015).....	13
Figure 2.2. Illustration of strain hardening and softening (Altoubat, 2018).....	13
Figure 2.3. Geopolymer structure at changing Si:Al ratios (Davidovits, 2002)....	21
Figure 2.4. Schematic outline of the geopolymerisation process (Van Deventer et al., 2007).....	23
Figure 2.5. Effect of Si:Al ratio on geopolymer structure, behaviour and applications (Davidovits, 2002).....	33
Figure 2.6. Predicted vs measured responses for compressive strength (MPa) of two groups of FA geopolymers (Diaz-Loya et al., 2013a)	37
Figure 2.7. Ternary plot representing the proportions of SiO ₂ , Al ₂ O ₃ and NME's (Duxson and Provis, 2008)	38
Figure 2.8. NBO/T vs compressive strength for 38 geopolymers (Diaz-Loya et al., 2013b)	39

Chapter 3

Figure 3.1. Flow chart illustrating research stages	61
Figure 3.2. SEM images of (A) fly ash (Terzano et al., 2005), (B) GGBS (Nagendra et al., 2018), (C) silica fume (Mindess, 2008), (D) metakaolin (Pillay et al., 2020) and (E) iron silicate (Gamonchuan et al., 2020)	63
Figure 3.3. Pozzolanic precursor powder being added to Hobart A200 mixer	67

Figure 3.4. 50mm mortar cube samples	76
Figure 3.5. ADR 2000 BS Non automatic compressive test machine.....	79
Figure 3.6. Flexural test rig to ASTM C947-03.....	81
Figure 3.7. Leica M165C stereo microscope.....	82
 Chapter 4	
Figure 4.1. Compressive strength and flow vs L/S ratio of MK based geopolymer mortars.....	88
Figure 4.2. Set times of MK/potassium silicate based geopolymer mortars.....	88
Figure 4.3. Effects of superplasticiser dose on mortar MK4.....	89
Figure 4.4. MK replacement with single industrial waste materials and 7-day compressive strength.....	91
Figure 4.5. MK replacement with single industrial waste materials and 28-day compressive strength.....	92
Figure 4.6. MK replacement with single industrial waste materials and S/A ratio.....	92
Figure 4.7. Setting times with GGBS content	93
Figure 4.8. Ternary plots of 7-day strength (a-c) and combined ternary plots of 28-day strength and embodied CO ₂ (d-f)	98
Figure 4.9. Silica/Alumina, Liquid/Solid and Activating solution to Binder powder ratios vs 7- and 28- day compressive strength.....	103
Figure 4.10. Relationships between flow and L/S ratio for various binder combinations.....	116
Figure 4.11. Indicative mix design worked example.....	117

Figure 4.12. Experimental factors vs compressive strength.....	118
Figure 4.13 Experimental factors vs carbon embodiment and mortar flow.....	119
Figure 4.14(a-d). MK mortars: Analysed equations.....	120
Figure 4.15(a-d). GGBS/MK mortars: Analysed equations.....	124
Figure 4.16(a-d). GGBS/SF mortars: Analysed equations.....	128
Figure 4.17. Contour plots for prediction of the 7-and 28 -strength (MPa), embodied carbon (kgCO ₂ /kg) and flow (mm) of MK-based mortars with increasing free water content.....	132
Figure 4.18: Contour plots for prediction of the 7-and 28 -strength (MPa), embodied carbon (kgCO ₂ /kg) and flow (mm) of GGBS/MK-based mortars with increasing free water content.....	133
Figure 4.19. Contour plots for prediction of the 7-and 28 -strength (MPa), embodied carbon (kgCO ₂ /kg) and flow (mm) of GGBS/SF-based mortars with increasing free water content.....	134
Figure 4.20. Proposed contour-based mix design methodology.....	135

Chapter 5

Figure 5.1. Load/displacement curves for GRC control.....	139
Figure 5.2. Load displacement curves for Mortar A with glass, basalt, and steel fibre reinforcement (0,1 and 2% volume).....	141
Figure 5.3. Load displacement curves for Mortar B with glass, basalt, and steel fibre reinforcement (0,1 and 2% volume).....	142
Figure 5.4. LOP and MOR results (GRCA method).....	143

Figure 5.5. Load displacement curves for GRC material and basalt composites.....	149
Figure 5.6. Flexural strength of geopolymer /basalt and GRC composites.....	151

Chapter 6

Figure 6.1. Foamed MK-based mortars at varied liquid to solid (L/S) ratios.....	156
Figure 6.2(a-c). Development and testing of foamed pastes (% by mass).....	157
Figure 6.3. Thermal conductivity and visual inspection of foamed mortars.....	161
Figure 6.4. Minimum required insulation thickness to meet specific U-values (0.2-0.35).....	163
Figure 6.5. Minimum embodied carbon required to meet specific U-values (0.2-0.35)..	164
Figure 6.6. Scale diagrams of proposed cladding panels.....	165

Chapter 7

Figure 7.1. Significance of L/S ratio to 28-day strength for primary and secondary data.....	167
Figure 7.2. Significance of A/B ratio to 28-day strength for primary and secondary data.....	169
Figure 7.3. Significance of S/A ratio to 28-day strength for primary and secondary data.....	171
Figure 7.4. Statistical comparison of 28-day strength prediction models.....	177
Figure 7.5. Comparison of thermal conductivity from primary and secondary data.....	181

Figure 7.6. Embodied carbon of GRC and basalt fibre geopolymer cladding panels.....194

Figure 7.7. Costs of GRC and basalt fibre geopolymer cladding panels.....196

List of Tables

Chapter 2

Table 2.1. Fire resistance requirements for residential buildings (DFPNI, 2012).....	8
Table 2.2. Typical GRC mix design (GRCA,2016).....	17
Table 2.3. Chemical composition of aluminosilicate source materials.....	24
Table 2.4. Embodied carbon content of pozzolanic precursor materials.....	56

Chapter 3

Table 3.1. Composition and environmental impact of source materials.....	62
Table 3.2 Particle size distribution of pozzolanic precursors and filler.....	64
Table 3.3 MK geopolymer mix designs for investigation of Na_2SiO_3 and K_2SiO_3 alkali reagents.....	69
Table 3.4 Geopolymer mix designs with binary combinations of precursor powder.....	70
Table 3.5 Geopolymer mix designs with ternary combinations of precursor powder.....	72
Table 3.6 Geopolymer mix designs based on factorial experimental design.....	73

Chapter 4

Table 4.1. Mix designs for metakaolin based geopolymer mortars.....	86
Table 4.2. Mix design methodology for replacement of metakaolin with multiple waste materials.....	96
Table 4.3. Factorial mix design methodology and strength results.....	99

Chapter 5

Table 5.1. Performance properties and mix design of unreinforced geopolymer matrix mixes.....	138
Table 5.2. Relative LOP and MOR of fibre/matrix compositions.....	144
Table 5.3. Variation in flexural strength results from Phase one.....	147
Table 5.4. Mix design and strength gain of GGBS/MK mortar and GRC control.....	148
Table 5.5 Composite combinations.....	148

Chapter 6

Table 6.1. Mortar mix designs for foaming.....	153
Table 6.2. Maximum allowable U-values (Technical Booklet F).....	161
Table 6.3. Properties of foamed geopolymer insulation and other common alternatives.....	163
Table 6.4. Geopolymer mortar mix design and properties.....	164
Table 6.5. Properties and composition of cladding panels based on typical GRC (Rieder).....	164
Table 6.6. Properties and composition of cladding panels based on typical concrete sandwich panel design (Creagh).....	165

Chapter 7

Table 7.1. Data set information for comparison of L/S ratio to 28-day strength.....	168
Table 7.2. Data set information for comparison of A/B ratio to 28-day strength.....	170

Table 7.3. Data set information for comparison of S/A ratio to 28-day strength.....	172
Table 7.4. Model information for primary and secondary equations.....	177
Table 7.5. Types of GRC.....	179
Table 7.6. GRC strength grades.....	179
Table 7.7. Material costs.....	196

List of Abbreviations and Symbols

AaC - Autoclaved Aerated Concrete

AACM - Alkali Activated Cementitious Materials

A/B - Activating solution to binder powder ratio

ACI - American Concrete Institute

AR - Alkali Resistant

ASTM - American Society for Testing and Materials

BF - Basalt fibre

BSI - British Standards Institute

BT - BanahTherm

CAD - Computer Aided Design

CASH - Calcium Alumino Silicate Hydrate

CIOB - Chartered Institute of Builders

CSH - Calcium Silicate Hydrate

CT - Computed Tomography

DFPNI - Department of Finance and Personnel Northern Ireland

EDX - Energy Dispersive X-Ray Analysis

ESFA - Education and Skills Funding Agency UK

FA - Fly Ash

FGI - Foamed Geopolymer Insulation

F/M - Fibre/Matrix ratio

FRM - Fibre Reinforced Mortar

GGBS - Ground Granulated Blastfurnace Slag

GRC - Glass Reinforced Concrete

GRCA - Glass Reinforced Concrete Association

HPFRCC - High Performance Fibre Reinforced Cementitious Composite

HSE - Health and Safety Executive

ICE - Institution of Civil Engineers

IS - Iron Silicate

ISO - International Standards Organization

IWM - Industrial Waste Materials

KASH - Potassium Alumino Silicate Hydrate

KOH - Potassium Hydroxide

LCA - Life Cycle Analysis

LOP - Limit of Proportionality

L/S - Liquid to solid ratio

MK - Metakaolin

MOR - Modulus of Rupture

NASH - Sodium Alumino Silicate Hydrate

NBO - Non- Binding Oxygen

NF - No fibre

NI - Northern Ireland

NME - Network Modifying Elements

NMR - Nuclear Magnetic Resonance

PC - Portland cement

PCE - Poly-Carboxylate Ether

PVA - Poly-Vinyl Acetate

PVC - Poly-Vinyl Chloride

RIBA - Royal Institute of British Architects

RILEM - International Union of Laboratories and Experts in Construction Materials,
Systems and Structures

S/A - Silica (SiO_2) to alumina (Al_2O_3) ratio

SEM - Scanning Electron Microscopy

SF - Silica Fume

SHCC - Strain Hardening Cementitious Composite

UNEPSBCI - UN Environment Programme Sustainable Buildings and Climate Initiative

UV- Ultra-Violet

VMA - Viscosity Modifying Admixture

XRD - X-Ray Diffraction

Chapter 1 – Introduction

This introductory chapter provides relevant background information to illustrate the need for the research proposed and presents the overall project aim and objectives. A summary of the thesis structure is also presented.

1.1 Background

Fibre reinforced cementitious cladding systems, using lightweight materials such as Glass Reinforced Concrete (GRC) are extremely popular in today's construction industry for creating the exterior facings and claddings of buildings. Cladding systems are usually composed of inter-connected individual GRC panels with insulation materials attached to meet the specific thermal resistance requirements of each project.

GRC is carbon and energy intensive to produce, as it chiefly comprises Portland cement (PC) that accounts for 5-7% of worldwide CO₂ emissions (Benhelal, 2013). Due to the need for high quality surface finishes and robustness, these composites typically use white cement, high cement to aggregate ratios, chemical admixtures and are therefore have increased costs, embodied carbon content and embodied energy (GRCA, 2016-b).

However, GRC suffers from a fatigue process due to the degradation of glass reinforcement fibres over time in a high alkaline cement paste; whereby fibre diameter decreases. Glass fibres are coated with zirconia, a cost and carbon intensive material, to limit degradation but cannot totally mitigate against degradation effects. As a consequence, GRC cannot be used in many load bearing, structural applications (Enfedaque et al, 2012).

This research intends to develop a new generation of cladding materials involving the use of geopolymer mortars reinforced with basalt fibres, which will comprise an external shell

and intrinsic foamed geopolymer insulation section. This is intended to form an all-in-one, monolithic cladding panel that is suitable for structural applications and fireproof.

Geopolymer mortars have been demonstrated to provide similar performances to PC mortars but have 60- 90% less embodied carbon and can be created using binders composed of 100% waste materials, such as fly ash or GGBS (Davidovits, 2013). As such, these mortars have the potential to significantly reduce the environmental impact of the cladding industry and find new uses for materials that otherwise would be landfilled. Basalt fibres were chosen as reinforcement as they are cheaper and more environmentally friendly than glass fibres (Branston, 2016). Furthermore, when combined with geopolymer mortars as opposed to PC mortars, basalt fibres may not require zirconia (coating) to prevent degradation (Branston, 2016; Palmieri et al, 2009).

The combination of this fibre reinforced structure with fireproof, low impact, foamed geopolymer insulation would allow sufficient thermal resistance for use in any structure and can improve safety and limit carbon embodiment in the cladding industry. This research aims to contribute towards the commercialisation and standardisation of geopolymers, along with their widespread adoption in the construction industry. The adoption of low impact construction materials such as geopolymers and their incorporation into building products such as high performance cladding panels is vital in order to meet government climate change commitments such as ensuring average global temperatures do not rise by more than 1.5°C and the complete decarbonisation of society through Net zero by 2050. To achieve this will require rapid transformation of the construction industry over the next ten years and the widespread adoption of new technological solutions such as proposed in this research before 2030. (Skidmore, 2023).

1.2 Aim

The aim of this research was to develop innovative cladding panel systems using low impact, fibre reinforced, geopolymer cement composites and foamed geopolymer insulation. This solution is intended to produce engineering performances that are comparable with GRC cladding systems.

1.3 Objectives

In order to achieve the above aim, the following objectives require fulfilment:

- The development of mix design procedures suitable for a wide range of geopolymer mortars and identification of mix parameters significant to strength, flowability and carbon embodiment. This will enable identification of an optimal geopolymer mortar to comprise the matrix of a low CO₂, high strength fibre composite cladding panel.
- The creation of foamed geopolymer insulation materials with thermal conductivity of approximately 0.03 W/mk and assessment of the efficacy and necessity of PC sizing techniques and methodologies in geopolymer mortar fibre composites.
- Identification of optimal fibre composition, geometry, and dosage for maximum flexural strength in the geopolymer mortar matrix and proposal of fibre reinforced geopolymer mortar cladding panels with foamed geopolymer insulation that are low CO₂ and meet UK building regulations including benchmarking of composite performance against similar materials in common usage for cladding applications.

1.4 Thesis structure

Chapter 1 – Introduction

This chapter presents the research background, the aim and objectives of the research and a clear outline of the final document contents.

Chapter 2 – Literature review

Chapter 2 presents a critical review of the relevant literature relating to the following:

1. Requirements of modern building cladding
2. Cementitious cladding systems
3. Geopolymers chemistry, design and performance
4. Geopolymer matrix fibre composites
5. Foamed geopolymers for insulation
6. Summary and knowledge gaps

Chapter 3 – Research methodology

Presented in chapter 3 is a summary of sample preparation and laboratory testing methodologies that were employed to assess the engineering performance of geopolymer mixtures.

Chapter 4 – Geopolymer mortar development

This chapter focusses on the development of geopolymer mortars that form the panel structure. A range of pozzolanic precursors and alkali activators were trialled and mix designs were developed to identify optimal mixtures in terms of strength and carbon embodiment. Mix design methodologies were created such that they made specification simpler and more familiar to the construction industry. Empirical equations were successfully developed to predict performance properties, such as strength flow and carbon embodiment.

Chapter 5 – Assessment of fibre reinforced geopolymer mortar panels

Based on the result of the previous chapter, chapter 5 focussed on the development of optimised fibre-reinforced geopolymer mortar designs to investigate the efficacy of using

different types and dosages of fibre reinforcement to improve the mechanical properties of the mortars produced.

Chapter 6 – Development of foamed geopolymer insulation materials

Chapter 6 presents results from the development and performance of novel foamed geopolymer mixtures, through thermal assessment. These findings were used to create cladding design options of specified thermal resistance, which were benchmarked against current standardised engineering materials.

Chapter 7 – Discussion

This chapter critically appraises the significance of the findings of this research, with comparisons made against published datasets for existing cladding materials and geopolymers, including engineering performance, practicality, sustainability and cost. This enabled a review of the potential benefits of using basalt fibre geopolymer composite cladding panels in future construction, highlighted future challenges in their use and commercialisation.

Chapter 8 – Conclusions and recommendations

This chapter summarises the main conclusions derived from this research and provides recommendations for further research.

Chapter 2 – Literature Review

2.1 Introduction

In modern building construction, cladding systems are widely used for providing the outer skin of new and retrofitted buildings - comprising interconnected panels. These provide design flexibility through a range of forms for aesthetical purposes. Cladding systems are designed to provide protection against the environment (e.g. weather extremes), provide privacy, security and fire protection for occupants (Theodosiou, 2015).

This literature review investigates modern cementitious building cladding systems, specifically their applications, technical material design requirements and their limitations. Focus will also be paid towards the potential benefits of geopolymeric or alkali activated cementitious materials (AACMs) if upscaled for commercial use. The following sections will be presented in turn:

1. Requirements of modern building cladding
2. Cementitious cladding systems
3. Geopolymers: A possible solution
4. Geopolymer matrix fibre composites
5. Foamed geopolymers for insulation
6. Conclusions from this literature review

2.2 Requirements of modern building cladding

In the UK, building cladding must meet prescribed minimum standards set out in the national building regulations for their use in the construction industry. The most important of these to consider when developing new cladding systems include: structural safety, fire resistance and thermal performance when in-situ.

2.2.1 Thermal performance of structures

The UK Building Regulations Technical Booklets F1 and F2 (DFPNI, 2022a and b) provide the minimum acceptable levels of thermal resistance that structures must exhibit in terms of specified minimum ‘U-values’. This U-value describes the thermal resistivity ($\text{W/m}^2\text{K}$) that must be achieved by the envelope of different types of buildings.

These regulations stipulate that, in non-domestic or commercial buildings, walls must provide an average U-value of $0.21 \text{ W/m}^2\text{K}$ across its entire area, and no single point must have a value higher than $0.6 \text{ W/m}^2\text{K}$. In domestic construction such as houses or flats, requirements are more stringent with a minimum average of $0.18 \text{ W/m}^2\text{K}$ and not greater than $0.7 \text{ W/m}^2\text{K}$. Cladding for roof structures must achieve maximum average U-values below $0.16 \text{ W/m}^2\text{K}$ for domestic and $0.2 \text{ W/m}^2\text{K}$ for non-domestic structures, with no values exceeding $0.3 \text{ W/m}^2\text{K}$ in either case. Most cladding materials cannot achieve this level of thermal resistivity independently. As such, cladding systems often use air cavities, rockwool or expanded polyurethane insulation boards to achieve the required level of thermal protection.

Limiting of cold bridge protrusion through cladding systems is important to the overall thermal performance of a building. Any suitable method of construction must be designed and constructed to mitigate against this effect as much as possible. Structures must also prove through on-site testing that the quality of construction will provide at least the minimum required air tightness of less than $10\text{m}^3/(\text{hour/m}^2)$. Technical Booklets F1 and F2 also stipulates that solar heat transfer through the structure must be limited to reduce the need for excessive air conditioning or capitalised upon to limit excessive heating requirements, depending on the local climate and nature of seasonal weather. This limits the use of fully transparent skins, such as glass curtain walling and most often necessitates the use of opaque cladding (DFPNI, 2022-a; DFPNI, 2022-b).

2.2.2 Fire resistance

A vitally important aspect of cladding design for buildings is fire and safety resistance, as highlighted in June 2017 by the tragic Grenfell Tower disaster. Such events have often led to the development and implementation of more stringent regulatory controls and an increase in minimum fire resistance over time. In response to the Grenfell Tower disaster, the UK House of Commons passed a bill that requires the Health and Safety Executive (HSE) to establish a new building safety regulator (GOV.UK, 2021).

Building Regulations Technical Booklet E (DFPNI(c), 2012) states that building exteriors must be designed and installed to limit the possibility of ignition from an external source and the spread of fire both across and through its structure. This is quantified through the rate of heat transfer and release. The regulations also limit the extent of unprotected areas (e.g. windows, glass walling) on a building exterior, to limit radiative heat and fire transfer. This implies that the use of opaque cladding options is often unavoidable. In practice, DFPNI (c) (2012) specifies a minimum time of fire protection that specific purpose groups or elements of the structure must provide when tested to BS476 (BSI, 2009). Table 2.1 shows an example of the minimum requirements for various residential buildings.

Table 2.1. Fire resistance requirements for residential buildings (DFPNI(c), 2012)

Building type:	Number of floors	Minimum fire resistance time
Residential	<5	30 mins
	>5 but <18	60 mins

In commercial construction, the process to determine these minimum times is determined by factors including the building purpose and whether sprinkler systems are considered to have been installed. In most simple cases, these will be as stated above for residential but for certain high-risk activities in tall, un-sprinklered buildings, these minimums could

rise to 120 minutes. Any method used to clad a building must not interfere with fire breaks or compartmentalisation used to divide areas, such as separate dwellings in a block of flats, as this would undermine the entire fire safety design strategy (DFPNI(c), 2012).

2.2.3 Structural safety

In terms of structural safety, Building Regulations Technical Booklet D (DFPNI, 2012d) states that buildings, and therefore cladding elements, must be designed and constructed such that they can withstand the combined dead, imposed and wind loads acting on the building. Furthermore, cladding elements must then transfer these forces through the structure to adequate underlying foundations. Buildings and their components must also be designed to ensure that for damage occurring to any part of the building, the resulting collapse will not be disproportionately acute. Cladding design and installation should be given the same care and consideration as the primary structure during design and construction to ensure safety, reliability and durability with specific attention focussed on the design of safety critical aspects such as connectors and fixings. Cross UK commissioned a safety report entitled ‘Structural issues with cladding’ reiterates these points and recommends that a single appointed entity has overall control of the cladding system, along with its connections to the structure to ensure applied loads are adequately supported at all points (Cross UK, 2020).

In terms of structural safety, design and installation of fixing and support systems are perhaps the most vital design concern for building cladding. Interactions between cladding panels and the building superstructure are often not well understood, and can be a major source of structural failure as a consequence. An example of stiff cladding panels fixed to the edge of a concrete floor slab can create composite load bearing between the panels and structure, where load is distributed and can overload individual fixings (Cross UK, 2020). BS 8297:2017 gives guidance on how fixings and support systems for panels can be designed to eliminate this composite action and provide consistent predictable load

distribution to the supporting structure (BSI, 2017). Fixings should only be selected if they have proven performance against the risks associated with the application and materials used. Redundant fixing systems are recommended to ensure that if an individual fixing fails, the load it supports can be transferred and shared by adjacent fixings to avoid disproportionate cladding failure and panel detachment (Cross UK, 2020). CIRIA report RP 566 outlines good practice for the selection, design and installation of fixings in concrete and masonry construction to ensure structural safety and durability of cladding systems (CIRIA, 2010).

To design fixing systems suitable for safe cladding, the forces that act on the panels must be accurately ascertained and reflected in the cladding composition. These forces are often not consistent across the cladding area or over time with local, transient maxima that must be sustained. Cladding panels must not only sustain their own weight but also those forces arising from activities inside or around the structure and local environmental conditions such as wind, rain and thermal gradients (Cross UK, 2020). Wind loads incident on cladding can be ascertained based on BS EN 1991-1-4:2005 and its local annex, which provides consideration for local increases in suction from wind funnelling in between buildings (BSI, 2005). Changes in load distributions should be accounted for when cladding is required to support other fixtures such as handrails or signage, act as a pedestrian barrier or withstand lateral pressure from crowds of people. Cross UK also report the importance of having sufficient expansion or movement joints integrated into the overall cladding design to control the stresses placed on individual fixings by factors such as wind loading or thermal expansion and contraction (Cross UK, 2020).

Building cladding elements will often need to endure significant flexural loads from environmental loadings such as wind, which cause material fatigue over time, or simply through an aesthetic-lead design that features large spans or cut outs (Donà, 2017). A cladding panel must have high flexural strength to cope with differential movement

between itself and the structure and the uneven loading often encountered. Typical limit of proportionality (LOP) and modulus of rupture (MOR) values for the GRC panels range from 5-10 MPa and 5-30 MPa respectively. These panels also exhibit compressive strength ranging from 40-80 MPa and tensile strengths between 3-12 MPa. Benchmarking against values such as these and a similar material that is currently used for building cladding systems in the UK will be the simplest way to ensure sufficient structural strength is achieved by any new systems developed (RIBA, 2020; Rieder, 2020; Oscrete, 2016; CIRIA, 2010).

When flexural loads are applied to unreinforced cementitious materials, such as the mortars developed in Chapter 4, a stress/strain curve of the reaction will follow Hooke's law showing linear, elastic deformation until the material yields. At this point, due to the brittle nature of the material, cracks will form and propagate rapidly causing nearly instantaneous structural failure (Visintin, 2018). Fibre reinforcement of brittle, cementitious materials has been shown in the literature to be an effective, lightweight method of increasing flexural strength (Yan et al, 2016). The ultimate performance and strength levels achieved by a fibre reinforced composite is a product of three factors: 1) the matrix properties, 2) the properties of the reinforcement fibres and 3) the interfacial bonding that holds the composite together by transferring applied stresses from the weak matrix to the strong fibres. This is accomplished through both chemical and frictional bonding between the fibre surface and the surrounding matrix, acting to bridge cracks that would otherwise cause catastrophic failure of the brittle matrix materials (Callister, 2014).

When flexural loads are applied to a single fibre embedded in cementitious material, the resulting stress/strain curve follows Hooke's law until a crack appears. While this will cause fibre debonding and rupture of chemical bonding between the two, a frictional force will still be present to hold the composite together and prevent the fibre from being pulled out. In a successful fibre composite the first crack strength will be significantly higher

than the matrix alone. Due to fibres blocking the propagation of cracks, brittle failure can be avoided and a higher total force can be sustained. Some composites even exhibit a slip hardening, where the frictional bond created from fibres being pulled out allows greater loads to be endured after the first crack before composite failure (Li & Wu, 1992; Lin and Li, 1997; Rienhardt et al, 2015).

The LOP or first crack strength of a composite is a vital parameter in determining the field performance of a cladding panel, as often once cracking begins the panel is no longer fit for purpose. Panels will likely be replaced or repaired once cracks begin forming and below the MOR level (ESFA, 2018). The difference between LOP and MOR values allows for a modicum of design safety where instant, catastrophic failure will be avoided. An MOR/LOP ratio ~ 1 signifies totally brittle failure, with higher values indicting greater composite action and a delayed failure after the first crack. Materials that can sustain significantly higher loads after first cracking but before total failure are strain hardening materials (Figure 2.1) (Altoubat, 2018). This occurs when the force required to break the combined chemical and frictional fibre/matrix bonds are greater than those that hold the matrix material together. This can provide greater structural safety and lifespans without catastrophic, instantaneous failure. The area under the load/displacement curves of plotted from bending tests of composites represents the total energy absorbed and is analogous to toughness. This metric describes both the strength and ductility of materials simultaneously and was analysed in this study for a correlation with the LOP and MOR.

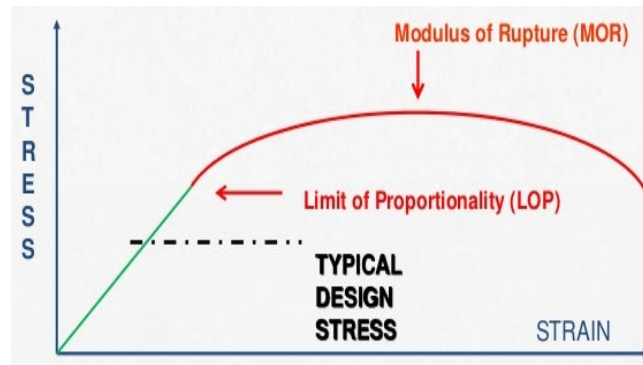


Figure 2.1. Typical stress/strain curve for GRC materials (White, 2015).

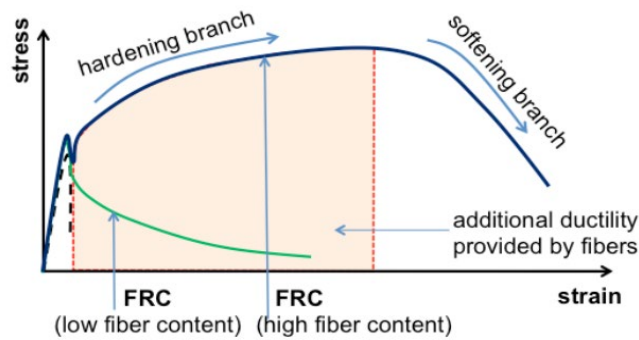


Figure 2.2. Illustration of strain hardening and softening (Altoubat, 2018).

2.2.4 The future of the cladding industry

Lightweight, non-structural cladding systems currently in use meet and surpass minimum engineering strength and fire resistance standards. Progressively higher levels of thermal performance, fire safety and aesthetically pleasing surface finishes are highly sought after by the construction industry and clients, with the added pressure of minimising greenhouse gas emissions, energy use and financial costs. These demands are likely to intensify over coming years if the UK's construction industry is to deliver net zero carbon emission targets by 2050 (Skidmore, 2023). Furthermore, there are international environmental / climate change agendas such as the Kyoto Protocol (1997) and the Paris agreement (2015), which have a significant influence on the development of new materials and new construction projects (European Council, 2018). However, it is

plausible that existing cladding material technologies may not be able to deliver on such targets, highlighting the need for innovation.

Perhaps the greatest factor driving change in the British and European standards required from building cladding is the increasing public and political awareness of anthropogenic climate change and its effects on the natural environment. In 2018, worldwide carbon dioxide (CO₂) levels were reported to be the highest in human history. Without making significant reductions in such emissions by 2100, global temperatures are predicted to rise by up to 6°C leading to rising sea levels, extreme environmental changes and ecosystem destabilisation (Cockburn, 2018). With the UK government committed to limit global warming to 1.5°C by 2050 new technological solutions must be funded and developed to facilitate the changes required (Skidmore, 2023).

Building construction and operation accounts for around 40% of the energy used and one third of the greenhouse gases emitted worldwide (UNEP SBCI, 2009). In 2018, this equated to 14.67 billion tonnes of greenhouse gases released into the atmosphere to further fuel temperature increases. As a result, buildings and energy use within them has become a vital area in need of improvement.

Pressure on the construction industry to create ever more sustainable, energy efficient and environmentally friendly building facades has seen the minimum standards of thermal insulation increase, and the acceptable levels of carbon embodiment reduce significantly.

2.3 Cementitious cladding systems

Cement-based cladding solutions typically include precast reinforced concrete and GRC panels, which can be designed to incorporate insulation as required. Precast, reinforced concrete cladding offers benefits such as intrinsic durability, robustness and precise architectural features with a wide range of surface finishes. Precast concrete panels can be supported by the structural frame of a building, or be self-supporting and restrained.

Cladding panels can also be designed to be load bearing and support a buildings floor deck. The high density, carbon footprint and panel thickness (for providing sufficient flexural strength) of reinforced concrete cladding make them disadvantageous for us as such heavy panels more difficult to install and require larger energy-intensive lifting equipment. Furthermore, such heavy panels must be supported by a stronger and heavier structure, which in turn must be supported by stronger foundations; all of which increase the cost, timespan and carbon footprint of the overall construction project.

Alternatively, GRC panels are typically thin, lightweight ($1800\text{--}2100\text{ kg/m}^3$ compared with precast reinforced concrete, $2400\text{--}2600\text{ kg/m}^3$) and possess high durability and strength properties; whereby they can be moulded using pre-cast or hand-spray manufacturing techniques. Developed in 1969, GRC is one of the most common forms of cementitious fibre composite, comprising a mixture of cement, fine aggregate, water, chemical admixtures and alkali resistant glass fibres.

GRC panels can be used for structural and non-structural applications with a range of surface finishes and shapes. In recent years, GRC structural applications have included industrial floors and roofs (Enfedaque et al, 2012; GRCA, 2016-a). Other applications include permanent formwork, tunnel cladding, building restoration and decorative products. Traditionally all applications have been non-load bearing, although structural GRC floors and roofs can experience static fatigue, due to the deterioration of glass fibres over time in the highly alkaline environment of the cement matrix (Enfedaque et al, 2012; GRCA, 2016-a). However, material innovations have mitigated against this.

Due to the quasi-brittle nature of concrete, the glass fibres within GRC panels aim to increase post crack toughness, flexural strength and reduce panel thickness. Through careful design, the engineering performance of GRC (i.e. mechanical strength, durability,

fire protection and corrosion resistance) can be tailored such that it is comparable to steel reinforced concrete (Choi et al, 2012; Steel Construction Info, 2016; Yan et al, 2016).

GRC is well suited to cladding applications due to its high (early) mechanical strength and fire resistance properties, along with practical factors including high production efficiency and easy mouldability. Due to the increased flexural strength, crack resistance and toughness provided by fibre reinforcement within GRC, this material can be used to produce much thinner panels compared with precast reinforced concrete; thereby reducing the bulk mass of building facades from 235 kg/m² for bulk concrete to approximately 85 kg/m² (GRCA, 2016-a; Fibre technologies international, 2020; RIBA, 2020). This can have wider financial benefits such as reduced costs for foundations, more flexibility for increased floor space and reductions in the carbon and energy embodiment of buildings.

2.3.1 Environmental impact of GRC

The manufacture and use of both precast reinforced concrete and GRC cladding panels does have environmental implications, owing primarily to their reliance on the use of Portland cement (PC). The manufacture of PC accounts for 5-7% of global CO₂ emissions (Benhelal et al., 2013); whereby it releases 0.912 kgCO₂/kg and requires 4.5 MJ of energy per kg of PC produced (Jones, 2019).

The carbon footprint of GRC is significantly greater per kg compared with traditional reinforced concrete, as the need for robustness and high-quality surface finishes necessitate the use of high cement to aggregate ratios, low water/cement ratios and high-grade white cement and silica sand (GRCA, 2016c). However, this is offset since up to 80% less GRC materials are required to fulfil the same application as reinforced concrete (RIBA, 2020). As a result, GRC structures will have lower carbon embodiment.

A typical formulation for cast GRC provided by GRCA is included in Table 2.2. The GRCA document ‘Specification for the Manufacture, Curing & Testing of GRC Products’ provides guidance on typical GRC composition and mix parameters for GRC suitable for a range of applications and strength requirements. Mix designs that fall outside these parameters may still be acceptable but “*must be fully scrutinised and tested before use*” (GRCA, 2021). It is evident that cement content is high, with a cement to aggregate ratio of 1, whereby the fine aggregate acts as a filler. This results in higher costs and environmental impacts compared with traditional precast concrete, which uses both coarse and fine aggregates as fillers. Furthermore, precast reinforced concrete will often use less than half the amount of PC in GRC per m³ and cement/aggregate ratios closer to 0.25. GRC also uses a Forton polymer additive to control surface cracking and increase early age strength. Superplasticising additives are used to give sufficient flowability to ensure surface quality and ease of casting, even at low water/cement ratios. However, the use of both additives further increases the cost and carbon footprint of the panels (GRCA, 2016-c; Ball, 2005) .

Table 2.2. Typical GRC mix design (GRCA,2016)

GRC constituents	kg/m³
White Portland cement	975
Fine aggregate	975
Plasticising admixture	10
Polymer	97.5
Water	312
AR glass fibre	2.5% total vol.

An example of a modern GRC cladding would be the GFRC M4 cladding panel created by Telling architectural. Telling describe these panels as lightweight, high performance, fibre reinforced, precast concrete, floor to floor cladding panels than can be moulded to

standard form profiles or almost any shape to accommodate window returns, column surrounds and roof level profiles. The panels use a cement to sand ratio of 1 and alkali resistant glass fibres as described in the example specification. Ribbing of 50-100 mm around the perimeter and across the rear face help achieve an LOP and MOR of 5-10 and 18-30 MPa, respectively. These are 12-15 mm thick with standard dimensions of 4m x 2m, which provide 1m² of building façade at a weight of just 50-70 kg. This is 80% less than what is provided by traditional precast concrete cladding (RIBA, 2020; Telling Architectural, 2019). Given that GRC possesses a higher carbon footprint compared with traditional reinforced concrete, this highlights the need to replace (complete or partial) high-carbon constituents (e.g. PC) with ‘greener’ alternatives to improve the environmental credentials of GRCs.

One alternative solution is to replace the PC matrix of the composite with geopolymeric or AACM systems, which are widely reported to produce superior engineering performances and significantly lower carbon and energy embodiments compared with GRC.

2.4 Geopolymers

Geopolymer and AACMs can form, cure, and gain strength rapidly in ambient temperatures by mixing user friendly alkaline reagents (e.g. Na or K silicates with SiO₂:H₂O ratios of 1.45-1.85), free water and alumina/silicate rich (i.e. pozzolanic) precursor powders. The latter can be commercially manufactured, such as metakaolin (MK) or involve the use of industrial by-products such as fly ash (FA), ground granulated blast furnace slag (GGBS), silica fume (SF) and biomass waste (Zeobond, 2012).

The geopolymerisation process produces a strong and durable matrix that behaves similarly to PC-based concretes, whereby it typically exhibits high strength over rapid setting times – thereby facilitating quick and efficient cladding panel manufacture.

Geopolymers have been widely reported to be superior to PC-based concretes in the following ways: they exhibit greater resistance against fire and chemical attack, possess a carbon footprint that can be up to 90% lower than Portland cement and have the ability to use a 100% recycled binder powder (Davidovits, 2013; Banah, 2014; Geopolymer Institute, 2016).

Geopolymer cements can harden more rapidly than PC, with marked strength gains being achieved within approximately two hours, thereby allowing for efficient pre-casting operations (Kim, 2012). Such short setting times are also practical for mixing on site in a batch plant and delivery by mixer truck to in-situ pours. As such, their usage in cladding panel systems offers technical, economic and environmental benefits to the construction industry.

2.4.1 Geopolymer definition and chemistry

Discrepancies exist in the literature regarding the distinction between geopolymers and AACMs (Davidovits, 2017). An AACM can be defined as “*any material produced from an alkali metal reacting with a solid silicate powder*”, whereas researchers such as Provis and Belena (Luukkonen, et al., 2018) would define geopolymers as simply a subset of these materials.

Joseph Davidovits, the inventor of geopolymers, considers these inorganic, polymerically bonded materials as discreet - specifically defined by a covalently bonded network of mineral molecules. Davidovits (2017) states that for an AACM to be classed as a geopolymer, the material must: 1) gain strength at ambient temperatures, 2) contain only covalent polymeric bonds, 3) not use a binder composed purely of slags to limit calcium content and the development of precipitate bridging particles characteristic of AACM - even though this would increase material strength (Davidovits, 2017; Chen, et al., 2020). Evidence of Sodium Aluminosilicate Hydrate (NASH) and Potassium Aluminosilicate

Hydrate (KASH) gel reaction products are considered a direct result of alkali activation and therefore should not be present within a geopolymerised matrix (Davidovits, 2017).

MacKenzie (2003) suggested several possible criteria for discerning the difference between geopolymers and AACMs, including the development of strength at ambient temperatures, lack of long-range atomic ordering, the presence of solely tetrahedral Al-O and Si-O units and thermal stability at high temperatures. Luukkonen et al. (2018) state that AACMs are characterised by lower Si co-ordination with 2-dimensional structural order and higher calcium content, whereas geopolymers exhibit higher, essentially 3-dimensional, structural coordination but lower calcium contents. This allows greater structural complexity to form. Luukkonen et al. (2018) further states that while these distinctions do exist, they are often ignored and the terms are often incorrectly used interchangeably in published work.

Geopolymer cements can be described as a mixture of compounds composed from repeating alumino-silicates, for example Silico-oxide (-Si-O-Si-O-), Silico-aluminate (-Si-O-Al-O-), Ferro-silico-aluminate (Fe-O-Si-O-Al-O-) or alumino-phosphate (Al-O-P-O). These materials exhibit only short-range structural order and the microstructure created is highly temperature dependant (Geopolymer Institute, 2016; Geopolymer Institute, 2006). At room temperature the geopolymers are amorphous in form but above 500°C this evolves into crystalline zeolite phases. The type and relative amount of reaction phases produced depends on formation parameters, such as the alumino-silicate source materials or the type of activator used (Kim, 2012).

Fletcher et al. (2005) state that geopolymers consist of tetrahedral AlO_4 and SiO_4 units polycondensed at ambient temperatures under highly alkaline conditions with charge stabilisation provided by alkali earth ions from the activating solution. Davidovits (2002) stated that poly-silicates which make up geopolymers, are amorphous to semi crystalline

and organised into three-dimensional aluminate chain or ring polymer structures in which Si^{4+} and Al^{3+} are Q4 structural order with oxygen. The gradual development of structures formed at changing Si:Al ratios according to this are shown in Figure 2.3 (Davidovits, 2002). Contrastingly, Provis and van Deventer (2009) suggest that these models imply one-dimensional chain structures, not the 3D network produced by geopolymerisation, and, only consider Si:Al ratios at integer values (1, 2 or 3) when this is likely not the case in reality.

Geopolymers are formed as a result of three main reactions; dissolution, condensation (oligomerisation) and polycondensation (polymerisation) (Davidovits, 2013). These reactions can occur simultaneously in different parts of the same mixture. A schematic outline of the geopolymerisation process is included in Figure 2.2 (van Deventer et al., 2007).

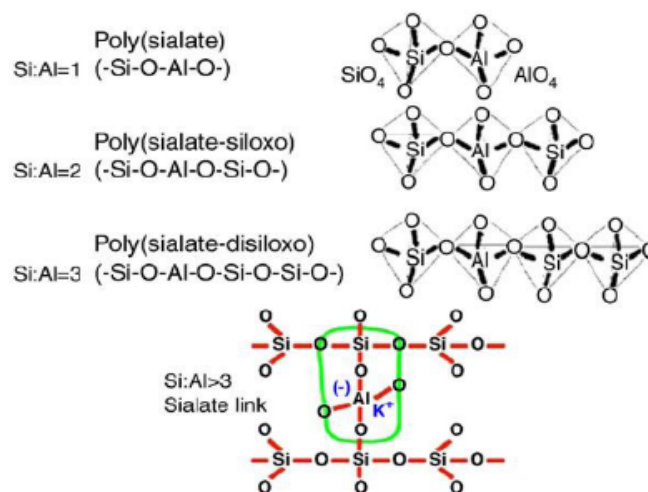


Figure 2.3. Geopolymer structure at changing Si:Al ratios (Davidovits, 2002).

Water is an integral part of a geopolymer mix design, but it does not become part of the aluminosilicate gel structure. Water provides a reaction medium, whereby if it is present in the bulk material – it is expected to be in isolated pore spaces. This directly contrasts with the hydration of PC (Lizcano et al, 2012). Much like in PC, if excess water is present

in the mixture it will limit the hardened properties such as strength and microstructure but due to increased pore volume and reduced density instead of altering the chemical composition of the binder. Liquidity, however, is required to facilitate reactions between the powders and the activating solution and to give fluidity. Therefore, a balance must be achieved (Aughenbaugh, 2015).

Unlike PC hydration where water is driving the reaction, geopolymerisation is initiated by contact between an aluminosilicate source material and an alkali reagent solution. This causes the aluminosilicates to depolymerise into separate alumina and silica monomers - the degree to which this happens is determined by the reactivity of the source material, the concentration (molarity) of the activating solution and the reaction time (Davidovits, 2013; Kim, 2012). The activating solution provides alkali and hydroxyl ions and combines with the precursor materials to form a disordered alkali aluminosilicate gel.

Over time this gel will then reorganise and condense into a rigid tetrahedrally orientated network made up of Si^{3+} and Al^{3+} cations linked by sharing O^{2-} anions and release water, thereby increasing workability (Mustafa al Bakri et al, 2011; Xu, 2000; Tempest et al, 2015). Hardening then inhibits precursor transport and therefore the reaction process, which may be initiated by the application of heat, a drop in pH or availability of nucleation sites by the inclusion of calcium (Davidovits, 2013).

Geopolymer hardening at ambient temperatures requires Ca cations. When a source of calcium is added (e.g., lime, Class C fly ash or GGBS), a typical PC hydration product is generally produced (e.g. CSH gel). This has been shown to increase susceptibility to chemical attack compared with alumino-silicate geopolymer gel and provide higher strength (Kim, 2012; Oh, et al., 2012; Austroads, 2016). The presence of calcium from GGBS however has also been shown to increase the degree of geopolymerisation, increase the mechanical strength and reduce set times in mortar mixes (Wilkinson, 2018)

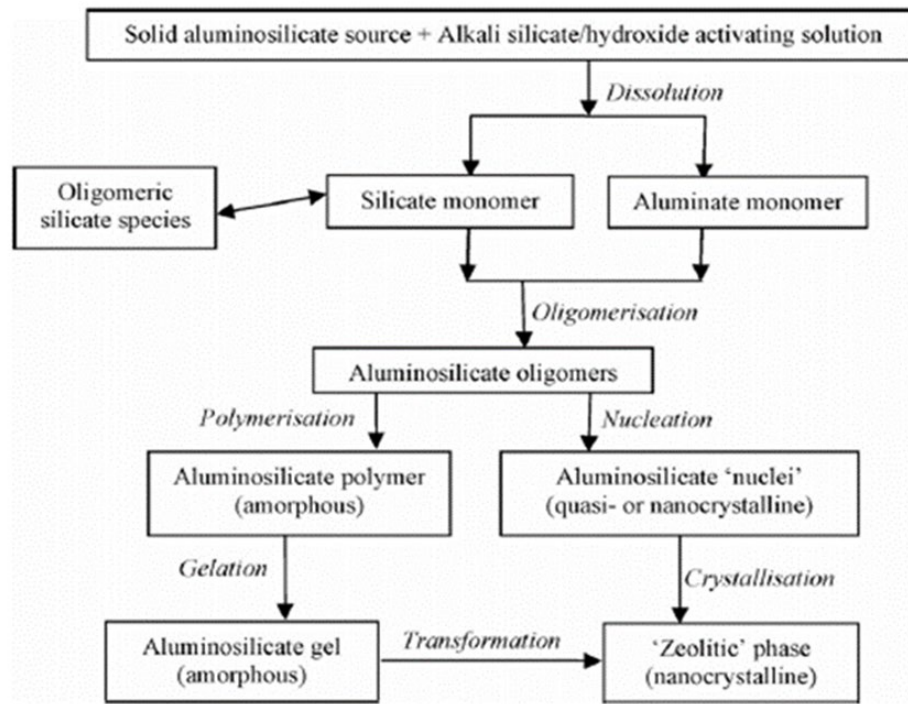


Figure 2.4 Schematic outline of the geopolymerisation process (Van Deventer et al., 2007).

2.4.2 Binder material options for geopolymers

Generally, aluminosilicate materials with high amorphous contents are preferable as precursor materials (Banah, 2014). Commonly used aluminosilicate materials include MK, FA, SF and GGBS. The chemical composition of various potential aluminosilicate source materials is summarised in Table 2.2, along with PC for comparison. As these materials contain similar metal oxides in varied concentrations, this allows customisation of the chemical structure using binder blends from multiple sources to control aspects such as the Si:Al ratio.

Precursors such as kaolin require thermal treatment (forming MK) to increase their reactivity and amorphous content. However, this is not required for materials like GGBS and FA, which were generated as waste products from heat-intensive processes associated with iron/steel manufacture and coal-fired electricity generation, respectively. Performing any extra pre-processing (e.g. heating) of precursors or alkali reagents has the adverse impacts of increasing cost and carbon emissions (Austroads, 2016). The use of industrial

by-products such as FA and GGBS possess the greatest potential for reducing the carbon footprint of PC and geopolymer concretes.

Table 2.3 Chemical composition of aluminosilicate source materials (Wilkinson, 2018; Bediako and Amankwah, 2015; Kwasny et al., 2016).

Material		Portland Cement	Meta-kaolin	GGBS	Silica Fume	Fly Ash	Iron Silicate	Banah CemA
Chemical composition (% by mass) NR = Not reported	SiO ₂	21	55	36.5	96	57	27	32
	Al ₂ O ₃	5	40	10.4	0.8	24	3.2	25
	CaO	64.2	0.3	42.4	0.5	3.9	1.8	25.2
	Fe ₂ O ₃	2.9	1.4	0	0.8	6	46	7.8
	TiO ₂	NR	1.5	0.5	0.02	1.4	>0.001	3.2
	MnO	NR	>0.001	0.4	>0.001	>0.001	>0.001	0.37
	MgO	1.7	0.3	8.1	0.5	2	0.7	1.71
	P ₂ O ₅	NR	>0.001	>0.001	>0.001	>0.001	>0.001	0.14
	Na ₂ O	0.24	0.4	>0.001	>0.001	0.4	>0.001	0.36
	K ₂ O	0.7	0.4	>0.001	>0.001	0.6	>0.001	0.15
	SO ₃	2.6	>0.001	>0.001	>0.001	1.6	>0.001	0.22

2.4.3 MK precursor

MK is a widely used and commercially available precursor (e.g., Metamax from BASF, Arigical M1000 and M1200S from IMERYS), which is typically manufactured by preparing, grinding and calcining mined kaolinite. Calcination causes the kaolinite to undergo dihydroxylation then recrystallisation, producing a more reactive amorphous material which can then be subjected to dissolution, as the first stage of geopolymerisation (Provis, et al., 2015). The processes of both dihydroxylation and recrystallisation are vital to MK reactivity and controlled by the heating regime; too cold and the kaolin particles have a low reactivity, too hot and the kaolinite recrystallises into less reactive

arrangements (Wan et al, 2017). Optimal calcination temperatures to ensure high strengths are achieved in geopolymers have been reported in the literature to vary between 650 and 850°C (Wan et al, 2017); whereby the most commonly used temperatures are 700°C (Yunsheng et al., 2009), 750°C (Rowles and O'Connor, 2009) and 800°C (Zibouche et al., 2009).

MK as a precursor material has high levels of consistency and can undergo dissolution more rapidly compared with materials such as FA (Provis et al., 2015). MK manufacture has a much lower environmental impact than PC manufacture, due to the lower energy requirements for thermal treatment. As such, partial or full replacement of MK with industrial waste products not only significantly reduces the environmental impact of the geopolymer, but can also produce impressive engineering performances in terms of reduced set times, increased strength and higher flowability (Austroads, 2016).

2.4.4 Fly ash precursor

FA is an inorganic mineral residue generated from coal-fired electric power stations, which has been the most widely used precursor in geopolymer research studies (Timakul et al., 2015; Austroads, 2016). From scanning electron microscope (SEM) data, FA particles are typically spherical with a diameter of 0.6-23 µm, with smooth exterior surfaces and occasional hollows, which may be infilled with finer FA particles.

The physical and chemical characteristics of FA depend on the type of coal burnt (i.e. chemical composition) and the efficiency of the power station facility. FA composition has been reported to vary significantly over time, even from the same source facility due to natural variations in the composition of the coal burnt. FA solidifies while suspended in the exhaust gases and is collected by electrostatic precipitators or filter bags. The powder mainly consists of two forms of SiO₂: an amorphous form which is smooth,

rounded and reactive, and a crystalline form which unreactive, sharp, pointed and hazardous; along with Al_2O_3 and Fe_2O_3 .

Variations in coal composition will produce variations in the ratio between these SiO_2 compounds, which will be reflected in the performance and composition of the FA produced. In general, higher amorphous content equates to higher reactivity, strength and flowability. FA contrasts to MK, whereby all oxides are soluble in alkali activating solutions, hence these crystalline phases cannot undergo geopolymerisation. As the glass to amorphous ratio defines reactivity and strength development, inconsistency in composition is a challenge when attempting to meet a specified strength or workability criteria (Aughenbaugh, 2015; McCarthy, et al., 2008). McCarthy et al. (2008) refers to this as ‘uncontrollable variability’, which represents the main drawback of using FA in geopolymers.

There are 2 classes of FA: Class C which has high calcium and alkali contents (making them suitable for PC replacement in traditional concrete mixes) and Class F which has lower calcium and alkali contents, and as such requires heat and alkali activation to promote pozzolanic activity. Due to the popularity of Class C FA as a PC replacement, the majority of studies into FA geopolymers concentrate on finding suitable applications for Class F FA. As such, little research attention has been given to Class C FA geopolymers. These materials have calcium content above 10% (by mass) and as such can set at ambient temperatures. However, they require higher alkaline activating agent contents making Class C FA geopolymers more expensive, less environmentally friendly and more user hostile than for Class F FA, MK or GGBS geopolymers (Davidovits, 2017).

2.4.5 GGBS precursor

GGBS is a hydraulic binder that is produced as a by-product of pig iron manufacture in blast furnaces (Srinath and Prabha, 2016). GGBS has been used for over 150 years, mostly

to improve the properties of traditional PC-based cements and concretes. This is a tightly controlled, as a uniform product with similar constituents to PC, but in different proportions (see Table 2.2). GGBS creation produces 35 kgCO₂/tonne of material due to post-production processes, such as grinding and granulation (Srinath and Prabha, 2016), which represents ~4% of the total emission for PC manufacture (Jones, 2019).

GGBS-based geopolymers also require a much smaller amount of activator solids for full dissolution when compared with MK or FA due to higher silica content. As activators are the most expensive components of geopolymers with the largest carbon footprint, GGBS-based geopolymers exhibit environmental and economic benefits compared with MK or FA based geopolymers. Using GGBS as a source of calcium in MK, FA, and SF geopolymers also leads to an increase in the formation of Calcium Aluminosilicate Hydrate (CASH) and increased compressive strength (Komnitsas, 2011).

2.4.6 Silica fume precursor

SF is a by-product from the production of silicon and ferrosilicon alloys used in semiconductors and other electronics, which are manufactured by reducing quartz with coal in an electric furnace. The material has extremely high silica content (>95%), is extremely fine-grained and is strongly pozzolanic. Hence, SF has been used for decades as PC replacement to improve mechanical strength and durability by increasing binder reactivity, density and particle packing and decreasing porosity. SF reacts with the calcium hydroxide produced during primary PC hydration and creates a secondary CSH, which may differ in Ca/Si ratio, molecular water content, molecular density and increase the potential for reactions with external ions (Al, Cl etc) (Khater, 2013).

In geopolymers, SF has been used to increase Si:Al ratio as it partially dissolves in the activating solution and releases silicon. This increased silicon content is reported to increase the number of Si-O-Si bonds present, which, theoretically should create

increased strength development (Austroads, 2016). Unreacted SF particles, however, can also remain in geopolymer pastes and limit mechanical performance. SEM images have shown that these particles do not fill the pores in the unreacted metakaolin particles present and therefore do not successfully reduce binder porosity even if they act to densify the structure. Ascertaining the proportion of dissolved SF to unreacted SF in the geopolymer structure is vital to the prediction of strength development. Due to these dual actions of the SF, irregular correlations exist between SF content and compressive strength trend, which depends on the SF used and the S/A of the source materials is reported (Park, et al., 2020).

The optimal SF dosage for strength development of geopolymers is based on the silica contents required to achieve a specific, optimal Si:Al ratio. Park et al. (2020) reported an optimal Si:Al ratio = 1.67. When Si:Al values are too far below or above this value, these result in longer setting times and lower compressive strength. As such, if MK or FA based geopolymer mix designs developed with optimised Si:Al ratios are to successfully incorporate SF; then silica from other sources must first be reduced to preserve the Si:Al ratio and achieve maximum performance. This can be achieved by diluting silicate-based activating solutions or blending with precursor powders that possess lower silica contents, such as GGBS or iron silicate (IS).

2.4.7 Novel geopolymer precursors from waste materials

IS fines are produced during copper manufacturing and can become pozzolanic if processed in a similar manner to GGBS. Hence, the CO₂ emissions and embodied energy associated with IS are anticipated to be similar to GGBS. Typical composition data for IS is provided in Table 2.3 (Aurubis, 2017). IS contains lower silica contents than MK or FA (Table 2.2) and as such its incorporation into MK or FA based geopolymers can be used to reduce precursor silica content, control the Si:Al ratio and allow optimum strength development for ternary precursor blends containing SF.

The use of locally sourced aluminosilicate materials has the potential to significantly reduce embodied energy and CO₂ for geopolymer cements. Pozzolans containing large proportions of amorphous material (i.e. high specific area) will exhibit high levels of reactivity (Cabrera and Frias Rojas, 2001).

McIntosh (2014) stated that due to the difficulties in obtaining a consistent source of FA, the high cost of MK and long transportation distance between the kaolinite mine and processing facility, low purity lateritic clays are an attractive alternative source of aluminosilicates, which are common worldwide. A suitable source was identified in the lithomarge layer (5-25m depth) of the County Antrim Lava Group's (Northern Ireland) inter-basaltic formation, which has been exposed by historic mining in many local basalt quarries. This local resource offers real potential as a low cost geopolymer precursor for Northern Ireland to help boost adoption here; whereby SEM, energy dispersive x-ray (EDX) analysis and XRD confirmed the amorphous and geopolymeric nature of the binder produced (McIntosh, 2014).

The world's first large scale production facility for geopolymer cement was opened in August 2016, in Northern Ireland, by Banah UK Ltd to utilise this source of aluminosilicate precursor and produce 200,000 tonnes per year of BanahCEM (CIOB, 2016). The chemical composition of the iron rich aluminosilicate precursor powder, Banah A, is given in Table 2.2 which shows the same oxides are present as in PC, MK, FA and GGBS but in differing proportions (Kwasny, et al., 2016). The material is fired at 750°C and ground to increase reactivity, with significantly lower CO₂ emissions from cradle to gate manufacturing than PC fired at 1450°C (0.184 vs 0.912 kgCO₂/kg) (McIntosh, 2014; Jones, 2019).

The group aimed to supply 3rd party manufacturers with commercially available geopolymer cements. However, Banah UK Ltd have ceased trading, leaving a gap in the local market for these materials (CIOB, 2016).

2.4.8 Alkali activators for geopolymers

The most financially and environmentally expensive component of a geopolymer is the alkali reagent. These are typically used in solution form and can include one or a combination of products such as NaOH, KOH and Na₂SO₃ (Mustafa al Bakri et al, 2011).

Zhang et al (2017) found that the difference in dissolution tendency between Na⁺ and K⁺ based activating solutions produced different geopolymeric structures and affected the compressive strength of MK geopolymers. Na promoted higher strengths at the same Si:Al ratio and cation concentration due to excessive unreacted MK in the K⁺ activated geopolymers. This occurred due to the lower dissolution tendency of K⁺ and that Na⁺ activated geopolymers contain more continuous monolithic structures and extensive crosslinking; both of which provide additional strength. The compressive strength was improved by using Na or K silicate solution as opposed to Na or K hydroxide, as this increased the number of stronger Si-O-Si bonds present (Zhang et al, 2017).

K silicate based activating solutions are double the price of their sodium silicate counterparts per litre (Davidovits, 2017). However, given that geopolymer mixtures only require half the amount of K silicate compared with Na silicate reagents, their costs are similar. Due to the fact Na silicate is much more widely used, its costs have already been reduced via economies of scale. With increased future use and the resulting cost reductions, K-based reagents will likely become the most cost-effective option (Davidovits, 2017).

2.5 Mixture proportioning of Geopolymers

One of the main challenges for commercialising geopolymer cement as a replacement for PC is the lack of recognised mix design methodologies for producing concretes with specified values of compressive strength and/or workability.

While many studies have investigated a range of geopolymer cement/concrete mix designs, the importance of mix parameters on compressive strength has not been fully quantified (Lahoti, et al., 2017). The design of these mixes depends on mixing a suitable activating solution with an alumina-silicate precursor and enough free water to facilitate monomer transport and allow full geopolymerisation. Several methods can be adopted to design mixes, including the use of constituent oxide ratios or factors such as liquid/solid ratios with oxide ratios fixed (Aughenbaugh, 2015). The most important and well known of these oxide ratios is the silica (SiO_2) to alumina (Al_2O_3) ratio, which is known to directly affect geopolymer concrete mechanical strength and microstructure. Other common ratios used include Na_2O or K_2O (activators)/ Al_2O_3 , $\text{H}_2\text{O}/\text{Na}_2\text{O}$, $\text{CA}:\text{Si}$ and $\text{Na}_2\text{O}/\text{SiO}_2$ (Davidovits, 2013; Austroads, 2016). The relative significance of these ratios to strength performance is unclear in the literature, due to the variation in curing and activation techniques and the ranges of pozzolanic precursors used. This research will attempt to better ascertain the significance of various mix parameters on performance.

Most studies on geopolymer mix design have focussed on specific binders and mixture compositions, most commonly FA systems that tend to require heat curing – thereby making them of limited use for ambient cured systems, which have the greatest potential for reducing embodied CO_2 . Furthermore, most geopolymer cement studies have used Na-based activating solutions, with very few using only K-silicate activation and even fewer studies that focus on the specific mix design of these materials (Austroads, 2016; Timakul et al, 2015)

Previous research on mix design methods has focussed on single proportioning ratios such as silica/alumina (S/A), activating solution to binder powder (A/B) or liquid to solid (L/S). This approach is analogous to the water/cement ratio in PC-based concrete (Austroads, 2016). Other studies have used multiple parameters synergistically to create empirical formulas and neural networks to predict strength (Wilson, 2015; Diaz-Loya, et al., 2013-b; Diaz-Loya, et al., 2013-a). As such, these methods are of little relevance to wider groups of geopolymer binder systems and K-silicate activation. Many methodologies are only suited for analysing consistent source materials such as MK or GGBS, as the inherent variability in composition of FA complicates the process (Aughenbaugh, 2015). Controlling the proportion of each pozzolanic precursor to achieve specific ratios allows customisation of the geopolymer properties (Austroads, 2016).

Figure 2.5 shows how the chemical structure and material behaviour evolves in geopolymers with increasing Si:Al ratios. At low Si:Al ratios (<1) the material is highly crosslinked with a 3D structural order and therefore brittle and relatively weak. As the Si content increases the degree of crosslinking is reduced, with more 2D polymeric structures created and fire-proof, rubber like materials formed (Si:Al >20) (Davidovits, 2002).

Geopolymer concrete designed for compressive loading is optimised with Si:Al ratios of ~ 2 (Geopolymer Institute, 2006), but for cladding applications flexural strength is vital. Optimal values for panel creation that provide a suitable compromise between the two values will likely use higher Si:Al ratios. Silica rich materials such as SF are often added to increase this ratio and therefore the theoretical strength of geopolymers. As Si:Al dictates the molecular- and nano-scale structures formed during geopolymerisation, theoretically there should be a direct correlation between silica content and strength due to increasing quantities of stronger Si-O-Si bonds until the loss of 3D ordering (Si:Al >15) (Kim, 2012). With that said, owing to other impacting mixture proportioning

parameters such as L/S or activating solution composition, optimum levels of S/A reported by researchers vary.

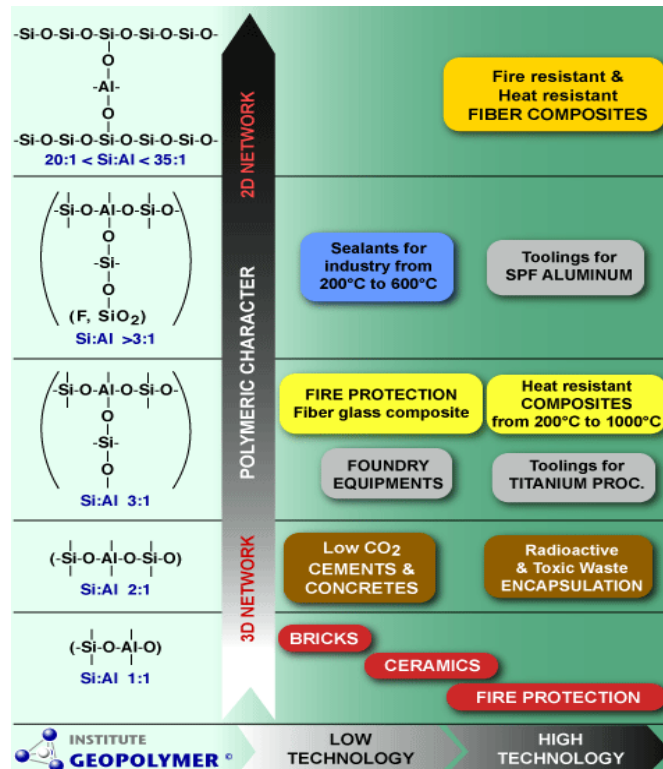


Figure 2.5. Effect of Si:Al ratio on geopolymer structure, behaviour, and applications (Davidovits, 2002).

The current literature reports many different Si:Al ratios to produce the highest compressive strength. Kim (2012) determined that MK geopolymers with a Si:Al ratio below 1.4 are very porous and provide little strength. When this figure reached 1.65 a large increase in compressive strength was reported, which can be attributed to the development of a more homogenous microstructure. An optimal ratio for compressive strength development was found to be approximately 1.85. Any higher ratios resulted in defects of unreacted MK.

Duxson et al. (2007) reported this optimum Si:Al ratio to be slightly higher at 1.9 for MK geopolymers, whereas Silva et al. (2007) reported 1.7 and Rowles and O'Connor (2009) a ratio of 2.5. This variance is to be expected, due to the large number of possible

components, parameters and mix designs for geopolymers. It is very unlikely that research groups use the same designs.

Fletcher et al. (2005) adopted the same approach as Barbosa et al. (2000) in defining geopolymer mix designs based on molar ratios of SiO_2 to Al_2O_3 (S/A). A geopolymer made from MK alone would have an $\text{S/A} = 2$. However, in atomistic terms it would be a polysialate with $\text{Si:Al} = 1$. Fletcher et al. (2005) used Metamax as the primary precursor with additions of amorphous alumina and very fine amorphous silica to create both high and low S/A ratio mixes and tested their resultant engineering properties. High alumina samples ($\text{S/A} = 0.5\text{-}2$) set and hardened, but XRD showed significant crystalline phases such as gibbsite, thermanatrite and a zeolite-like phase of sodium aluminosilicate hydrate. No evidence of the expected amorphous structure was present at the 0.5 ratio. As the ratio increased to 1, amorphous peaks began to appear in the XRD data, but crystalline phases remained. When $\text{S/A} = 2$, the amorphous phase was predominant with only a single peak remaining, which represented a zeolite-like structure. These samples set at ambient temperature but did not resemble geopolymers in many aspects, including not providing comparable strength and containing octahedral (not tetrahedral) sites under visible Al^{27} NMR. These materials were also found to contain both Al and Si rich phases visible under Si^{29} NMR as opposed to the broad spread of Si expected in geopolymers. Instead, the samples formed several discrete compounds rather than a single tetrahedral aluminosilicate structure.

The high silica ($\text{S/A} = >2\text{-}300$) samples exhibited considerable variation in setting and hardening behaviour; whereas samples with a ratio <24 set in a consistent way. For samples with $\text{S/A} >30$, the material became increasingly rubber-like - thereby limiting the ability to measure meaningful crushing strength data due to large deformation. This change in failure mode is a very interesting property, although Fletcher et al. (2005) highlighted that no explanation exists in the structural parameters to explain this

behaviour. Based on Figure 2.5, it would seem evident that the lower level of crosslinking and more 2D structure would have this effect at higher S/A ratios. XRD and NMR data show much more characteristic amorphous geopolymer structures at this level of silica content compared with the crystalline formations below this S/A range.

To create MK geopolymers with a desirable microstructure and strength, Si:Al ratios should be 2-24, whereby a ratio of ~ 16 is expected to produce the highest strength (Fletcher et al., 2005). In terms of atomic Si:Al ratios previously used, this equates to a value of 8 – over four times greater than optimum values reported by other researchers.

The adaptability of geopolymer chemistry to a range of materials is a great advantage for future adoption in various engineering applications. Augenbaugh (2015) stated that development of systems to effectively proportion geopolymers for optimum property development is one of the critical path points for its widespread adoption. Using the S/A ratio alone allows the correct prediction of the strength of 6/8 FA geopolymers, which was more significant than the Na_2O or K_2O (activators)/ Al_2O_3 ratio. When this method failed, it was attributed to factors unaccounted for in the equations, such as particle size and vitreous content. Hence a S/A ratio below 4.3 was recommended as mixtures containing higher ratios possessed significantly lower compressive strengths. While this is much closer to the findings of Fletcher et al. (2005), this value still highlights the great variation in reported optimums across the literature. To compare MK and FA systems, XRD must be used to identify the reactive content of the FA for inclusion in calculations.

Timakul et al. (2015) investigated the effects of Si:Al on the compressive strength of Class C FA and MK geopolymers. These were activated with a NaOH, Na_2SiO_3 and water mixture at a ratio of 1:1:4. The samples were cured at 750°C for 24, 48, 72 and 96 hours before a further 28 days at ambient temperatures. Density of the samples also increased with curing time, whereby the most successful mix design was cured at 750°C for 96

hours, had a S/A ratio of 2.65 and a compressive strength of 40 MPa. The compressive strength was observed to increase from 32 to 40 MPa when the S/A ratio increased from 2.6-2.65, thereby suggesting that marginal differences in proportioning had a significant impact on the resulting strength properties. For S/A ratios >2.65, the resulting compressive strength was observed to degrade. An improved understanding of the nature of this sensitivity is required to ensure the commercial use of FA and MK geopolymers as low carbon construction materials.

Empirical correlations have been developed to predict specific material properties such as strength for a wide range of geopolymer mix designs. Diaz Loya et al. (2013a&b) proposed a new correlation for geopolymers comprising precursors activated with NaOH/Na₂SiO₂, cured for 24 hours at 23°C then 72 hours at 60°C, and finally 24 hours at 23°C. The correlation was based on the reactive oxide content of FA, loss on ignition and mean particle size distribution; all of which strongly affect reactivity. Accurate predictions were reported for 6/8 samples, with those that failed due to similar reasons for the Si:Al predictions. The correlation, given below (Equation 1), was successful in predicting the strength of FA geopolymers ($R^2 = 0.78$, predicted $R^2 = 0.73$). The most influential factor in compressive strength development was mean particle size (d_{50}), followed by reactive Al₂O₃ content, LOI, reactive SiO₂ content and reactive CaO content. Predicted vs actual values from validations (Figure 2.4) shows prediction accuracy is relatively consistent across the range of strength values and achieves a level of accuracy expected from an R^2 value of 0.73.

$$f'c = -3.62 + 0.59 * RSiO_2 + 3.35 * RAl_2O_3 - 0.48 * RCaO - 0.74 * d50 - 4.39 * LOI (N/mm^2) \text{ (Equation 1)}$$

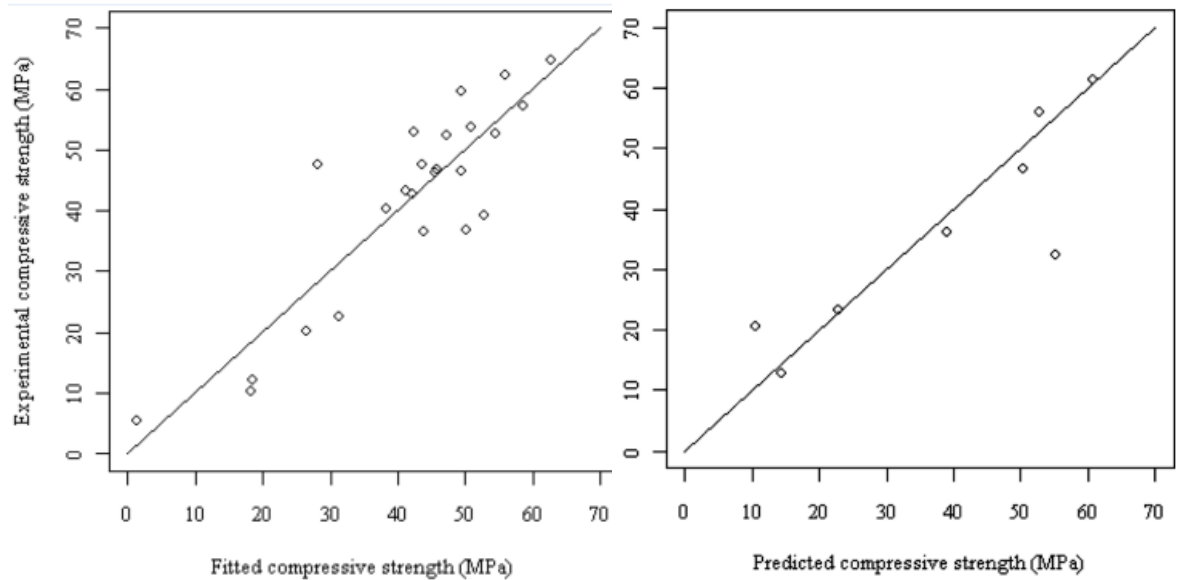


Figure 2.6. Predicted vs measured responses for compressive strength (MPa) of two groups of FA geopolymers (Diaz-Loya, et al., 2013-a).

The amounts of Network Modifying Elements (NME) (i.e. Ca^{2+} , Mg^{2+} , Na^{+} , K^{+}) present in Class F FA influence the compressive strengths of the geopolymer created (Aughenbaugh, 2015). These elements balance the negative charge in tetrahedral aluminium allowing it to take on 4-fold co-ordination. This provides greater solubility than the 6 co-ordinated state of an AACM it would otherwise be in (Davidovits, 2013; Davidovits, 2017). If there are any remaining NMEs present, they can alter the glass structures of FA by bonding with the oxygen and preventing it from creating a bridge between adjacent SiO_4 tetrahedra. The presence of these Non-Binding Oxygens (NBOs) therefore increases reactivity. This method does not consider vitreous content, distribution of NMEs in the glassy phases, particle size or the potential contribution of calcium. As such, it must be more fully developed before being used to form precise predictions (Aughenbaugh, 2015).

A ternary diagram was created by Duxson and Provis (2008) based on the relative amounts of silica, alumina and NMEs in FA. Figure 2.7 illustrates that compressive strength typically increased with NME content and alumina content. Oh et al (2015)

examined a range of Class F FAs and the resulting compressive strength, stating that NME content was the best predictor of compressive strength. A graph plotting this strength against NME content had an exponential curve ($R^2=0.952$). The ratio of NBO to tetrahedra (NBO/T) has also been successfully used to predict the strength of PC concrete with FA (Bumrongjaroen, et al., 2007), and then for FA geopolymers. Diaz Loya et al. (2013b) identified a strong linear relationship between the two for 38 different high Ca FAs (Figure 2.6).

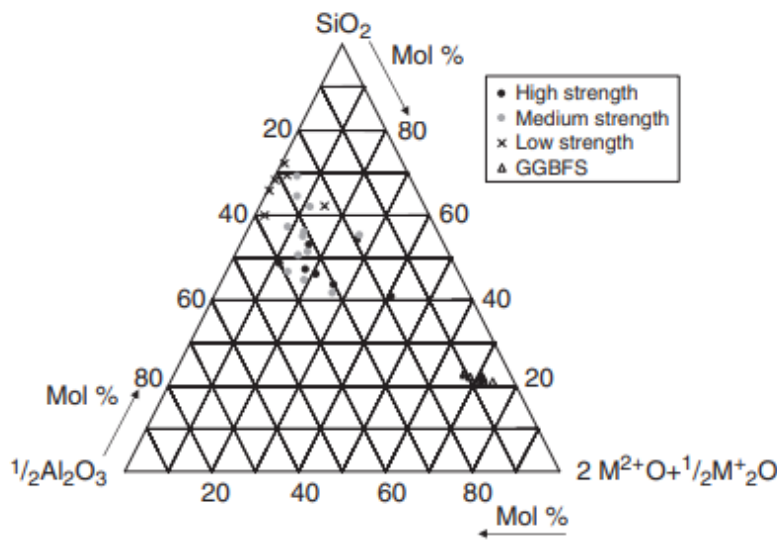


Figure 2.7. Ternary plot representing the proportions of SiO_2 , Al_2O_3 and NME's
(Duxson and Provis, 2008).

$$\frac{NBO}{T} = \frac{2(\text{Na}_2\text{O} + \text{K}_2\text{O} + \text{CaO} + \text{MgO} - \text{Al}_2\text{O}_3)}{\text{SiO}_2 + \text{Al}_2\text{O}_3 + \text{Fe}_2\text{O}_3}$$

(Equation 2)

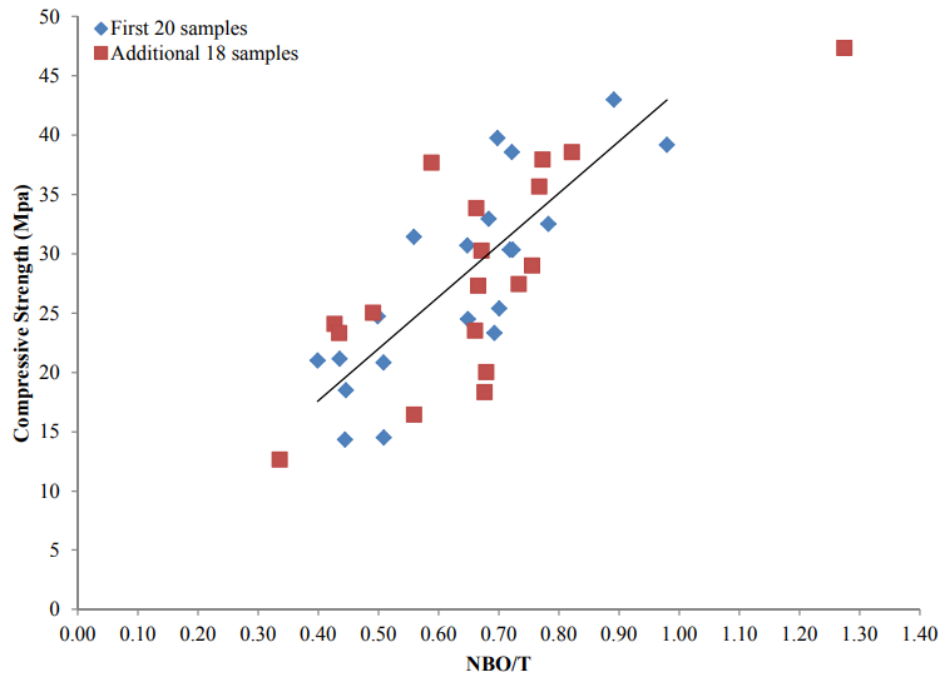


Figure 2.8. NBO/T vs compressive strength for 38 FA geopolymers (Diaz-Loya et al., 2013b).

Another ratio reported in the literature to significantly affect strength development in geopolymers is the L/S ratio. This parameter is reported to be analogous to the water/cement ratio in PC concretes (Austroads, 2016). A low L/S ratio is reported to create a high viscosity slurry and high strength product. If water content is too low, a lack of paste fluidity will begin to hinder monomer transport and reorganisation during geopolymerisation. This will result in low strength materials with unreacted aluminosilicate phases and low levels of binder formation. A high L/S ratio has been found to be associated with low viscosity, long reaction and setting times, and generally lower strength (Heah, et al., 2012). Zuhua et al. (2009) stated that high L/S ratios could accelerate the dissolution process but was not beneficial to the reorganisation process at high concentrations of NaOH activator.

Water does not become part of the geopolymer gel structure, but is stored in micropores and significantly decreases the mechanical strength. Thus, creating an optimally high strength geopolymer mix design involves finding a L/S level that provides just enough

fluidity to allow full monomer transport and reorganisation, with as little excess as possible. Heah et al. (2012) stated that for MK geopolymers, an L/S ratio = 1 produced the highest compressive strength.

Water reducing or superplasticising admixtures are not designed for use in geopolymers since they are attacked by highly alkaline solutions, causing rapid degradations in engineering performance. Nematollahi and Sanjayan (2014) reviewed the effect of available superplasticisers (SP) on GGBS and FA based geopolymers, corroborating the correlation between SP content and susceptibility to alkali attack.

In general, polycarboxylate SPs are the most effective type for increasing flowability in NaOH and Na_2SiO_3 activated FA geopolymers; whereas NaOH activated GGBS geopolymers exhibited highest flowability using naphthalene-based SP systems. In general, their use slightly decreased the compressive strength but, in some cases, slightly increased the flexural strength. Furthermore, it is difficult to predict the effect of SPs on FA based geopolymers due the inherent variability of the source material (Nematollahi & Sanjayan, 2014).

2.6 Geopolymer matrix fibre composites

Geopolymer cements exhibit good compressive strength and thermal properties but weak tensile or flexural strength, which can be enhanced by fibre reinforcements. Fibre materials typically used include carbon, silicon carbide, basalt, plastics, animal derived fibres, graphene, and steel. Fibre contents vary from 0.5% by weight for short fibres to 20% for matt reinforcement systems. Fibre addition is also an efficient method of improving fracture toughness, impact absorption, resistance to deformation and flexural strength of concretes. Furthermore, fibre reinforcement suppresses brittle behaviour, limits the extent of damage caused by cracking and enhances ductility (Davidovits, 2016).

Cementitious composites have been developed to improve the toughness of the quasi-brittle base materials through micromechanical design. These can exhibit significant tensile strain capacity, typically $>3\%$ at fibre dosages of $<2\%$ by volume. Comparing this strain capacity to that of ultra-high strength concrete, which is only $0.3\text{--}0.7\%$, demonstrates the effectiveness of these materials (Choi et al, 2012). Al-Majidi et al. (2017) reported that the mechanical performance of fibre reinforced cementitious composites depend on many factors. These include fibre properties such as their composition, strength, aspect ratio, Poisson's ratio and shape, as well as matrix properties such as strength, shrinkage, and stiffness. However, the friction and physiochemical bonding developed between the fibre and the matrix components is the primary driver of composite action and dictates composite performance.

Strain hardening cementitious composites can possess tensile strain capacity over one hundred times higher than standard PC concrete through the inclusion of a small proportion of short, randomly orientated fibres (Yang et al., 2012). These composites require high cement content to develop interfacial bond strength and overcome the absence of coarse aggregate in the mix design. High cement content leads to a material with an increased heat of hydration, higher shrinkage potential and a larger carbon footprint. Bernal et al. (2012) attempted to manufacture an environmentally sustainable fibre reinforced cementitious composite using an 85% FA binder and reported reduced drying shrinkage, reduced crack width and improved tensile ductility, but a reduction in compressive strength. Choi et al. (2012) carried out a similar study and reported that FA improves bending and tensile behaviour due to stronger Fibre/Matrix (F/M) bonding.

While fibre reinforcement plays a vital role in the aerospace, automotive and biomedical sectors, the construction industry has been slow to capitalise on the potential benefits. Carbon and glass fibres are the most commonly used fibre reinforcements, with glass approximately one order of magnitude less expensive. Glass accounts for 95% of the

fibres used for reinforcement in the composite industry due to the performance / price ratio offered (Thomason and Adzima, 2001).

Hammell et al. (1998) developed a method to reduce composite costs by using alternating layers of E-glass and carbon fibre, reporting the reduction of strength to be minimal and that the E glass bonded well with the matrix and created an interlaminar plate between layers. The addition of the E glass layers to the carbon fibre increased the deflection and therefore, energy adsorption before failure. However, the flexural strength was reduced due to the much lower elastic modulus of glass compared with carbon fibres. The dual fibre composite had lower stiffness, but the strength was similar to the carbon fibre at 504 and 525 MPa respectively. The methods used show how multiple fibre types can work in unison to improve composite behaviour and reduce costs/impact.

PC reinforced with steel fibres is a commonly used material in the construction industry where the fibres act to provide post crack strength to the brittle matrix. Replacing the PC with a geopolymer cement blend would reduce the cost and environmental impact of the material and reduce the likelihood of failure due to corrosion. Ranjbar et al. (2016) studied the effects of wettability, chemical characterisation and nanometric roughness of polypropylene and micro steel fibres at dosages of 0.5-4% by volume in a FA geopolymer matrix. Results showed the steel had a strong bond with the geopolymer paste matrix as it behaved as a hydrophilic material providing significant improvements to energy adsorption and flexural strength. The 3% volume steel fibre reinforced, FA geopolymer exhibited 35 MPa flexural strength compared with 8 MPa for the polypropylene fibres.

Steel fibre reinforcement has several drawbacks, the most significant of which are high cost and environmentally unfriendly to manufacture. It is also three times as dense as concrete, therefore adding unnecessary weight to the composite and creating the possibility of corrosion (Choi et al., 2012).

Fibre-reinforced composites within a geopolymer matrix have been developed and used since 1988; whereby the most common types of fibre reinforcement include carbon and glass fibres (Davidovits, 1988). These materials exhibit excellent performances such as a high strength to weight ratio, fire resistance with non-toxic fumes and resistance to all organic solvents. This makes them ideal as a matrix material, i.e. to protect the fibres that provide the majority of the strength (Duxson et al., 2007; Callister, 2014). Many applications such as manufacturing automobile and aircraft engine components take advantage of high fire and heat resistance, whereby in applications over 200⁰C, most other organic cementitious matrix composites cannot be used. The ability of a geopolymer matrix to withstand extremely high temperatures, whilst being easy to manufacture at ambient temperatures are qualities that have previously been considered inconceivable (Davidovits, 2002)

Natalie et al. (2011) created geopolymer fibre composites from a range of fibres including glass, carbon, PVA and PVC and demonstrated that all types significantly improved the flexural strength and post crack ductility. Zhang et al. (2008) investigated the impact properties of MK and MK/FA geopolymer based extrudates incorporating PVA fibres. These materials were reported to outperform similar fibre-reinforced PC concretes and that the flexural strength and failure mechanisms varied as a function of matrix composition and F/M bond.

Aydin and Baradan (2013) investigated the effects of steel fibre reinforcement on a range of alkali-activated GGBS and SF mortars, which confirmed improved flexural toughness and reduced drying shrinkage compared with non-reinforced control samples. Bernal et al. (2012) investigated the permeability and engineering properties of GGBS geopolymers with the addition of steel fibre reinforcement. Their study reported a reduction in compressive strength when steel fibres were present. This highlighted that

the effects of reinforcement must be considered for all engineering performance properties and not just those that are of interest for the intended engineering application.

Nematollahi and Sanjayan (2014) identified two challenges associated with creating fibre composites for geopolymer cements. First, that they may require viscous liquid activators, which can be hard to safely handle, and secondly, that they may require heat curing, which can be impractical on site, costly and increase carbon emissions. Hence, Nematollahi and Sanjayan (2014) developed strain hardening geopolymer composites from FA and GGBS pastes and cured them at ambient temperatures. The material exhibited 43-52 MPa compressive strength, a tensile strain capacity of 2.6-4.2% and tensile strength of 4.3-4.6 MPa at a density of 1800-1874 kg/m³. The ambient cured GGBS based mortars achieved superior uniaxial performances compared with the heat treated or gypsum slag-based options. Slag type and curing conditions had significant effects on the fibre matrix bond exhibited by the composites. Ambient temperature curing increased the chemical bond strength on the GGBS based samples. The composites developed were characterised by 76% lower CO₂ emissions and 36% lower embodied energy than PC alternatives. Hence, the material was classified as a lightweight composite (Nematollahi & Sanjayan, 2014).

Researchers such as Davidovits (2017) have been proposing the use of more user friendly geopolymers where the alkaline activator is used at a lower molar ratio to limit corrosivity. However, Al-Majidi et al. (2017) identified that no studies have been carried on such geopolymer mixtures with strain hardening characteristics. Al-Majidi et al. (2017) used a ternary blend (FA/GGBS/SF) geopolymer activated with K₂SO₃ (molar ratio = 1.25) and reinforced with discontinuous steel, PVA and glass fibres. The effects of using a lower molar ratio on the mechanical performance and microstructure of the composite were assessed by performing compressive and flexural strength tests and SEM imaging. The research also developed a new methodology for manufacturing such composites; whereby the order of constituent mixing was: 1) precursor powder, 2) alkali

reagent and water, 3) fibres and 4) sand filler. Samples were covered with polyethylene sheets to prevent moisture loss and permit curing at room temperature. The compressive strength increased by 15-20 MPa with the steel and PVA fibres, but not with glass. The steel fibre content and aspect ratio significantly affected the compressive strength of the composites; whereby longer, straight fibres in higher dosages resulting in better compressive and tensile strength, and post-crack behaviour. The optimum mix design used 3% 13mm long fibres by volume. This mix produced 70 MPa compressive strength, the highest flexural strength and with almost 20 times higher deflection at peak load than those without fibres, and four times greater than those using 6 mm steel fibres (Al-Majidi, et al., 2017).

Lin et al. (2008) took a geopolymer matrix carbon fibre composite and investigated the effect of different fibre lengths. In the absence of fibres, the material exhibited a flexural strength of 16 MPa. With 2 mm and 7 mm fibres, flexural strengths of 62 MPa and 90 MPa were achieved, respectively. This decreased slightly to 86 MPa when using 12 mm fibres, highlighting the importance of careful fibre length selection.

Basalt fibres are a potential replacement for the steel, plastic, glass or carbon fibre options used for geopolymer composites. Basalt fibres are manufactured from the volcanic rock basalt, which is melted in a blast furnace at 1450-1500 °C and forced through platinum/rhodium crucible bushings to create fibres in a similar manner to glass fibre production. The continuous spinning process used can create short or continuous fibres and no additives or complex equipment is required for production (Fiore et al., 2015). Basalt fibres show promise due to their relatively low cost, high tensile strength, similar material density to steel-reinforced PC concrete, resistance to corrosion/chemical attack and fire, and are more environmentally friendly to manufacture compared with glass fibres – producing less toxic fumes (Sim et al., 2005; Jiang et al., 2014).

Basalt fibres have been shown to produce a strong chemical bond with cementitious matrices (1.8 times higher than would be the case for PVA fibres), with higher first crack strengths - albeit these materials show more softening behaviour after cracking (Choi et al, 2012). Furthermore, adding basalt fibres to cementitious composites promotes a more ductile failure mode, similar to glass fibres (Choi et al 2012). Past research into basalt fibre reinforced mortars and concretes has focussed on the fundamental mechanical properties of the material, such as compressive, flexural, and tensile splitting strength. The basic properties and composition of basalt fibres have been summarised by Choi et al. (2012), whereby they have a density of 2.65 kg/m^3 , tensile strength of 1773 MPa and the following chemical composition: SiO_2 (48-59%), Al_2O_3 (15-18%), B_2O (1%), CaO (6-9%), MgO (3-5%), $\text{Fe}_2 + \text{FeO}$ (7-12%) and $\text{NaO}+\text{K}_2\text{O}$ (4-5%).

Branston (2016) suggested that the same alkali attack damage that occurs to unprotected glass fibres in PC concretes also deteriorates basalt fibres, but to a lesser extent. Due to the lower alkalinity of geopolymer matrix composites ($\text{pH} = 11-11.5$) compared with PC mixtures ($\text{pH} = 12-12.5$), the addition of basalt fibres to an optimally designed, low alkalinity geopolymer matrix may reduce or eliminate the impact of alkali attack. This would mean that the use of zirconium dioxide to protect fibres would not be required and would promote more structural applications (Branston, 2016). Hence, there is the possibility of developing new high-performance basalt fibre composites with reduced fibre degradation, similar mechanical performance and a lower carbon footprint than glass fibre-based equivalents.

Hyde et al. (2017a) developed geopolymer based cladding panels with a hybrid, ambient cured binder system, comprising GGBS, SF and basalt quarry dust precursors, K-silicate activation and steel/PVA fibre reinforcement. These were designed for retrofitting existing buildings to improve aesthetics and, through the use phenolic foam and vacuum insulation, improving the thermal performance of the building exterior. Two 20 mm thick

high-strength geopolymer cladding sections were combined with 80 mm of insulation (20 mm phenolic foam board / 40 mm Slimvac insulation / 20 mm phenolic foam board) to produce a 120 mm thick panel that exhibits U-values of 0.1135 W/m²K. Compressive strengths of geopolymer mortar of 40 and 84 MPa at 24 hours and 90 days respectively were reported (Hyde and Kinnane, 2016; Hyde et al., 2017b).

2.6.1 Fibre / matrix interface bond and sizing technologies

One of the frequently overlooked aspects of fibre reinforced cementitious composites is the fibre matrix interface, which is usually controlled by fibre surface treatments such as sizing compounds (Callister, 2014).

Sizings are a 30-100 nm thick fibre coating applied for adhesion enhancement and protection during handling and when in-situ. These compounds can provide a physio-chemical bond between fibres and the cementitious matrix, even if the composition or surface of the virgin materials do not create high bond strength. A large proportion of the ultimate strength exhibited by a composite depends on the extent of interfacial bonding. Adequate bonding is essential to maximise the stress transmittance from the relatively low tensile strength matrix to the high tensile strength fibres (Downey and Drzal, 2016; Korniejeko et al, 2016).

Fibre sizing is a fundamental stage during the manufacture of glass and basalt fibres, which is one of the simplest and most cost-effective methods for promoting adhesion (Ralph, et al., 2019). Individual constituents of these aqueous compound solutions fulfil a specific function such as increasing adhesion or protection from chemical attack. Sizing agents are generally composed of an organofunctional silane coupling agent to increase F/M bond and a film former for fibre protection. They are highly customised for specific applications and therefore may also contain lubricants to reduce abrasion between the fibres, emulsifiers, wetting agents, chopping aids and antistatic agents depending on

applications and production processes. The quantity of sizing used is a carefully controlled parameter and commonly expressed as a loss on ignition figure that represents the mass of sizing agent burned off the fibre (Thomason and Adzima, 2001).

Silane coupling agents are multifunctional molecules that perform many other roles other than adhesion. Their non-coupling aspects require further understanding (Mason, 2006). Thomason and Adzima (2001) suggested that there is great scope for the development of better and more cost-effective silane agents and an improved screening method for F/M interaction to judge their effects. This is especially true for geopolymer composites where the literature is lacking in comparison to thermoset, thermoplastic and PC based composites.

Silane molecules are highly effective in providing enhanced F/M bond, but if used in isolation they will make fibres brittle and prone to damage in manufacture. Therefore, they require the use of a film forming additive to prevent this. These additives hold filaments together in a strand, protecting them from damage through fibre/fibre and processing contacts and is chosen to be closely compatible with the intended matrix material. Commonly used materials for this application include polyvinyl acetates, polyurethanes, polyolefins and modified epoxies (McMican, 2012). Many fundamental areas in the science of sizing remain unexplored. The development of sizing and composite interface science could be advanced by establishing a better understanding of molecular adsorption over short time frames from complex sizing onto surfaces, high speed dynamic wetting and spreading of sizing onto and into fibre assemblies (Thomason and Adzima, 2001).

The proportions of each constituent of the sizing solution present at any specific point along the fibre length is hard to predict, due to slight inconsistencies in application and the level of sorption by the fibre (Ivashenko, 2009). No reference material to assist in

resolving this problem is currently available. As a result, design of solutions with a small number of or single components have attracted attention as this would enable more accurate micromechanical design. Ivashenko (2009) proposed the use of a system containing only three components via the dispersion of grafted polyvinyl acetate copolymer and allyloxy methyl cellulose in water. These would still provide film-forming capabilities, adhesion and plasticiser functions, whilst maintaining its composition at a specific point of the interface that is more easily predicted and controlled. Water used in sizing cools the fibres, acts as a carrier and dilutant for the sizing compounds, thereby ensuring good coverage. The water also wets glass, helping to boost the F/M interaction and bond. Lower sizing viscosities and fibre packing density generally lead to better adhesion to the fibre with the relative level dependant on the material the sizing must displace (Thomason and Adzima, 2001).

Sizing composition is the primary parameter used by fibre manufacturers to adapt their products for different applications (Mason, 2006). No general-purpose sizings are available as they are tailor designed to provide a specific type of fibre to suit the concrete matrix material, protect the fibre during the specific production processes they undergo and control how the material behaves to suit each unique application. Specialised sizings are not yet available for geopolymer fibre composites. Great scope exists for the development of innovative sizing techniques through partnership with fibre suppliers, which could revolutionise the performance levels of the material. Ivashenko (2009) identified that the improvement of sizing systems and their creation for different specific matrix and fibre types is a major concern and represents a significant knowledge gap.

For glass and basalt fibre composites, sizing is one of the most vital components influencing the success or failure of reinforcement systems. When applying sizing to glass fibres that are being drawn at 60 m/s and chemically cooled, inconsistency in the proportions of each sizing component is expected due to selective sorption of some

components by fibres and aggregation of sizing components. Within milliseconds of the glass forming, it is coated with an aqueous mixture of coupling agents, lubricants and emulsified polymers at a dosage of 0.5-10% solids content in a water substrate. This coating takes place in under 10mm drawing distance or 0.5 milliseconds contact with an applicator. Successful sizing during manufacture should deliver an undamaged product without defects from the process, a clean-cut surface for short fibre products, low fibre fuzzing/damage during handling, high application efficiency and reduced costs.

During composite manufacture, well-sized fibres should exhibit high strand integrity with low fuzz and fines, continuous processing, successful impregnation of sizing into the fibre, good of sizing dispersal and predictable behaviour. The fibres should provide composites with high mechanical strength and thermal resistance performance, high durability and fatigue resistance, low void contents and clean surfaces with consistent colour and easy means of recycling. The reason for the composite possessing these features is due to the effects this sizing has on the interfacial bond between the fibre and the matrix; including high F/M interaction, good wetting, high levels of stress transfer and high fibre strength retention (Thomason and Adzima, 2001).

Recent technological developments have produced new sizing techniques that can improve the engineering performance of fibre composites in the future. One example is UV o-zone treatment, which increases the amount of reactive oxygen groups on the fibre surface and reduces the amount of fibre defects to enhance the fibre/matrix bond. The fibres are exposed to both oxygen and o-zone in the presence of energetic UV photons. Some surface material is removed, creating a reactive surface for the oxygen to chemically bond to. This treated surface is then able to bond strongly with either the fibre sizing or matrix (Tiwari and Bijwe, 2014). For more high-cost technology applications, such as carbon fibre composites intended for lightweight racing cars or the aerospace industry, new sizing techniques using materials such as graphene have been developed.

Zhang et al. (2012) investigated the interfacial properties of carbon fibre composites in which fibre surfaces were modified by dispersing 5% weight graphene oxide into the sizing agent. This significantly enhanced the interfacial shear strength but would be financially too expensive to implement for use in geopolymer composites intended for construction and cladding applications.

Fibres can also be treated with low molecular compounds to promote bonding between the sizing, fibres and the matrix; thereby providing F/M bonding. An example of such bonding would be an epoxy matrix system using an amine hardener to provide reactive amine groups. These chemically bond with the epoxy groups and provide high adhesive strength of 5-22 MPa (Ivashchenko, 2009).

European patent EP 25406853A1 states that glass fibres are usually sized with a silane compound, so Si-O-Si bonds are formed between the glass fibre surface, the sizing and adjacent silanol groups to create a crosslink on the fibre surface. This creates a strong bond and enhances resistance to corrosion and hydrolysis. As the stronger bonds in a geopolymer structure are also Si-O-Si bonds, this would create the potential where the fibres could be bonded to the matrix with the same strength the matrix itself is held together with; a drastic improvement when geopolymer cement mixes can have compressive strengths of over 100 MPa (Piret et al., 2013).

US Patent 20060204763 for an Al⁺ sizing for glass fibre composites has potential for use as geopolymer specific sizing. An aluminosilicate coupling agent was used, which could exhibit a chemical affinity for geopolymer matrices. This would seem more likely to form increased (-Si-O-Al-O-) bonds, which are slightly weaker but would still have the potential to provide high interfacial bond strength (Hartman et al., 2006).

2.7 Foamed geopolymers for insulation

Geopolymers can provide thermal insulation through chemical or mechanical foaming to present a promising alternative to polyurethane insulation boards typically mounted to GRC cladding. This is based on their high strength, lightweight, resistance to fire and high temperatures, and low environmental impact. However, there are currently no standard parameters or procedures for geopolymer foam manufacture; whereby each mix design is unique and optimised for locally available source materials and engineering applications (Lach et al., 2016).

Geopolymer foams have been produced with density and thermal conductivity as low as 300 kg/m^3 and 0.03 W/mK , respectively (Lach et al., 2016) and have great potential for use as insulation materials. In use, these materials are similar in form and function to the phenolic foam insulation boards commonly used in cementitious cladding systems, but have a much lower cost and carbon embodiment. These materials are also intrinsically inflammable and will compartmentalise fire risks rather than contribute to fire spread.

Geopolymer foams are most often created through two processes: endogenous foaming and mechanical foaming. Endogenous foaming uses the highly alkaline environment of the geopolymer paste to decompose chemical foaming agents such as hydrogen peroxide or aluminium powder. This reaction produces gases including hydrogen and oxygen, which can then be trapped in the paste to create a porous structure (Kaddami, 2017).

Mechanical foaming introduces pores into the paste either through the addition of a preformed foam or through mechanically mixing air bubbles into a paste containing surfactants to promote a foamed structure. The preformed foam comprises foaming agents including detergents, resin soap or hydrolysed proteins and water, and is added from a foam generator to the wet paste. Research has been undertaken on the combined use of endogenous and mechanical foaming methods, with a view to producing an enhanced

microstructure, mechanical strength and thermal resistance properties (Narayanan & Ramamurthy, 2000).

The most important factors that determine compressive strength, thermal conductivity and permeability of foamed geopolymers are the size, volume and interconnectivity of pore spaces developed. Pores present in the hardened material will include interlayer pore space in reaction products like CSH (<1 nm), gel pores in the materials structure (1-10 nm) and capillary pores between gel clusters (>10 nm). This is in addition to the air voids (1-2 mm) introduced via foaming (Nambiar and Ramamurthy, 2007).

Extensive research has been undertaken on the pore structure of foamed PC concretes and how foams affects microstructure, mechanical strength and thermal resistance properties, with several models developed to define the relationship between strength and porosity. However, it has yet to be determined whether these models are applicable for geopolymer foams. Very few models have been developed for geopolymer foams due to the complexity of geopolymer formulation. Further research on ranges of geopolymer formulations is required to understand the effect of pore characteristics and intelligently design these materials (Zhang and Wang, 2016).

The total pore volume and the percentage of interconnected open pores are both approximately inversely proportional to the compressive strength and thermal conductivity of the materials produced. The level of pore interconnectivity depends on the foaming method and agents used. Endogenous foaming by aluminium powder and hydrogen peroxide generates fewer interconnected pores than mechanical foaming with a surfactant, even at a lower total density (Masi, et al., 2014).

Pore size in foamed geopolymers is dependent on the foam dosage, foaming agent and its distribution, which significantly influences compressive strength development - especially at high porosity (where higher dosages result in larger pores of an ellipsoidal

shape). Large pores have a greater influence on compressive strength than smaller pores for the same volume. Zhang and Wang (2016) reported that critical voids (pores $>100\text{ }\mu\text{m}$) were the primary factor influencing the strength of geopolymer foams. The shape of pores remained relatively constant and had little influence on mechanical properties.

A geopolymer foam that is optimised for thermal insulation applications will comprise a large volume of small, closed, uniform, spherical pores, which act to limit heat transfer through the material. Many methods have been employed to achieve this, such as a gel templating procedure similar to the manufacture of aerogel. A gel/liquid structure is created and doped with hydrophobic compounds. The pore liquid is then exchanged with a solvent, which is then slowly expelled under controlled pressure in an autoclave. This allows customisation of pore structure and reduces the effects of capillary drying forces and the likelihood of pore collapse or coalescence (Glad and Kriven, 2014). Other researchers have included porous or hollow aggregate, such as expanded perlite or polystyrene and microspheres in their paste to create sections of the materials with controlled porosity (Duan et al., 2017).

Geopolymer foams based on perlite have been created with densities and thermal conductivities as low as 200 kg/m^3 and 0.03 W/mK ; approximately ten times lower than what can currently be achieved in FA foams. This is similar to the level achieved by Rockwool based insulation, but higher than more effective board systems providing suitable insulation for buildings at approximately 100 mm thickness. This highlights the importance of material selection for ensuring successful development of foamed geopolymers (Szabo and Mucsi, 2016). TROLIT is a commercially available inorganic geopolymer foam insulation created using peroxide and perborate foaming agents and a recycled silica/alumina source. It has a density of $200\text{--}800\text{ kg/m}^3$, thermal conductance of $\geq 0.037\text{ W/mK}$ depending on density and a pore parameter range of 0.5–3.0 mm (Lach et al., 2016).

Zhang and Wang (2016) concluded that geopolymer foams are a greener alternative to PC foams for construction and insulation applications and gave two important guidelines for creating these materials. Firstly, the foaming method employed must be able to produce fine bubbles which should be kept stable during mixing to avoid coalescence into larger pores. Secondly, this state can be achieved by introducing foam stabilisers or adjusting the setting behaviour of the geopolymer. One complication in the development of geopolymer foam insulation is that the foamed paste must be suitably viscous to trap gas bubbles throughout the geopolymerisation process, until the porous structure is retained by hardening. As geopolymer concretes have lower yield stresses compared with PC concretes, their composition must be carefully controlled. Methods used to combat this problem include using additives or heat to increase the materials viscosity and hardening rate or delaying foaming or foam addition until a suitable viscosity level is reached (Kaddami, 2017). For geopolymer pastes, it has been shown that high L/S ratios and paste viscosity increase the materials foaming-ability but reduces its ability to retain its porous structure (Masi et al., 2014).

2.8 Environmental impact of Geopolymers

Since the mid-1900s PC production globally has experienced exponential growth. PC manufacturing is estimated to be responsible for producing 5-7% of global CO₂ emissions, whereby its usage continues to grow by 10% each year (Austroads, 2016; Benhelal, 2013). This is largely being driven by the growth of the Chinese economy and associated rapid large scale urbanisation, which necessitates the construction of major civil engineering infrastructure networks. China consumed 2.23 billion tonnes of cement in 2018, which represents 54% of the global total. This equates to an estimated 4,460,000 m³ of concrete (Statista, 2020; World Cement Association, 2019).

CO₂ accounts for around 65% of the global warming effect due to anthropogenic activities. Hence, it is vital to reduce CO₂ emissions to alleviate the catastrophic effects

of climate change. The manufacture of PC releases CO₂ in three major ways; 50% from the de-carbonation of limestone, 40% from the burning of fossil fuels used to heat the kiln (using operating temperatures of 1000 – 1200°C) and 10% from generating the electricity required (Srinath and Prabha, 2016). Geopolymers offer the ability to eliminate the first of these two stages of CO₂ release as they do not contain limestone and can be created from secondary materials generated from existing processes. Table 2.4 shows the carbon embodiment of the average UK PC compared with values from geopolymer precursor materials. It is evident that significant carbon savings can be made and that secondary materials have the greatest potential. MK, a popular option, is calcined at temperatures less than half the 1450⁰C required for PC production to form alite. As such, MK has significantly lower embodied carbon than PC (Yunsheng et al., 2009). Geopolymer cement production also does not require as much financial investment in plant equipment. Thermal processing of common, naturally occurring pozzolanic materials presents a multitude of precursor feedstocks that are available worldwide (Davidovits, 2015).

Table 2.4. Embodied carbon content of pozzolanic precursor materials

<i>Materials</i>	<i>PC</i>	<i>MK</i>	<i>GGBS</i>	<i>SF</i>	<i>FA</i>	<i>IS</i>
Carbon embodiment (kgCO ₂ /kg)	0.912 ⁽¹⁾	0.347 ⁽²⁾	0.032 ⁽³⁾	0.064 ⁽⁴⁾	0.004 ⁽⁵⁾	0.057 ⁽⁴⁾

⁽¹⁾ Jones (2019); ⁽²⁾ Komkova and Habert (2023), ⁽³⁾ EPD Ireland (2019),
⁽⁴⁾Values provided by Elkem and Aurubis, ⁽⁵⁾McGrath, T et al (2018)

There are many methods currently used in industry to quantify the carbon footprint of materials; the most popular of which is Life Cycle Assessments (LCA) – which considers all of the material / energy inputs and products / emissions outputs for each step of the manufacturing process. There are three approaches that can be taken for performing LCA analyses: ‘cradle-to-gate’, ‘cradle-to-grave’ and ‘cradle-to-cradle’. ‘Cradle-to-gate’ LCA’s calculate and report the carbon required for all processes required to manufacture the final product, including acquiring the raw materials, transport to the manufacturing

facility and any processing required before the product reaches the factory gate. 'Cradle-to-grave' LCA's go a step further and quantify the carbon footprint arising from the whole life of the product, including installation, maintenance, demolition, removal and disposal. (Clearloop, 2021).

The first full cradle to grave LCA of the CO₂ emissions from geopolymer cement production was proposed by Habert at the 2010 Geopolymer Camp, who suggested that geopolymer concretes generate more CO₂ emissions than PC concretes, due to the use of Na silicates. This was then clarified in greater detail by Habert et al. (2011), which considered numerous mix designs. However, most of the mixtures considered were identified by Davidovits (2017) as AACMs and that many methodological errors had been identified in Habert et al.'s (2011) LCA methodology. Furthermore, Habert et al. (2011) stated that the data used for the Na silicate solution was sourced from Fawer (1999), who considered a 100% pure sodium silicate. However, Habert et al. (2011) considered alkali silicate activators that were often used in a 0.55:0.45 ratio with water. It can therefore be reasonably stated that the CO₂ emissions calculations published by Habert et al. (2011) could be reduced by ~50% before being added to the data for the rest of the components (Davidovits, 2013). This error has been repeated in other papers attempting LCAs of geopolymers, such as Turner and Collins (2013). As stated by Austroads (2016), Habert et al. (2011) did not consider FA to be a by-product of coal fired power stations and attributed CO₂ emissions from electricity generation to the material. This further discredited their earlier assertions.

Jones (2019) reported that a MK750 and Na silicate geopolymer mix used five times more alkali silicate than would typically be required today. This formed the basis of the claim that geopolymer cement production produced twice as much CO₂ as PC. The mix specified was also considered a binder and not a cement, due to its inability to harden at ambient temperatures. When compared with an epoxy resin, there was great potential for

CO₂ emissions savings using this blend. Carbon embodiment of 286 vs 6663 kg CO₂/1000 kg was expected for the geopolymers and epoxy resin, respectively (Davidovits, 2015; Jones, 2019).

McLellen et al. (2011) performed an analysis of the CO₂ emissions from the average geopolymer concrete mix created in Australia and compared this with a PC mix, using accurate values for the Na silicate solution. A CO₂ emissions reduction of 44-64% was achievable, depending on the materials used. However, the financial costs were 7-39% higher. These figures were greatly influenced by the large transportation distances required for geopolymeric materials in Australia compared with PC, due to the less developed infrastructure. A similar situation would be apparent in other large countries such as the USA, but less so in smaller countries such as the UK and across Continental Europe. With increased usage, supply chains and economies of scale will help to reduce costs and carbon embodiment (Davidovits, 2015). Davidovits (2015) stated that datasets from local and specialised environments were being generalised for the whole world and suggested using two values, with the other being where travel distances are estimated for 5-10 years after industrialisation begins.

It is apparent that most published literature on LCAs for geopolymer cements were actually for AACMs, with the scientific community not understanding the differences and neglecting to research the patent literature available for geopolymer cement (Davidovits, 2017; Austroads, 2016). LCAs of available proprietary geopolymer cement blends are exceptionally rare as this information can be commercially sensitive. One produced by Start2see (2012) for E-Crete, a GGBS/FA/alkali silicate-based geopolymer cement, found that using this product could reduce CO₂ emissions by 62-66% and embodied energy by 80% against a comparable PC mix.

Based on the above studies and reported data, a geopolymer-basalt fibre composite cladding panel could potentially be created with similar design specifications to GRC, without the need for AR glass fibres, polymeric additions or superplasticising admixtures. With careful design, the composite could have embodied energy of just 54 MJ/m² and an embodied carbon content of 20.4 kgCO₂E/m². For comparison, a standard bulk concrete cladding panel would have 1057.5 MJ/m² embodied energy and 171.6 kgCO₂E/m² embodied carbon, whereas the GRC panel would have 624 MJ/m² embodied energy and 64.2 kgCO₂E/m² embodied carbon. As such, geopolymer cladding panels, if used to replace bulk concrete cladding, could achieve a 95% reduction in embodied energy and an 88% reduction in embodied carbon. If used to replace GRC building cladding, it has the potential to reduce the embodied energy by 91% and embodied carbon contents by 68%. However, these figures are an approximation. Once the embodied energy and carbon required to produce the basalt fibre reinforcement for such a composite are considered, the energy and carbon savings may not be as significant (RIBA, 2020; Jones, 2019).

2.9 Summary and knowledge gaps

Cementitious cladding systems are required to possess high engineering performances (e.g. strength and fire resistance), with the smallest possible carbon footprint. Geopolymers offer a low impact alternative to PC-based claddings with comparable engineering performances and up to a 90% reduction in embodied carbon. Despite these benefits, a key barrier to the commercial use of geopolymers and AACMs is the lack of recognised mix design methodologies. A consistent method capable of producing materials with specified values of compressive strength and/or workability, that is applicable to most precursor sources, must be developed to drive forward its commercial use in the construction industry.

Against this background, one of the aims of this research is to produce a simplified preliminary mix design method, which allows easy selection of geopolymer and AACM mortars by industrial practitioners who are more familiar with performance-based specification of PC cement systems. This research also aims to create a methodology that will enable strength prediction for K-silicate activated geopolymer mortars comprising a wide range of binder combinations and mix parameters. In this way, the intention is to drive forward the adoption of these systems as a high performance, low impact alternative to PC-based materials such as GRC in building cladding components.

As geopolymers undergo brittle failure and possess low tensile strengths, randomly orientated fibre reinforcement is often incorporated. Basalt fibres have several technical advantages over glass fibres for this application such as lower costs and lower carbon embodiment. Suitable sizing on reinforcement fibres is vital for creating a strong interface bond and composite. However, it is currently unclear whether sizing developed for PC composites would perform similarly in a geopolymer composites or the optimal fibre type, geometry and dosages for maximum flexural strength.

Geopolymers can also serve as a low carbon alternative to traditional insulation boards through either mechanical foaming, endogenous chemical foaming or a combination of the two. The choice of method, materials and dosages significantly affects the pore structure achieved and therefore the strength and thermal conductivity exhibited by the final product. The optimal method, mix designs, rheology and processes for creating these foams in geopolymer pastes have yet to be identified.

There are no recognised mix design methodologies capable of producing foamed industrial waste-based geopolymeric material of specific strength, density or thermal conductivity and one must be developed. Current research in the field highlights the need for this research and similar attempts made by other researchers have shown great promise.

Chapter 3 – Materials and testing methodologies

3.1 Introduction

This chapter describes the methods and materials used throughout this thesis to fulfil the research aims and objectives. Where possible, readily available materials and reputable test methodologies (BS-EN, ASTM etc) have been used to maximise the reproducibility and impact of this research. This research was carried out in four main stages, which are outlined in Figure 3.1.

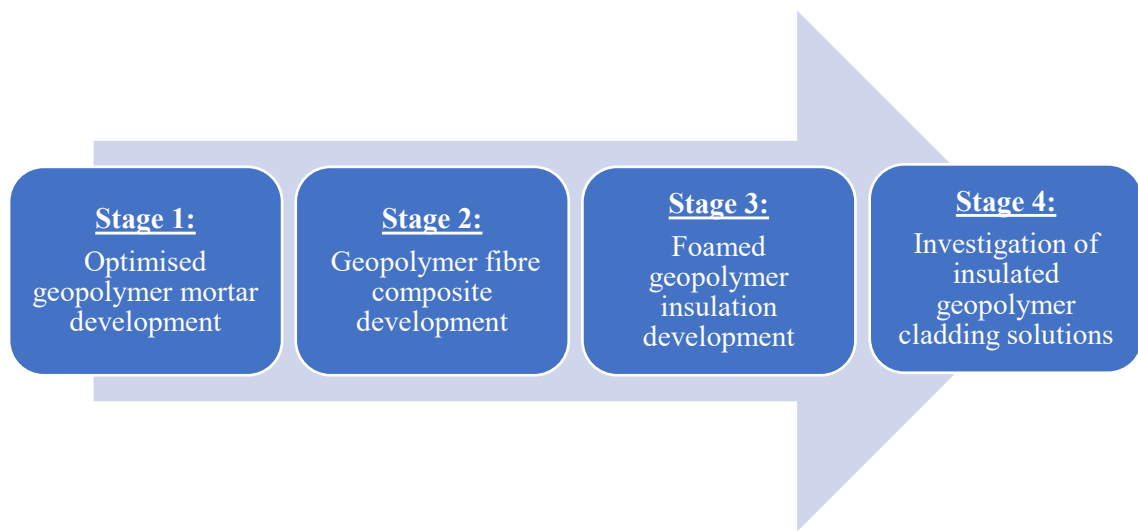


Figure 3.1. Flow chart illustrating research stages.

3.2 Materials

3.2.1 Geopolymer precursors

Five precursor materials were investigated to facilitate national/international commercial use of the methodologies presented and beneficial reuse of prevalent local waste streams. Metastar 501 MK from Imerys UK was used as the primary pozzolanic precursor due its commercial availability, consistency, high amorphous content, rapid dissolution and geopolymerisation at ambient temperatures (Provis et al., 2015).

To reduce the environmental footprint of the MK precursor, whilst providing reduced setting times, increased strength and flow values (Austroads, 2016), industrial by-products were used to partially or completely replace MK. These included GGBS from ECOCEM Ireland, SF from Elkem, FA from Kilroot power station in Northern Ireland and IS fines from Aurubis (Bulgaria). IS is a low impact by-product of copper production and novel in its usage as a geopolymer source material. GGBS geopolymers require less alkali reagent content and, therefore, have lower environmental impact than MK systems which have a lower Si:Al ratio, necessitating more reagent to be used for full dissolution to occur (Komnitsas, 2011). SF has been shown by Okoye (2016) to increase the Si:Al ratio of the binder and thereby promote increased strength development between 7 and 28 days.

The mineralogies (from XRF data published by Wilkinson, 2018) and published embodied CO₂ values (derived from cradle to gate LCA, according to BS EN 15804) for the precursors considered are presented in Table 3.1, together with typical values for PC for comparative purposes. Particle size distribution data is provided in Table 3.2, which shows that SF is finer than the other precursors.

Table 3.1. Composition and environmental impact of source materials used in this study.

Material	Chemical composition (% by mass)				Embodied carbon (kgCO ₂ /kg)
	SiO ₂	Al ₂ O ₃	CaO	Fe ₂ O ₃	
PC	20	4.6	64.6	3.8	0.92 ⁽¹⁾
MK	55	40	0.3	1.4	0.347 ⁽²⁾
GGBS	36.5	10.4	42.4	0	0.032 ⁽³⁾
SF	96	0.8	0.5	0.8	0.064 ⁽⁴⁾
FA	57	24	3.9	6	0.004 ⁽⁵⁾
IS	27	3.2	1.8	46	0.057 ⁽⁴⁾

(Wilkinson, 2018), ⁽¹⁾ Jones (2019); ⁽²⁾ Komkova and Habert (2023), ⁽³⁾ EPD Ireland (2019), ⁽⁴⁾ Values provided by Elkem and Aurubis, ⁽⁵⁾ McGrath, T et al (2018) .

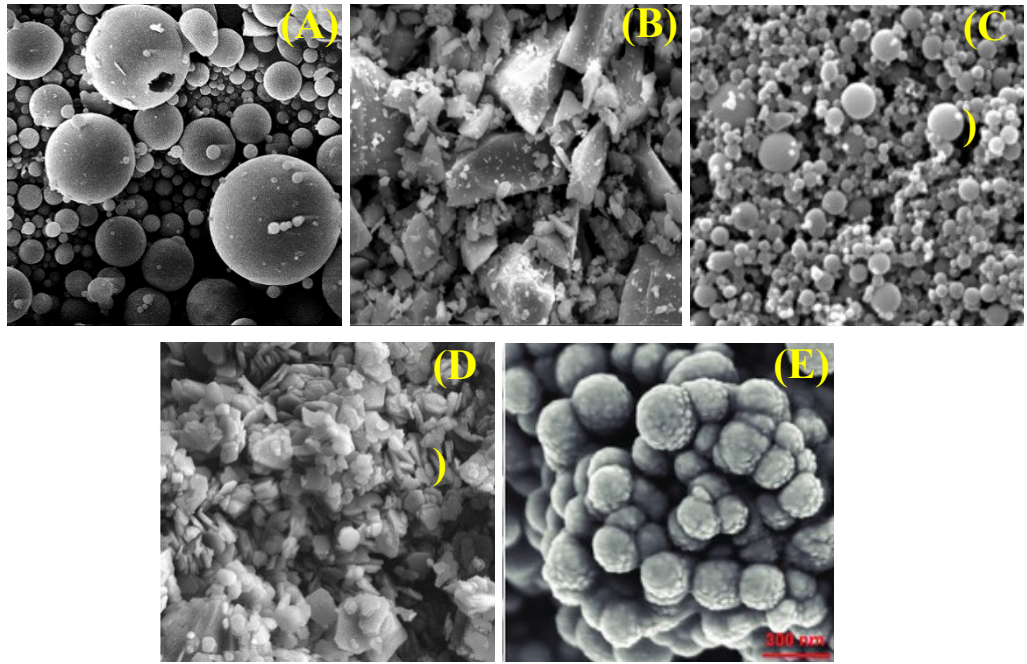


Figure 3.2. SEM images of (A) fly ash (Terzano et al., 2005), (B) GGBS (Nagendra et al., 2018), (C) silica fume (Mindess, 2008), (D) metakaolin (Pillay et al., 2020) and (E) iron silicate (Gamonchuan et al, 2021).

Figure 3.2 shows the varied particle shapes of the precursor powders; whereby the FA, SF and IS powders chiefly comprised smooth spherical particles. Contrastingly, the GGBS and MK powders were characterised by angular flaky particles. As such, GGBS and MK create higher water demand in fresh geopolymer pastes before they are broken down into individual silica and alumina monomers, therefore requiring higher shear mixing to achieve dissolution. As water in geopolymers remains in pores after geopolymerisation, pastes that require increased water contents to provide sufficient liquidity for dissolution will possess inferior mechanical strength properties. The blending of the highly reactive, but angular and flaky MK and GGBS with the spherical, smooth FA, SF and IS particles has the potential to reduce early water demand and therefore provide increased strength and durability (Provis et al., 2010).

Table 3.2 Particle size distribution of pozzolanic precursors and filler.

<i>Material:</i>		MK	GGBS	SF	FA	IS	Filler
Particle Size (µm)	D ₁₀	0.9	1.1	0.053	2.9	5.8	164
	D ₅₀	2.7	5.3	0.21	18.8	42.1	311
	D ₉₀	8.2	22.5	8.7	124.6	99.8	1799

3.2.2 Filler material

Fine sand aggregate was sourced locally from Stanley Emerson & Sons Ltd (Northern Ireland), for use as an inert filler material and mixing with precursors, alkali reagents and water to create geopolymer mortars. Particle size distribution data for the sand is given in Table 3.2, which was dredged from the south bank of Lough Neagh. The mineralogy of the sand resembled the following parent rocks: 1) amphibolite, 2) altered granite, 3) metagranite, 4) quartzite and 5) schist – all of which possessed a relatively high quartz content (Wilkinson, 2018).

3.2.3 Activators and additives

To ascertain the most effective activating solution for the geopolymer mortars studied in this research, two alkali reagents were considered: 1) Geosil 14515 (K_2SiO_3 , molar ratio = 1.5, solids content = 45% by mass, provided by Woellner and 2) Na silicate solution (Na_2SiO_3 , molar ratio = 1.7, where values of 1.45-1.85 are user-friendly (Geopolymer Institute, 2016). This was formulated in the lab by mixing Na-silicate powder with distilled water and comprised 45% solids content by mass).

A PCE based superplasticising admixture sourced from Sika, Visco-crete 25 MP, was trialled to ascertain its efficacy for increasing flowability in MK-based geopolymers, compared with the PC-based materials it is designed to work with. The use of superplasticising admixtures allowed the creation of highly flowable geopolymers, with

low L/S ratios and increased strength (Callister, 2014). This additive was chosen as it is a popular option used in many PC concrete pre-casting operations.

3.2.4 Fibres

Fibre types used in this study included glass, basalt and micro steel fibres. The glass fibres (NEG ARG Fibre AR2500H103) were sourced from Fibre Technologies International. This material came as a roving and was cut to length by hand in the laboratory to lengths of 12 mm, to ensure consistency with the basalt fibres and facilitate comparisons. The fibres were composed of soda lime glass made by Nippon Electric Company, which possessed a flexural strength of 1.5 GN/m² and a Youngs modulus of 74 GN/m². A proprietary sizing called H103 specifically designed for use in cementitious composites was then applied with a minimum zirconia content of 17% by mass. The glass fibres had a roving tex of 2500 g/1000 m, a strand tex of 78 g/1000 m and had 200 filaments woven together to make each strand.

Chopped basalt fibres were sourced from Mafic Black Basalt (Ireland) Ltd, which had a length of 12 mm. Four fibre types were considered, one with no sizing and the other with a proprietary silane-based sizing (0.15-2 wt%) designed to optimise performance in a PC-based composites. However, both fibre types had a diameter of 13 µm. The remaining two fibre types were 17 µm in diameter with the same treatments applied. These were compared against the GRC-RTU control. The 13 µm fibres had tensile strength of 3.1 GN/m² and Young's modulus of 90 GN/m², while the 17 µm fibres were slightly weaker at 3 GN/m² and 88 GN/m² respectively. Fibre diameter (13 µm and 17 µm) and dosage range variation (0-2% volume of total mix) allowed optimisation of fibre reinforcement type and mechanical properties. Sizing variation allowed the identification of the extent to which sizing requirements differ between geopolymeric materials and PC. This information was considered important for the future design of geopolymer specific sizing systems for basalt fibre composites.

The copper coated, micro-steel fibres used in this study, SD-2013, were sourced from SDS Fibres for Concrete Ltd and manufactured by Tengzhou Star Smith Metal Products Co. These fibres had a diameter 200 μm , a length of 13 mm tensile strength of 2.85 GN/m².

GRC-RTU is a blend of white cement, silica sand, alkali resistant glass fibres, superplasticisers and polymers that have been specifically developed for use in GRC. Oscrete state that the product should deliver compressive and flexural strengths of up to 40 MPa and 8 MPa after 1 day, respectively. Oscrete report enhanced early age strength gain, improved OP and maximum load before failure MOR (Equations 3 and 4, Figure 2.1), faster demoulding and improved dry curing times over traditional GRC without their novel admixture and polymer blend.

3.2.5 Foaming agents

This work investigated four types of materials used to increase the porosity of a MK or commercially available binder paste. This included endogenous foaming agents, surfactant based foaming agents, pre-formed foam and porous aggregates.

A hydrogen peroxide solution (35% H₂O₂ by mass) was used as an endogenous foaming agent. This material decomposed in highly alkaline paste environments to produce hydrogen gas bubbles that could then be trapped by a viscous geopolymer paste. Industrially available non-ionic surfactant Glucopon 225 DK was used to create porosity by trapping air through the mixing process, due to reduced surface tension created in the geopolymer paste. This material is an aqueous solution of alkyl poly-glucosides based on a natural fatty alcohol C8 – C10. Preformed foam addition was trailed using two types of *Gillette* shaving foam products, a traditional white foam (*Gillette* foamy regular shaving foam) and a more modern gel that foams with mixing (*Gillette* series sensitive shave gel). Both of which were composed mainly of water, palmitic acid, triethanolamine, isopentane

and steric acid. Expanded perlite aggregate Silvaperl P45 was also trialled to provide controlled porosity. This aggregate had a 0-5 mm particle size range and a bulk density between 90-120 kg/m³.

3.3 Preparation of geopolymer mortars and pastes

3.3.1 Structural mortar preparation

Geopolymer mortar samples were prepared in laboratory conditions, whereby batches were mixed using a Hobart A200 mechanical mixer, as shown in Figure 3.3. Powdered precursor materials were first placed into the mixer on a medium setting (113 rpm) for 1 minute to achieve a homogeneous mix. Additives and alkali reagents were then added. The free water was used to wash out the container that previously held the activating solution into the mixer bowl. This ensured that none of the viscous activator remained in the measurement pot. The materials were then mixed at a medium speed for approximately five minutes.



Figure 3.3. Pozzolan precursor powder being added to Hobart A200 mixer.

Any material adhering to the sides of the bowl was scraped in periodically with a plastic spatula to ensure full dissolution. Half of the sand filler was then added to the paste and mixed for 30 seconds before the remaining sand was added. The mortar was mixed for a further 2 minutes. For sample mixtures which comprised fibres, they were added with the second batch of sand.

The GRC-RTU material was created according to the manufacturer's instructions. 4.5 litres of water per 25kg of powder were combined in the following sequence:

- 3/4 of the water was added to a clean mixer;
- 3/5 of the GRC-RTU was then added while mixing until homogenous;
- 1/2 the remaining water was added and mixed until homogenous;
- The remaining 2/5 of the GRC-RTU was then added while mixing;
- The sides of the mixing vessel were then scraped to remove any build up;
- The remaining water was added and mixed until the required consistency was obtained.

A summary of all the geopolymer design mixtures tested in this research are summarised in Tables 3.3 – 3.6.

Table 3.3. MK geopolymer mix designs for investigation of Na₂SiO₃ and K₂SiO₃ alkali reagents.

Materials (kg/m³):		MK	GGBS	FA	SF	IS	Alk. Rea	Water	Sand	L./S ratio	A/B ratio	S/A ratio	Sand / Binder
MK/K ₂ SiO ₃	1	547	0	0	0	0	436	135	1351	0.505	0.80	1.84	1.209
	2	544	0	0	0	0	434	140	1351	0.512	0.80	1.84	1.209
	3	534	0	0	0	0	426	158	1351	0.540	0.80	1.84	1.209
	4	542	0	0	0	0	453	134	1340	0.514	0.84	1.86	1.187
	5	540	0	0	0	0	451	139	1340	0.521	0.84	1.86	1.187
	6	530	0	0	0	0	443	157	1340	0.549	0.84	1.86	1.187
MK/Na ₂ SiO ₃	7	547	0	0	0	0	436	135	1351	0.505	0.80	1.84	1.209
	8	544	0	0	0	0	434	140	1351	0.512	0.80	1.84	1.209
	9	534	0	0	0	0	426	158	1351	0.540	0.80	1.84	1.209
	10	542	0	0	0	0	453	134	1340	0.514	0.84	1.86	1.187
	11	540	0	0	0	0	451	139	1340	0.521	0.84	1.86	1.187
	12	530	0	0	0	0	443	157	1340	0.549	0.84	1.86	1.187

Table 3.4. Geopolymer mix designs with binary combinations of precursor powder.

Materials (kg/m ³):		MK	GGBS	FA	SF	IS	K ₂ SiO ₃	Water	Sand	L./S ratio	A/B ratio	S/A ratio	Sand / Binder
MK/GGBS	13	488	54	0	0	0	453	134	1340	0.514	0.84	1.94	1.187
	14	434	108	0	0	0	453	134	1340	0.514	0.84	2.03	1.187
	15	380	163	0	0	0	453	134	1340	0.514	0.84	2.14	1.187
	16	325	217	0	0	0	453	134	1340	0.514	0.84	2.26	1.187
	17	271	271	0	0	0	453	134	1340	0.514	0.84	2.42	1.187
	18	217	325	0	0	0	453	134	1340	0.514	0.84	2.61	1.187
	19	163	380	0	0	0	453	134	1340	0.514	0.84	2.86	1.187
	20	108	434	0	0	0	453	134	1340	0.514	0.84	3.16	1.187
	21	54	488	0	0	0	453	134	1340	0.514	0.84	3.59	1.187
	22	0	542	0	0	0	453	134	1340	0.514	0.84	4.16	1.187
MK/FA	23	488	0	54	0	0	453	134	1340	0.514	0.84	1.92	1.187
	24	434	0	108	0	0	453	134	1340	0.514	0.84	1.99	1.187
	25	380	0	163	0	0	453	134	1340	0.514	0.84	2.08	1.187
	26	325	0	217	0	0	453	134	1340	0.514	0.84	2.16	1.187
	27	217	0	325	0	0	453	134	1340	0.514	0.84	2.39	1.187
	28	108	0	434	0	0	453	134	1340	0.514	0.84	2.59	1.187
	29	0	0	542	0	0	453	134	1340	0.514	0.84	2.85	1.187
MK/SF	30	488	0	0	54	0	453	134	1340	0.514	0.84	2.18	1.187
	31	434	0	0	108	0	453	134	1340	0.514	0.84	2.57	1.187
	32	380	0	0	163	0	453	134	1340	0.514	0.84	3.10	1.187
	33	325	0	0	217	0	453	134	1340	0.514	0.84	3.75	1.187

Materials (kg/m³):		MK	GGBS	FA	SF	IS	K₂SiO₃	Water	Sand	L./S ratio	A/B ratio	S/A ratio	Sand / Binder
	34	217	0	0	325	0	453	134	1340	0.514	0.84	6.53	1.187
	35	108	0	0	434	0	453	134	1340	0.514	0.84	12.81	1.187
	36	0	0	0	542	0	453	134	1340	0.514	0.84	232.10	1.187
MK/IS	37	488	0	0	0	54	453	134	1340	0.514	0.84	1.97	1.187
	38	434	0	0	0	108	453	134	1340	0.514	0.84	2.10	1.187
	39	380	0	0	0	163	453	134	1340	0.514	0.84	2.27	1.187
	40	325	0	0	0	217	453	134	1340	0.514	0.84	2.50	1.187
	41	271	0	0	0	271	453	134	1340	0.514	0.84	2.80	1.187
	42	217	0	0	0	325	453	134	1340	0.514	0.84	3.21	1.187
	43	108	0	0	0	434	453	134	1340	0.514	0.84	4.92	1.187
	44	0	0	0	0	542	453	134	1340	0.514	0.84	14.49	1.187

Table 3.5. Geopolymer mix designs with ternary combinations of precursor powder.

Materials (kg/m ³):		MK	GGBS	FA	SF	IS	K ₂ SiO ₃	Water	Sand	L./S ratio	A/B ratio	S/A ratio	Sand / Binder
TERNARY PRECURSOR MIXTURES	45	325	108	108	0	0	453	134	1340	0.514	0.84	2.21	1.187
	46	217	217	108	0	0	453	134	1340	0.514	0.84	2.51	1.187
	47	217	108	217	0	0	453	134	1340	0.514	0.84	2.42	1.187
	48	108	217	217	0	0	453	134	1340	0.514	0.84	2.87	1.187
	49	108	325	108	0	0	453	134	1340	0.514	0.84	2.97	1.187
	50	108	108	325	0	0	453	134	1340	0.514	0.84	2.68	1.187
	51	325	108	0	108	0	453	134	1340	0.514	0.84	2.94	1.187
	52	217	217	0	108	0	453	134	1340	0.514	0.84	3.50	1.187
	53	217	108	0	217	0	453	134	1340	0.514	0.84	4.62	1.187
	54	108	217	0	217	0	453	134	1340	0.514	0.84	6.18	1.187
	55	108	325	0	108	0	453	134	1340	0.514	0.84	4.43	1.187
	56	108	108	0	325	0	453	134	1340	0.514	0.84	21.40	1.187
	57	325	108	0	0	108	453	134	1340	0.514	0.84	2.38	1.187
	58	217	217	0	0	108	453	134	1340	0.514	0.84	2.78	1.187
	59	217	108	0	0	217	453	134	1340	0.514	0.84	2.98	1.187
	60	108	217	0	0	217	453	134	1340	0.514	0.84	3.81	1.187
	61	108	325	0	0	108	453	134	1340	0.514	0.84	3.45	1.187
	62	108	108	0	0	325	453	134	1340	0.514	0.84	4.28	1.187

Table 3.6 Geopolymer mix designs based on factorial experimental design

Materials (kg/m³):		MK	GGBS	FA	SF	IS	K ₂ SiO ₃	Water	Sand	L./S ratio	A/B ratio	S/A ratio	Sand / Binder
MK 100% FACTORIAL	63	490	0	0	0	0	400	100	1143	0.478	0.82	2.19	1.155
	64	490	0	0	0	0	500	100	974	0.524	1.02	2.40	0.893
	65	590	0	0	0	0	500	100	875	0.460	0.85	2.24	0.736
	66	590	0	0	0	0	400	100	1045	0.416	0.68	2.07	0.959
	67	490	0	0	0	0	500	160	820	0.608	1.02	2.40	0.713
	68	590	0	0	0	0	500	160	722	0.534	0.85	2.24	0.577
	69	490	0	0	0	0	400	160	990	0.567	0.82	2.19	0.943
	70	590	0	0	0	0	400	160	891	0.494	0.68	2.07	0.775
	71	540	0	0	0	0	450	130	933	0.508	0.83	2.22	0.833
	72	540	0	0	0	0	500	130	848	0.529	0.93	2.31	0.725
	73	540	0	0	0	0	400	130	1017	0.486	0.74	2.13	0.951
	74	490	0	0	0	0	450	130	982	0.545	0.92	2.30	0.918
	75	590	0	0	0	0	450	130	883	0.476	0.76	2.15	0.755
	76	540	0	0	0	0	450	100	1009	0.468	0.83	2.22	0.926
	77	540	0	0	0	0	450	160	856	0.549	0.83	2.22	0.744
GGBS/SF FACTORIAL	78	0	440	0	110	0	400	70	1186	0.397	0.73	8.18	1.163
	79	0	440	0	110	0	500	70	1017	0.445	0.91	9.00	0.908
	80	0	520	0	130	0	500	70	923	0.394	0.77	8.37	0.756
	81	0	520	0	130	0	400	70	1092	0.349	0.62	7.67	0.975
	82	0	440	0	110	0	500	130	863	0.523	0.91	9.00	0.731
	83	0	520	0	130	0	500	130	769	0.463	0.77	8.37	0.601
	84	0	440	0	110	0	400	130	1033	0.479	0.73	8.18	0.956

Materials (kg/m³):		MK	GGBS	FA	SF	IS	K ₂ SiO ₃	Water	Sand	L./S ratio	A/B ratio	S/A ratio	Sand / Binder
	85	0	520	0	130	0	400	130	939	0.422	0.62	7.67	0.796
	86	0	480	0	120	0	450	100	978	0.433	0.75	8.28	0.850
	87	0	480	0	120	0	500	100	893	0.455	0.83	8.66	0.744
	88	0	480	0	120	0	400	100	1062	0.410	0.67	7.90	0.966
	89	0	440	0	110	0	450	100	1025	0.462	0.82	8.59	0.932
	90	0	520	0	130	0	450	100	931	0.408	0.69	8.02	0.776
	91	0	480	0	120	0	450	70	1055	0.396	0.75	8.28	0.942
	92	0	480	0	120	0	450	130	901	0.470	0.75	8.28	0.763
GGBS/MK FACTORIAL	93	110	440	0	0	0	400	70	1206	0.397	0.73	4.61	1.182
	94	110	440	0	0	0	500	70	1036	0.445	0.91	5.18	0.925
	95	130	520	0	0	0	500	70	946	0.394	0.77	4.74	0.775
	96	130	520	0	0	0	400	70	1116	0.349	0.62	4.26	0.996
	97	110	440	0	0	0	500	130	883	0.523	0.91	5.18	0.748
	98	130	520	0	0	0	500	130	793	0.463	0.77	4.74	0.619
	99	110	440	0	0	0	400	130	1052	0.479	0.73	4.61	0.974
	100	130	520	0	0	0	400	130	962	0.422	0.62	4.26	0.815
	101	120	480	0	0	0	450	100	999	0.433	0.75	4.68	0.869
	102	120	480	0	0	0	500	100	914	0.455	0.83	4.94	0.762
	103	120	480	0	0	0	400	100	1084	0.410	0.67	4.42	0.985
	104	110	440	0	0	0	450	100	1044	0.462	0.82	4.90	0.949
	105	130	520	0	0	0	450	100	954	0.408	0.69	4.50	0.795
	106	120	480	0	0	0	450	70	1076	0.396	0.75	4.68	0.961
	107	120	480	0	0	0	450	130	922	0.470	0.75	4.68	0.782

3.3.2 Mortar/paste preparation for foaming

Paste mix designs for foaming were created using the following methodology:

- The powder binder materials were placed into the mixer on a medium setting for 1 minute to achieve a homogeneous composition;
- Additives and alkali reagent solution were poured in;
- The free water was then poured into the container that contained the activating solution, and then transferred into the mixer bowl. This ensured that none of the viscous alkali reagent remained in the measurement pot;
- The materials were then mixed at a medium speed for approximately 5 minutes with any materials stuck to the sides scraped in periodically with a plastic spatula to ensure full dissolution.

From this point, methods varied for each method of foaming. Perlite aggregate, pre-formed foams and foaming agents were added. Mixing times for materials were judged by visually inspecting the paste as easily identifiable peaks in porosity were identifiable while mixing. This point varied based on mix compositions and porosity degraded with overmixing.

3.4 Casting and curing of samples

3.4.1 Cubes for compressive strength tests

Once prepared, geopolymer mixtures were cast in a variety of methods, including in 50 mm cubes, 500 mm beams and poured out onto plastic sheeting to replicate both cast and sprayed applications.

Three 50 mm steel cube moulds were coated with demoulding agent (Eco-lease MR2 from LogCo manufacturing) to ensure easy release without damage. The mortar was then added in two layers and tamped with a rod to ensure full compaction as per BS EN 1015-11 (BSI, 1999). Any excess material was removed with a pallet knife. Mortars with low

workability were further compacted using a vibration table to ensure full compaction. The filled moulds were sealed with polyethylene sheeting to eliminate moisture loss and left for 24 hours to harden. Samples were then removed from the mould (Figure 3.4) and placed in an airtight tub to cure at 20°C until testing.



Figure 3.4. 50mm mortar cube samples.

3.4.2 Fibre reinforced panels

Fibre reinforced panels were created using two methodologies. The first based on GRCA standard test 3 (2017) and the second in accordance with ASTM C947-03 (2016).

While the GRCA methodology requires samples to be cut from an existing panel, due to limitations in mould availability and cutting methods it was decided to cast a thick beam of each sample (100 x 100 x 500 mm) and slice these using a diamond tipped circular saw to the correct dimensions (300 x 50 x 12.5 mm). This ensured that the sample ends were

flat, parallel, smooth, and thus ensured an even stress distribution throughout samples during loading.

As stipulated in ASTM C947-03 and C1228-96, a bespoke mould to produce panels and an articulation rig for the test device was required. These were designed using AutoCAD and manufactured within the university. Six test panels measuring 300 x 50 x 13 mm were taken from a marked location on a single test board for 1, 7 and 28-day testing of flexural strength.

Fibre reinforced panels were cast by adding the total amount of mortar to the mould in quarters and spreading evenly with a palette knife. A vibration table was then used to ensure full compaction. Vibration was carried out in 10 second intervals until the mortar had fully consolidated within the mould and air bubbles had stopped being released from the top surface. The vibration times used varied due to the differences in rheology of the mortars studied. The filled moulds were sealed with polyethylene sheeting to eliminate moisture loss and prevent cracking, then left for 24 hours to harden. After this they were removed from the mould and placed in an airtight bag to cure at 20°C until testing.

3.4.3 Foamed mortars and pastes

Foamed mortars were cast in three 50 mm steel gang moulds with the mortar carefully added in two stages to preserve the foam structure. After 24 hours the foamed mortar was removed and cured in an airtight container for 7 days at 20°C.

Foamed pastes were cast and cured using various cube and beam moulds, and poured out onto plastic sheeting to replicate both cast and sprayed applications. These procedures are described in greater detail in chapter 6. Samples that underwent thermal conductivity testing were cast into 100 mm cubes and cured using the same method described from the foamed mortars.

3.5 Test procedures

3.5.1 Fresh properties

The rheological behaviour of mortar mixes was determined by flow table testing in accordance with BS EN 1015-3:1999, to ensure sufficient workability and limited void areas. While this standard specifies the use of a 250 mm wide flow table, this was not large enough to assess some highly flowable mixes. As a result, a modified methodology was created using a 700 mm flow table as specified in BS EN 12350-5:2000.

The setting time for each of the designed mortar mixes is of vital importance for efficient pre-casting, which was determined using Vicat testing in accordance with BS EN 196-3. Initial and final setting times were measured to the closest 5- and 15-minute intervals, respectively.

3.5.2 Uniaxial compressive strength

A fundamental mechanical property for assessing the engineering performance of geopolymer concrete or mortar is uniaxial compressive strength. This was assessed at 1, 7 and 28 days in accordance with BS EN 1015-11:1999. An ADR 2000 BS Non automatic compressive test machine was used (Figure 3.5) with a loading rate of 10 N/s to crush 50 mm cubes, allowing the effects of important mix variables to be quantified and strength optimised.



Figure 3.5. ADR 2000 BS Non automatic compressive test machine

3.5.3 Flexural strength

Preliminary fibre matrix investigations on a range of fibre matrix compositions and combines involved performing 4-point bending tests to determine the flexural strength, and therefore the most suitable high-performance combinations for use in cladding panels. These tests were carried out and reported in accordance with the ‘Determination of flexural strength of glass fibre reinforced concrete material’ test method described in part 3 of the ‘GRCA Methods of testing glass fibre reinforced concrete (GRC)’ standards document and compared flexural strength of the GRC composites developed against a commercially available pre-bagged GRC material sourced from Oscorete, GRC-RTU. This standard was chosen as none currently exist for fibre reinforced geopolymer composites, and GRC is a similar but much more widely studied material. This allowed comparative

analysis of test results through proven methodologies and direct benchmarking against GRC data found in the literature (GRCA, 2017).

The parameters used to examine the flexural performance included LOP and MOR. These values were calculated using Equations 3 and 4 from GRCA, 2016 where: W_1 = load at which the load/deflection curve deviates from linearity (newtons), W_2 = maximum load before failure (newtons), L = major span, b = width and d = thickness (GRCA, 2017). All LOP and MOR values presented were average values based on the results of multiple individual samples.

$$LOP = W_1 / bd^2 \text{ (Equation 3)}$$

$$MOR = W_2 / bd^2 \text{ (Equation 4)}$$

(GRCA, 2017)

To benchmark the flexural strength level achieved by the geopolymer composites, a commercially available pre-bagged GRC product (GRC-RTU) was used as a control. Geopolymers can significantly outperform PC materials in terms of strength development and the costly additives for these materials are not as well developed or understood. Therefore, additives were not used in the geopolymer composites. As such, any geopolymer composites achieving comparable strength to the control sample was considered a success, indicating that through further development much higher performance could be achieved with suitable admixtures employed.

After analysing the process and results of the preliminary test methodology (GRCA, 2017), a suitable mould and testing rig were custom-built to carry out further 4-point bending tests to the more well defined, less specialised methodology in ASTM C947-03 ‘Standard test method for Flexural properties of thin section Glass fibre reinforced concrete (Using simple beam with third point loading)’. This methodology was then

followed for the remainder of flexural strength testing. Adopting the ASTM C947 standard required a force centring rig that increased testing precision and allowed more consistent samples and test results to be generated. The force centring device was required to provide articulation of the loading head to load the samples more evenly. This attachment was designed in Auto-CAD and manufactured as shown in Figure 3.6.

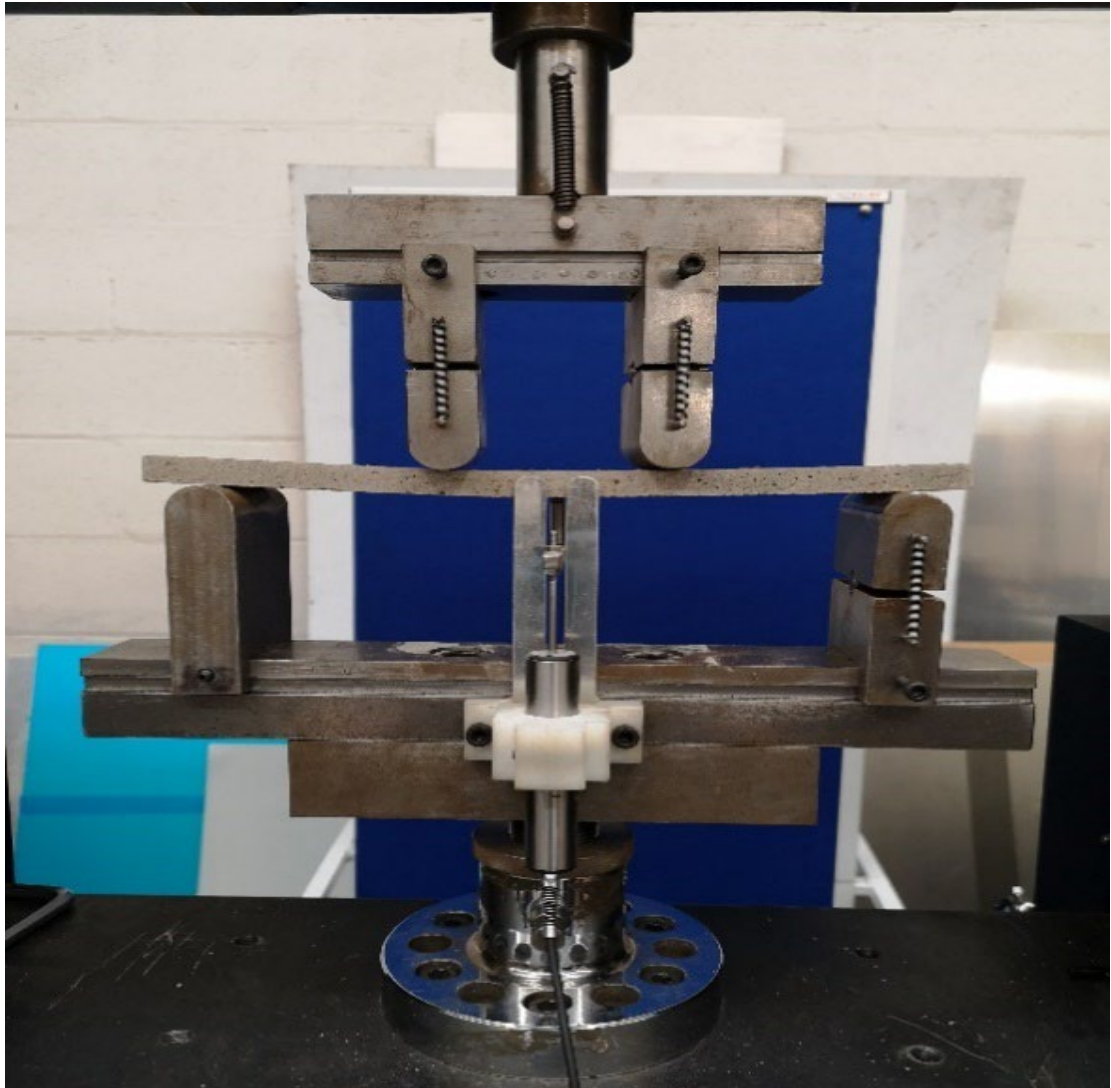


Figure 3.6. Flexural test rig to ASTM C947-03.

3.5.4 Foamed materials

The method of foam generation/addition and the viscosity of the base paste was predicted to have significant effects on the pore structure developed. Hence, four methods of foaming were investigated (endogenous foaming, surfactant-based foaming, pre-formed

foam addition and porous aggregate addition) in a range of geopolymer mortars and pastes, to identify optimal foam compositions and creation methods.

The experimental programme was carried out in the following four phases:

- Phase 1 - Investigation of foamed MK-based mortars

Due to the much lower cost and carbon embodiment of mortar compared with paste, initial investigations studied mortar mix designs, which were with endogenous and surfactant-based foaming agents and expanded perlite aggregate.

Optical microscopy and mass comparisons were used to identify successful compositions, analyse the materials produced – specifically regarding the pore structure created by each method over a range of L/S ratios. The microscope used was a Leica M165C stereo microscope (Figure 3.7); whereby images of samples were taken for a 1 cm² field of view.



Figure 3.7. Leica M165C stereo microscope

- Phase 2 - Investigation of foamed MK-based pastes

After foaming of mortars was unable to produce materials with high enough porosity, the research then focussed on the use of a paste-only base mix. As for phase 1, the same mix designs, foaming agents and expansive lightweight aggregates were used to optimise the porosity and pore structure developed. A second control base paste provided by Banah UK Ltd, intended for use in foaming applications was also investigated. Viscosity modifying admixtures (VMA) and fibre additions were also trialled to control mix viscosity. Macro scale visual inspections were used to assess the integrity and microstructure of the MK-based pastes, with a view to selecting optimum compositions for further testing. Density comparisons were not possible as many of these materials collapsed or could not be cut to a uniform volume due to their brittleness.

A small selection of samples underwent 3D CT scanning using a Skyscan 1272 device (CT-analyser: Version: 1.16.9.0). This allowed 3D visualisation and quantification of the internal pore structure (including closed and open pores). Samples for CT scanning were cut into small cubes (50 x 50 x 50 mm) using a diamond tipped circular saw. Proprietary analysis software systems CTVOX, CTAN and CTVOL were used to analyse the data and create 3D images of sample pore structures.

- Phase 3 - Thermal conductivity testing and proposed cladding panels

Thermal conductivity testing was carried out on three iterations of an optimised foamed geopolymer mix design created in Phase 2 to ascertain exact density and R-values. The thermal resistance of insulation and structural cladding materials was analysed by Gearing Scientific Ltd., whereby thermal conductivity testing was performed in accordance with ISO 8301. The apparatus used was a Fox 304, which was calibrated to 10°C mean T ($\pm 2\%$ accuracy). Each 100mm cube sample was weighed, measured and placed in the apparatus at 20-22°C. A holding pressure of 1 bar was applied from the top

plate with a constant temperature set at 0°C. The lower plate was set at 20°C for a mean of +10°C. Every 0.5 seconds, values of heat flow and lamda were recorded and averaged every four minutes to form one block. Lambda was defined as the heat (watts) transferred through a 1m³ wall when the temperature differential is 1°C. The last seven blocks were averaged for the equilibrium reading. As the sample of fibre reinforced, structural mortar was so dense and conducting +5 and +15 °C Ts were used.

- Phase 4 - Proposed claddings panels

Based on the thermal conductivity results for both the foamed insulation and the structural geopolymeric materials, cladding panels have been proposed to meet the thermal resistance requirements laid out in UK building regulations (technical booklets F1 and F2) for a range of domestic and non-domestic applications.

AutoCAD drawings illustrating each option (Figure 6.6) have been created and are presented alongside the calculated U values (Tables 6.3 and 6.4) and benchmarked against currently available options. U values were calculated using the conventions outlined in BRE 443 (2019) based on the thermal conductivity (W/mK) and the thickness (mm) of each component (Anderson and Kosmina, 2019).

Chapter 4 – Geopolymer mortar development

4.1 Introduction

The aim of this chapter is to identify suitable geopolymer mix designs for use in fibre reinforced cladding panels and create simplified, preliminary mixing methods that are practical for proportioning of geopolymers and AACMs. Furthermore, this chapter will focus on developing methodologies for predicting compressive strength, flowability and carbon embodiment for K-silicate activated mortars comprising a wide range of precursor combinations and mix parameters. In this way, the intention is to facilitate adoption of these systems as a high performance, low impact alternative to PC-based materials in buildings. This chapter is presented in the following phases:

Phase A: Geopolymer mortars created from single source materials

Phase B: Single replacement of MK geopolymers with industrial by-products

Phase C: Replacement of MK with multiple industrial by-products

Phase D: Influence of singular mixture proportioning ratios

Phase E: Simplified preliminary mix design methodology

Phase F: Synergistic influence of multiple mixture proportioning ratios

4.2 Phase A: Geopolymer mortars created from single source materials

4.2.1 MK based geopolymer mortars

The first phase in the development of the mortar component of the geopolymer cladding panel was to investigate Metastar 501 MK as the pozzolanic precursor. Two alkali reagent solutions were selected for mixing with MK, including K-silicate solution Geosil 14515 (45% solids by mass) and a laboratory made, Na-silicate water glass with the same solids content. A range of mix designs titled MK1-6 were developed for this preliminary testing and compositions repeated using each activating solution.

The mix designs for these mortars are given in Table 4.1. These value ranges were identified to provide high performance in previous work (Wilkinson, 2018).

The flow of each mortar mix was measured prior to casting in 50 mm steel cubes. While the K-silicate mortars hardened sufficiently in 24 hours, those using Na-silicate fell apart as the moulds were removed. As a result, setting times and hardened property testing of these mortars was not possible. Therefore, K-silicate was chosen as the most suitable activation medium for the geopolymer mortars going forward. This result was unexpected based on the literature review (Zhang et al., 2017; Alves and Leklou, 2020) where Na-silicate activators were reported to have higher dissolution tendency, provide more continuous monolithic structures and more extensive crosslinking; all of which should create increased strength.

Significant variation in flowability was found between MK mortars activated with the two different solutions. The K-silicate activated mortars had on average 52% higher flow than those activated with the Na-silicate. The chemical reaction that causes dissolution of aluminosilicate source materials creates water, which increases flow. This trend combined with low strength gain indicates that the Na was not as successful in depolymerising MK into individual monomers required for geopolymerisation.

Table 4.1. Mix designs for metakaolin based geopolymer mortars

<i>Materials (kg/m³)</i>	Mixture ID					
	MK1	MK2	MK3	MK4	MK5	MK6
MK	547	544	534	542	540	530
Alkaline reagent	436	434	423	453	451	443
Water	135	140	158	134	139	1567
Sand	1351	1351	1351	1340	1340	1340
L/S ratio	0.505	0.512	0.540	0.514	0.521	0.549
A/B ratio	0.797	0.797	0.797	0.835	0.835	0.835
S/A ratio	1.84	1.84	1.84	1.86	1.86	1.86
Sand / Paste	1.21	1.21	1.21	1.19	1.19	1.19

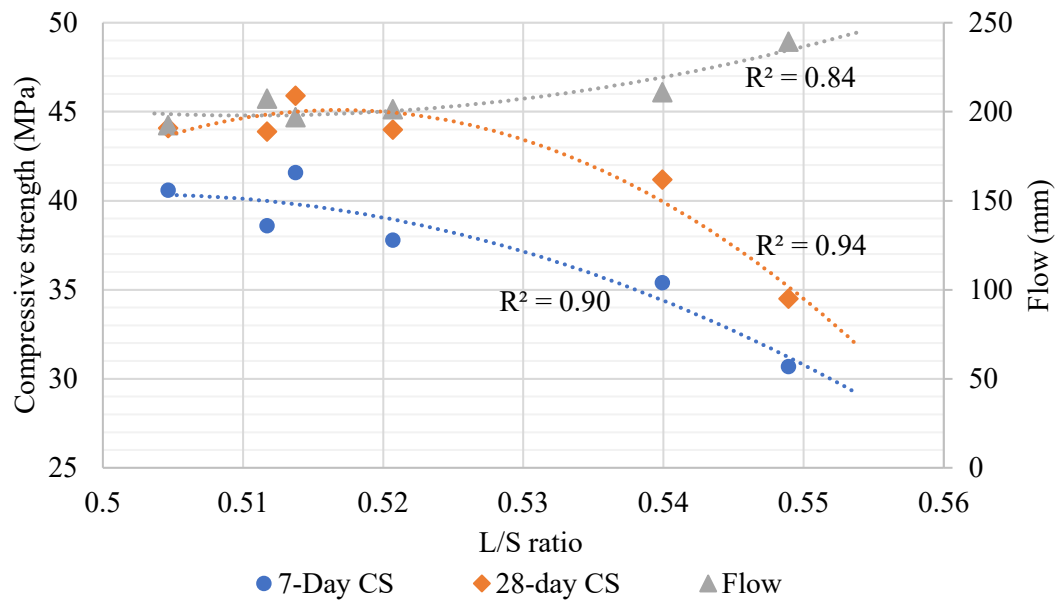
According Austroads (2016), the L/S ratio of geopolymetric material is comparable with the water/cement ratio of traditional cementitious materials and should significantly affect the flow, setting times and strength levels. As the L/S or W/C ratio increases, material flowability and setting times should increase, whereas the strength should decrease.

Figure 4.1 plots the compressive strength achieved for each of the 6 mix designs against their respective L/S ratios. High R^2 values in the range 0.84-0.94 indicate that the strong relationships predicted in the literature apply in this study, even with variations in other mix parameters. This shows that the L/S ratio plays a fundamental role in controlling the performance of MK based geopolymer mortars.

Figure 4.2 shows similar strong relationships between setting times and L/S ratio. In all three of the ways tested (flow, setting times, strength), the L/S ratio has been confirmed as analogous to the water to cement (W/C) ratio in PCs and dictates many performance properties in a similar manner.

MK1-3 which had lower average L/S ratios also had higher average 7- and 28-day strength, lower setting times and flowability than MK4-6 at 0.835. However, the strongest mix design at both 7 and 28 days was MK4, not MK1 or MK2 as expected – given their lower L/S ratios. This indicates a complex relationship. MK4 was also found to have the lowest flowability of the mortars tested. This shows that other mix parameters may have significant effects. An optimal L/S ratio has been found at 0.514, which provides the liquidity required for monomer breakdown, transport and reorganisation without the excess that becomes detrimental to performance.

The S/A, A/B and sand to paste ratios were constant for MK1-MK3 and then again for MK4-6. As such, it was impossible to separate the significance this change had in each.



Flow equation = $y = 24,836.69x^2 - 25,357.39x + 6,670.10$ (RMSE = 6.16)

28-day CS equation = $y = -9,652.20x^2 + 9,977.57x - 2,533.38$ (RMSE = 0.89)

7-day CS equation = $y = -4,253.31x^2 + 4,275.36x - 1,034.04$ (RMSE = 1.14)

Figure 4.1. Compressive strength and flow vs L/S ratio of MK based geopolymer mortars.

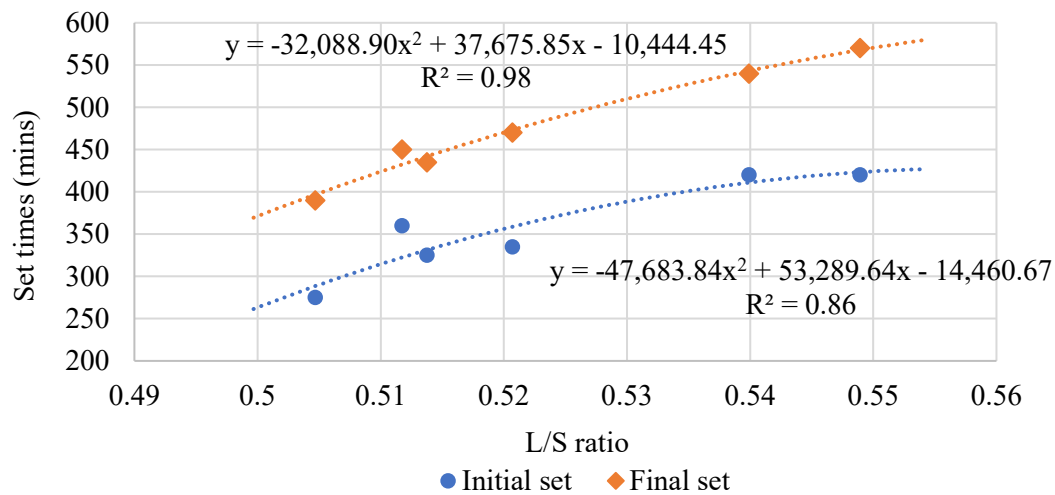


Figure 4.2. Set times of MK/potassium silicate based geopolymer mortars.

Based on the results presented in Figures 4.1 and 4.2, MK4 was selected for further investigation as it produced the highest compressive strength performance. As these mortars are intended for applications requiring high flexural strengths, the relationship between the compressive and flexural strength was investigated. Flexural strengths were

found to be on average 17% of compressive strength values. Knowledge of this relationship enabled initial estimations of flexural strength.

A preliminary trial was then carried out to determine if superplasticising additives could provide the same performance benefits as in PC-based materials. This was assessed by measuring the flow of mixes containing 0-3% (with respect to mass of MK) of PCE-based admixture Sika Visco-crete 25 MP. As shown in Figure 4.3, at dosages below 1% by mass MK4 flowability was inconsistent with minimal actual impact from the additive. Increases in flowability beyond 1% by addition rate were insignificant (<10 mm) and likely created by the additional water the admixture contains rather than its active components. As the main reaction of the superplasticising additives involves C_3A , as present in PC, this was not a surprising result. It is widely reported that the effects of these admixtures in geopolymeric materials is inconsistent and unproven (Austroads, 2016).

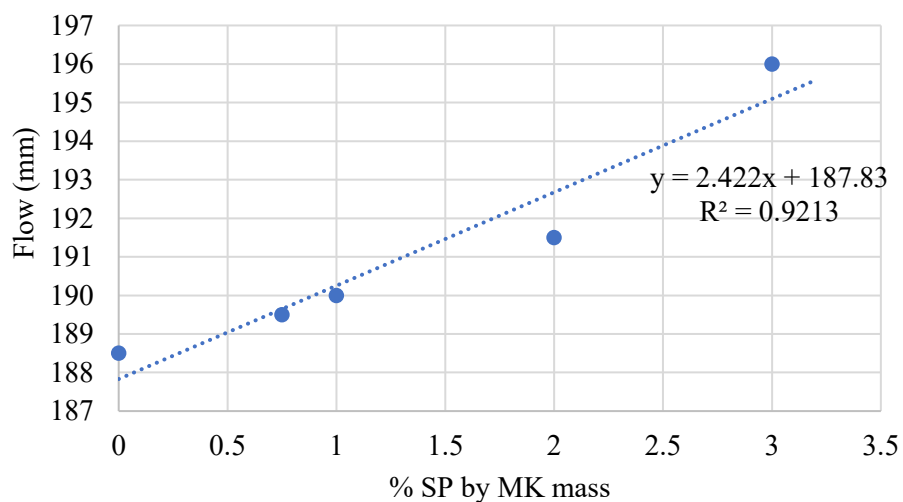


Figure 4.3. Effects of superplasticiser dose on mortar MK4.

4.3 Phase B: Single replacement of metakaolin geopolymers with industrial waste materials

While MK has a lower environmental impact compared with PC, partially or fully replacing it with industrial by-products has been shown to both significantly reduce this

impact, reduce setting times, increase strength and flow values (Austroads, 2016). As such, the industrial by-products considered in this phase B of testing included GGBS, SF, FA and IS fines.

From Table 3.1 it is evident that significant variation exists in the major oxide contents of these materials, suggesting that there is potential to produce geopolymer mixes with a wide range of tailored engineering performances. To investigate this, mortar mix (MK 4) was selected as a base with its mix composition held constant except for the binder powder composition to enable investigation of effects on mortar compressive strength, flow and setting times. The results of this work are presented in Figures 4.4-4.7.

4.3.1 MK replacement with GGBS

GGBS has been shown in the literature to have the greatest potential from the industrial by-products considered for replacing MK in the creation of high strength geopolymers. GGBS was used to replace the MK in mortar MK4 in 10% increments from 10-100% (Figure 4.4-4.6).

Initial and final setting times were dramatically reduced with increasing GGBS content, down to a minimum of 35 and 45 minutes respectively beyond 80% replacement (Figure 4.7). Hence, these mortars would be well suited for efficient pre-casting of fibre reinforced cladding panels. GGBS incorporation also increased the 7-day and 28-day compressive strength of MK4 by up to 41% and 46% respectively, and exhibited significantly higher strength gain between these ages.

Figure 4.4 shows that all GGBS additions, except 10%, improved the 7-day compressive strength up to a maximum of 70 MPa at 80% replacement. All levels of GGBS addition increased the 28-day strength up to a maximum of 86 MPa, whereby the highest performing mixture involved using 80% replacement of MK with GGBS (Figure 4.5).

These MK/GGBS mortars all had increased flowability, such that they spilled over the edges of the 255 mm flow table used and could not be measured. These mortars had a S/A range between 1.86-4.16, which increased with GGBS content. With maximum compressive strengths emerging at 80% replacement and reductions observed at 90 and 100% replacement, this may indicate that an optimal S/A ratio was determined at 3.16. This will be confirmed through further testing later in Phase D.

Furthermore, the geopolymer gels and CASH hydration products resulting from the GGBS formed simultaneously and bonded well together. The needle like CASH hydrates could be reasonably inferred to have expanded into the geopolymer gel pores to create a stronger, interlocked, homogenous microstructure and provide increased mechanical strength. 80% GGBS content may provide the optimal phase distribution to allow this type of structural formation. Future SEM investigation would be required to confirm this postulation, which will be highlighted in Chapter 7.

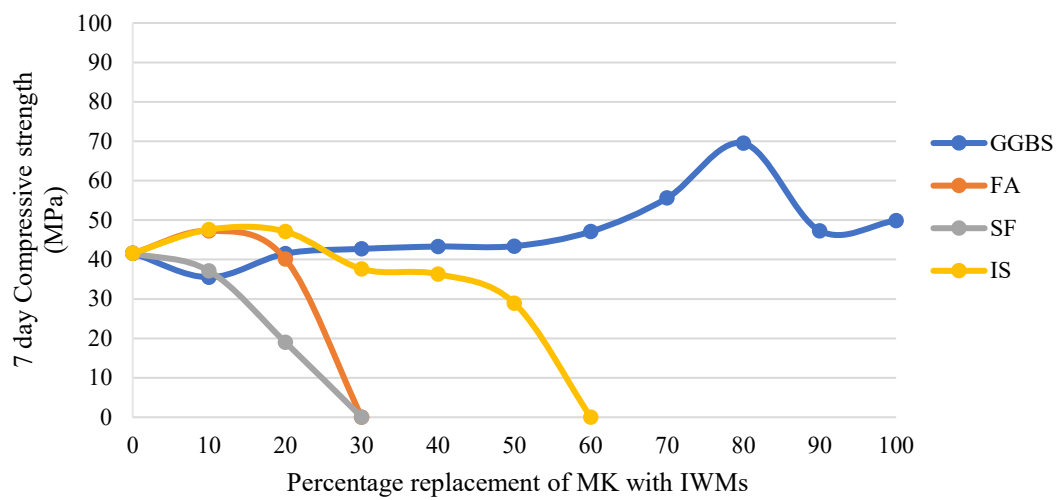


Figure 4.4. MK replacement with single industrial waste materials and 7-day compressive strength

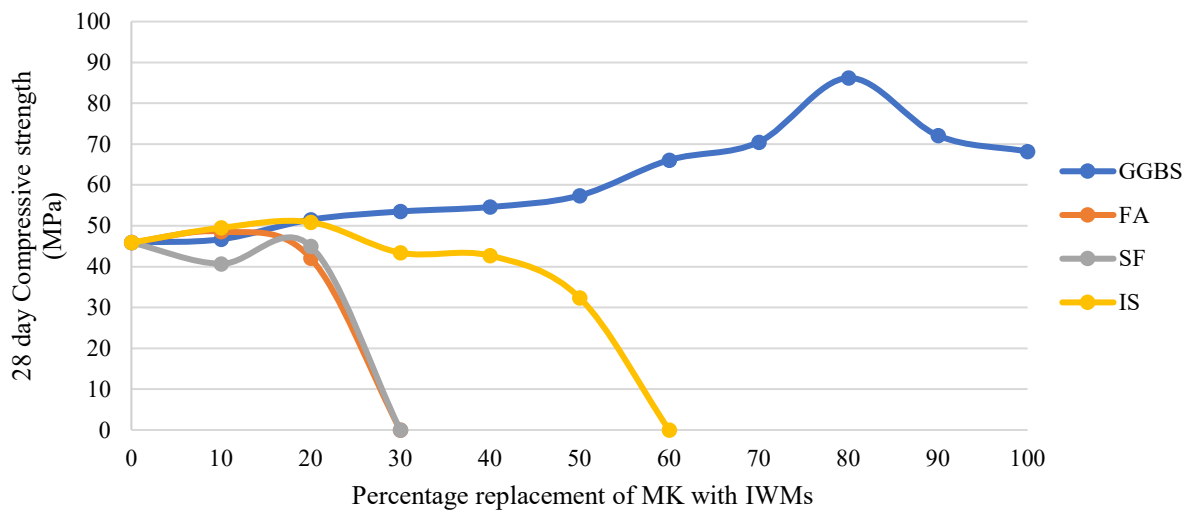


Figure 4.5. MK replacement with single industrial waste materials and 28-day compressive strength.

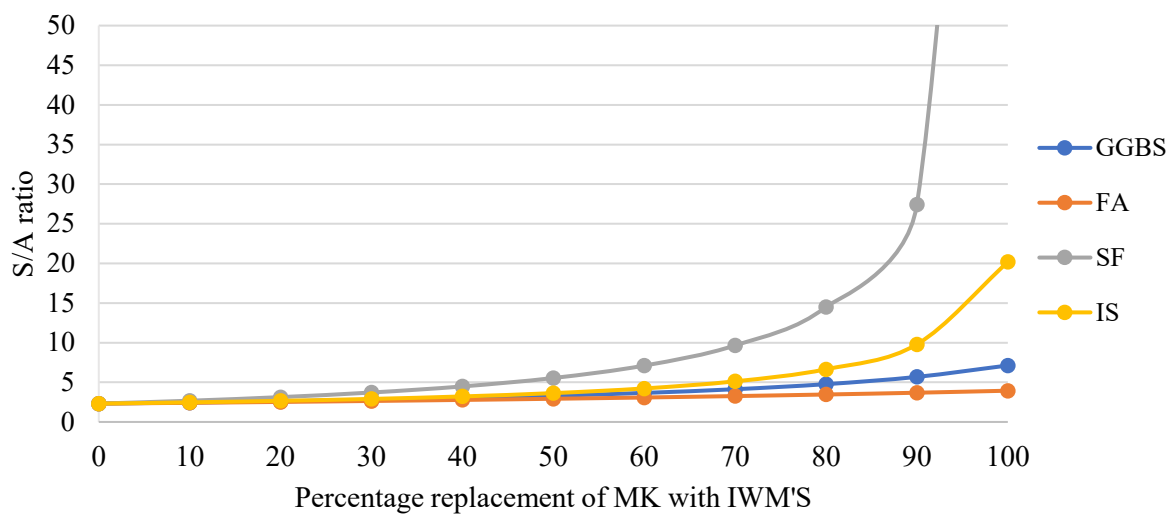


Figure 4.6. MK replacement with single industrial waste materials and S/A ratio.

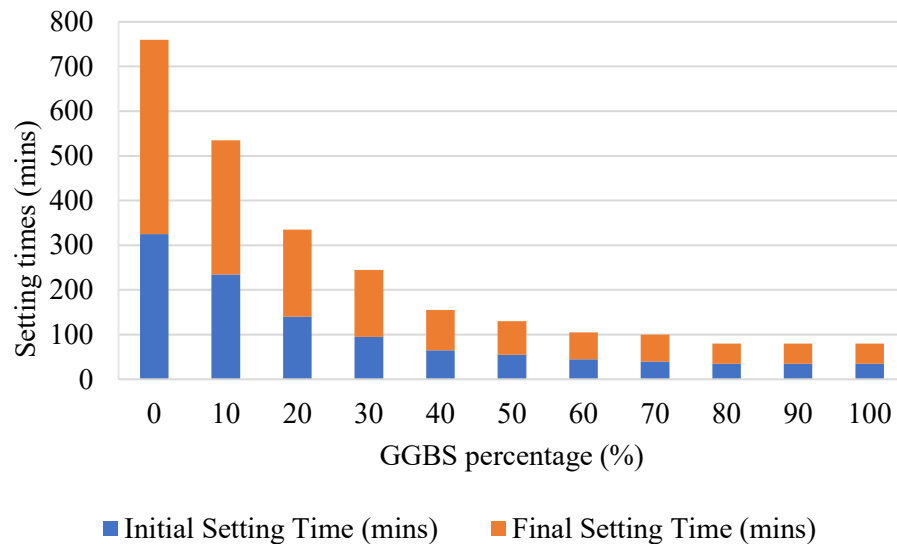


Figure 4.7. Setting times with GGBS content.

4.3.2 MK replacement with FA

Figures 4.4-4.6 show the effect of MK replacement with FA on mortar MK4. FA addition resulted in a small increase in compressive strength at 10% replacement, but reduced strength beyond this level. No mortars were able to set within 24 hours which contained >30% FA content. However, all mixtures (except MK4) exhibited diminished strength gain between 7 and 28 days.

All mortars that did set, did so within 10 hours allowing efficient pre-casting. These mortars exhibited S/A ratios between 1.86-1.99 with the highest strength found at 1.92. The highly spherical nature of FA particles acted to increase the flow of the mortar at all addition levels.

The non-uniformity of FA composition and its amorphous to glassy content must be measured consistently and accounted for when using these materials for ongoing production. Mortars with less than 30% FA do, however, have potential due to the reduced costs, emissions and embodied energy from this pre-fired waste material albeit with slightly lower performance.

4.3.3 MK replacement with SF

SF reduced the 7-day strength at all addition levels (Figure 4.4). At 28 days the compressive strength of the 20% SF mortar was similar to MK4 (Figure 4.5). This late strength development was significantly greater (137% increase) than for any other mortar combination investigated. Setting times increased with SF content until mortars no longer set at >20%. These mortars had increased flowability due to the small, smooth, spherical SF particles, indicating that the material could be used to increase the workability of geopolymer mortar mixes like in PC. However, SF powders do have additional health and safety concerns, which this must be safely managed during production.

4.3.4 MK replacement with IS

Replacement of MK with IS resulted in an increase in the compressive strength of the mortar at 10% and 20% replacement, with a maximum 28-day strength of 51 MPa achieved by using 10% replacement (S/A=2.1) (Figure 4.5). Setting times and mix flowability increased with IS contents and mortars set with up to 60% replacement.

The fact that this material is magnetic and metallic may create unforeseen phenomena with regards to thermal conductivity, electrical conductivity and thermal bridging. As such, these mortars may require further investigation before adoption for use in cladding panels.

4.3.5 Summary

Using industrial by-products to replace MK in these mortars was found to increase their setting times, with the exception of GGBS, which was well suited for efficient pre-casting of these mortars. In general, GGBS was the most successful MK replacement and produced high compressive strength mortars up to 100% GGBS content. The strongest mortar produced at both 7- and 28-days contained 80% GGBS content and an S/A ratio

of 3.16. The FA, SF and IS mixes continued to produce high strength until they no longer set. As many geopolymers need some form of heat curing to initiate their hardening phase, these could still potentially provide high performing mixes. Many of the materials were found to increase mortar strength when their contents were low but then drastically reduce this as their content increases.

4.4 Phase C: Replacement of MK with multiple industrial waste materials

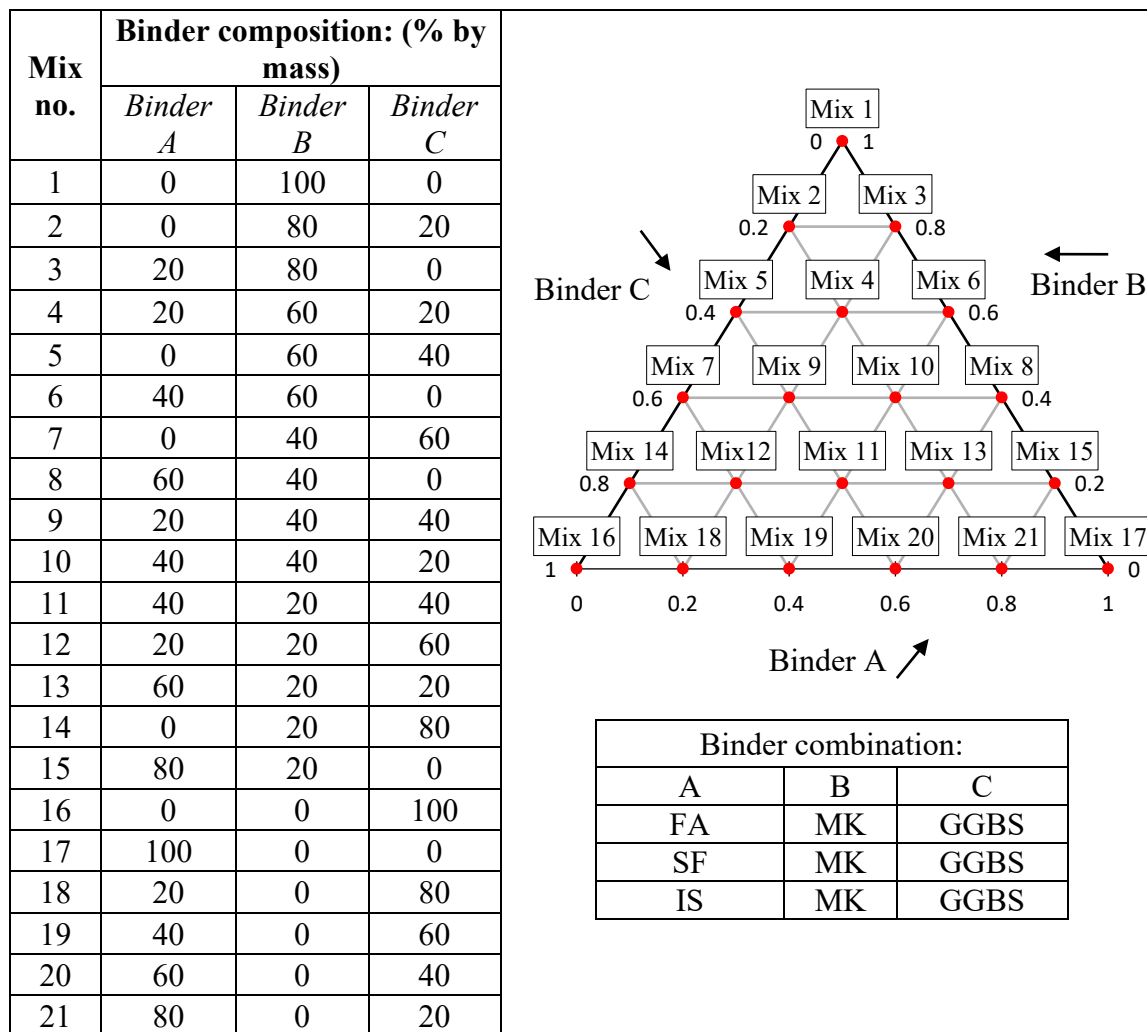
The same base MK mortar used in Phase B was used as the basis for developing further mortar mix designs, which included a combination of industrial by-products. The binder combinations considered included MK/GGBS/FA, MK/GGBS/SF and MK/GGBS/IS, with full ranges of unary, binary and ternary binders considered for each by considering respective binder increments of 20% in the range 0-100% by mass.

By adopting this approach, it was recognised that performance levels were likely to vary and potentially beyond limits of suitability. MK-based mixes, for instance, are reported to require more liquids than FA or slag-based geopolymers to ensure monomer transport, full dissolution and reorganisation (Lahoti et al., 2017). The mix design methodology used is illustrated in Table 4.2.

In terms of mortar flowability, results varied significantly for the binder combinations considered and, at almost all increments of MK replacement, were in excess of 250 mm. As such, flow rates were generally too high for accurate measurement or making any meaningful comparisons. While this high range was clearly influenced by the L/S ratio of the base mix used (0.51), the ability of industrial by-products to increase flowability was considered a positive finding in terms of industrial-scale cladding panel production, for example, a factory-based precast production process demanding high-flow and high-strength materials.

Table 4.2. Mix design methodology for replacement of metakaolin with multiple waste materials.

Material quantities (kg/m ³)				L/S ratio	Paste/sand ratio
Binder	Activator	Water	Sand		
542	453	134	1340	0.514	0.843



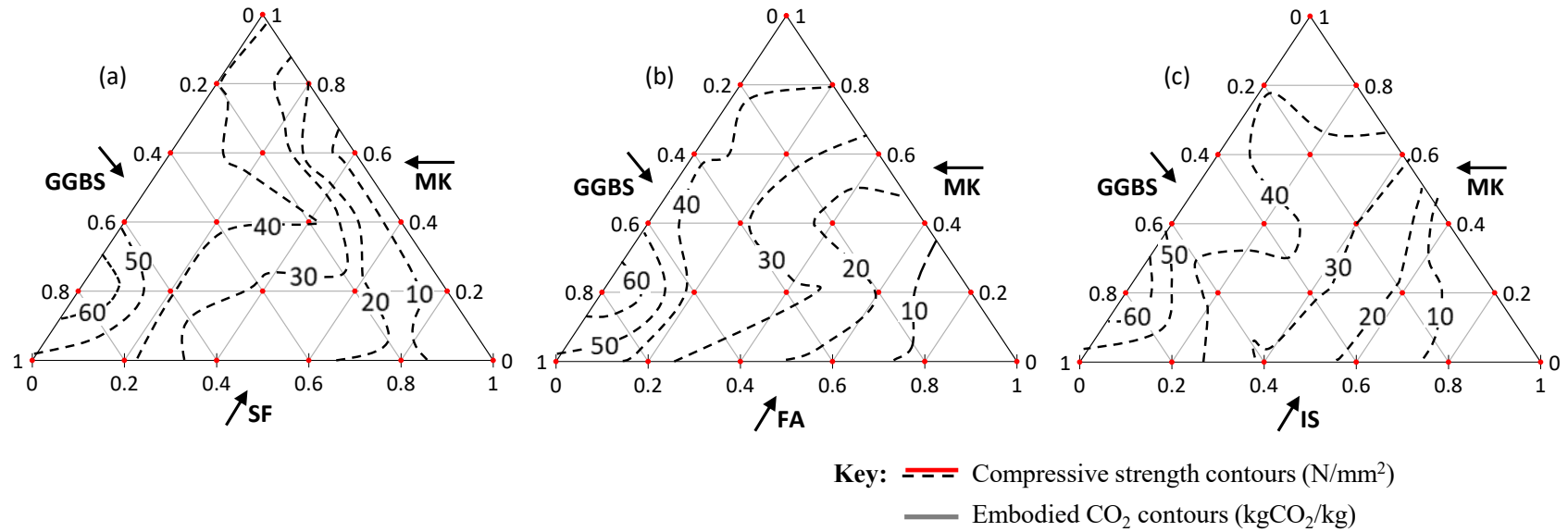
Based on the mixes considered, Figure 4.8 presents contoured ternary plots illustrating the significant influence of binder powder composition on both 7- and 28-day mortar compressive strength. Represented at the pinnacle of each ternary plot in Figure 4.8, the 100% MK mix attained 7 and 28-day strengths of 41.5 and 46 MPa, respectively. At both 7 and 28 days, GGBS was proven to be a successful replacement for MK, with respective strengths of 69.5 and 85 MPa recorded for the binary 20%MK/80%GGBS combination.

This binder blend outperformed the 100%GGBS mortar, suggesting that in these mixes geopolymer gels and CASH hydration products likely formed to create a strong, homogenous microstructure. While at 7 days (Figures 4.8a-c), the 20%MK/80%GGBS combination delivered the highest strength of all combinations considered (70 MPa), at 28 days this was achieved by the 20%SF/80%GGBS binary blend (106 MPa). As suggested previously, these performance levels reflect increasing quantities of Si-O-Si bonds present due to associated increasing S/A ratios.

In comparison with these maximum binary combinations, similar general trends were noted from the three ternary plots considered at both 7 and 28 days (MK/GGBS/SF, MK/GGBS/FA and MK/GGBS/IS), with strengths steadily decreasing as levels of MK and GGBS were replaced with increasing levels of either SF, FA or IS. While this was perhaps unexpected given the significant disparity of the chemical compositions of these binders, it confirmed the dominance of GGBS and MK in resultant geopolymerisation reactions and performance levels. From Figures 4.8 and 4.9, compressive strength values ranged from 4-70 and 5-106 MPa at 7 and 28 days, respectively across the range of binder combination considered, offering significant performance and mix design flexibility.

Overlaid on the 28-day strength ternary plots (Figures 4.8d-f) are embodied CO₂ contents for each binder combination, based on published Stage A-1 (raw material extraction and processing only) LCA's created using the methodology described in BS EN 15804. This enabled both environmental- and performance-informed decision making. From these plots, embodied CO₂ values generally decrease with corresponding reductions of MK; reflecting the fact that it is commercially mined and calcined, as opposed to a by-product from other industrial activities. Of significance from these combined plots in Figure 4.8 (d-f) is that for the binder combinations considered, improving levels of compressive strength generally correspond with reducing levels of embodied CO₂. This is contrary to trends typical of conventional PC-based concrete mixes.

7-day strength results (L:S ratio = 0.51)



28-day strength results and embodied CO₂ levels (L:S ratio = 0.51)

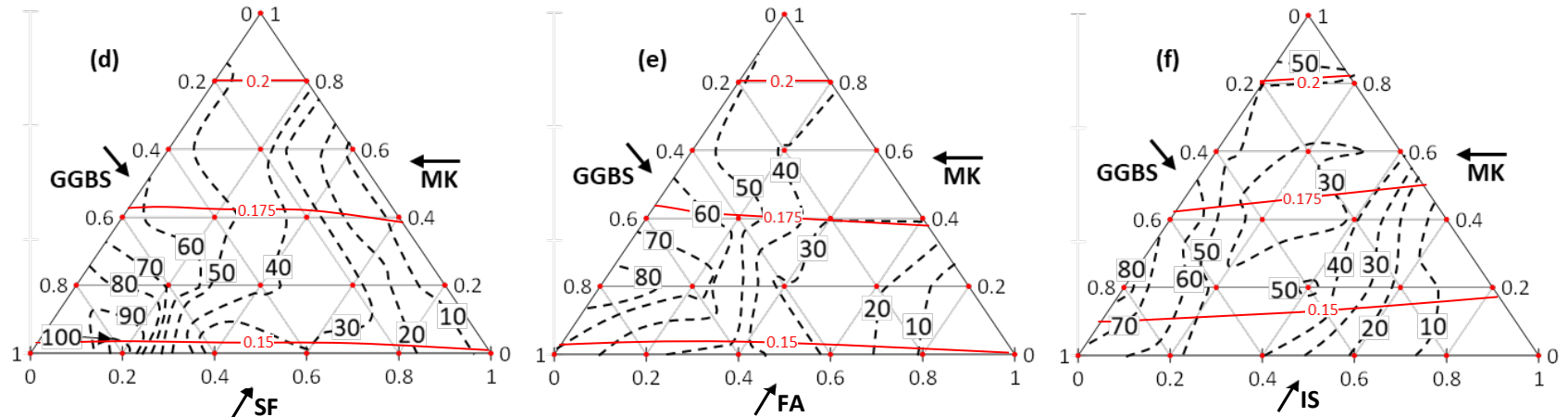
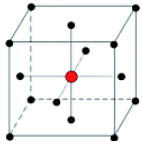


Figure 4.8. Ternary plots of 7-day strength (a-c) and combined ternary plots of 28-day strength and embodied CO₂ (d-f).

Table 4.3. Factorial mix design methodology and strength results

⁺1: 100% MK; 2: 80%GGBS/20%MK; 3: 80%GGBS/20%SF

Mix no.	Central composite design variables				7-day compressive strength (MPa)			28-day compressive strength (MPa)		
	A	B	C	 100% MK	Binder combination: ⁺			Binder combination: ⁺		
					1	2	3	1	2	3
1	-1	-1	-1		42.5	75	48	58.5	100	93
2	-1	1	-1		42	69	53.5	46.5	83	116.5
3	1	1	-1		58	86	60	56.5	93	118.5
4	1	-1	-1		-	82.5	68.5	-	102.5	92
5	-1	1	1	-1 0 1	38	67.5	38.5	43.5	72.5	84
6	1	1	1	A. Binder 490 540 590	39	79	51	38.5	88	83.5
7	-1	-1	1	B. Activator 400 450 500	33	72	34.5	33	86.5	75
8	1	-1	1	C. Free water 100 130 160	-	79.5	44.5	-	96	94
9	0	0	0		42	77.5	55.5	51.5	93.5	79
10	0	1	0	80% GGBS / 20%MK	41.5	73.5	54.5	41.5	88.5	84
11	0	-1	0	80% GGBS / 20% SF	-	71	52.5	-	104	86.5
12	-1	0	0	-1 0 1	35	75	50.5	46.5	86.5	87.5
13	1	0	0	A. Binder 550 600 650	46.5	82.5	57	52.5	96.5	89.5
14	0	0	-1	B. Activator 400 450 500	51	85	52.5	59	88	88.5
15	0	0	1	C. Free water 70 100 130	39	79	47	47	77.5	87

4.5 Phase D: Influence of singular mixture proportioning ratios

While previous work was effective in identifying the influence of binder composition on geopolymer mortar performance, this was established for one mix design only, with other important and inter-relating mix parameters not considered. As such, the following three binder powder blends were selected for further investigation: 100% MK; 80%GGBS/20%MK and 80% GGBS/20% SF. The latter two were chosen as they achieved the highest strength at 7 and 28 days, respectively.

4.5.1 Mix designs

As shown in Table 4.4, a ‘face centred central composite’ mix design approach was used to consider three mortar component variables (pozzolanic precursor, activator and free water content) across three levels (Low -1, Medium 0, High +1) in order to ascertain their significance to performance properties for each selected binder blend.

In section 4.3, the L/S solid of 0.51 used provided a wide range of flowabilities across the different binder types considered, with pure MK geopolymers exhibiting significantly lower values than hybrid or GGBS-based blends. This was due to the MK geopolymers requiring higher L/S and A/B ratios than FA or GGBS geopolymers for full dissolution, monomer transport and reorganisation to take place. This trend was addressed by lowering the binder mass and increasing water mass for the 100% MK mixes to maximise the potential of forming homogenous geopolymer matrices.

The ranges of pozzolanic precursor, activator and free water content considered for the MK mixes were 490-590, 400-500 and 100-160 kg/m³, respectively; whereas the corresponding ranges for the GGBS/MK and GGBS/SF mixes were 550-650, 400-500 and 70-130 kg/m³. This facilitated further investigation of the influences of the following key relationships, as presented in the literature (Kim, 2012; Wilson, 2015; Provis et al., 2015; Austroads, 2016; Lahoti, 2017) as being significant for geopolymers: S/A, L/S and

A/B. Values of A/B and L/S ranged from 0.76-1.02 and 0.46-0.57, respectively for the 15 MK mixes. Corresponding ratio ranges for the GGBS/MK and GGBS/SF mixes were 0.62-0.91, 0.35-0.52.

4.5.2 Compressive strength

The 7- and 28-day compressive strength results achieved by the geopolymer mortar mixes considered are presented in Table 4.4. As expected, and reflecting the mix constituent ranges introduced as part of the experimental design, broad ranges of strength were recorded for each binder mixture investigated. For the 100%MK, 80%GGBS/20%MK and 80%GGBS/20%SF combinations, these were 33.0-58.0, 67.5-86.0 and 34.5-68.5 MPa, respectively.

Of the 15 mixtures considered for each binder blend, mix no.4 was perhaps expected to produce the greatest compressive strength as it possessed the lowest L/S ratio, highest mass of precursor, the lowest amount of activating solution and free water. This was provided that sufficient activating solids existed in the mixture for full dissolution to occur without leaving unreacted binder, which would promote microdefects. Indeed, for the 100%MK binder, mix no. 4 (as well as for mix no.8 and no.11) this proved not to be the case, with the material failing to set or gain any appreciable strength.

Alternatively, all the GGBS/MK and GGBS/SF mixtures successfully depolymerised the precursor and had enough liquidity for monomer transport and reorganisation, allowing homogeneous hardened geopolymer mortar to form in all 15 mix iterations, irrespective of the lower ratio values considered. This suggests that the amount of activator solids required for geopolymers based on these industrial by-products was significantly lower. As this is likely to be the most significant component of these geopolymer mixtures from both economic and environmental standpoints, the benefits of partially replacing the MK with these are clear. As expected from results presented in section 4.3 the GGBS/SF

mixes exhibited the greatest strength gain between 7 and 28 days with many over doubling in strength.

4.5.3 Relationships between singular mixture proportioning ratios and strength

As illustrated in Table 4.4, work progressed to explore if clear relationships existed between the strength results obtained and the aforementioned ratios reported as being significant for geopolymer mix design (i.e. S/A, L/S and A/B). Figure 4.9 plots these ratios versus 7- and 28-day compressive strength for all 15 mixes considered for the three binder combinations under investigation.

The S/A ratio of source materials used to create geopolymers dictates the formation of molecular- and nano-scale structures. Theoretically, there should be a direct correlation between silica content and compressive strength due to increasing quantities of strong Si-O-Si bonds. With that said, owing to other impacting mixture proportioning parameters such as L/S or activating solution composition, optimum levels of S/A reported by researchers have been noted to be variable (Kim, 2012; Austroads, 2016).

However, in this study the influence of S/A ratio on 7-day strength was less significant as previously reported, with insignificant R^2 values of 0.06, 0.28 and 0.07 at 7 days and 0.08, 0.53 and 0.03 noted for the MK, GGBS/MK and GGBS/SF mixtures, respectively. While the MK mix designs had the most significant relationships between S/A ratio and compressive strength as there was only one binder type used in these mixes, this value is a stronger reflection of the binder mass level being used.

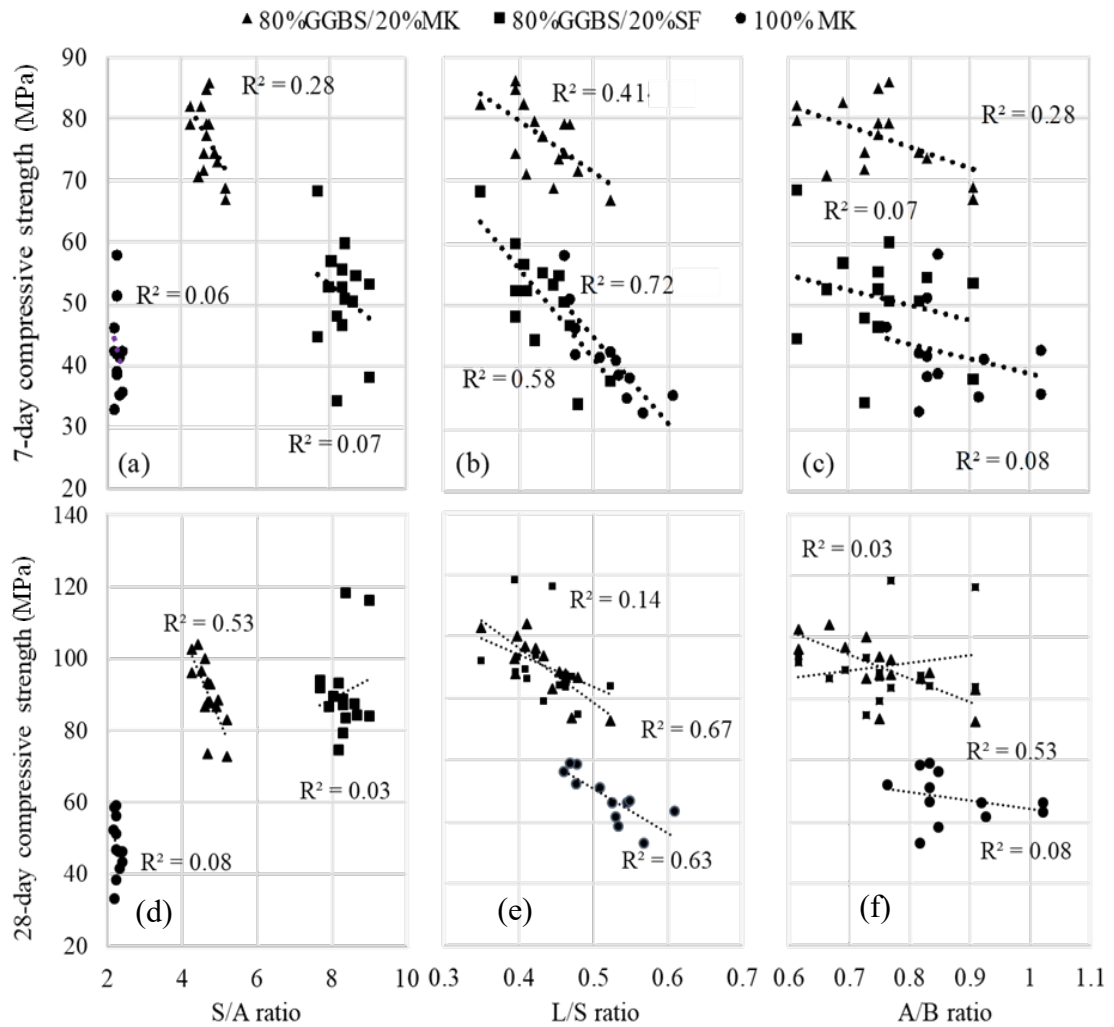


Figure 4.9. Silica/Alumina, Liquid/Solid and Activating solution to Binder powder ratios vs 7- and 28- day compressive strength.

A/B ratio is one of the most important factors in the successful design of geopolymer mixes, enabling full dissolution of the original aluminosilicate chains in the precursor and geopolymerisation without defects from unreacted binder powder (Wilson, 2015). Three of the 100%MK mortar mixes (MK4, MK8 and MK11) were unable to form geopolymeric bonds owing to insufficient activator solids in the mix to depolymerise the binder powder. With no release of silica and alumina monomers, along with chemically bound water, dry sandy mortars lacking any cohesion or liquidity were formed. All MK mixes with an A/B ratio less than 0.75, or an activator solid to binder ratio of 0.34 reacted in this way. While vital to geopolymer formation, this ratio was of little relevance in trying

to predict strength, with R^2 values ranging from 0.07 to 0.28 at 7 days and 0.03 to 0.58 at 28 days.

L/S ratio in geopolymer materials is reported to be analogous to the water/cement (W/C) ratio in PC concrete mix designs in terms of its impact on properties such as flowability and compressive strength. In PC-based materials, compressive strength is inversely proportional to W/C. Relationships which are similar, albeit varying and with diminished significance, were noted for the three geopolymer binder compositions considered, reflecting the probable influence of other key mix variables that are not present in PC concrete. The R^2 values ranged from 0.41 to 0.72 at 7 days, indicating a stronger correlation between L/S ratio and strength. At 28 days this range varied from 0.14 to 0.67 with the GGBS/SF mortars showing the lowest significance. This was likely due to the large strength gains exhibited by these mortars between 7 and 28 days not being a product of the L/S, but indicative of the material properties of the SF.

From Figure 4.9, no principal mix proportioning ratio can be used to accurately predict 7- or 28-day compressive strength. With that said, of the three considered, L/S was the most significant; albeit with differing relationships apparent for the different binder compositions investigated.

The data presented in Figure 4.9 was manipulated further to investigate and develop generic relationships of performance versus L/S ratio and to explore its applicability to a wide range of geopolymer binder types. To this end, further laboratory work was undertaken to assess flowability and compressive strength performance of additional selected representative binder types across a range of L/S ratios (0.35-0.61).

Binder combinations considered included: 100% MK; 100%GGBS; 80%GGBS/20%MK; and 60%GGBS/20%MK/20%SF. Primary data was additionally supplemented by performance versus L/S ratios published in the literature (Gao et al.,

2013; Kumar, 2015; Shivarajan et al., 2016; Lahoti, et al., 2017; Guzmán-Aponte et al., 2017). The results with respect to compressive strength are presented in Figure 4.10. From Figure 4.10(a), it is evident that while clearly distinctive and inconsistent relationships exist for individual mix types (determined by differences in binder types, associated geopolymerisation reactions, testing times, experimental variables, etc. used), families of generic relationships are identifiable. While recognised not to closely fit all primary and secondary data sets compiled in Figure 4.10(a), a proposed normalisation of this observation is presented in Figure 4.10(b) for use within a preliminary mixture proportioning methodology. Similar normalised relationships for flow versus L/S ratio are presented in Figure 4.10(c, d).

4.6 Phase E: Simplified preliminary mix design methodology

Combining the results presented from phases A-D, a simplistic mix design procedure is hereby proposed for geopolymer mortar mixes comprising any binder combination of MK/GGBS/FA (see Figure 4.11). This methodology is intended to be reproducible for the other geopolymer combinations. Included in Figure 4.11 are values of embodied CO₂ and 7-day compressive strength for mixes with L/S ratio of 0.51, as well as generic relationships linking both 7-day compressive strength and flow with L/S ratio in the range 0.30-0.65. In this way, the figure enables estimations of approximate mixture proportions for specified values of compressive strength and/or flow.

In the example presented, initial mix design requirements include a maximum value of embodied CO₂ content (0.15 kgCO₂/kg) and 7-day strength (50 MPa). Using Figures 4.11(a) and (b), the 7-day strength can be estimated for geopolymer cement mortar comprising a suitable binder combination and L/S ratio of 0.51.

In the example shown, a value of 35 MPa is predicted for a 30%MK/50%GGBS/20%FA binder combination. This value can then be transposed onto Figure 4.11(c) to estimate the L/S ratio required to achieve a 7-day strength of 50 MPa. An L/S value of 0.38 is estimated, leading to an approximate flow value of 260 mm. It is recognised that by not accounting for other mix design criteria (e.g. aggregate size/type/properties and paste/aggregate ratio), this mix design procedure requires refinement for geopolymer cement mortar/concrete. However, a provisional user-friendly methodology is hereby proposed to enable rapid estimation of performance for a wide range of low impact binder material options.

4.7 Phase F: Synergistic influence of multiple mixture proportioning ratios

While the mixture proportioning method presented in section 4.4 was capable of providing preliminary mixture proportions for a variety of geopolymers and AACMs, its limitations were recognised given its sole reliance on L/S ratio as a performance predictor. Thus, work in this phase proceeded to ascertain whether combinations of several mix parameters could be used synergistically with more success.

Data analysis programme Design Expert 12 was used to determine mix parameters most closely linked with performance properties, to represent these relationships in easily identifiable forms and to create equations that can predict important performance properties. For each of the three mix types (MK, GGBS/MK and GGBS/SF) separate models were developed to map and predict the 7- and 28-day compressive strength, flowability and carbon embodiment based on variation of the three experimental factors (A= binder mass, B= activator mass, C= free water mass). While the aim at the outset was to generate generic models capable of predicting the value of performance properties across all binder combinations, this was found not to be possible within acceptable limits of accuracy. Significantly different factors and equations were found to better predict geopolymer performance across the binder types studied.

Figures 4.12 and 4.13 show the experimental factors (binder powder, alkaline reagent and water contents), plotted against compressive strength at 7 and 28 days, carbon embodiment and flowability for each binder type. For the 100% MK mortars water content was the most significant factor for both 7- and 28-day strength. However, R^2 values were relatively low (0.53 and 0.46 respectively). In MK/GGBS mortars the binder content was of the greatest significance to 7-day strength ($R^2 = 0.55$), whereas this factor had less significance towards 28-day strength. Activator and water contents were more significant to 28-day compressive strength ($R^2 = 0.18$ vs 0.32 and 0.30 respectively). GGBS/SF mortar strength development was primarily influenced by water contents, followed by binder content.

The significance of alkaline reagents contents to strength development was minimal at 7 days. However, by 28 days an increased significance was apparent for all binder types. For all mortars, the carbon embodiment was primarily determined by alkaline reagent contents as they possessed high carbon embodiment relative to the other mix components such as precursors and filler ($R^2 = 0.77$ -0.87). Binder contents were only significant in MK mortars ($R^2 = 0.44$) since MK is a commercial material specifically manufactured as a geopolymer precursor as opposed to industrial by-products. Flowability of all mortars was found to be a product of water and alkaline reagent contents with binder contents surprisingly of negligible significance for all binder types ($R^2 < 0.1$).

Based on the relatively low R^2 values exhibited by the factors across all binder types, further analysis and more complex equations are required to accurately map and predict the performance of these geopolymer mortars. In isolation, each factor was of limited importance and none would allow accurate performance prediction. Examples of effects that could not be accounted for in the simple analysis of Figures 4.12 and 4.13 include: 1) the most suitable alkaline reagent content is dependent on the binder content; 2) a suitable A/B ratio must be achieved to allow full dissolution of the binder 3) the alkaline

reagent solution is water based therefore minimum free water contents required to provide sufficient early workability are dependent on alkaline reagent contents contribution towards total water content. This minimum total water content is vital to allow dissolution, monomer transport and homogenous mixing of K-silicate through the binder powder. However, excess water creates porosity and lowers strength; and therefore has significant influence on performance. Using equations that can identify the interaction effects present between these interconnected factors allowed a more comprehensive understanding of factors that significantly impact performance properties and the types of relationships present.

Figures 4.14-4.16 show the models created for each binder type and analysis of their ability to make accurate predictions. Each figure is composed of four individual sub-figures (a-d) that represent individual performance properties (7-day compressive strength, 28-day compressive strength, embodied carbon content and flowability). The top of each figure contains both the actual and coded equations for predicting the performance property described, or assess the significance of each factor respectively. The graphs provided illustrate the predictions made from these models vs the measured values used to create them, allowing the identification of predictive accuracy at specific points within the value range. For example, from Figure 4.15(a) for GGBS/MK mortars, 7-day strength prediction accuracy generally increases with the compressive strength achieved. Thus, predictions for high strength mortars can be used with more confidence. Finally, relevant statistical analysis of the model is presented including factors such as adjusted and predicted R^2 used to assess model significance.

Based on the models presented in Figures 4.14-4.16, Figures 4.17-4.19 show sets of contour graphs illustrating the relationship between Binder mass (A) and Activator mass (B) in terms of the four response outputs; (1) 7-day strength, (2) 28-day strength, (3) carbon embodiment and (4) flowability, respectively. For each response, three plots are

presented, which represent increasing Free water content (C) i.e., left = minimum, centre = medium, right = maximum. This allowed easy identification of the relationships present and the predicted performance of specific mix compositions. A graphical example of how the plots contained in Figures 4.17-4.19 could be used as mix design methodology is presented in Figure 4.20.

4.7.1 Compressive strength

For all binder types studied, significant variation existed between factors that were vital to performance. The equations which were most successful at predicting performance are slightly different between the binder types and for strength development at different curing times.

Generally, for MK-based mortars lower water contents correlated with higher compressive strengths. However, the relationships between strength, binder contents and activator contents were more complex. At low binder dosage (490 kg/m^3), the optimum activator content for strength development was predicted to be approximately 450 kg/m^3 . When the dosage increased to 590 kg/m^3 , the optimal activator content also increased up to a maximum of 480 kg/m^3 . At higher water contents, contours in Figure 4.17 merged showing that maximum strengths were predicted at these two distinct points and decreased between them.

From the coded equations in Figures 4.14-4.16, the contribution of the activator content was the most significant factor in determining the 7-day compressive strength, followed by the free water content. The binder content and its interaction with the activator content, while forming a fundamental part of the predictions, was of lower significance. Activator content was more important regarding the development of 28-day than for 7-day compressive strength. The effect of free water content became insignificant.

Equations predicting the 7- and 28-day strength of MK mortars used similar components and had relatively similar success at modelling strength development. Quadratic functions were introduced to allow the effects of each variable to be scaled, dependent on other mix parameters. The actual equation used for predicting performance is shown in Figure 4.17 as well as a coded equation used to identify the significance and effect of each parameter on the output value. Adjusted R^2 values around 0.8 and predicted R^2 values of over 0.6 illustrate that while the models can make successful predictions, a significant proportion of the variation in the results will not be accounted for. This is confirmed in the predicted vs actual results graphs. The models were also unable to successfully predict when a mortar would be unable to set before mould removal and would therefore score 0 MPa.

Strength development in GGBS/MK mortars was driven by many of the same factor effects as for the 100%MK mortars. The equation found to be most successful at predicting 7-day strength values used the same factors as the equation for MK mortars, albeit with variation in the coefficients applied to each. The 28-day equation was also similar and all R^2 values of both the 7- and 28-day strength equations were higher than for the MK mortars.

The only difference between the MK and MK/GGBS equations for 28-day strength is that a term AB (Binder mass*Activator mass) is replaced with a C^2 term (Free water content²) in the latter. However, the contour graphs in Figure 4.17-4.19 show slight differences in form between the two mortar types, whereby they each provide different mix compositions for optimal compressive strength.

While MK mortars have consistent factor responses for 7- and 28-day strength development, this was not the case in MK/GGBS mortars. In MK/GGBS mortars the most significant factor that determined strength development at 7-days was the binder content. However, by 28 days the activator content became dominant – as for MK mortars.

After 7 days curing, instead of the two optimal areas evident in MK mortars, GGBS/MK mortars provided maximum compressive strength when the water content was lowest (70 kg/m³), the binder content was highest (590 kg/m³), and the activator content was approximately 450 kg/m³. Contrastingly, maximum 28-day strength development in GGBS/MK mortars was produced when activator to binder ratios were at their lowest.

As expected, the equations used to model strength development in GGBS/SF mortars exhibited significant differences to those used for MK mortars. The most dominant factor that determined 7-day compressive strength was the free water content, with binder content also found to be significant. The effect of activator content was insignificant at this age and therefore not used in the predictive equation. R^2 statistics ($R^2 = 0.91$, Adjusted $R^2 = 0.86$, Predicted $R^2 = 0.78$) for the 7-day strength equations illustrate similar success to that achieved by the GGBS/MK mortar equations.

After 28-days curing, the free water content remained the dominant factor in strength development. Precursor contents became insignificant, whereas the increased significance of activator content became apparent. However, this model had the lowest significance of any model developed, whereby it only accounted for 64% of the variation in the responses measured (adjusted R^2) and exhibited a Predicted R^2 value of only 0.45. Predictions from this model were therefore likely to be less accurate and some trends identified may be a result of model inadequacies rather than real behaviour.

4.7.2 Flowability

Factors that determined mortar flowability and the equations that were most successful at predicting this value varied significantly with binder type. For MK mortars, activator content was the dominant parameter and the interactions between this and the binder content determined mortar flowability irrespective of free water content. Contour graphs in Figure 4.17 show that the same mortar compositions that provide the greatest

flowability also provide the greatest strength. Rapid and effective dissolution of the pozzolanic precursors will produce the water required for this increased flow and reactive monomers in sufficient quantities to build a high strength geopolymerised matrix. This combination of properties indicates an optimal A/B ratio was determined at 0.93.

In GGBS/MK mortars, the activator and precursor contents still dominated flow predictions, but free water contents also became significant. A more complex equation and contour topography was required to accurately model flowability, which produced R^2 values > 0.95 . From the contour plots in Figure 4.18, it is evident that the greatest mortar flow was not generated when activator contents were highest and precursor contents were lowest. This was expected but also affected by the variable release of chemical water with changing A/B ratios. Maximum flowability was found instead when activator and free water contents were maximised, binder contents were in the mid-range around 580 kg/m^3 , and the A/B ratio was around 0.86.

The A/B content interactions that determined flow in MK and GGBS/MK mortars were also present in GGBS/SF mortars. However, these effects had less influence on the predictions made. Free water content was the primary determinant of flowability in GGBS/SF mortars and the model was extremely accurate in making predictions of flow values (predicted $R^2=0.91$). When activator content was highest, the greatest flowability was achieved using a binder powder mass in the centre of the mass range. This is likely to be the point where the flow reduction from increased precursor content was overcome by the rate of chemical water release during dissolution. Additional precursor content reduced the A/B ratio and therefore dissolution efficiency compared with the optimum A/B ratio found at 0.83. This lower optimal A/B ratio for both GGBS/MK and GGBS/SF mortars corroborates the literature, whereby the geopolymers containing GGBS require lower amounts of activating solution.

4.7.3 Embodied carbon

For each of the three binder types studied, the activator content was the primary factor that determined the embodied carbon of the mortars produced, followed by the binder content. Furthermore, increasing the activator and binder contents increased the embodied carbon content and the contours plots describing the relationships are very similar to each other. The higher carbon embodiment of MK means that carbon contents can be described as MK>GGBS/MK>GGBS/SF. Predicted R^2 values were between 0.99-1 and highlight how successful these models were in determining carbon embodiment.

4.8 Contour based mix design methodology

In a similar manner to the simplified mix design presented in section 4.6, the contour plots created to define the influence of multiple mix parameters on strength and flowability performance properties can be used as a mix design tool. This method will allow the selection of MK, GGBS, FA, IS-based geopolymer concretes that can meet specified design strength, flowability and carbon footprint requirements in a simple manner and will have much greater accuracy and applicability than the previous attempt.

A summary example is provided in Figure 4.20 based on a proposed client brief that stipulates the following:

- 7-day compressive strength must be >40 MPa;
- 28-day compressive strength must be >90 MPa;
- Flowability must be 275-350 mm to enable casting;
- Embodied carbon content must be <0.24 kgCO₂/kg.

A major advantage for this method is that the predicted vs measured response graphs in Figures 4.14-4.16 allow the exact variation level and error direction that should be expected at a specific point in the output value range to be analysed (7-day day strength etc.). This implies that mixes can be selected based on optimised criteria or controlled

predictive error. As a result, increased confidence can be placed on mix design predictions made and safety margins can be employed to ensure compliance in practice.

Not all combinations of performance properties are achievable. Alteration of other mix parameters may be required to modify resulting mixes in order to meet all demands simultaneously. For example, a small amount of GGBS may be added to the MK based mixes to lower CO₂ content. Conversely, a small amount of MK could be added to reduce the flowability of GGBS/SF mortars. The mix designs proposed can all be modified using the techniques previously discussed to have significance on engineering performance, such as the L/S ratio.

4.9 Chapter summary

The goal of the work reported in this chapter was to develop performance-based mix design methodologies capable of reliably producing K-silicate-activated geopolymer mortars, based on MK and a range of industrial by-products with specified levels of strength, flowability and/or embodied carbon content.

For a given geopolymer mix design, the influence of binder composition on the resulting reactions and corresponding values of compressive strength gain has been shown to be significant. High performance geopolymer mortars were developed, exhibiting high flowability and 7- and 28-day compressive strengths of up to 87 and 106 MPa respectively; whereby the latter used a binder system comprising 100% by-product precursor powder.

Many of the highest performing mortars investigated had embodied CO₂ binder levels around 30% lower than corresponding PC-based mixes. This is deemed to be a major benefit of geopolymers, where a broad range of structural performance levels can be attained using various combinations of, ideally, locally available, low impact binders.

Further improvements to the engineering performance for geopolymer mixes are possible via further adjustments to mixture proportioning parameters, such as the mass of alkali reagents, as these are the environmentally and financially expensive component. The reagent dosages are relatively high in industrial by-product-based binders, in the absence of MK. While the CO₂ savings reported here are modest compared with some published in the literature (Davidovits, J (b) 2013), if similar geopolymer systems are to be used for replacing all PC-based materials, the theoretical reduction in total global carbon emission would be approximately 2.1% (Jones, 2011; Benhelal, 2013).

This chapter confirmed that the use of single proportioning ratios is not the optimum approach for accurate strength prediction and that combinations of mixture design parameters can have a bearing on performance. Of the single ratios studied, L/S ratio appeared to show the strongest correlation with strength, albeit that mixes with low L/S values did not consistently provide the greatest strength in the mix designs studied. Mix designs with the lowest L/S ratios often had the lowest A/B ratio, causing difficulties in precursor dissolution and subsequent geopolymerisation. In MK based mortars, A/B ratios below 0.75 produced dry, sandy mortars due to the lack of activating solids present causing incomplete dissolution.

Experimental design software was successfully used to develop empirical equations for accurately predicting performance properties of geopolymer mortars based on a mix design. These equations and contour graphs representing important relationships are a vital mix design tool in increasing the ease of geopolymer adoption by the construction industry.

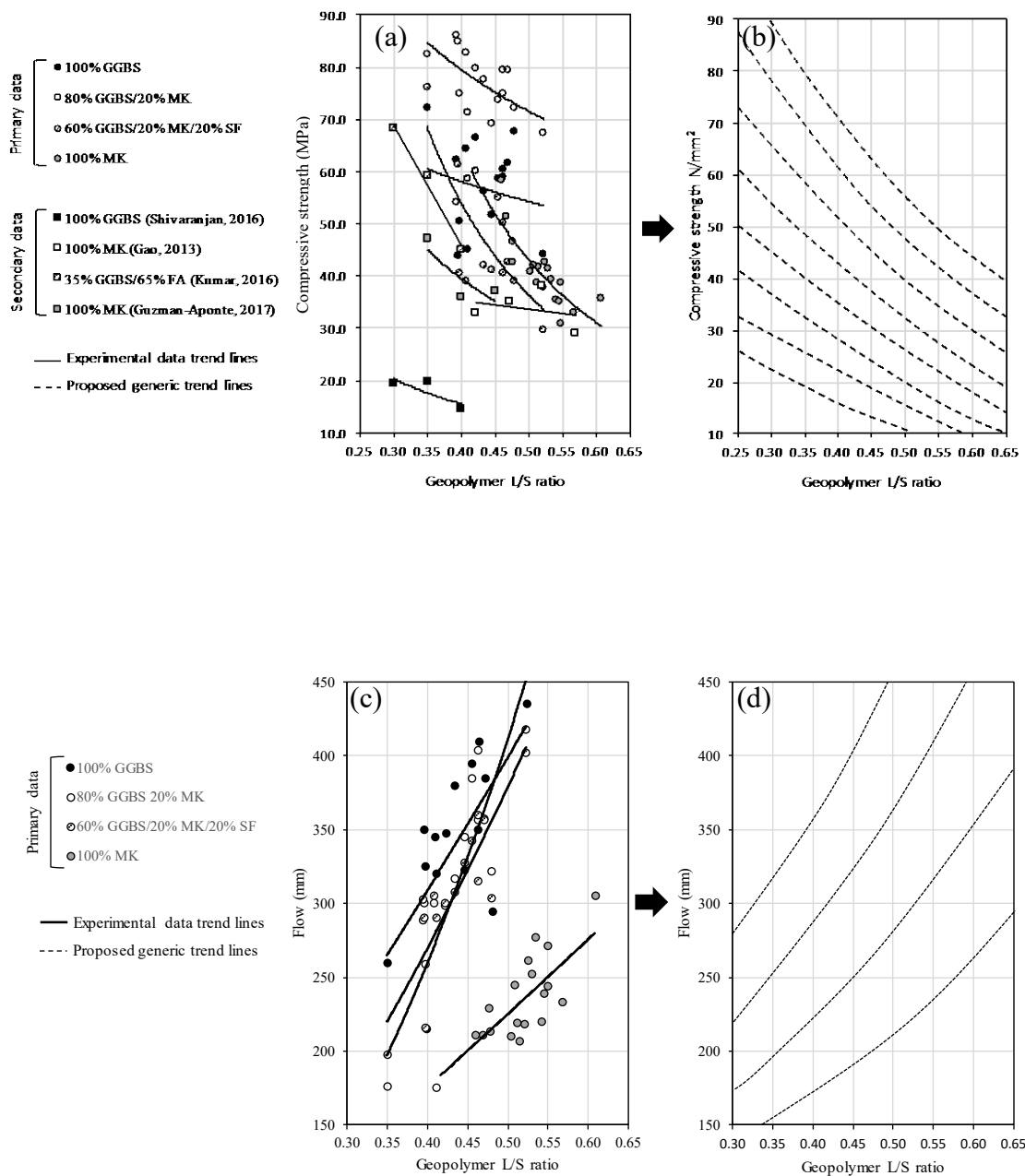
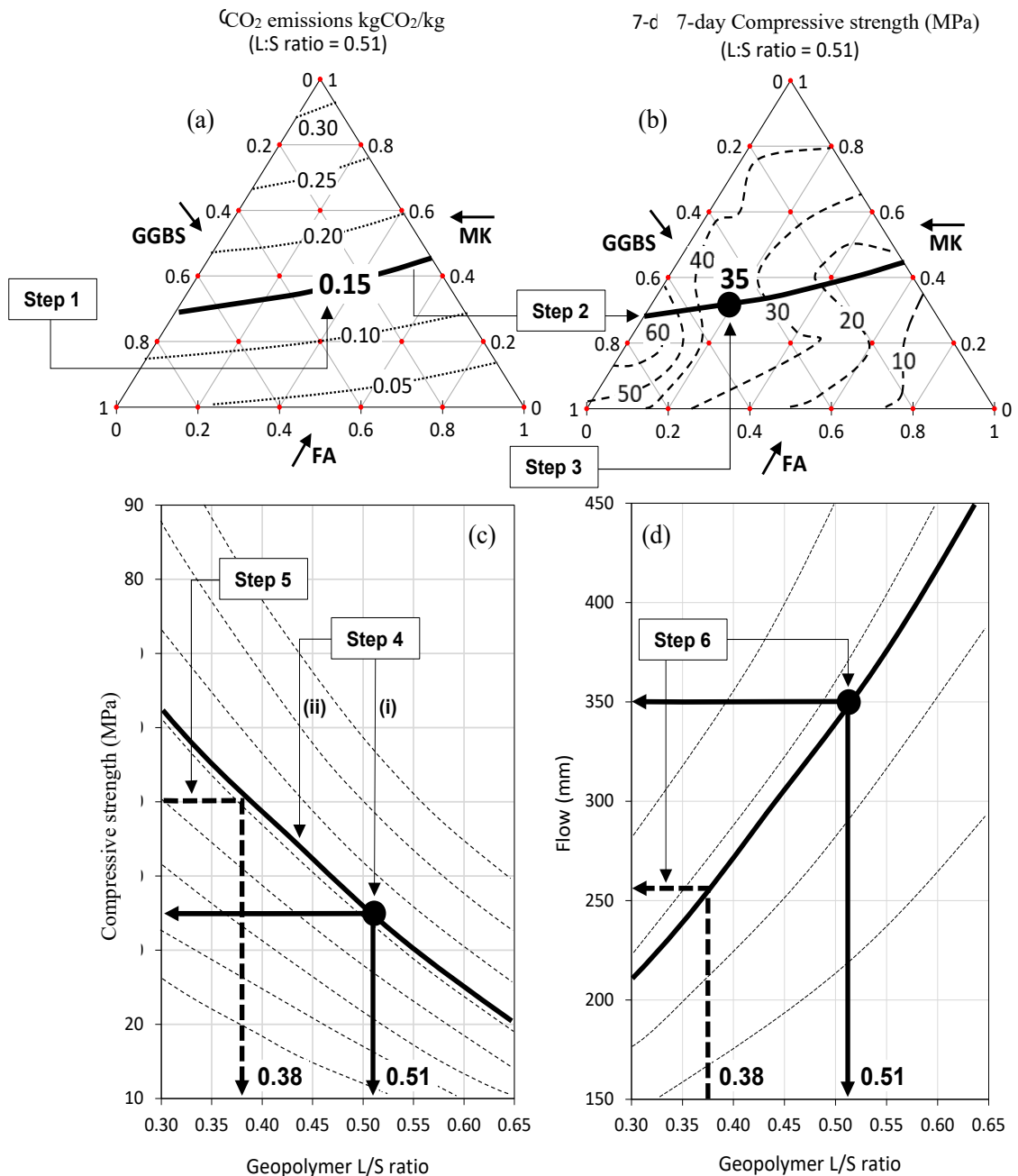


Figure 4.10. Relationships between flow and L/S ratio for various binder combinations



Example mix design requirements: 1) Max. embodied CO_2 content = $0.15 \text{ kgCO}_2/\text{kg}$; 2) 7-day strength = 50 MPa

Step 1: Highlight required embodied CO_2 equivalence line on ternary plot ($0.15 \text{ kgCO}_2/\text{kg}$ in example shown);

Step 2: Transpose embodied CO_2 equivalence line on to compressive strength ternary plot;

Step 3: Select appropriate binder combination (30% MK/50% GGBS/20% FA in example shown) and note corresponding 7-day compressive strength at L/S ratio of 0.51 (MPa in example shown) ;

Step 4: (i) Transpose performance level of chosen binder combination at L/S ratio 0.51 onto generic strength versus L/S ratio chart; (ii) Plot corresponding strength versus L/S ratio relationship curve for binder combination chosen;

Step 5: Use plotted curve to identify approximate L/S ratio required to achieve target strength (0.38 in example shown);

Step 6: Repeat steps 4 and 5 to predict approximate flow levels (260 mm in example shown);

Step 7: Undertake trial mixes and adjust proportions accordingly (not shown on figure).

Figure 4.11. Indicative mix design worked example

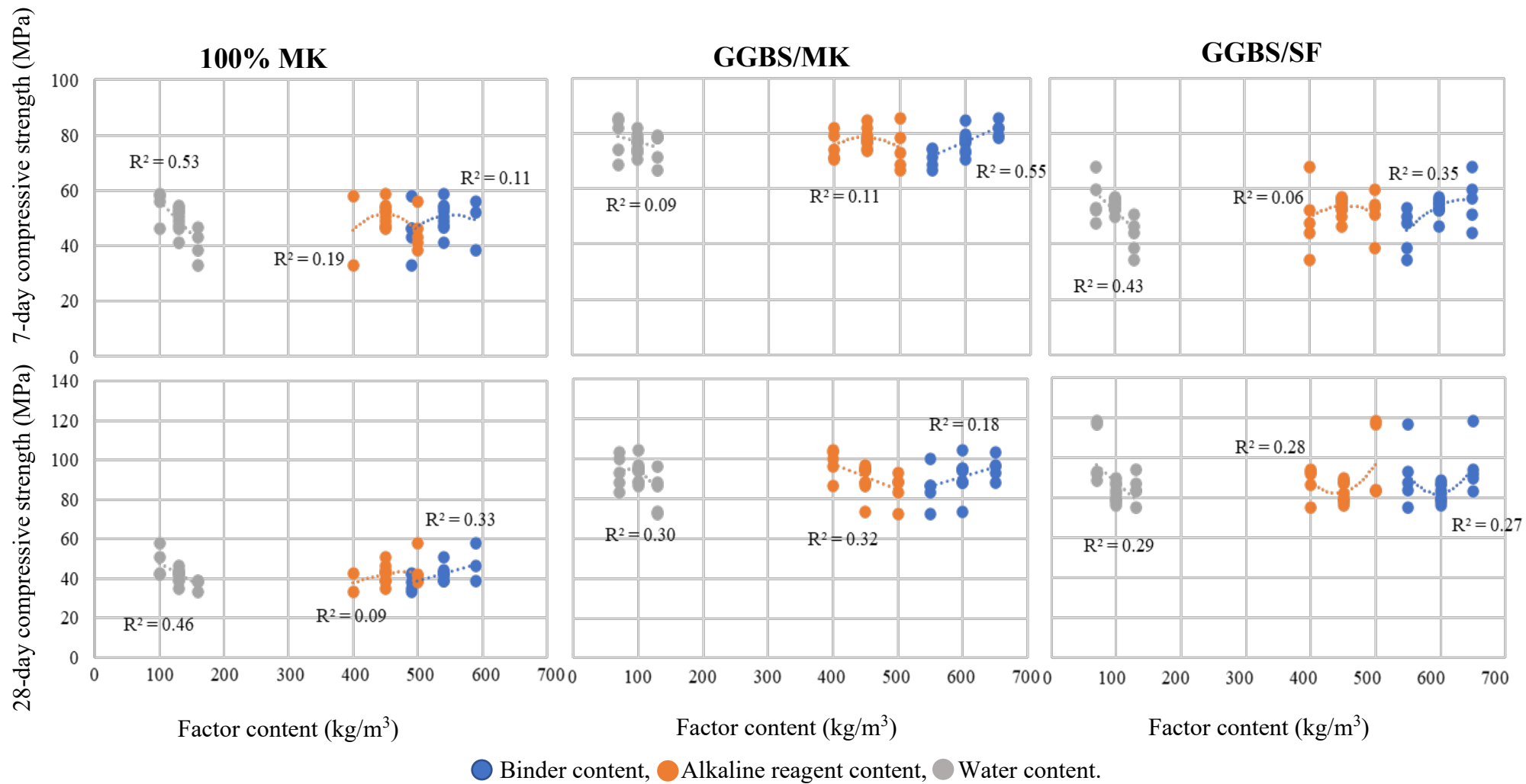


Figure 4.12. Experimental factors vs compressive strength

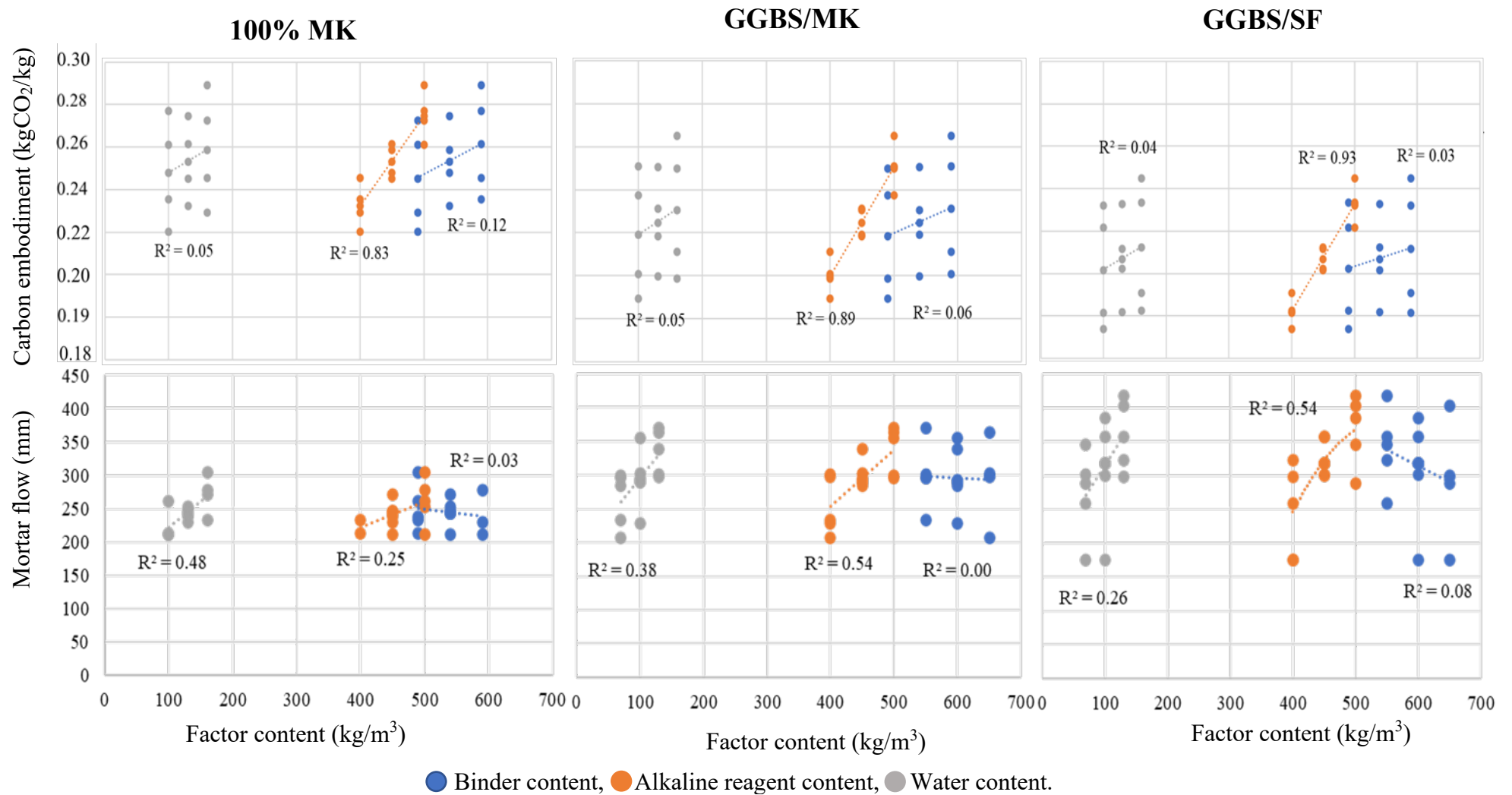


Figure 4.13 Experimental factors vs carbon embodiment and mortar flow

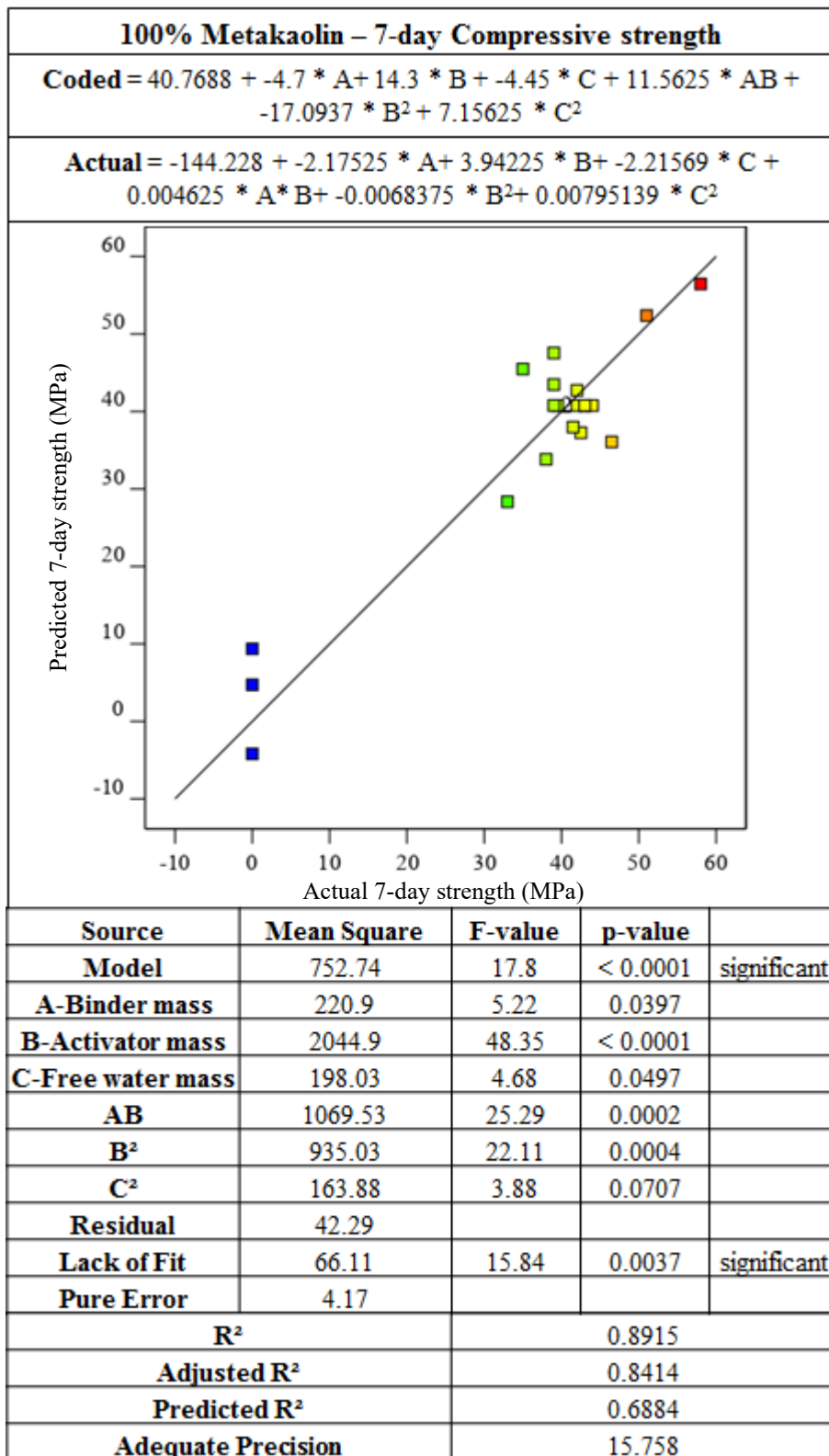


Figure 4.14(a). MK mortars: Analysed equation for 7-day Compressive strength

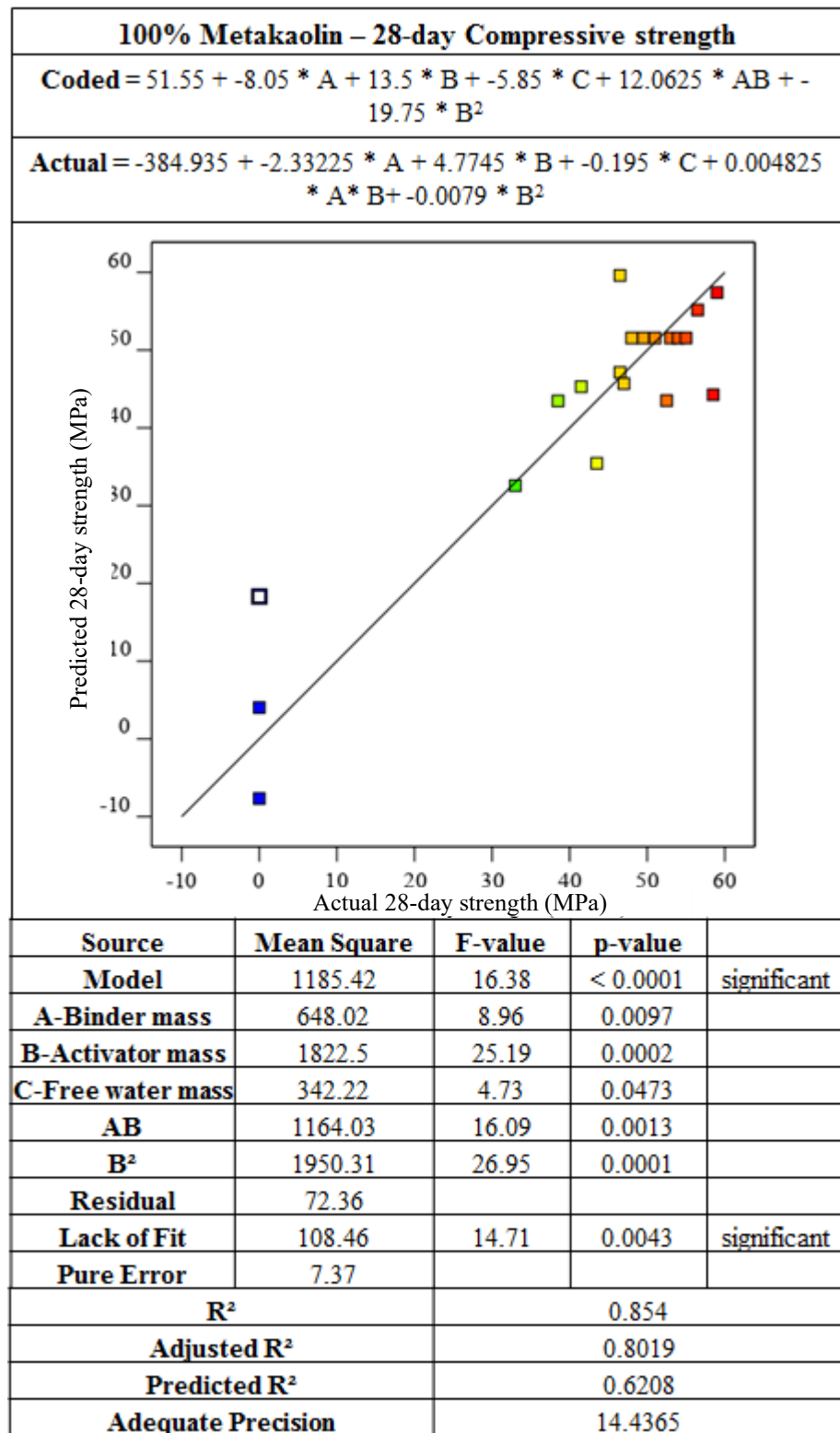


Figure 4.14(b). MK mortars: Analysed equation for 28-day Compressive strength

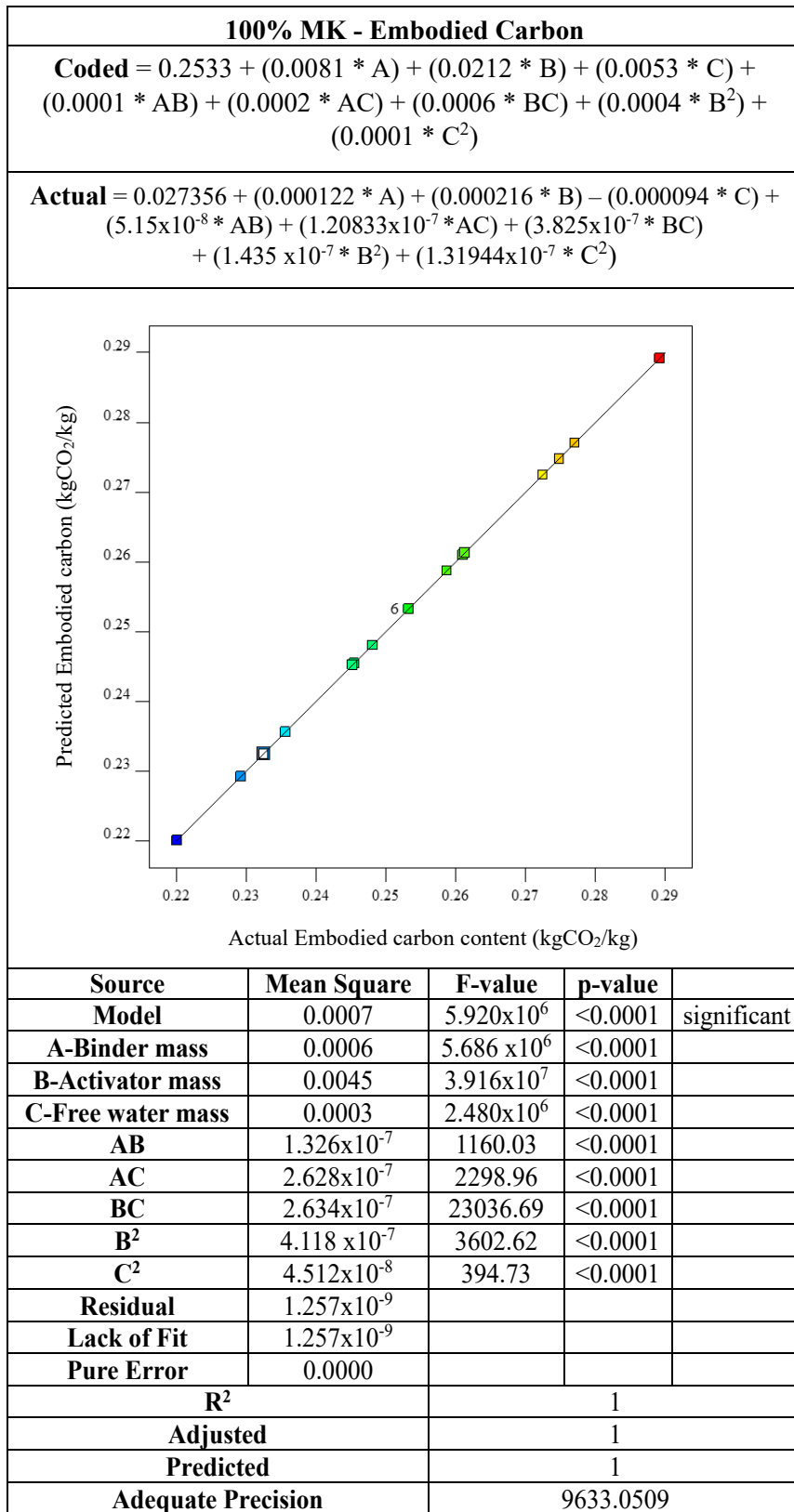


Figure 4.14(c). MK mortars: Analysed equation for embodied carbon contents

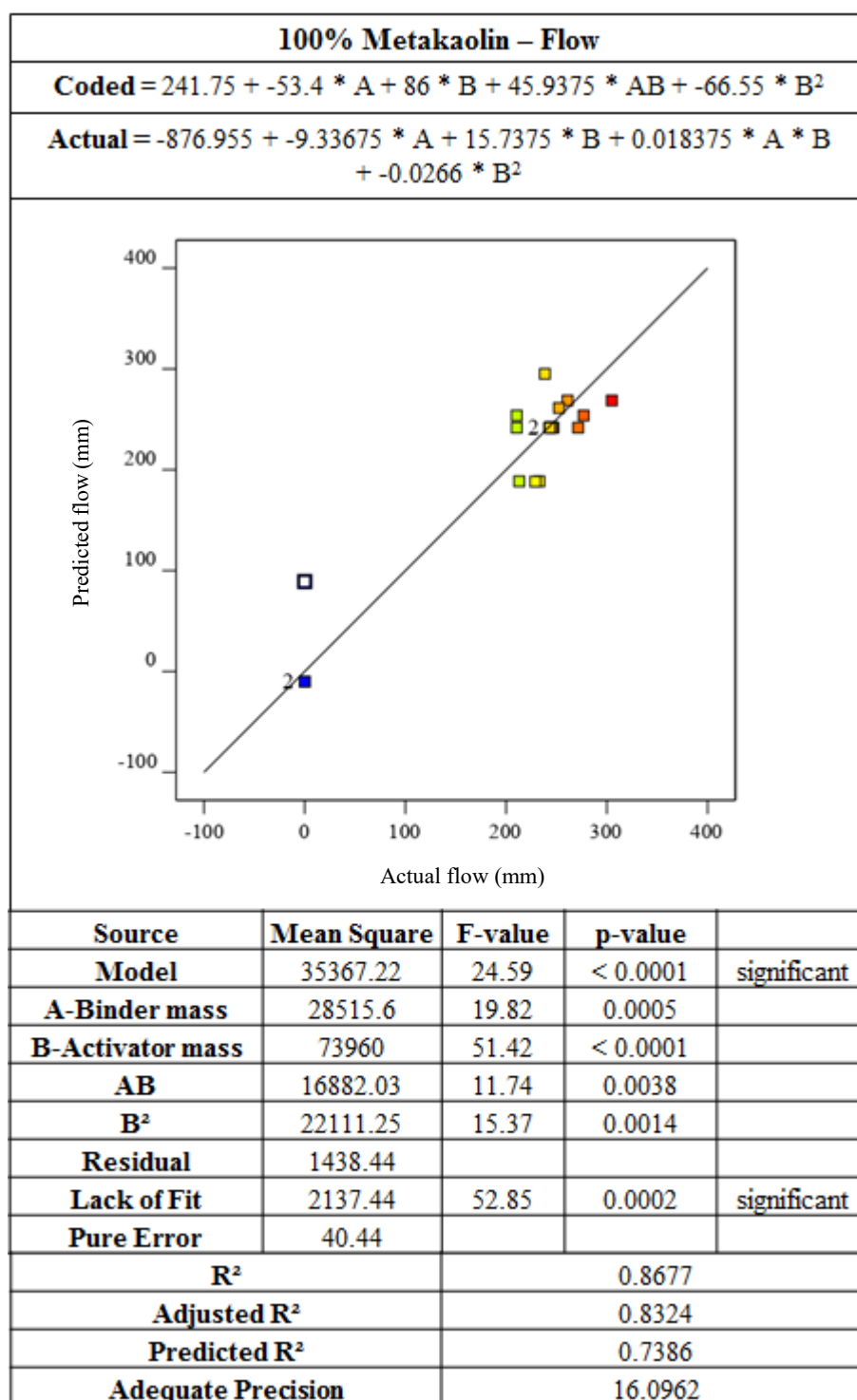


Figure 4.14(d). MK mortars: Analysed equation for flow

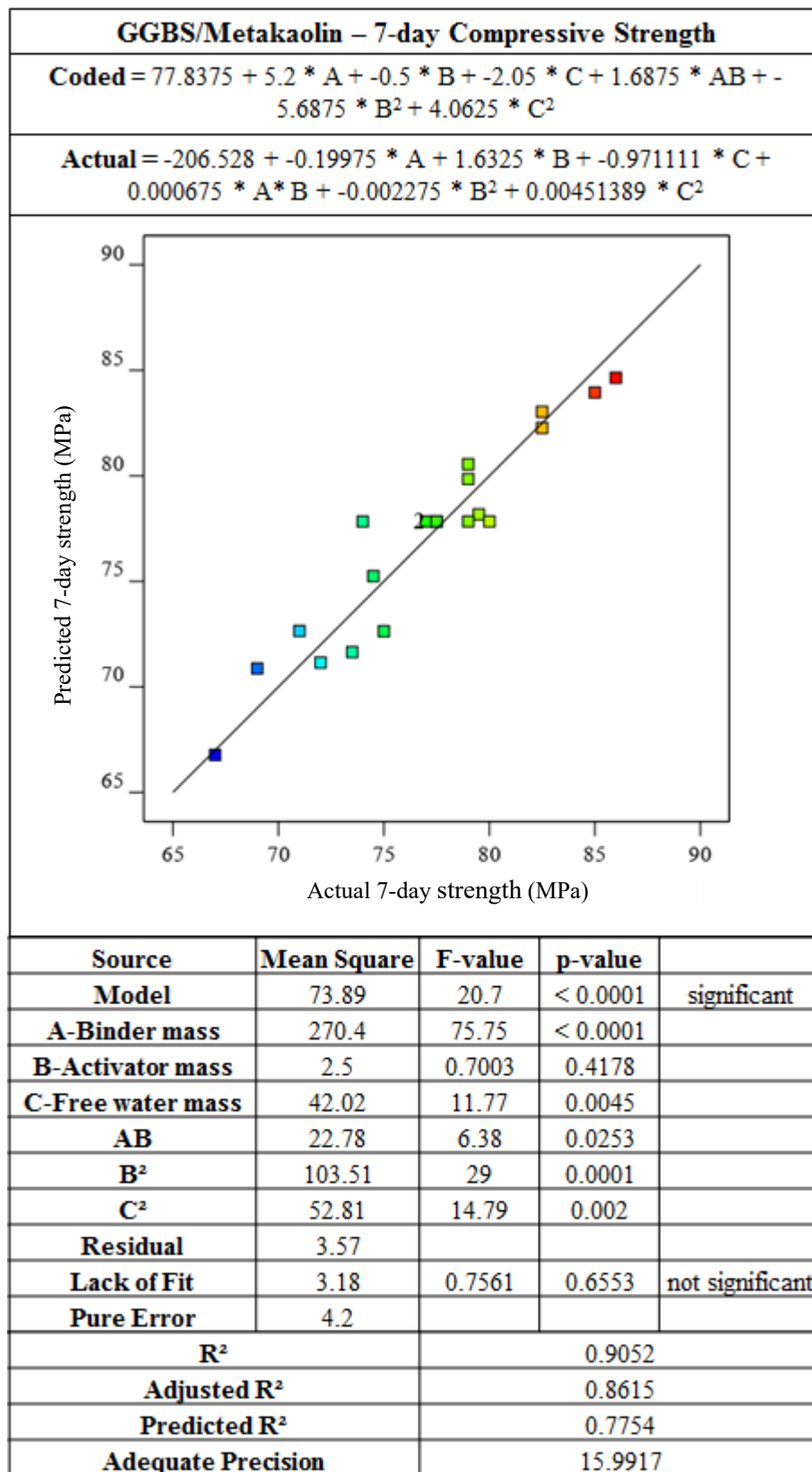


Figure 4.15(a). GGBS/MK mortars: Analysed equation for 7-day compressive strength

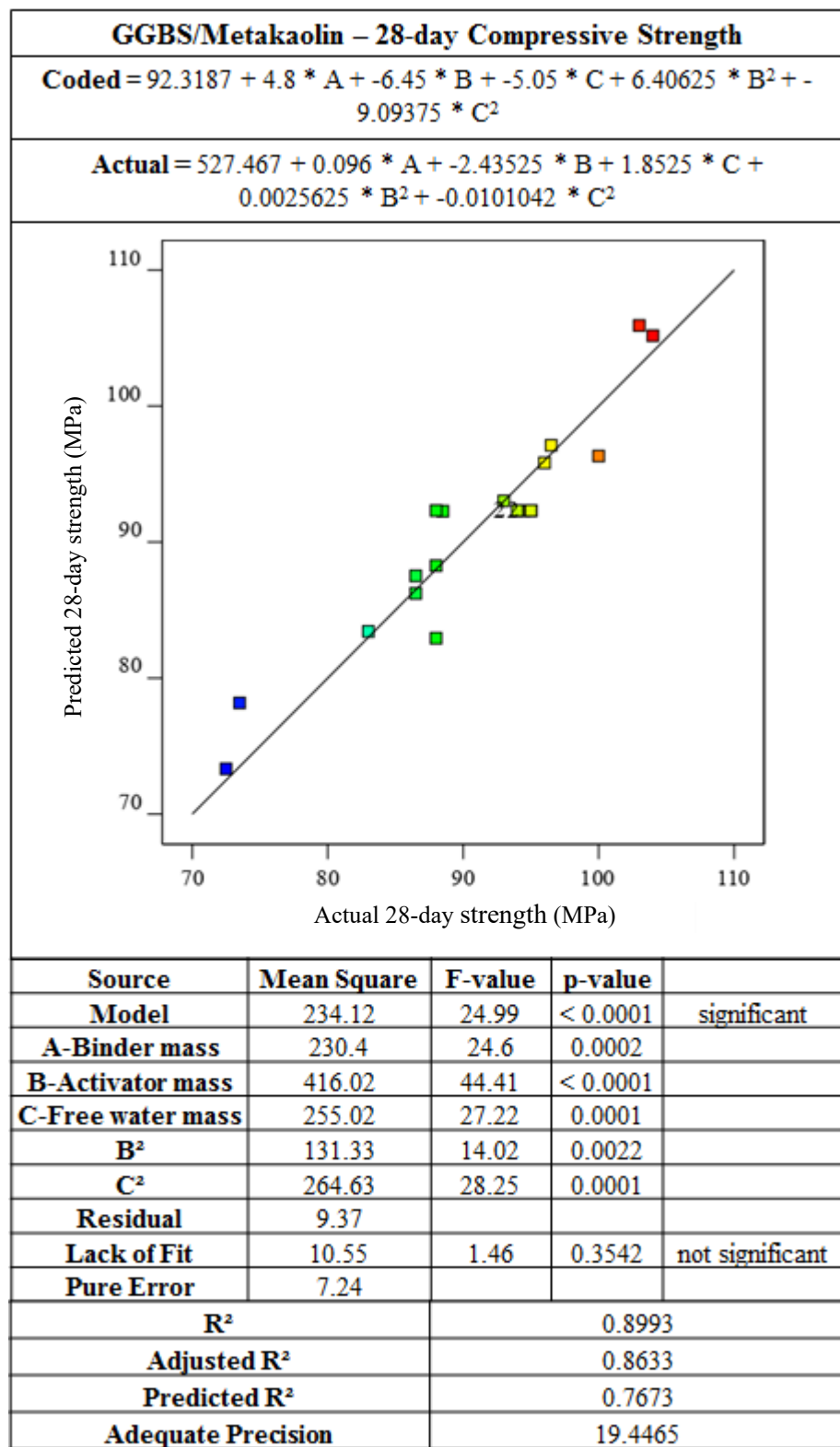


Figure 4.15(b). GGBS/MK mortars: Analysed equation for 28-day compressive strength

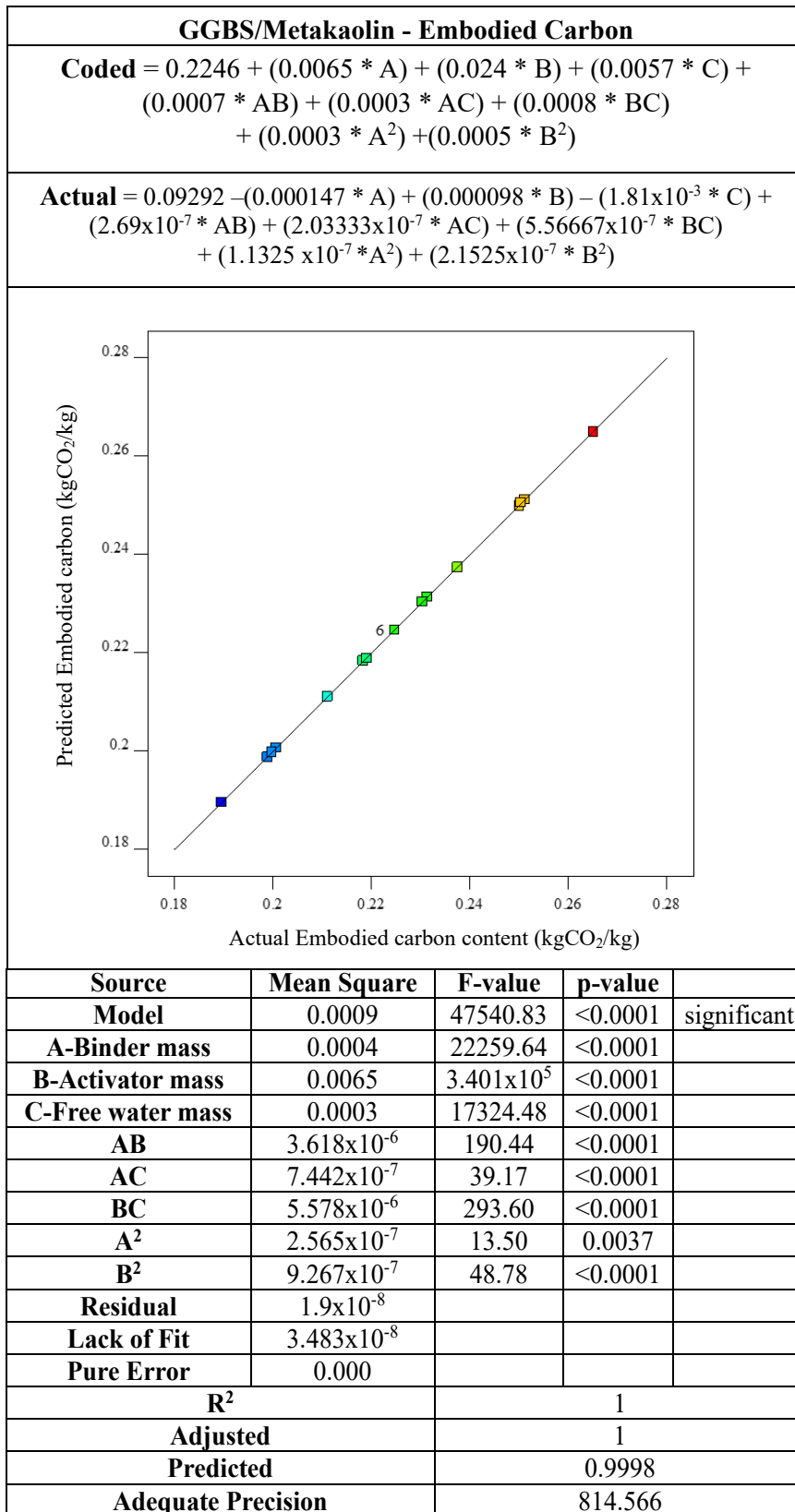


Figure 4.15(c). GGBS/MK mortars: Analysed equation for embodied carbon contents

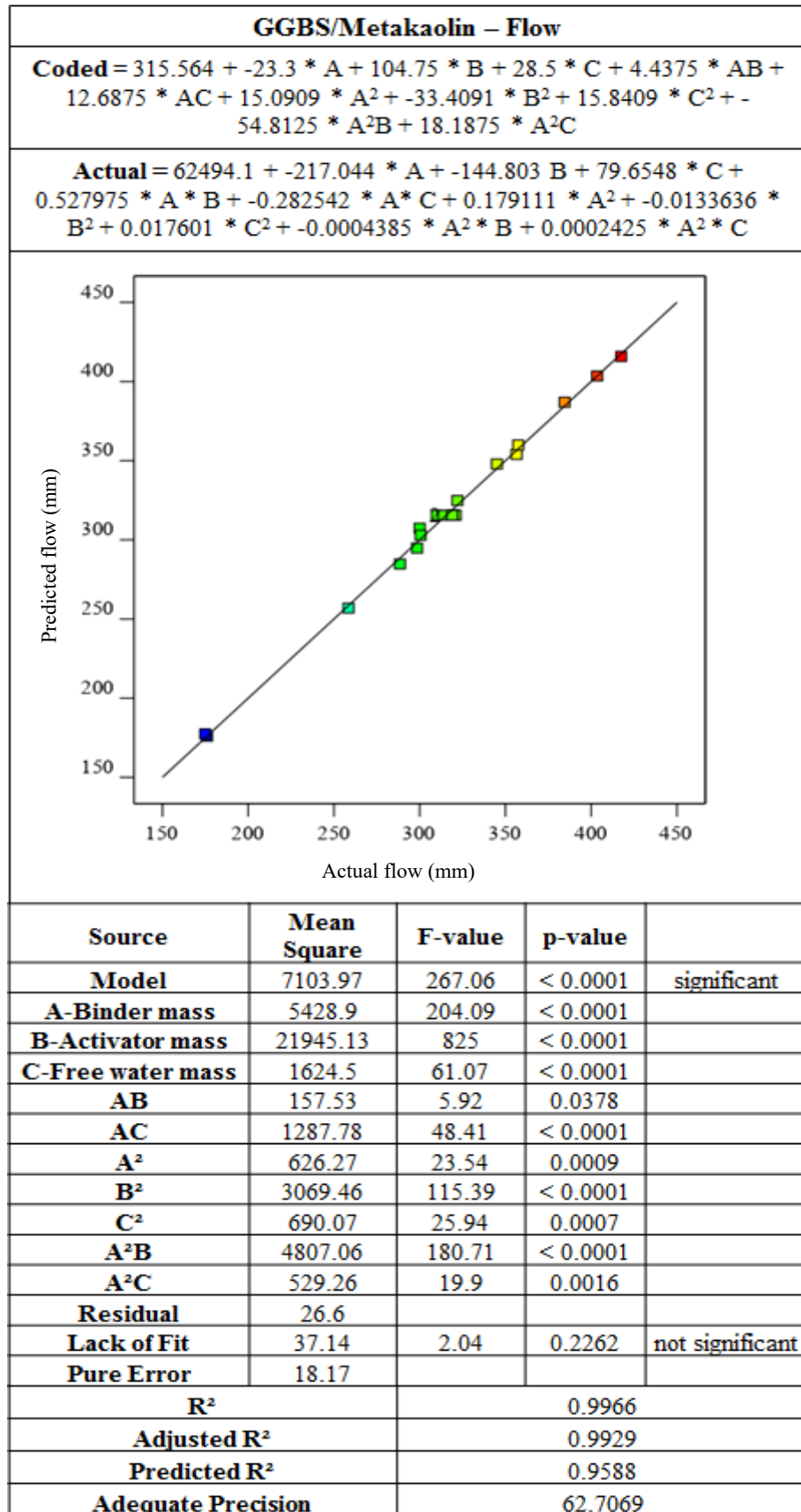


Figure 4.15(d). GGBS/MK mortars: Analysed equation for flow

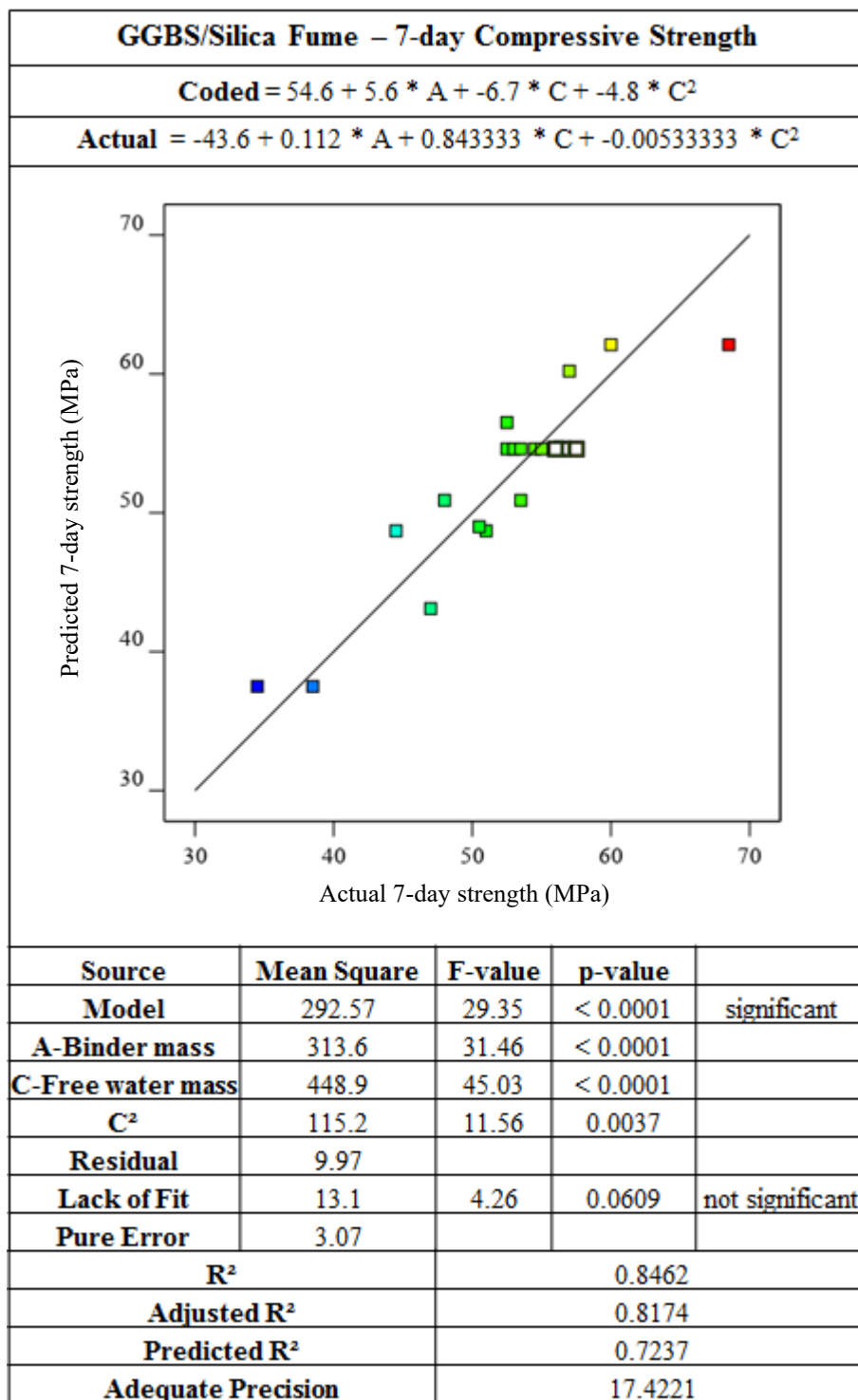


Figure 4.16(a). GGBS/SF mortars: Analysed equation for 7-day compressive strength

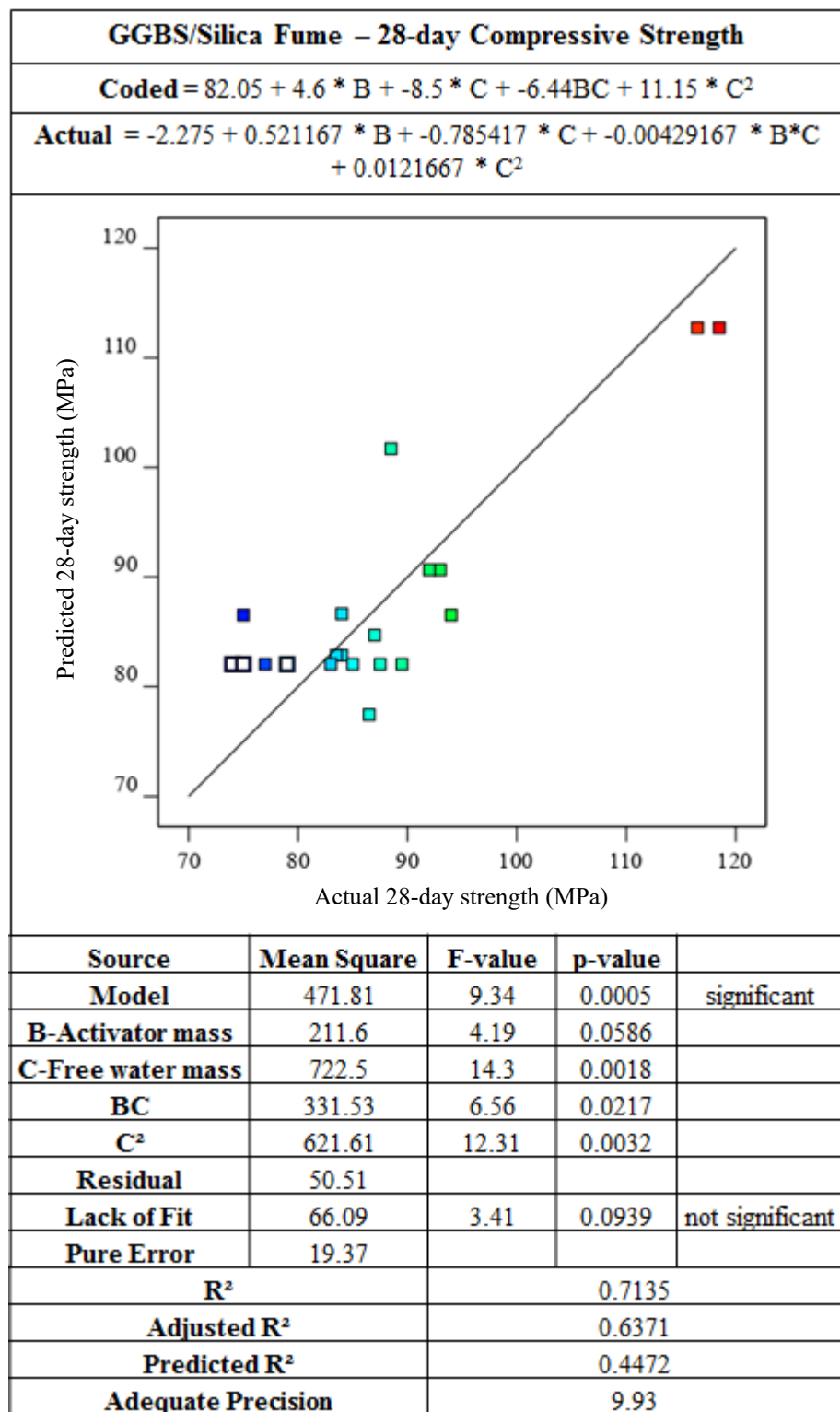


Figure 4.16(b). GGBS/SF mortars: Analysed equation for 28-day compressive strength

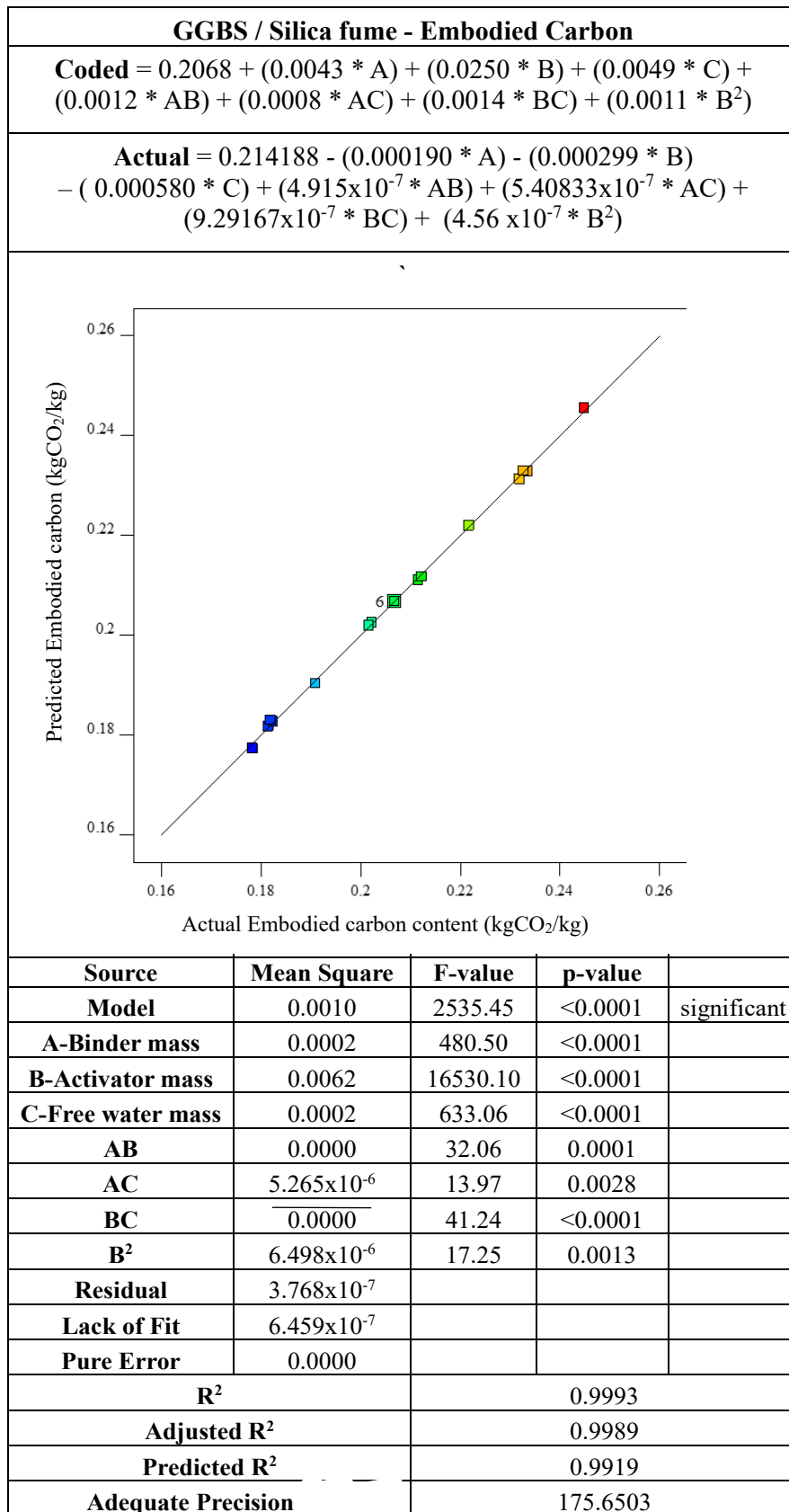


Figure 4.16(c). GGBS/SF mortars: Analysed equation for embodied carbon contents

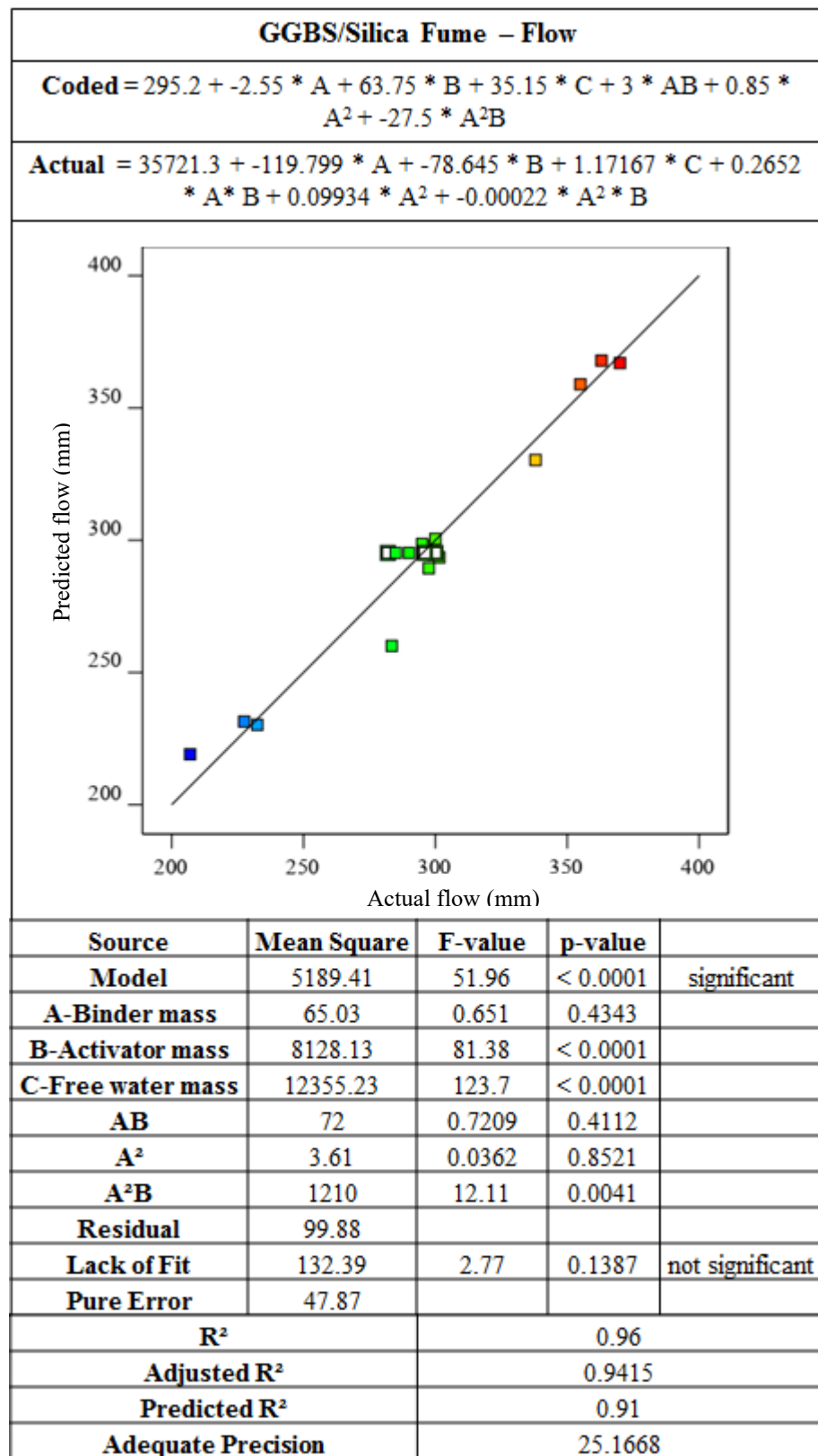


Figure 4.16(d). GGBS/SF mortars: Analysed equation for flow

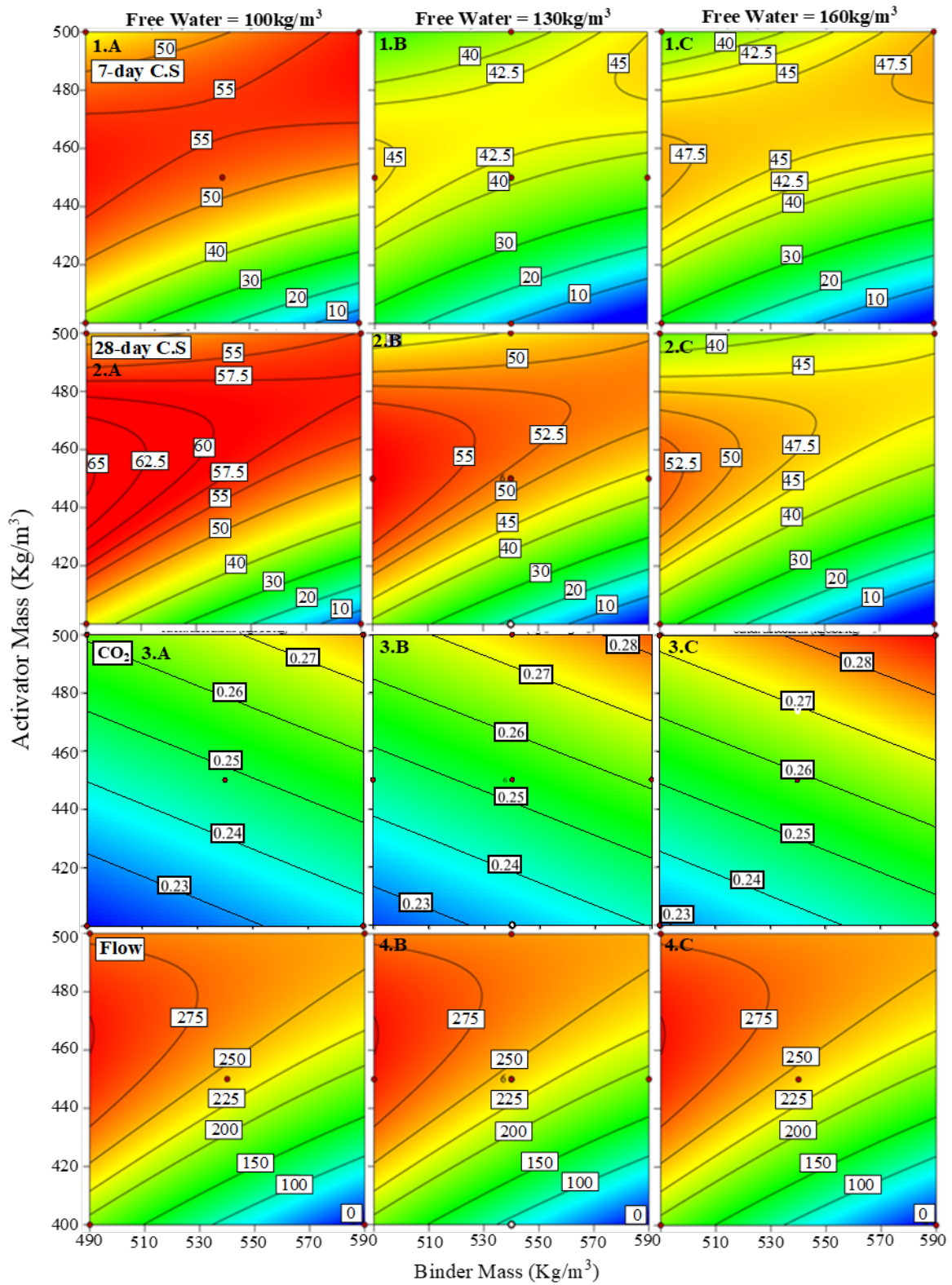


Figure 4.17. Contour plots for prediction of the 7-and 28 -strength (MPa), embodied carbon (kgCO_2/kg) and flow (mm) of MK-based mortars with increasing free water content

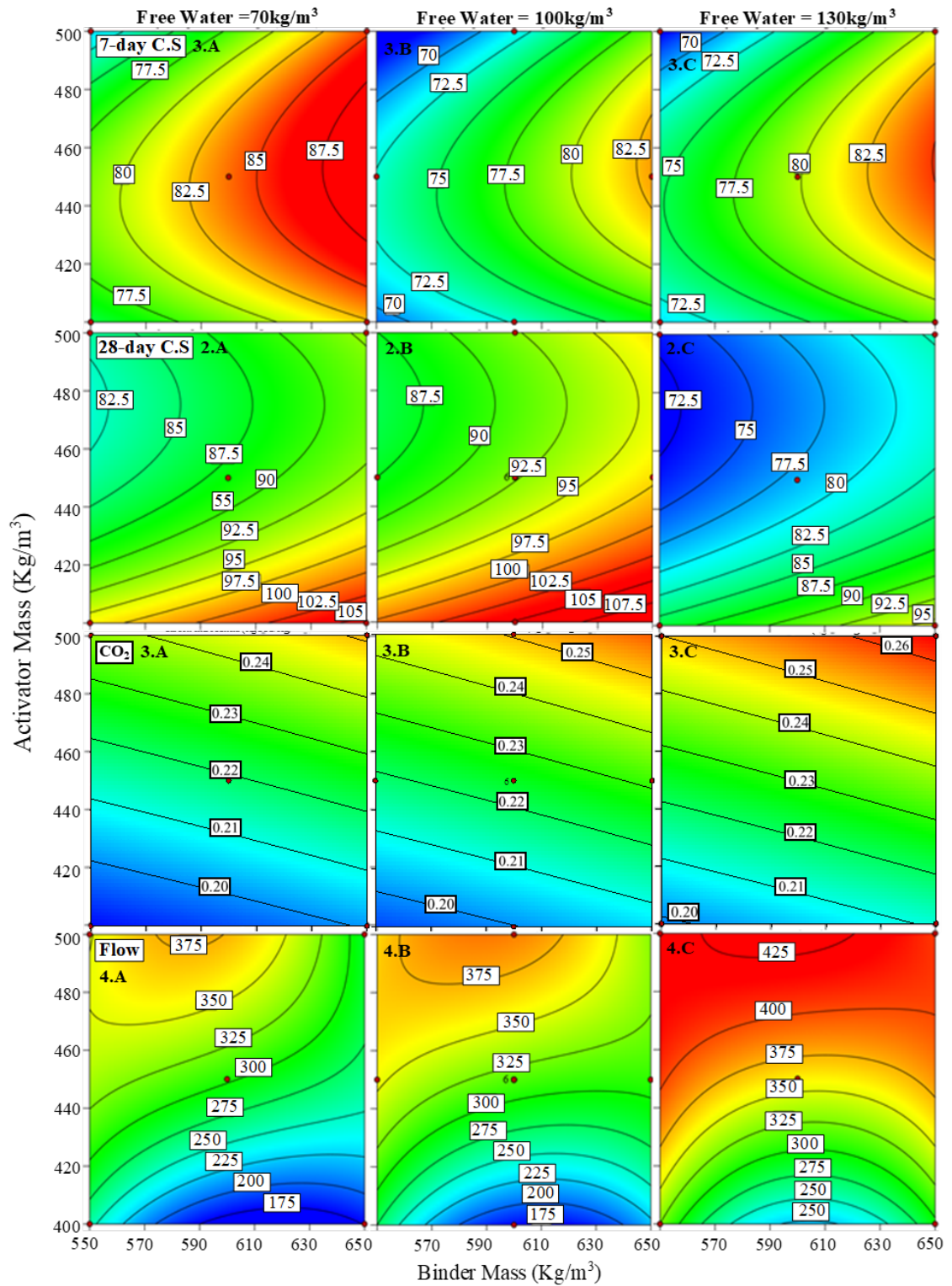


Figure 4.18: Contour plots for prediction of the 7-and 28 -strength (MPa), embodied carbon (kgCO₂/kg) and flow (mm) of GGBS/MK-based mortars with increasing free water content

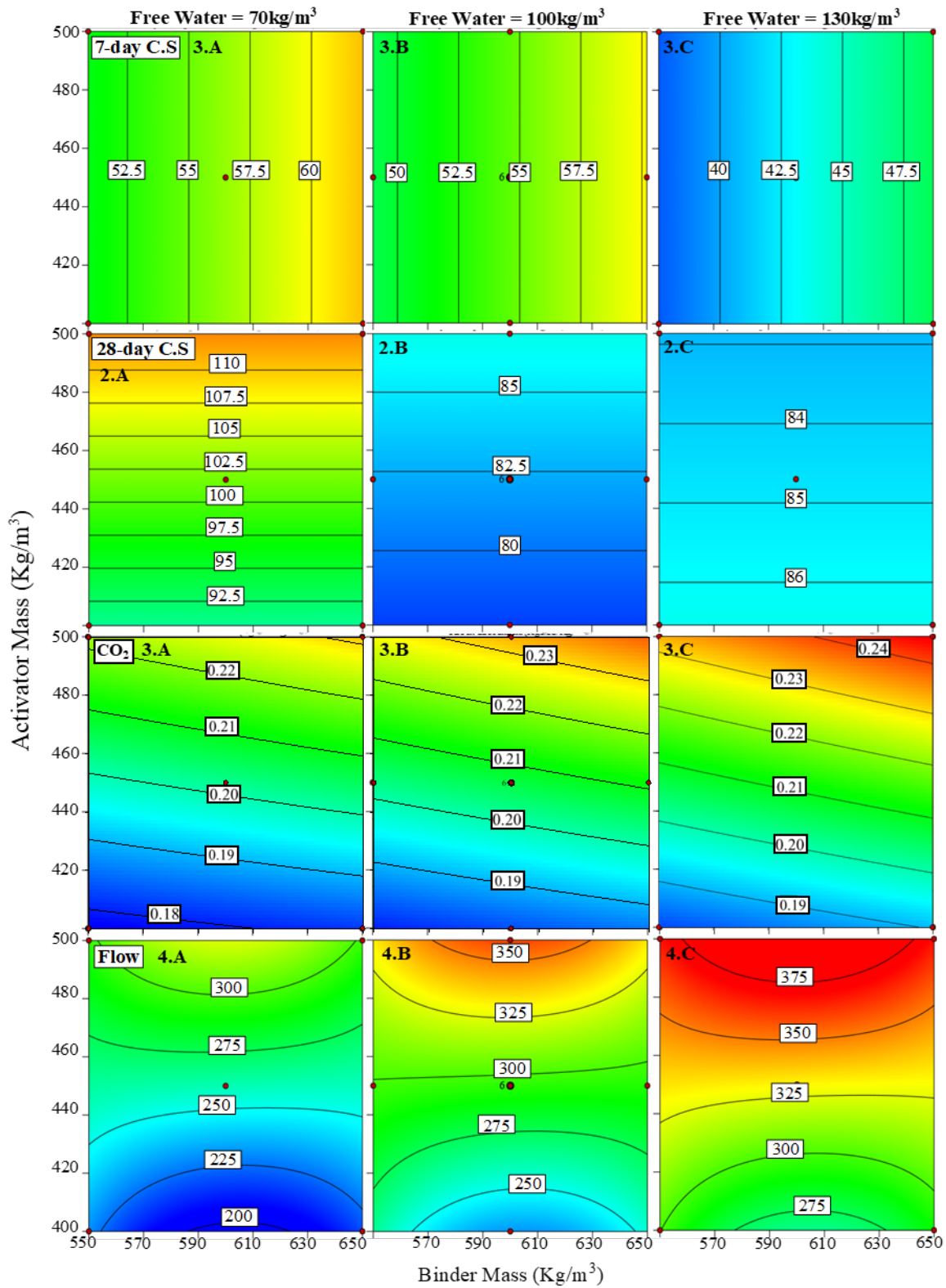
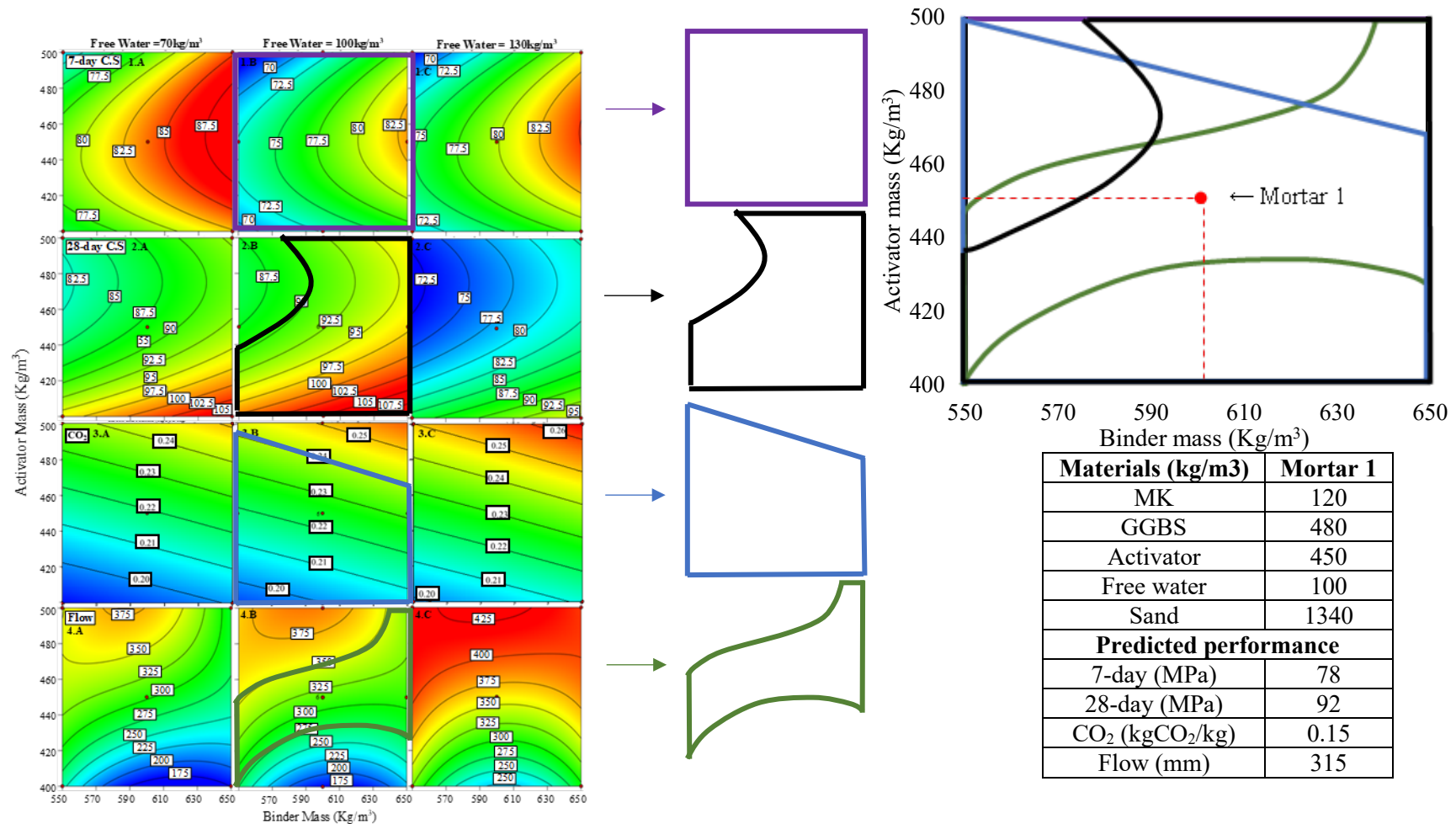


Figure 4.19. Contour plots for prediction of the 7-and 28 -strength (MPa), embodied carbon (kgCO₂/kg) and flow (mm) of GGBS/SF-based mortars with increasing free water content



Specification: 7-day strength > 40 MPa , 28-day strength > 90 MPa, flow = 275-350 mm, embodied carbon <0.24kgCO₂/kg

Step 1: For a given binder type (GGBS/MK) select a water content likely to produce the required performance levels.

Step 2: Create an outline of the areas in each contour plot where values are predicted to meet or exceed requirements.

Step 3: Super-impose these shapes onto a clean contour plot at the same scale to create a Venn diagram.

Step 4: Select any point inside the area confined by all four outlines (see mortar 1). This will give the binder and activator mass required.

Figure 4.20. Proposed contour-based mix design methodology

Chapter 5 – Assessment of fibre reinforced geopolymer mortar panels

5.1 Introduction

This chapter investigates a range of fibre/matrix compositions to identify an optimal method for combining the high strength geopolymer mortars created in the previous chapter with fibre reinforcement. This aimed to improve the flexural strength of these mortars such that they would become suitable materials for cladding structures in a similar manner to GRC.

Geopolymeric materials are often less alkaline than PC materials and basalt fibres have increased resistance to alkaline degradation (Ivashchenko, 2009; Geopolymer Institute, 2006). Hence, there is the potential to create a GRC-like material from basalt fibre reinforced geopolymer mortars that may not require zirconium dioxide protection. No general-purpose sizings are available as they are bespoke and designed to give a specific type of fibre a strong affinity to the choice of matrix material. Sizing also protects the fibre during the specific fibre production processes and control how the material behaves to suit each unique application (Lin et al., 1999; Downey and Drzal, 2016; Ivashchenko, 2009). To date, no specialised sizing treatment has been developed for geopolymer fibre composites. Hence, opportunities exists for the development of innovative sizing techniques that could revolutionise the performance levels of the materials.

This chapter focusses on assessing whether existing sizing technologies for optimising fibre/matrix bond in PC-basalt fibre composites can be applied to geopolymer-basalt fibre composites. Flexural strength was selected as the chief engineering parameter for assessing the effectiveness of such sizing technologies for a range of fibre/geopolymer mortar combinations. These composites were based on the mortars developed in chapter 4 (Tables 3.3-3.6), which were reinforced with different fibre types and addition levels to enable the identification of the most suitable material configurations.

Once basalt fibres and a GGBS/metakaolin mortar were selected, work proceeded to identify which fibre diameters and sizing techniques provided the greatest performance. Flexural strength was monitored over time.

The ultimate goal of this chapter was to produce a fibre composite configuration with flexural strength values similar to that of the GRC control, as this would make the resulting materials suitable to form a strong, lightweight building cladding panel. The metrics used to assess flexural strength included LOP and MOR; whereby the difference between these values is representative of the post crack toughness. Finally, the compressive strength of the fibre matrix compositions was assessed against those of the unreinforced mortar. The results were compared against a benchmark set by a pre-mix GRC product that is currently used for building cladding applications. This work was carried out in two phases to consider the 4-point bending testing of GRC vs glass, basalt and steel fibre reinforced geopolymer composites when undertaken to GRCA standards (Phase 1) and then to ASTM C974-03 (Phase 2).

5.2 Phase 1: 4-point bending testing of GRC vs glass, basalt and steel fibre geopolymer composites to GRCA standard

5.2.1 Introduction

Preliminary fibre matrix investigations used 4-point bending tests (GRC standard test method 3) to calculate the flexural strength achieved by a range of fibre matrix compositions and determine the most suitable (GRCA, 2017). The fibres used in this preliminary testing included chopped glass, basalt and micro-steel fibres. This GRC standard was initially chosen as none currently exist for the testing of fibre reinforced, geopolymer composites and GRC is a similar material used in similar applications. These standards are widely used and allowed analysis of test results and secondary data through proven methodologies and direct benchmarking against GRC. Samples were tested at 7

days to give an early understanding of the relative success of both the test method and material studied before taking further time to age samples.

5.2.2 Composites

The geopolymer composites considered were based on two of the highest performing binders developed in Chapter 4; namely Mortar A composed solely of GGBS and Mortar B, a 80%GGBS/20%SF binder. These mix designs were selected due to their high flowability, high strength and low embodied CO₂ contents, which are shown in Table 5.1. The mixes have slightly lower compressive strength at 7 days compared with the 73 MPa achieved by the GRC control.

Table 5.1. Performance properties and mix design of unreinforced geopolymer matrix mixes.

Mix Components (kg/m³)	Mortar A	Mortar B
GGBS	605	484
Silica fume	0	121
Activator	453	453
Water	134	134
Sand	1340	1340
Fibre volume 1% (cm³)	9.4	9.5
Fibre volume 2% (cm³)	18.75	19
Performance Properties		
Flow	323 mm	260.5 mm
7-day Compressive strength	57 MPa	52 MPa
28-day Compressive strength	68 MPa	106 MPa

Four-point bending tests were initially performed on unreinforced mortar samples without fibre reinforcements and then with chopped glass, basalt and micro-steel fibres at dosages of 1 and 2% of the total composite volume. The fifteen composite iterations considered and their relative values of LOP and MOR are shown in Tables 5.2 and 5.3. The composite abbreviations adopted (for example, A-G2), refers to the mortar used (Mortar A or B), fibre type (G= glass, B=basalt, S=steel, NF=no fibres) and fibre dosage (1 or 2% by volume).

5.2.3 Load/displacement curves

The load/displacement curves from the GRC control samples are presented in Figure 5.1, whose general shapes are similar to theoretical curves as shown on Figure 2.2. However, there is a significant deviation between the 4 load/displacement curves. This is likely associated with the rough surface texture of the samples and the lack of force centring capabilities of the test device stipulated in the GRCA test standard (GRCA, 2017). Evidence of some strain hardening was exhibited by most samples after LOP had been reached, prior to reaching their respective yield points.

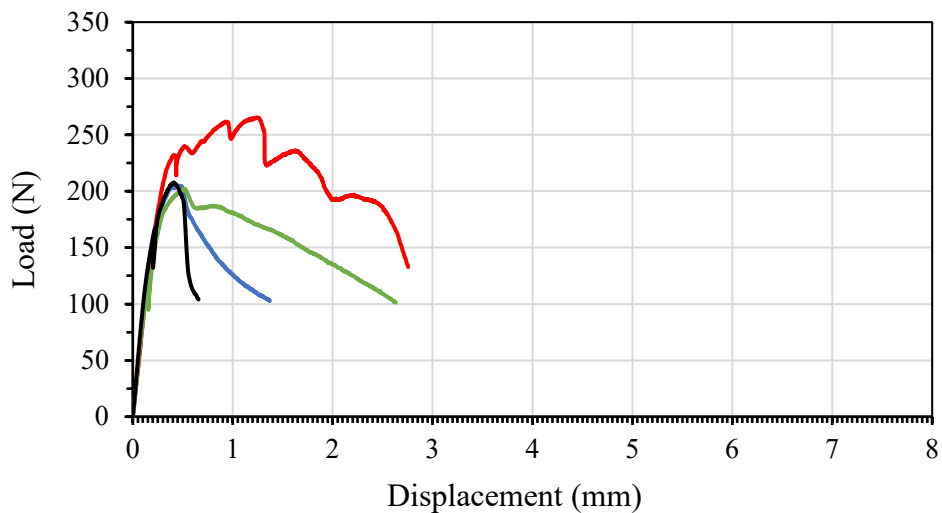


Figure 5.1. Load/displacement curves for GRC control samples.

Load/displacement curves for the geopolymer-fibre composite samples are presented in Figures 5.2 and 5.3. The curve morphologies for glass and basalt fibre reinforced composites were similar to those of the GRC control, indicating similar behaviour in response to loading. This is beneficial for the material, if it is to satisfy engineering standards and fulfil the same building cladding applications as GRC. Furthermore, the load/displacement curves generally exhibited successful development of composite action between the fibres and the cementitious matrix of the mortars, indicating suitability for their synergistic use.

Load/displacement curves for the steel fibre reinforced samples exhibited more complex behaviour and larger variation in results compared with samples containing other fibre materials; whereby some samples experienced brittle failure once first crack was initiated. An irregular trend in the load/displacement curves after the formation of the first crack signified the pull out (or failure) of individual crack bridging fibres, often after the matrix had crumbled away. Little to no fibre reinforcement was to be found at the point of failure in samples that experienced brittle failures, and a greater volume than would be expected were present in those with more ductile failure modes. Composites A-S1 and B-S2 showed some evidence of an increase in load after first crack, signifying a modest strain hardening effect.

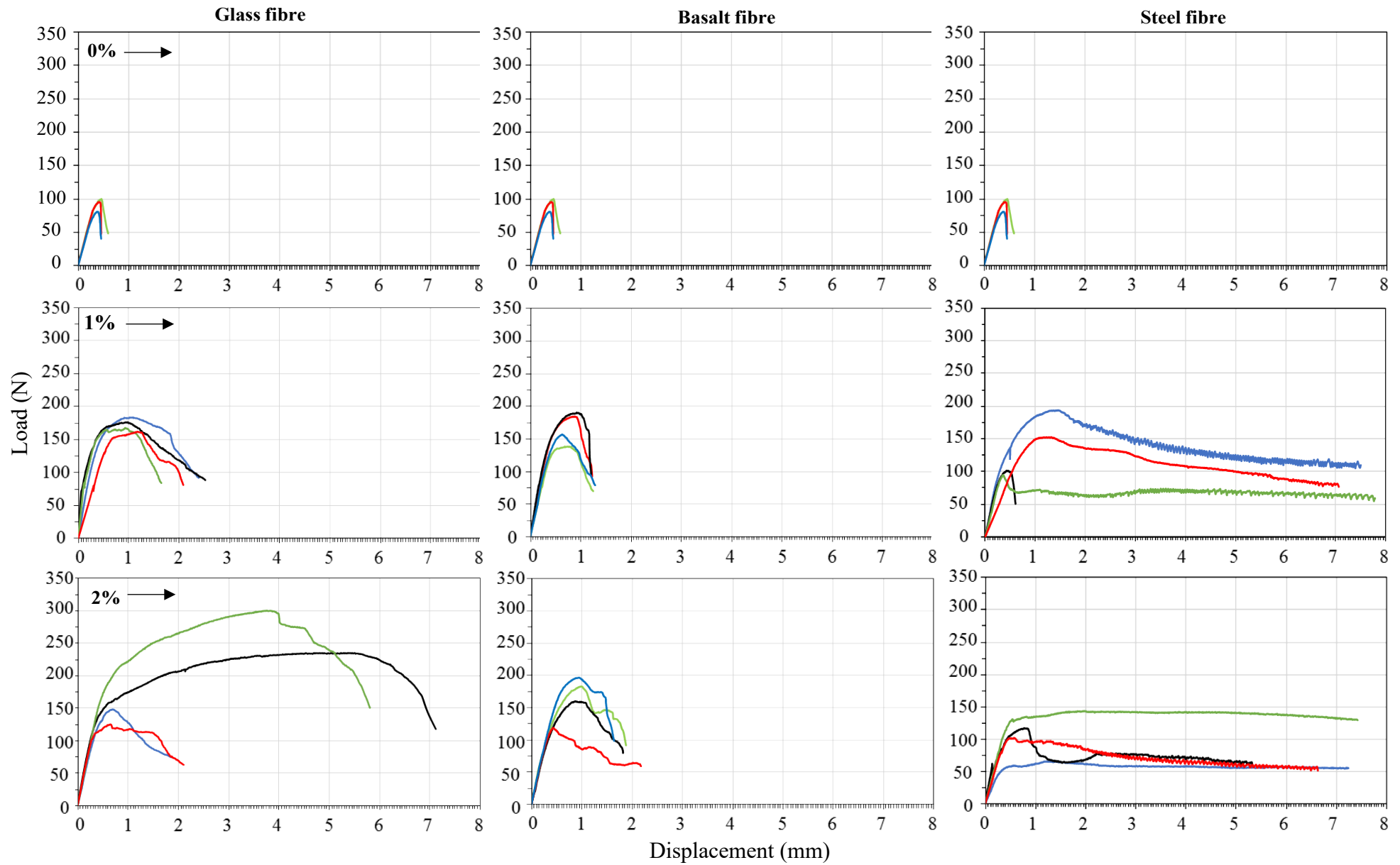


Figure 5.2. Load displacement curves for Mortar A with glass, basalt, and steel fibre reinforcement (0, 1 and 2% volume).

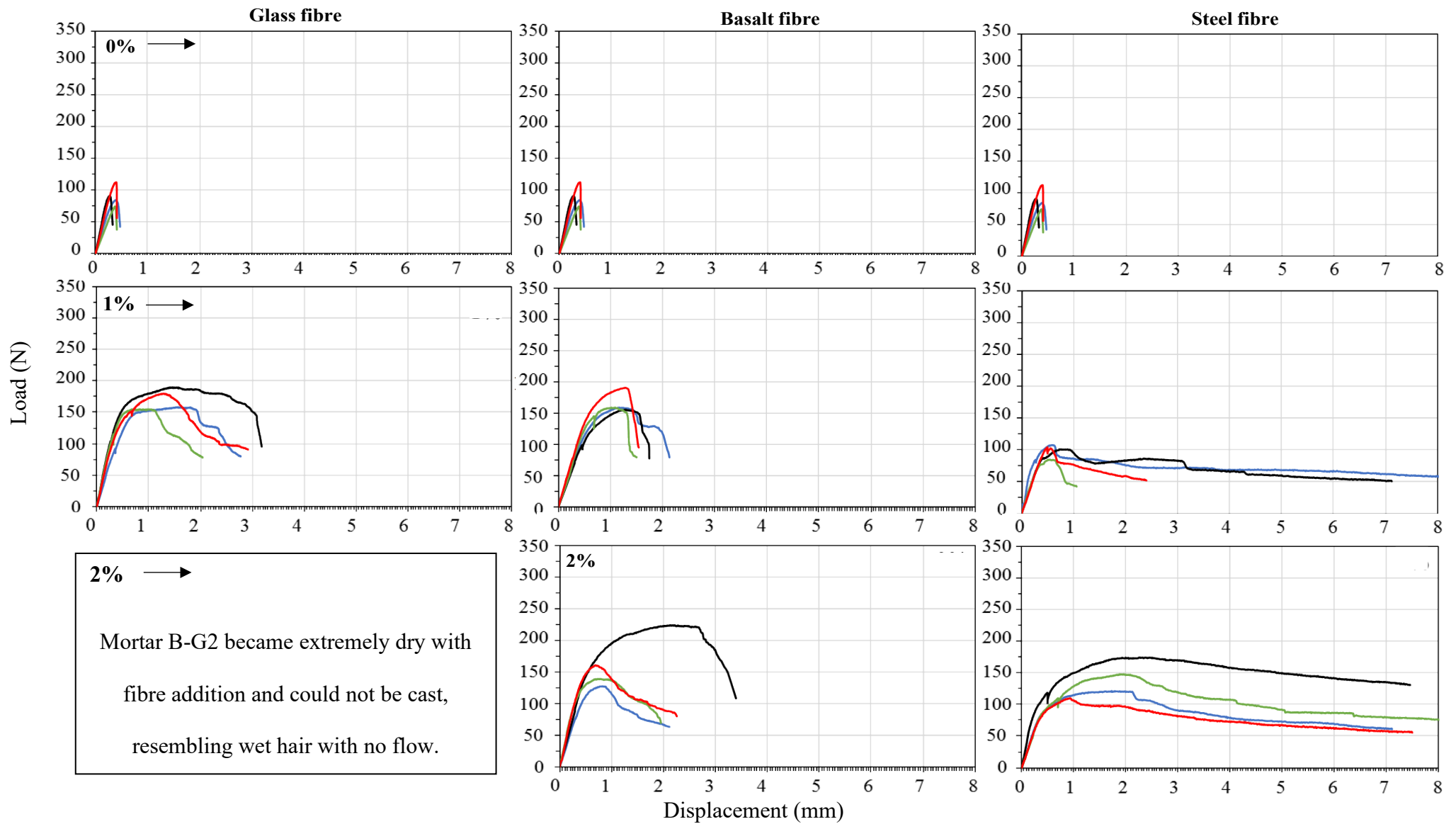


Figure 5.3. Load displacement curves for Mortar B with glass, basalt, and steel fibre reinforcement (0, 1 and 2% volume).

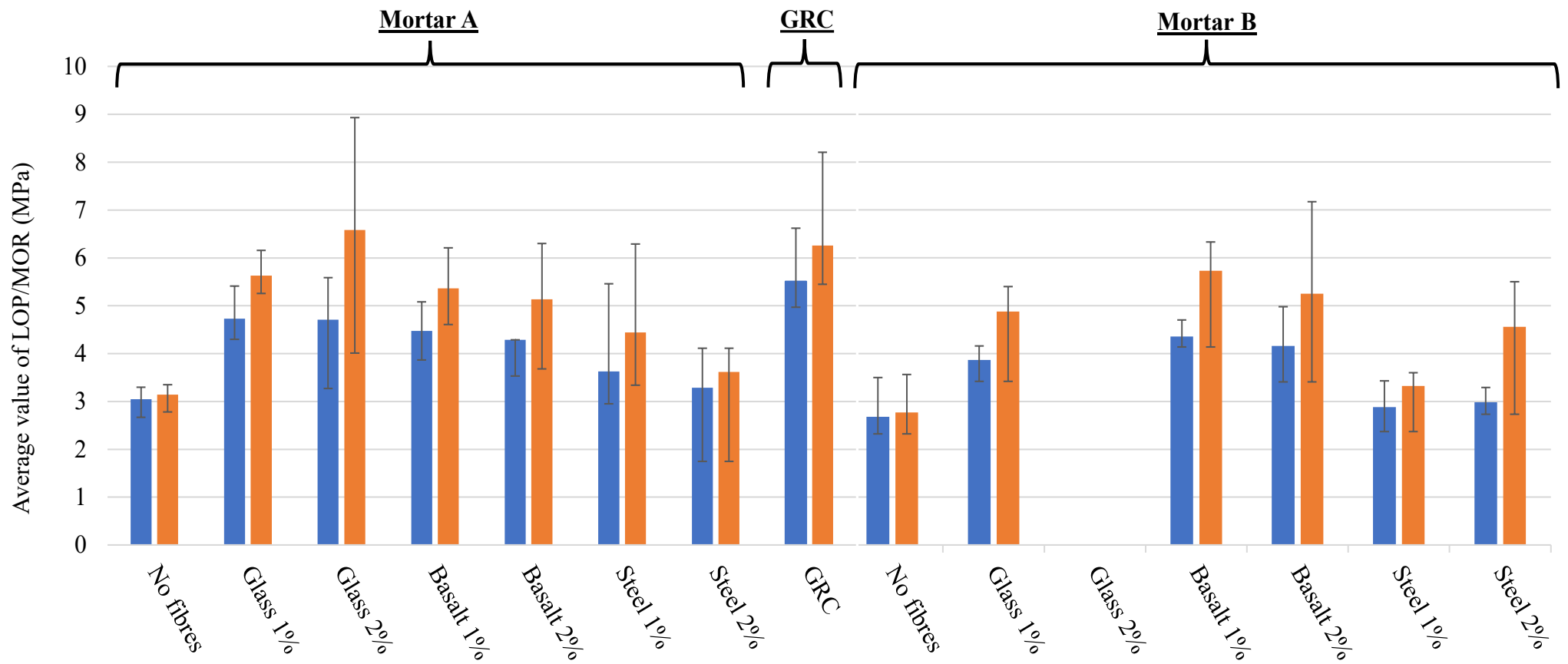


Figure 5.4. LOP (■) and MOR (■) results (GRCA method). Note: error bars represent maximum and minimum values from 4 tested samples.

5.2.4 LOP and MOR results

With regards to LOP, the commercial GRC product exhibited the highest average value of 5.5 MPa. In comparison for Mortar A mixes, values for the glass, basalt and steel reinforced samples were on average 86%, 79% and 63% of this value, respectively.

In terms of Mortar B, the glass, basalt and steel fibres achieved on average 70%, 77% and 53% of the control value, respectively. The low average LOP of the glass fibres in Mortar B compared with Mortar A can be partially attributed to samples reinforced with 2% glass fibres were too dry to form or be tested, and therefore were given a value of 0 MPa.

Mortar A provided greater LOP values than Mortar B when they contained no fibres, contained all fibre types and addition levels. This was unsurprising as the compressive strength of the mortar was higher and viscosity was lower, which allowed all compositions to be formed and tested.

Table 5.2. Relative LOP and MOR of fibre/matrix compositions.

Mix abbreviation	Mix composition		Relative LOP	Relative MOR
	Mortar	Fibre addition		
GRC	Pre-bagged product		1 st (100%)	2 nd (95.1%)
A-G1	Geopolymer mortar A	1% glass	2 nd (85.8%)	4 th (85.6%)
A-G2		2% glass	3 rd (85.5%)	1 st (100%)
A-B1		1% basalt	4 th (81.1%)	5 th (81.6%)
A-B2		2% basalt	6 th (77.9%)	7 th (77.9%)
A-S1		1% steel	9 th (65.9%)	10 th (67.5%)
A-S2		2% steel	10 th (59.7%)	11 th (55%)
A-NF		No fibres	11 th (55.4%)	13 th (47.7%)
B-G1	Geopolymer mortar B	1% glass	8 th (70.1%)	8 th (74.2%)
B-G2		2% glass	15 th (0%)	15 th (0%)
B-B1		1% basalt	5 th (78.9%)	3 rd (87.1%)
B-B2		2% basalt	7 th (75.5%)	6 th (79.8%)
B-S1		1% steel	13 th (52.3%)	12 th (50.5%)
B-S2		2% steel	12 th (54.1%)	9 th (69.3%)
B-NF		No fibres	14 th (48.6%)	14 th (40.7%)

Unlike LOP, the GRC control was outperformed in terms of MOR by mix A-G2, which exhibited an MOR = 6.6 MPa. The GRC control exhibited an average MOR = 6.3 MPa. In comparison for Mortar A, average MOR values for the glass, basalt and steel reinforced samples were 98%, 84% and 64%, respectively of the GRC's MOR value. In Mortar B, these values were 78%, 88% and 63%, respectively.

While fibre additions significantly increased the MOR value achieved by Mortars A and B (Figure 5.5), significant differences in behaviour were evident between them. The average MOR value achieved by Mortar A across all compositions was higher than that of Mortar B (4.84 vs 3.79 MPa).

Mix B-G2 became too dry during mixing to form, successfully distribute the fibres or be cast. As such, this composition was unable to form a homogenous composite and therefore could not be tested. The mortar dried out and flash set in the bowl directly after fibre addition and mixing, making successful casting impossible. However, mix B-G1 (which contained a lower fibre dosage) did not exhibit the same problems. The slightly higher flowability of Mortar A may have helped fibre dispersal and allowed mix A-G2 to form successfully, albeit with significant data spread.

When mix B-G2 was excluded from average MOR calculations, the average values for Mortar A and B were more comparable (4.56 vs 4.42 MPa). Fibre type and dosage were therefore shown to be the most significant factors of variation than mortar type.

Basalt fibres provided the highest average MOR value of any fibre addition at 5.37 MPa, compared with 4.27 MPa for glass and 3.99 MPa for steel fibres. This represents an 81.7% increase in the maximum load that the composite could sustain before total failure compared with the unreinforced mortars.

The mortar that provided optimal performance to steel fibre composites varied with fibre dosage, but none of the composites created performed satisfactorily. The dense fibres

sank through the relatively thin mortars and tended to agglomerate at the bottom of the mould, even before being vibrated. Thus, fibre distribution was heterogeneous and the weakest samples showed no sign of fibres at the point of failure. The brittle failure shown in the load/displacement curves for these samples provided further evidence of a lack of bridging fibres. Even those samples that exhibited high MOR values were often completely devoid of matrix material around the failure zone, which had crumbled away during the test, leaving only fibres. Failure of the composite occurred at a much lower load and much earlier than the test results alone would suggest.

The MOR value (6.26 MPa) achieved by the GRC control is at the lower limit of the range declared typical for GRC by the GRCA of 5-15 MPa (GRCA, 2017) . The value is also significantly lower than the MOR of 8 MPa declared by Ocrete (Ocrete, 2016). This indicates that the testing and manufacturing processes used are likely sub-optimal and improvement could increase performance across all composite types. Mix A-G2 achieved a higher MOR value of 6.58 MPa, indicating slightly better performance given the absence of additives. The relative MOR achieved by each composite is included in Table 5.3 along with their rankings.

5.2.5 Summary

The mortars selected for this investigation were too flowable and not viscous enough to hold the steel fibres in suspension, or prevent the drying phenomena that took place with the glass fibres. This highlights that a more viscous matrix with lower flowability was required for the next stage of testing. Steel fibres were the least effective reinforcement materials and, while this may have been due to the viscosity of the mortars, they also have high carbon embodiment and self-weight.

While glass fibres produced the strongest composites, basalt fibres produced higher levels of consistency in terms of compressive strength performance across the mortar types. This coupled with the lower environmental impact of basalt fibres, along with their ability to resist degradation and associated strength loss informed the selection of basalt fibres for further investigation in the next stage of testing.

5.3 Phase 2: 4-point bending testing of GRC vs basalt fibre geopolymer composites to ASTM C974-03

5.3.1 Introduction

This phase of testing aimed to evaluate the performance of basalt fibres with different diameters and sizings, relative to a GRC control material for multiple curing times. After analysing the process, the variation in load/displacement curves and the relative standard deviation in test results from the preliminary flexural testing (Table 5.3), a mould was manufactured to carry out further 4-point bending tests to ASTM C947-03.

Table 5.3. Variation in flexural strength results from Phase 1.

Composition	GRC	Mortar A	Mortar B
Average relative standard deviation (%)	17	20	14

An 80%GGBS/20%MK mortar developed in Chapter 4 was selected for this investigation, which was characterised by a higher viscosity than the preliminary test mortars, to more easily incorporate high fibre dosages. Hence, the geopolymer mortar was selected to match the strength gain of the GRC as closely as possible to allow for easier comparisons between the glass and basalt fibres at different ages. Table 5.4 gives the mix design of the geopolymer mortar and its strength gain compared with the GRC control. Four types of basalt fibre were used to create composites with this mortar, whose acronyms and descriptions are given in Table 5.5.

Table 5.4. Mix design and strength gain of GGBS/MK mortar and GRC control.

Material	Mix proportions (kg/m ³)		Compressive strength (MPa)		
			1-day	7-day	28-day
80%GGBS/20%MK geopolymer mortar	MK	96	19	70	86
	GGBS	387			
	Alkaline reagent	402			
	Water	119			
	Sand	1194			
Pre-bagged GRC	Proprietary information		39	73	83

Table 5.5. Composite combinations.

Material	Mix name	Fibre details			
		Type	Diameter (µm)	Length (mm)	Sizing applicability
80%GGBS/20%MK geopolymer mortar	GP-13-A	Basalt	13	12	None
	GP-13-B		13	12	Concrete
	GP-17-A		17	12	None
	GP-17-B		17	12	Concrete
Pre-bagged GRC	GRC	Glass	14	12	Unknown

5.3.2 Load/displacement curves

The load/displacement plots for the GRC and geopolymer composites tested at 28 days are presented in Figure 5.8. GRC composites experienced significantly less deformation compared with geopolymer composites, along with brittle failure modes without strain hardening. The load/displacement curves for GRC samples had greater consistency and less deviation than geopolymer composites.

Geopolymer composites, particularly mix GP-13-A, exhibited greater ductility than GRC. Larger displacements could be endured before failure and often exhibited strain hardening, albeit at loads below the LOP of GRC samples. Mix GP-13-B bared the most resemblance with the load/displacement curves for the GRC control. Geopolymer composites often showed significant strain hardening but this was limited in GRC samples.

The effects of fibre diameter and sizing were not easily identifiable in the load/displacement curves presented in Figure 5.8. In fact, the samples exhibiting the most similar curves had different diameters and sizing regimes, for example mixes GP-17-A and GP-13-B, or, GP-17-B and GP-13-A.

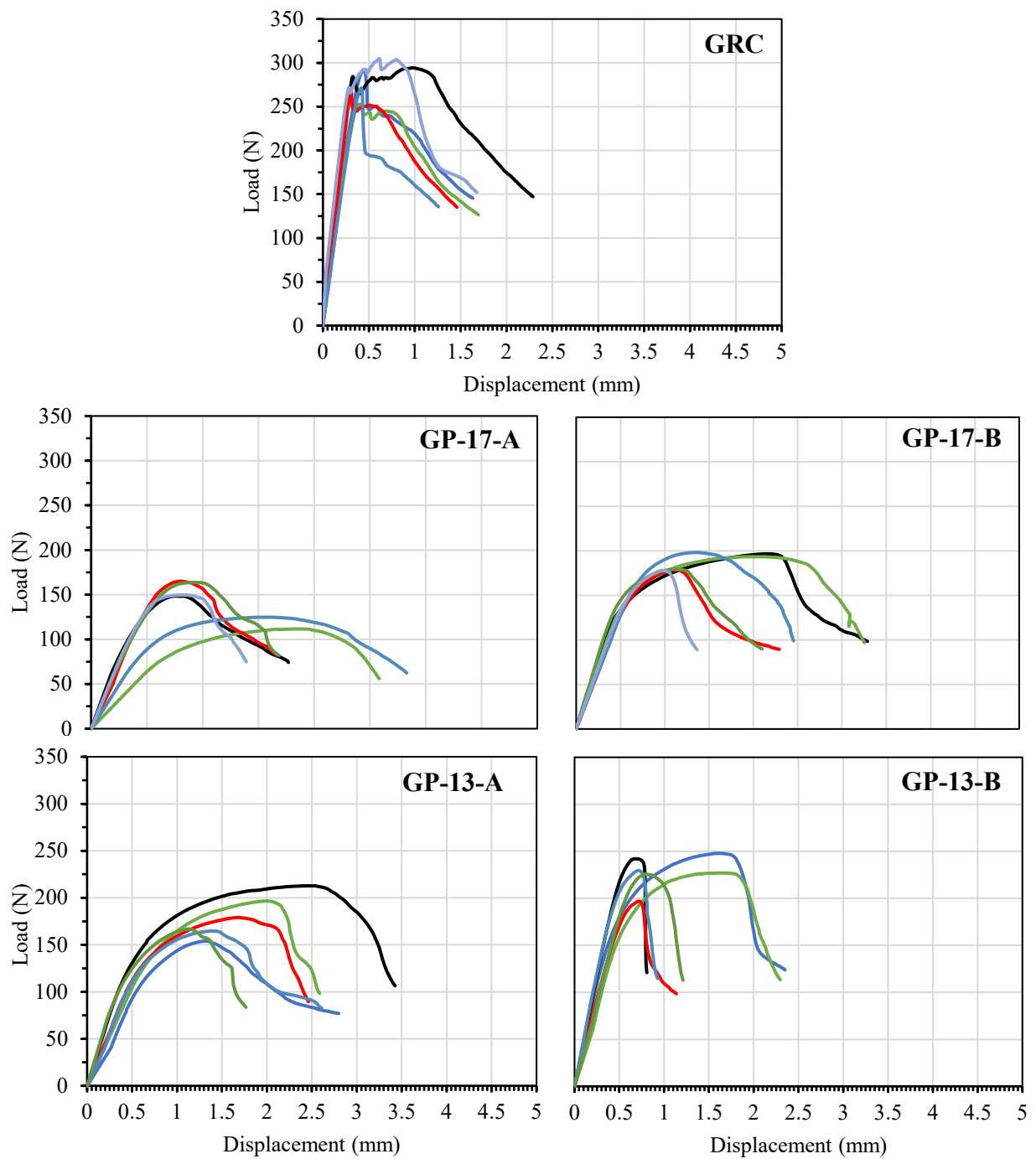


Figure 5.5. Load/displacement curves for GRC and geopolymer composites at 28 days.

5.3.3 LOP and MOR results

Figure 5.9 shows the LOP and MOR values achieved by the geopolymer-basalt fibre composites and the GRC control. As expected, after 28 days curing, GRC performed best with average LOP and MOR values of 7.21 and 7.51 MPa, respectively. In comparison, LOP and MOR values for the various geopolymer mixes were on average 40 and 30% lower than the GRC controls. 13 μm diameter fibres generally outperformed 17 μm diameter fibres, exhibiting average LOP and MOR values 12% and 16% higher, respectively. Concrete containing sized fibres clearly outperformed non-sized fibres with LOP and MOR values by 28 and 23%, respectively. The highest performing geopolymer composite (GP-13-B) exhibited LOP and MOR values 5.4 and 6.3 MPa, respectively – approximately 25% and 16% lower than values for the GRC controls. Average LOP and MOR values were strongly correlated ($R^2=0.95$), as the two most important factors dictating performance are common to both; fibre/matrix bonding and matrix hydration kinetics.

The GRC control material exhibited the highest LOP and MOR value after all curing times. However, the disparity between this and the highest performing geopolymer composites was found to reduce significantly with age. Early age results indicate that the benefits of sizing do not become apparent from the outset, but develops over time as the bond strength increases. This lower early strength may be a direct result of the waterproofing process and could indicate silane sizing may not be optimal for applications dependant on extremely high early strength.

Many geopolymer composites lost strength or showed a significant retardation of strength development between 7 and 28 days. This was partially due to the hydration kinetics of the GRC and geopolymer binders; both of which gained little strength after 7 days. Composites comprising larger diameter, unsized fibres were more significantly affected, indicating that fibre degradation may have played a key role in diminishing or reversing

strength gain. GP-13-B was the only composite that gained significant strength in this time showing that optimised fibre sizings and diameters may both play a significant role. However, if fibre degradation occurs, this is not dependant on the surface area of fibre/matrix contact.

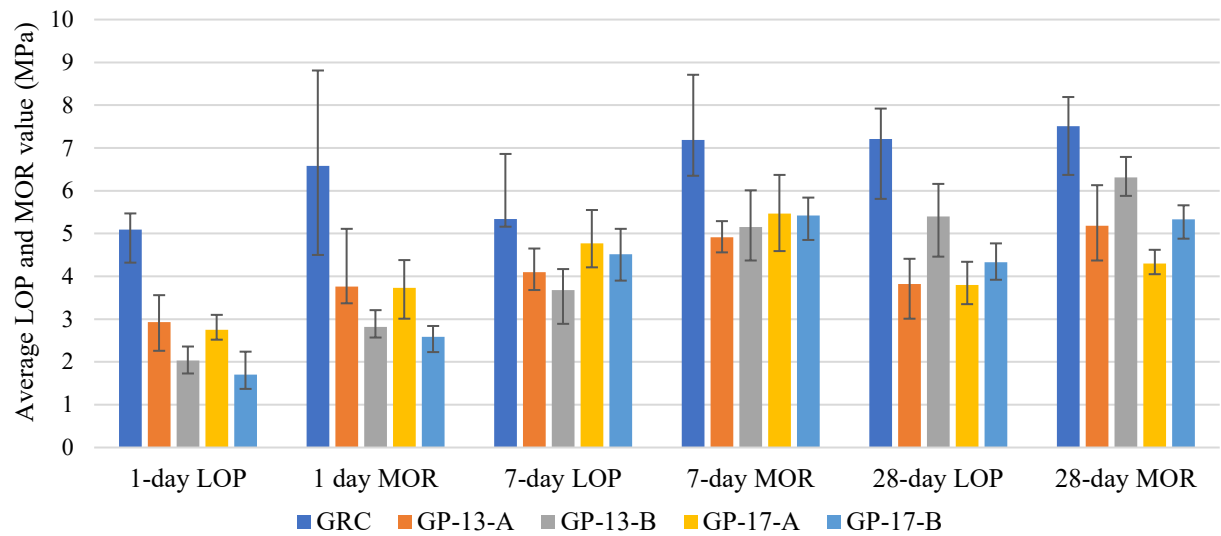


Figure 5.6. Flexural strength of geopolymer/basalt and GRC composites. Note: error bars represent maximum and minimum measured values from 6 tested samples.

5.3.4 Summary

Composite mix GP-13-B was the most successful composite and the closest to replicating the performance of the GRC control. This composite achieved an MOR value 16% lower than the control and exhibited the most similar load/displacement curves of any sample. While the GRC control is a fully developed commercial product that uses bespoke admixtures to improve performance the geopolymer composites developed here, they are in their preliminary stages of development. These compositions have scope to achieve better performances through the use of suitable additives or the reduction of the matrix water to binder ratio. As such this GP-13-B was selected to form the structural facing section of the building cladding panel and subject to further investigation in Chapter 6, when combined with thermal insulation materials.

Chapter 6 – Development of foamed geopolymer insulation materials

6.1 Introduction

This chapter investigates the efficacy of adopting geopolymeric materials to form the structure of a cladding panel system and the required thermal protection. The Foamed Geopolymer Insulation (FGI) materials developed in this chapter are intended to be combined with the Fibre Reinforced Geopolymer Panel (FRGP) developed in the previous chapter. This will represent a convenient and versatile lightweight, low impact, inflammable, building cladding solution for a wide range of applications.

6.2 Results of research phases

6.2.1 Phase 1 - Investigation of foamed MK-based mortars

In a geopolymer mix design the sand has the lowest cost and carbon embodiment, whereas the paste component (i.e., pozzolanic precursor and alkali reagent) has the highest. As such, any foamed mortar with similar performance and microstructure will be of much lower cost and carbon embodiment than those made from paste only. At the outset it was recognised that paste only foams are much more common and that the sand may be detrimental to generating and holding foam during mixing. The development of lightweight mortars is of interest in many applications, even if thermal conductivity and density is too high for use as an insulation material.

One common method for foaming cementitious materials is endogenous foaming. Hydrogen peroxide was used as an endogenous foaming agent in this study due its low cost, relatively low environmental impact and readily available. The highly alkaline geopolymer paste causes H_2O_2 to decompose, releasing bubbles of oxygen and hydrogen gas that can then be trapped to create a porous internal structure. Another method used surfactants to reduce the surface tension of the mortar/paste to facilitate foaming during the mixing process. The creation of controlled porosity using expansive perlite aggregate

was also trialled to ascertain the benefits or detriments this may have to structural integrity and pore structure. The MK mortar mixes shown in Table 6.1 were combined with H_2O_2 (endogenous foaming agent), and expanded perlite aggregate to maximise mortar porosity and understand which mix parameters control microstructure development.

Table 6.1. Mortar mix designs for foaming

Materials (kg/m³)	L/S=0.7	L/S=0.5
Metakaolin	386	428
Alkaline reagent	322	358
Free water	194	106
Sand	954	1058
Density	1857	1951

Figure 6.1 presents optical microscope images of the pore structures developed by each of the material options tested (Figure 6.1 (a)) alongside their measured densities (Figure 6.1(b)). All mortars studied had densities $>1500 \text{ kg/m}^3$, which would only account for a total porosity of approximately 19%. The pores generated were concentrated near the material surface, hence it is worth considering that microscope images in Figure 6.1(a) may give misleading insights into the total porosity. All samples still possessed significant mechanical strength based on visual inspection and may have some usage as lightweight mortars for structural applications.

The L/S ratio is the primary determinant of mortar viscosity and played a significant role in the development of a porous structure. In all samples, higher L/S ratios promoted higher porosity. However, the higher viscosity of the 0.5 L/S ratio mortars may have limited the formation of a foamed porous structure. The presence of sand also acts to increase mortar viscosity, which combined with the mechanical behaviour of the sand in the mixer, may be the primary cause of the low porosities generated.

Hydrogen peroxide was relatively successful in creating a porous structure, albeit that Figure 6.1(a) shows high density and a significant volume of open pores. The addition of

Perlite reduced the overall porosity of the mortars studied and increased the average size of the pores that remained. In the 0.5 L/S ratio mortars, significant void areas were present due to the reduced workability resulting from the aggregate particles. The expanded perlite aggregate possessed a much more closed pore structure than the foamed mortar, so even at reduced porosity, may provide greater thermal resistance.

While some useful data and knowledge of the foaming process was garnered in this phase, the mortars produced would not have sufficient thermal performance for use as an insulation material due to their high density and low porosity. Thus, further investigation focussed on using paste only foaming mixes, which were predicted to provide improved performance.

6.2.2 Phase 2 - Investigation of foamed MK pastes

In this phase a range of mix compositions and foaming methods were investigated to determine an optimal composition for foamed geopolymer paste insulation. The primary objective was to produce a low impact, high performance insulation material using natural, waste or low impact materials.

H₂O₂ was used for endogenous foaming and expanded perlite as a porous aggregate. This phase of testing also investigated commercially available materials as controls, including: 1) industrial surfactant *Glucopon*, and 2) *BanahTherm* - a geopolymer binder/activator system specifically designed for foaming applications. Figure 6.2 shows details of the mix designs investigated, comments on their form and structure, as well as 3D XRCT scan images of selected compositions. Figure 6.2(a) shows MK-based pastes foamed using H₂O₂. While the exclusive use of H₂O₂ provided significant porosity to the MK-paste (69.7%), this was predominantly in the form of open pores and, as such, less conducive to low thermal conductivity. The use of both VMA and a curing agent were found to provide benefits in this regard and warrants further investigation.

The use of Perlite aggregate increased the toughness and compressive strength of the geopolymer foams significantly (Figure 6.2(b)) but did not have a marked effect on either the total porosity or volume of closed pores. The addition of pre-formed foam in the form of a traditional shaving foam and a shaving gel was also trialled, but produced mortars with low porosity (Figure 6.2b). Higher L/S ratios and, therefore, lower viscosities allowed increased foam generation but also increased the likelihood of sample collapse. Due to the difficulties in finding compositions with suitable microstructures, an industrial, high-performance surfactant was trialled (Figure 6.2c). This material was effective in producing MK pastes with high porosity and a microstructure characterised by a large number of small, closed spherical pores. These materials had extremely high porosities, were resistant to crumbling and were mechanically similar to traditional insulation boards. MK paste was found to provide much higher porosity (>70%) than the industrially available alternative binder (45%), but was of slightly lower compressive strength.

An optimised MK-based mix design (57% MK, 40% Activator, 3% Glucocon) was selected as the best available option and underwent testing to determine its density and thermal conductivity (Figure 6.2c). A sample of the fibre reinforced geopolymer mortar developed in the previous chapter was also tested to allow the specification of cladding value with specified levels of thermal insulation. To ensure the mix design used was cost effective, mixes were tested with progressively lower dosages of surfactant to determine the relationship between surfactant dosage and thermal conductivity.

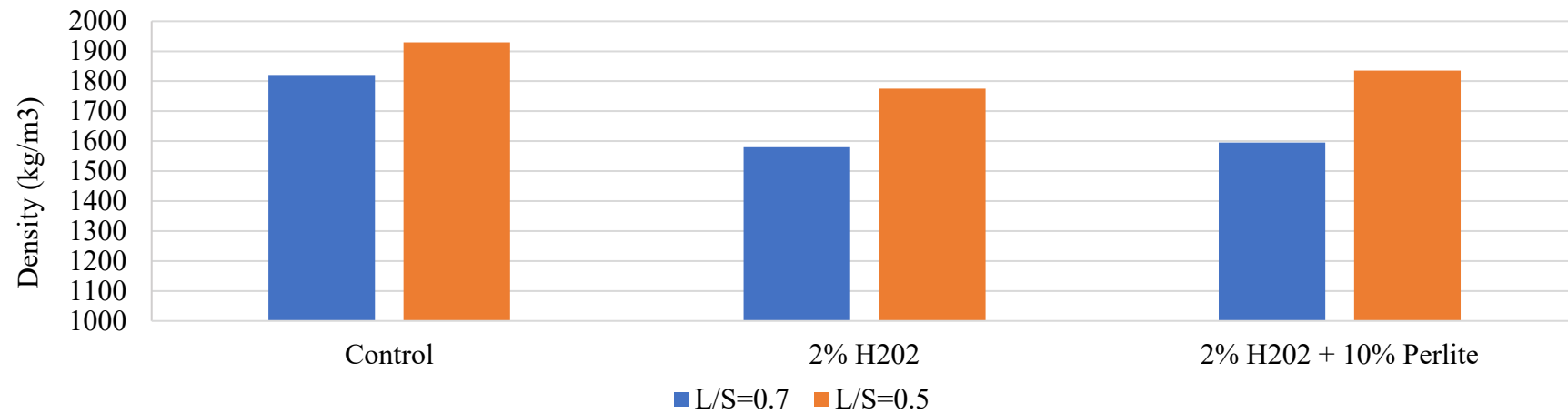
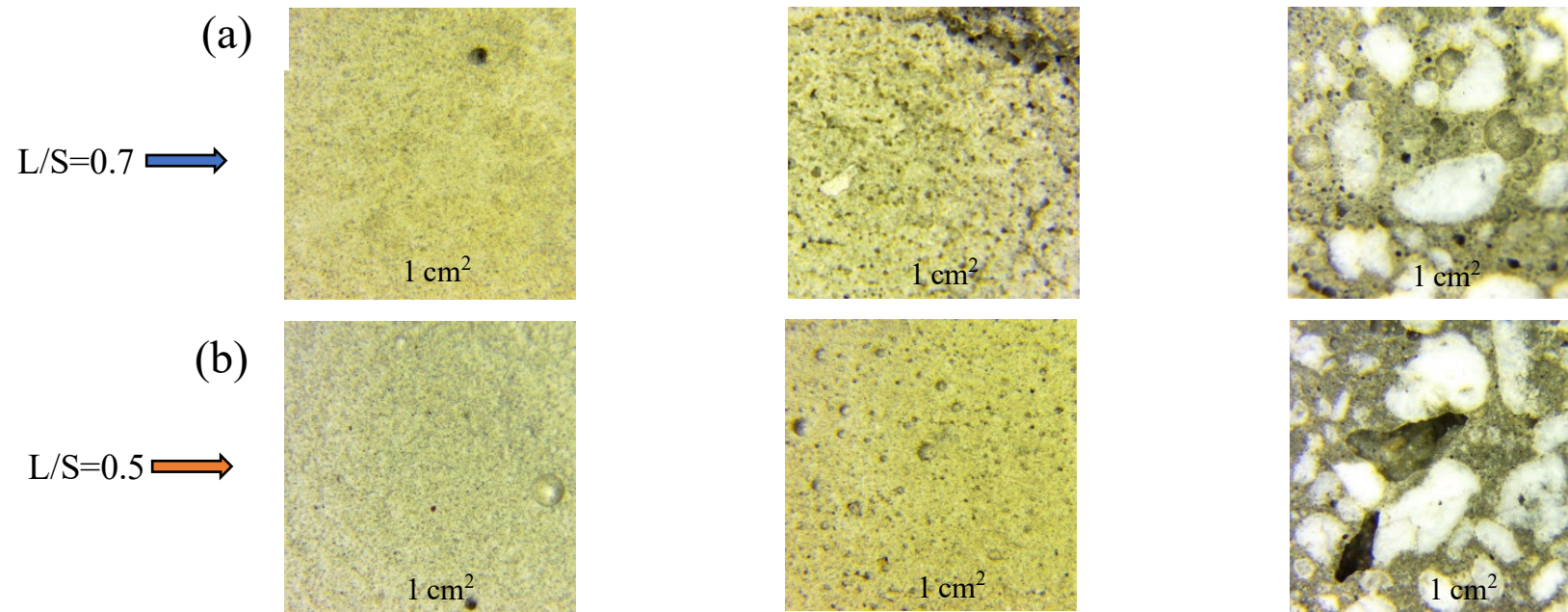


Figure 6.1. Foamed MK-based mortars at varied liquid to solid (L/S) ratios.

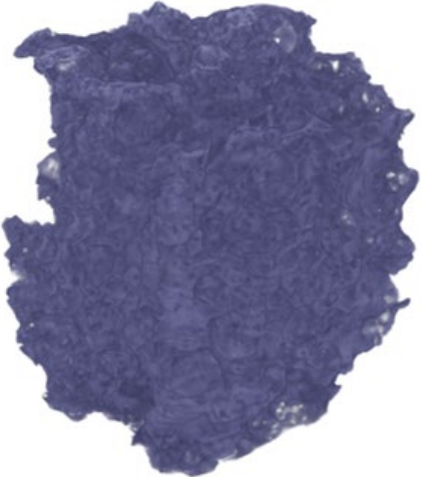

Foamed MK with hydrogen peroxide (H ₂ O ₂)						
Mix proportions (% by mass)						Comments
MK	Activator	Water	EW	H ₂ O ₂	VMA	
51	40	0	0	9	0	Uneven lumpy surface. Large, open pores. Overall high porosity.
<div>  <div> <p><u>CT Scan results</u></p> <p>Total porosity: 69.7%</p> <p>Open porosity: 69.5%</p> <p>Closed Porosity: 0.2%</p> </div>  </div>						

Figure 6.2(a). Development and testing of foamed pastes (% by mass).

Foamed MK with shaving gels					
Mix proportions (% by mass)					Comments
MK	Activator	Water	Gel foam	Foam	
50	38	0	12	0	Sunken, flat, little porosity, open pores, did not combine easily.
52	36	0	12	0	Flat, sunken, open pores, little porosity.
48	41	0	0	11	Flat, very good small pore structure, little porosity, high density.

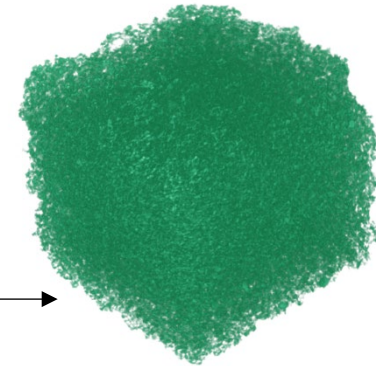


Foamed MK with Glucopon				
Mix proportions (% by mass)				Comments
MK	Activator	Water	Glucopon	
55	42	0	3	Flat, smooth, not sunken, no porosity visible.
53	44	0	3	Same but more porous, some large open pores present, generally small pores.
47	39	12	3	Flat smooth not sunken, excellent uniform small pore structure.
45	38	14	3	small uniform pores, too porous, open pores, low strength.
47	39	11	3	small uniform pores, too porous, open pores, low strength.
49	41	8	3	small uniform pores, too porous, open pores, low strength.
51	42	4	3	small uniform pores, too porous, open pores, low strength.
53	44	0	3	small uniform pores, too porous, mainly open pores, low strength.
55	42	0	3	small uniform pores, too porous, mainly open pores, low strength.
57	40	0	3	small uniform pores, stable foam, small, closed pores, best MK mix.



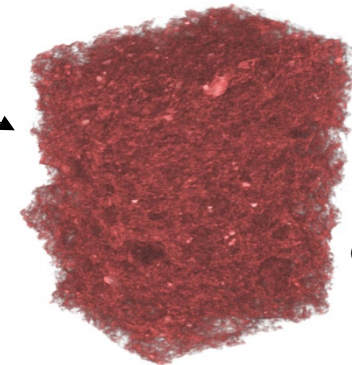
Figure 6.2(b). Development and testing of foamed pastes (% by mass).

BanahTherm (BT) with Glucopon					
Mix proportions (% by mass)					Comment
BT Binder	BT Activator	Water	Glucopon	VMA	
49	35	12	3	1	Flat surface with visible open pores. Excellent even small pore structure. Cast and cut perfectly. Stable foam.
46	33	18	3	0	Small uniform pores. Stable foam. Closed pores. Best Banah mix.



CT Scan
 Total porosity:
 45.1%
 Open porosity: 45%
 Closed Porosity:
 0.1%

Foamed MK with Perlite (P) and Basalt fibres (BF)						
Mix proportions (% by mass)						Comments
MK	Activator	Water	H ₂ O ₂	P	BF	
40	31	0	9	17	0	Lumpy surface. Small pores around aggregate. Uniform structure. Mechanically strong.
43	33	0	9	9	0	Uneven lumpy surface. Cracked and sunken. Irregular pores around aggregate. Large voids.
45	35	0	9	4	0	Flat, cracked surface. Irregular pores around aggregate. Large voids.
49	38	0	5	0	1	Flat surface with small cracks. Uneven pore sizes.



CT Scan
 Total porosity:
 73.1%
 Open porosity: 73%
 Closed Porosity:
 0.1%

Figure 6.2(c). Development and testing of foamed pastes (% by mass).

6.2.3 Phase 3 - Thermal conductivity testing and proposed cladding panels

The MK-based mix design previously described was dosed with 1, 2 and 3% Glucopon surfactant by mass and underwent thermal conductivity testing and density measurement, according to ISO8301 (ISO, 1991). The results are presented in Figure 6.3, which illustrate that thermal conductivity and density decrease with increasing surfactant dose. However, the effect created by adding additional surfactant diminishes after 2% dosage. Geopolymer foams were produced with densities as low as 608 kg/m^3 , a 68% decrease from that of the un-foamed paste (1927 kg/m^3), and thermal conductivities as low as 0.0933 W/mK . The thermal conductivity of geopolymer composite GP-13-B created in the previous section is also presented but is described as simply Fibre Reinforced Mortar (FRM) in this chapter. This allowed a full panel to be designed and its thermal conductivity and U-value to be calculated.

While these results are significant, the thermal conductivities achieved are approximately four times higher than expected from standard plastic based, foil faced, insulation boards, and twice that of mineral wool insulation. Therefore, designs incorporating these materials will likely require significantly greater depths of material for thermal protection. However, this increase will be minimised by the extremely thin cladding panel structure (13 mm). The images shown in Figure 6.3 illustrate that some damage or surface pore agglomeration during foaming occurred when surfactant dosage reached 3% (indicated by flat, non-porous areas). As there is little difference in thermal conductivity or density between the 2 and 3% dosage levels, the lower dosage may be optimal. The pore agglomeration noted was only surface deep, as the material still exhibited the lowest density and, therefore, must have greater internal porosity.

6.2.4 Phase 4 - Proposed claddings panels

Thermal conductivity values presented in Figure 6.4 are combined with material data taken from the literature to produce sample specifications for different applications designed to satisfy the building regulations (DFPNI, 2022-a; DFPNI, 2022-b). The building component which the materials are to form (roof, party wall and floor) and the use of the proposed structure (domestic and non-domestic) dictate the maximum permissible U-value for specific applications. These requirements for each structural component in domestic and non-domestic uses are given in Table 6.2.

Table 6.2. Maximum allowable U-values (Technical Booklet F).

Max area weighted U-value UK (W/m²K)		
Building element	Domestic	Non-domestic
Wall	0.18	0.21
Floor	0.18	0.21
Roof	0.16	0.16 - 0.2

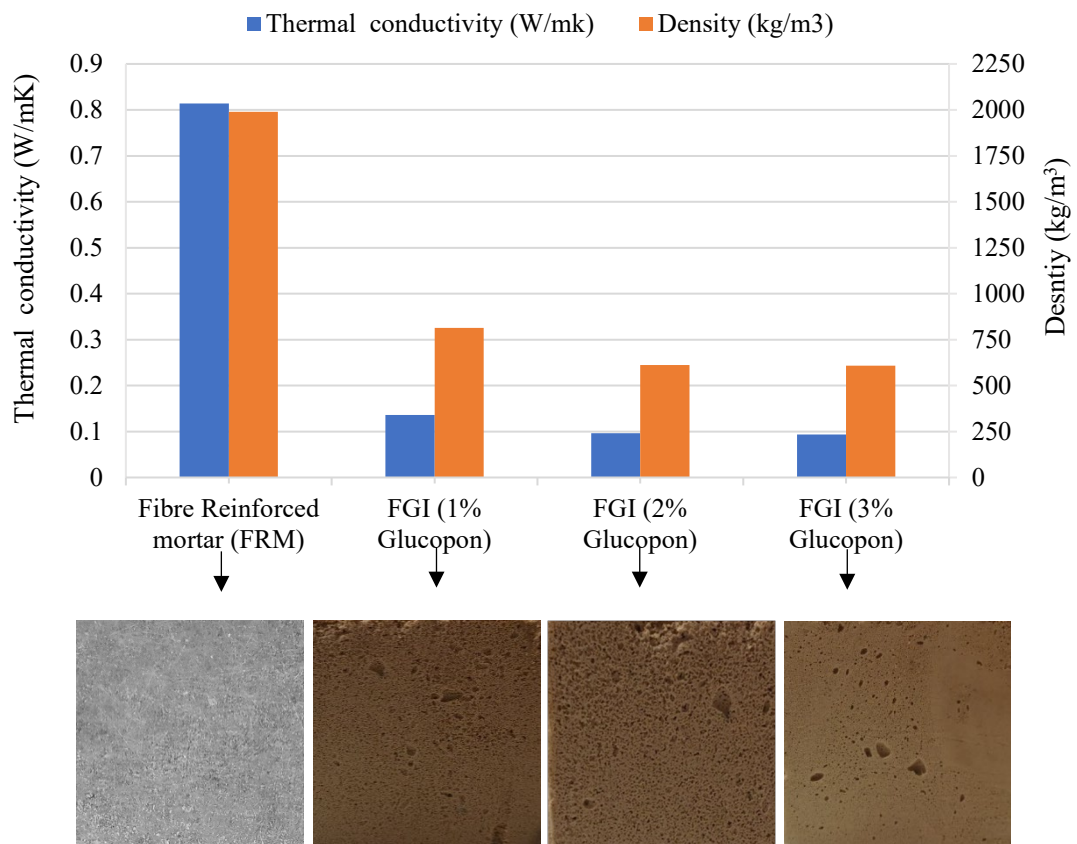


Figure 6.3. Thermal conductivity and visual inspection of foamed mortars (scale = 5 cm²).

Thermal conductivity, density and embodied carbon values for the foamed geopolymer insulation, fibre reinforced mortar (FRM) and a GGBS/SF mortar developed in Chapter 4 are presented in Table 6.3, which are compared with common insulation materials. The mix design for the unreinforced GGBS/SF mortar is given Table 6.4. Mineral wool and phenolic foam-based insulations have higher carbon embodiment per kg of material, but significantly lower density and thermal conductivity than foamed geopolymers. As such, these materials can be used in thinner panels that weigh less and therefore exhibit low carbon embodiment per m². The autoclaved aerated concrete (AaC) insulation block is a very similar material to the foamed geopolymer developed in this research and was included for comparative purposes. References for calculations were gathered from the following BS EN 15804 compliant stage A-1 LCA's, or provided by manufacturers when compositions are commercially sensitive (BASF, 2013; EPD Ireland, 2019; Mannock, 2021; Creagh, 2020; Foamglas, 2022; Kingspan, 2022; Rockwool Ltd, 2020; Rieder, 2020; Komkova, 2023; McGrath et al., 2018).

The minimum thickness of each insulation panel required to meet the U-values specified in Technical Booklet F is presented in Figure 6.4. The data illustrates that phenolic foam and mineral wool significantly outperformed the foamed geopolymer and AaC insulation, and met specified U-values using less materials. A similar trend can be identified in Figure 6.5, which presents the minimum carbon embodiment per m² required to meet specified U-values. The foamed geopolymer exhibited the highest carbon embodiment/m²; almost ten times that of the mineral wool.

Based on the data presented in Table 6.3, and collected from the literature, two example panels are proposed. The first is based on a typical GRC panel design (Rieder, 2020) and uses the FRM material developed in chapter 5 (Table 6.4). The second is based on a typical concrete sandwich panel design detail (Creagh, 2020) using the GGBS/SF mortar developed in chapter 4, converted into a typical concrete mix design (Table 6.4).

Tables 6.5 and 6.6 present the properties and composition of each proposed cladding option, which are then visually represented by scale drawings in Figure 6.7. Figure 6.5a presents a typical Rieder GRC panel and Figure 6.5b illustrates the increased insulation thickness required when using the foamed geopolymer insulation. A similar relationship is presented in Figures 6.5c and 6.5d for the typical Creagh concrete sandwich panel and the geopolymer mortar sandwich panel proposed, respectively.

Table 6.3. Properties of foamed geopolymer insulation and other common alternatives.

Material type	Product name	Thermal conductivity (W/mK)	Density (kg/m ³)	Embodied carbon (kgCO ₂ /kg)
Foamed geopolymer (FGI 3%)	N/A	0.0933	607	0.498
Fibre reinforced mortar (FRM)	N/A	0.814	2199	0.163
GGBS/SF concrete	N/A	0.9	2469	0.103
Autoclaved aerated concrete	Mannock Aircrete Super AaC insulation block	0.12	480	0.28
Mineral wool	Rockwool High Performance Partial Fill Cavity Slab	0.034	50	1.28
Phenolic foam	Kingspan Kooltherm K108	0.018	71	3.84

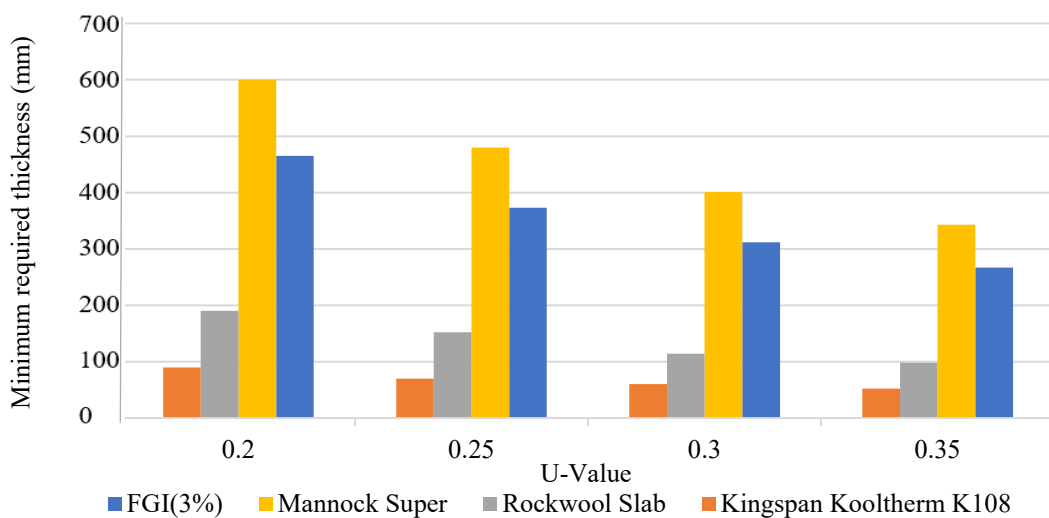


Figure 6.4. Minimum required insulation thickness to meet specific U-values (0.2-0.35).

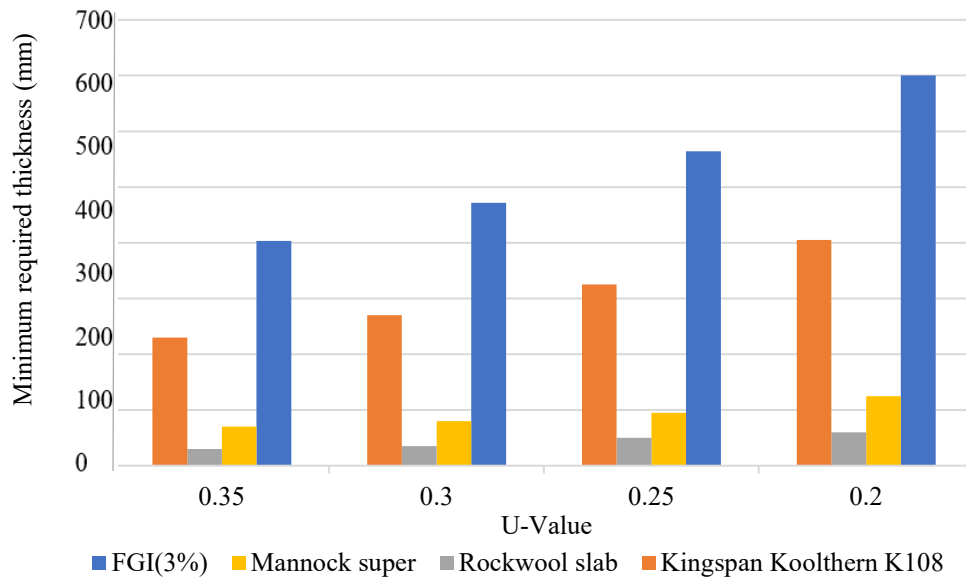


Figure 6.5. Minimum embodied carbon required to meet specific U-values (0.2-0.35).

Table 6.4. Geopolymer mortar mix design.

Material quantities (kg/m ³)					
GGBS	SF	Activator	Water	Sand	Aggregate
275	68	286	85	810	855

Table 6.5. Properties and composition of cladding panels based on typical GRC design (Rieder, 2020).

Panel type	Material	Thickness	Panel thickness	Embodied carbon	U-value
Typical Rieder GRC panel	GRC	13 mm	113 mm	38.9 kgCO ₂ /m ²	0.21
	Kingspan Kooltherm K108	50 mm			
	Cavity	50 mm			
Geopolymer composite panel	FRM	13 mm	320 mm	82.3 kgCO ₂ /m ²	
	Foamed geopolymer	257 mm			
	Cavity	50 mm			
Geopolymer composite/Kingspan panel	FRM	13 mm	113 mm	18.3 kgCO ₂ /m ²	
	Kingspan Kooltherm K108	50 mm			
	Cavity	50 mm			

Table 6.6. Properties and composition of cladding panels based on typical concrete sandwich panel design (Creagh, 2020).

Panel type	Material	Thickness	Panel thickness	Embodied carbon	U-value
Typical Creagh concrete sandwich panel	Precast concrete outer leaf	150 mm	430 mm	67.9 kgCO ₂ /m ²	0.24
	Foamglas	200 mm			
	Precast concrete inner leaf	80 mm			
Geopolymer concrete sandwich panel	Geopolymer concrete outer leaf	150 mm	603 mm	168.2 kgCO ₂ /m ²	
	Foamed geopolymer	373 mm			
	Geopolymer concrete outer leaf	80 mm			
Geopolymer concrete /Kingspan sandwich panel	Geopolymer concrete outer leaf	150 mm	280 mm	59.3 kgCO ₂ /m ²	
	Foamglas	200 mm			
	Geopolymer concrete outer leaf	80 mm			

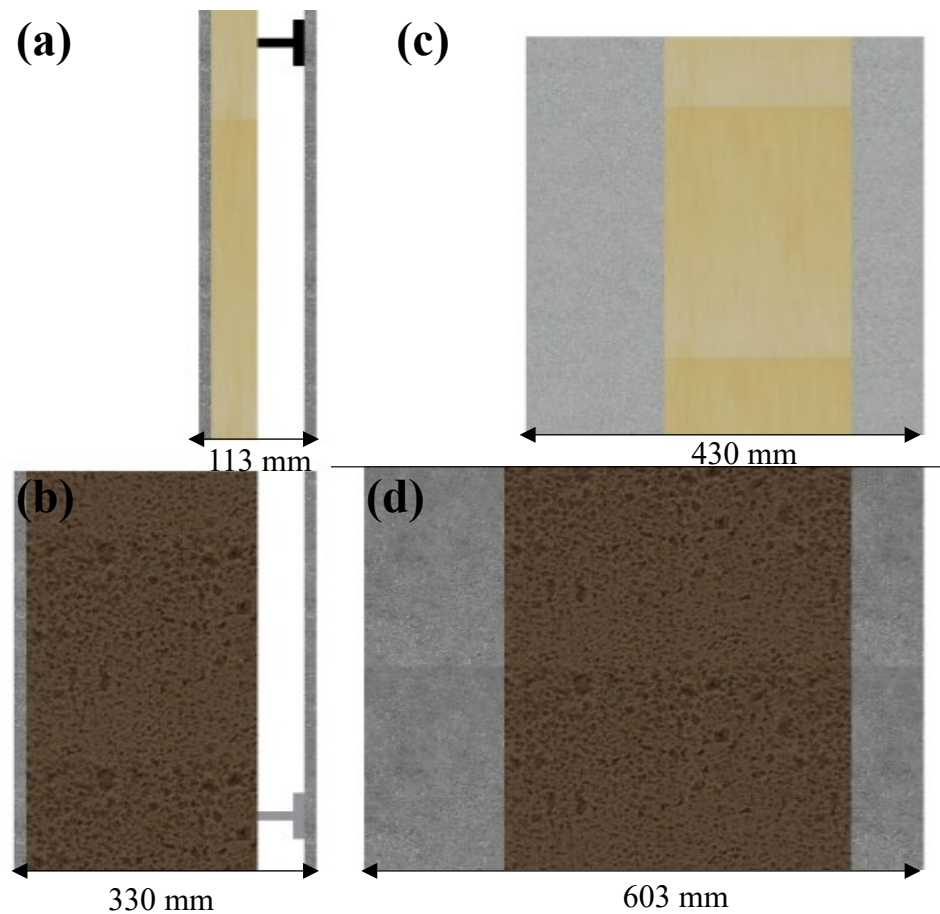


Figure 6.6. Scale diagrams of proposed cladding panels.

6.3 Summary

Several cladding options were developed using the foamed geopolymer insulation created in this chapter and the fibre reinforced geopolymer structure developed in Chapter 5, to meet the thermal requirements for use in a wide range of building structures. Industrial surfactant-based foaming was the most effective method and more successful in the MK-based pastes than the commercially available base materials. While thermal conductivities were greater than would be expected for common insulation materials, the developed panels can provide similar U-values/depth ratios due to the thin fibre reinforced structure.

These materials are low impact, fireproof and have the potential for improved performance as their development is still at a preliminary stage. Controlling paste viscosity or limiting the time over which gas bubbles are released in the MK pastes foamed with H_2O_2 would likely allow these to be suitable for use. The high porosity of these materials would often cause collapse. However, if this can be prevented through the methods described then it is likely that thermal conductivities would be less than or equal to those created with industrial surfactants.

Chapter 7 – Discussion

7.1 Engineering performance

7.1.1 Mortar performance

7.1.1.1 L/S ratio

Figure 7.1 compares the relationships between L/S ratio and 28-day compressive strength reported by this research (MK data, Factorial data) against others from the literature. The high R^2 values and similar trends exhibited by both primary and secondary data points indicate a strong inverse relationship between liquid contents and compressive strength. The primary data collected in this research corresponded with examples from the literature and helped confirm that L/S is a vital mix parameter for determining mechanical strength, and is consistently seen across a range of pozzolanic precursor compositions, alkaline reagent solutions and curing regimes (Table 7.1)

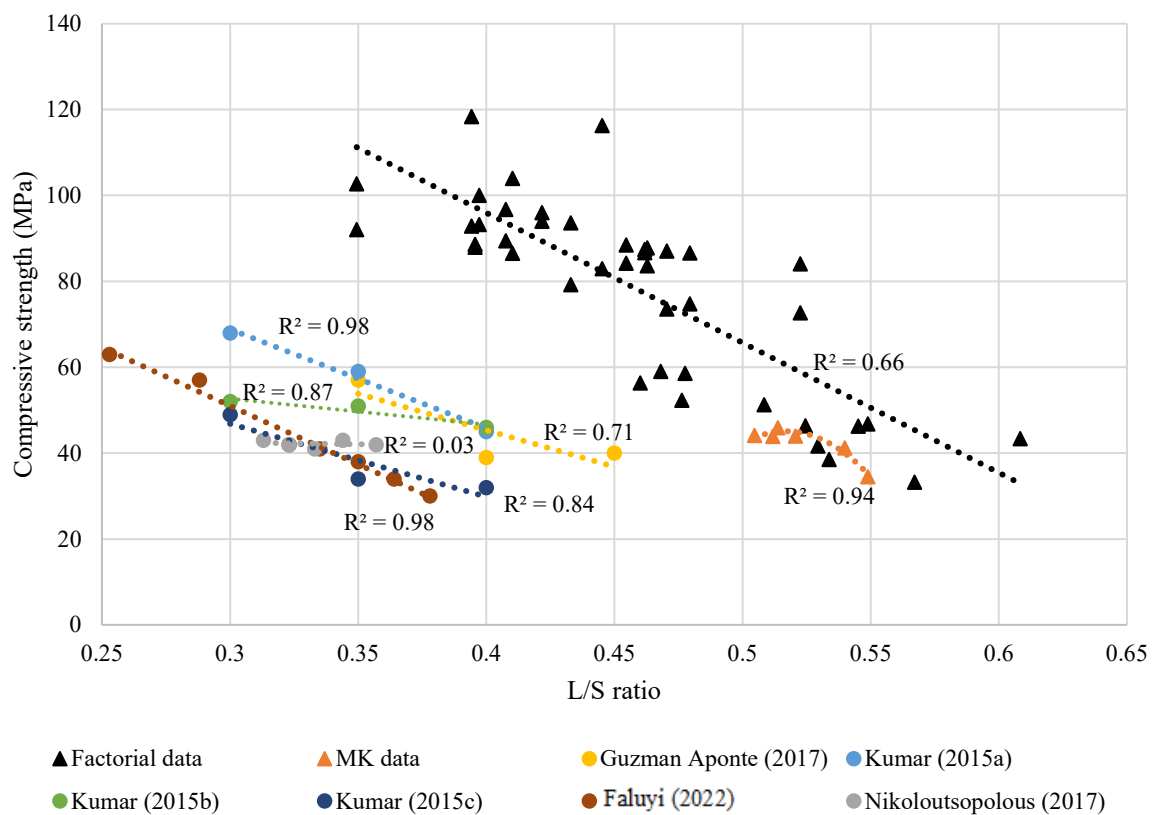


Figure 7.1. Significance of L/S ratio to 28-day strength for primary and secondary data.

Nikoloutsopolous (2017) reported the L/S ratio was insignificant to strength development or setting times in FA mortars, contrary to the rest of the reviewed literature. This can only be reasonably explained by the specific test methodology adoption or variation in mix components.

Table 7.1. Data set information for comparison of L/S ratio to 28-day strength.

Data set	Pozz. precursor	Activator	Curing	R ²
Factorial data	80%GGBS/20%MK, 80%GGBS/20%SF 100% MK	K ₂ SiO ₃	Ambient	0.66
MK data	100% MK	K ₂ SiO ₃	Ambient	0.94
Kumar (2015)	100% FA	Na ₂ SiO ₃ + NaOH	Ambient	a = 0.98 b = 0.87 c = 0.84
Guzman Aponte et al (2017)	100% MK	K ₂ SiO ₃ + KOH	Ambient	0.71
Faluyi (2022)	100% FA	Na ₂ SiO ₃ + NaOH	72 hours @ 60°C	0.98
Nikoloutsopolous (2017)	100% FA	Na ₂ SiO ₃ +NaOH	72 hours @ 70°C	0.03

From Figure 7.1 it is evident that the mortars produced in this study were of greater strength than those reported in the literature, even with higher L/S ratios. This indicates if the L/S ratio of these mortars was reduced further, especially for the GGBS/SF and GGBS/MK mortars which exhibited high flow, then mortars with higher compressive strength could be produced. Many of the studies used Class F FA geopolymers, which require heated curing for high strength. If these studies used Class C FA, the increased calcium content would increase compressive strength and allow ambient curing even at high inclusion levels. Diaz-Loya et al. (2013a) tested 24x FA geopolymer mortars, which used FA sourced from different power stations in the USA. Class C FA-based mortars produced on average 61% higher strengths than Class F FA-based mortars. However, Class C FA is more expensive due to its high demand as an SCM in traditional concretes, therefore cost/benefit analysis should be undertaken (Diaz-Loya et al., 2013b).

7.1.1.2 A/B ratio

Figure 7.2 presents compressive strength vs A/B ratio plots based on data collected in this research and published datasets. It is evident that the reported significance of A/B ratio on compressive strength varies based on the A/B value range and the pozzolanic precursors, activation solution and curing regime used.

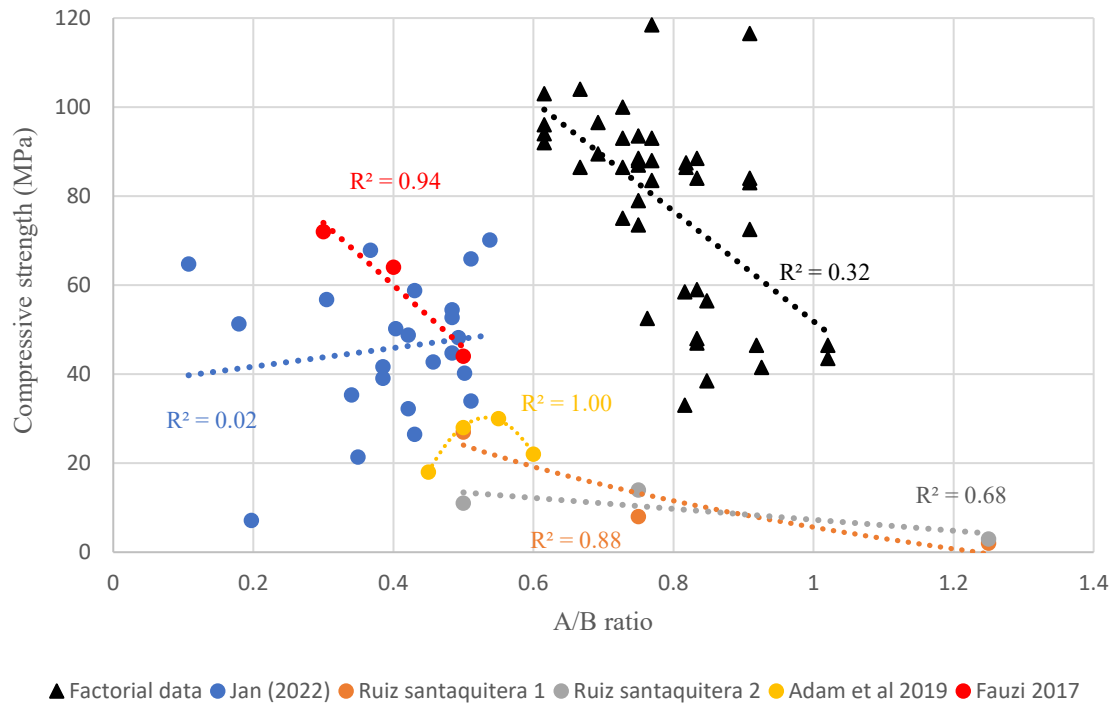


Figure 7.2. Significance of A/B ratio to 28-day strength for primary and secondary data

In general, for small datasets composed of a single precursor type, precursor/activator combination and curing regime, A/B ratio is reported to play a significant role in strength development (Adam et al., 2019; Ruiz-Santaquitera et al., 2012; Fauzi et al., 2017). Whereas for larger data sets composed of multiple precursor types, precursor/activator combinations and curing regimes, A/B is a poor predictor of compressive strength (Jan, et al., 2022).

Table 7.2. Data set information for comparison of A/B ratio to 28-day strength.

Data set	Pozz. precursor	Activator	Curing	R ²
Factorial data	80%GGBS/20%MK, 80%GGBS/20%SF 100% MK	K ₂ SiO ₃	Ambient	0.32
Jan et al. (2022)	100% FA 100% Class C FA 100% GGBS 100% Calcined clay 100% MK 70%FA/30% GGBS	NaOH Na ₂ SiO ₃ +NaOH	Varied depending on precursor	0.02
Ruiz-Santaquitera et al. (2021a)	70%FA/30%MK	NaOH	20 hours @ 80 °C	0.88
Ruiz-Santaquitera et al. (2021b)	70%FA/30%MK	Na ₂ SiO ₃ +NaOH	20 hours @ 80 °C	0.68
Adam et al. (2019)	95%FA/5% Slaked lime	Na ₂ SiO ₃ +NaOH	Ambient	1.0
Fauzi et al. (2017)	100%FA	Na ₂ SiO ₃ +NaOH	Ambient	0.94

This result is not unexpected as each precursor powder / activating solution combination will have a minimum A/B ratio required for successful dissolution of the precursor powder into silica and alumina monomers. This process is vital to develop the maximum possible strength. Any excess activating solution and the liquid it contains will act to increase the L/S ratio, creating increased porosity and reduced strength. As such, peak strength will be achieved where the minimum activating solution contents required for full dissolution is found; whereby strength will degrade at lower/higher values due to either the presence of unreacted precursor powder or excess liquidity.

Based on primary data, this minimum A/B ratio was ~0.75 for MK geopolymers and <0.6 for GGBS/MK and GGBS/SF geopolymers. If the dataset includes this peak strength close to the centre of the range investigated, then the A/B ratio to compressive strength plot will mirror that of (Adam et al., 2019). As a result, A/B ratio was unsuitable for strength prediction for a range of geopolymer mortars as each will have a different minimum activator content required for full precursor dissolution.

7.1.1.3 S/A ratio

A range of relationships between S/A ratio and compressive strength are reported in the literature with inconsistent significance. It has been widely reported that higher S/A ratios result in an increased number of Si-O-Si bonds and therefore increased geopolymer strength. However, this was not apparent for many of the data sets shown in Figure 7.3. No optimal S/A ratio that created the highest strength for all types of geopolymer could be identified. S/A ratios for optimal strength development varied across binder types, whereby Deghani et al. (2021) and Wang et al. (2021) reported the opposite effect from increasing to S/A in the same value range and both exhibiting high R^2 values.

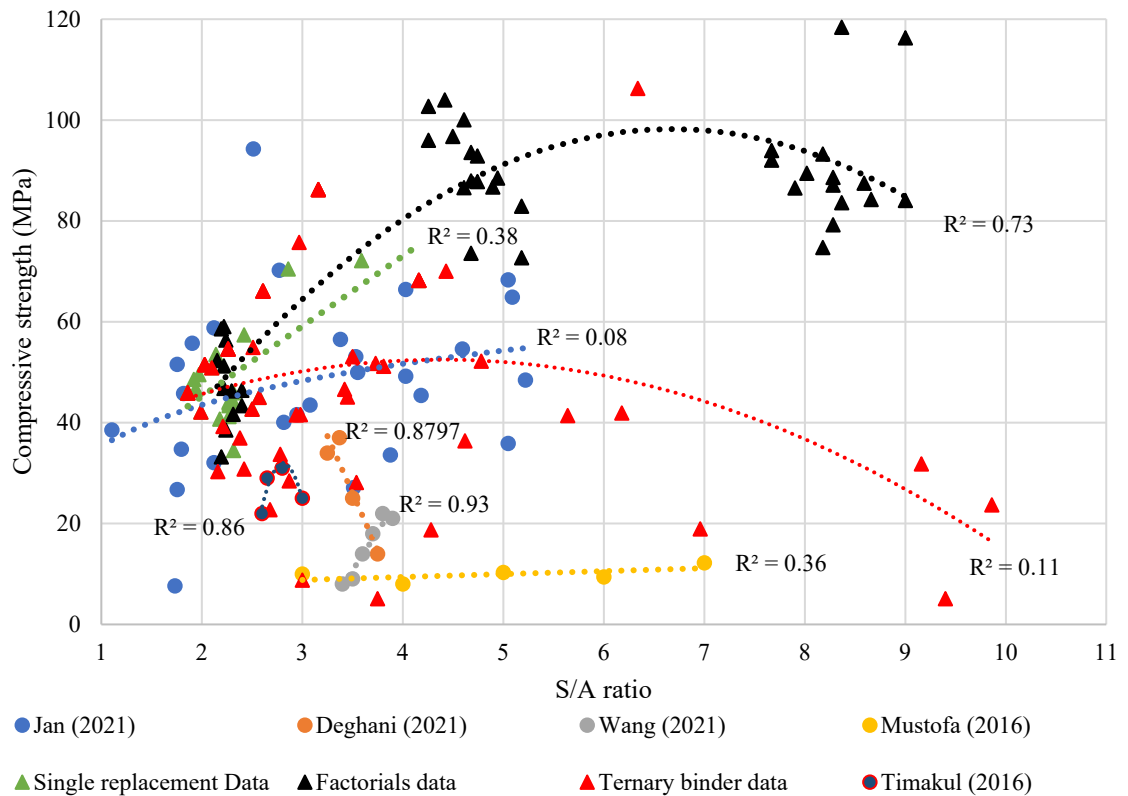


Figure 7.3. Significance of S/A ratio to 28-day strength for primary and secondary data.

Similar trends are present in the primary data presented. The high R^2 of 0.77 exhibited by the factorials data set is also slightly misleading as the three main clusters of data points represent three different binder types (MK, GGBS/MK, GGBS/SF). Within each of these datasets, as shown in Figure 4.9, significance is low ($R^2 = 0.03, 0.53, 0.08$). Discounting

this effect, all primary data shows that the relationship between S/A ratio and strength development is weak and inconsistent. Both the weakest and the strongest mortars shown in Figure 7.3 had very similar S/A ratios.

Table 7.3. Data set information for comparison of S/A ratio to 28-day strength.

Data set	Precursor	Activator	Curing	R ²
Single replacement data	MK/GGBS MK/IS MK/FA MK/SF	K ₂ SiO ₃	Ambient	0.38
Multi replacement data	MK/GGBS/IS MK/GGBS/SF MK/GGBS/FA	K ₂ SiO ₃	Ambient	0.11
Factorial data	80%GGBS/20%MK 80%GGBS/20%SF 100% MK	K ₂ SiO ₃	Ambient	0.73
Jan (2022)	100% FA 100% Class C FA 100% GGBS 100% Calcined clay 100% MK 70%FA/30% GGBS	NaOH or Na ₂ SiO ₃ +NaOH	Varied depending on precursor	0.08
Deghani (2021)	78-85%FA/15-22%GGBS	Na ₂ SiO ₃ +NaOH	Ambient	0.88
Wang (2021)	87.2-99%MK/0.1-12.8%SF	Na ₂ SiO ₃ +NaOH	Ambient	0.93
Mustofa (2016)	Ferronickel slag	Na ₂ SiO ₃ +NaOH	24 hours @ 80 °C	0.36

When datasets consisted of small groups of similar mortars, with variations in S/A being the only major difference, then high R² values were exhibited (Deghani et al., 2021; Wang et al., 2021). When large data sets of varied materials were studied, the effect of S/A ratio on compressive strength became insignificant (Jan et al., 2022). As such, S/A ratio in isolation was found both in the literature and through primary data collection to be unsuitable for strength prediction for a wide range of geopolymer mortars.

7.1.1.4 Strength prediction equations

As accurate compressive strength predictions were not possible using any compositional ratio in isolation, more complex models were established that used multiple mix parameters and considered the effects of important interactions between them.

The equations developed in this research to predict the 28-day compressive strength of MK mortars (Equation 5), GGBS/MK mortars (Equation 6) and GGBS/SF mortars (Equation 7) are presented and compared with similar attempts from the literature that vary in the techniques adopted, ease of use and complexity (Equations 8 - 12). The equations proposed are simpler and easier to use compared with any model equations previously published in the literature. Only three factors were used to predict strength in Equations 5-8, which uniquely corresponded to simple mix values and can be easily used by practitioners. Model outputs therefore easily combine to provide a full mix design. However, for the models presented in Equations 8 - 12, complex chemical analyses such as XRD, XRF and LOI are required to identify factor input values from the source materials – hence producing a complete mix design from their outputs is complex.

As illustrated in Table 7.4, a wide range of different mix and material composition parameters were found to influence strength development, with no two equations derived from the literature using the same parameters. Many of the more complex mix parameters that appear in Equations 8 - 12 are a function of the simpler metrics from Equations 5 – 7, such as L/S ratio. Many of the complex factors from Equations 8 - 12 do not appear in Equations 5 - 7 as they remain constant by experimental design features, such as the use of identical activating solution for all mixes. This means that for example metrics describing activator composition, molarity and water contents are represented in the models developed in this research, even if they are not a varied factor.

Figure 7.4 presents statistical analysis of the success each model had with respect to 28-day compressive strength prediction. Based on the model Si (scatter index) values exhibited by each, the methodology used to develop Equations 4 - 7 was successful. Models describing GGBS/MK and GGBS/SF exhibited good Si values similar to the secondary models from the literature. However, the model describing MK mortars was significantly less successful. Si values were over 200% greater any of the other models studied. The most successful model, developed by Shahmansouri et al. (2020) exhibited a Si value of 5.6%.

The most successful model developed in this study (GGBS/MK) exhibited the third lowest Si value, behind only the models established by Shahmansouri et al. (2020) and the most complex NLR model by Ahmed et al. (2022). The simplicity of the models developed in this research is highly advantageous. When combined with a similar level of prediction accuracy exhibited by the more complex, difficult to use models, this makes both the GGBS/MK and GGBS/SF equations a useful tool to facilitate adoption of these materials by the construction industry.

$$28 \text{ day } CS = -384.935 + (-2.33225 * A) + (4.7745 * B) + (-0.195 * C) \\ + (0.004825 * A * B) + (-0.0079 * B^2)$$

Equation 5. 28-day compressive strength of 100%MK mortars

$$28 \text{ day } CS = 527.467 + (0.096 * A) + (-2.43525 * B) + (0.0025625 * B^2) + \\ (-0.0101042 * C^2)$$

Equation 6. 28-day compressive strength of GGBS/MK mortars

$$28 \text{ day } CS = -2.275 + (0.521167 * B) + (* 0.195 * C) + (-0.00429167 * BC) + (0.121667 * C^2)$$

Where A= Binder contents, B = Activating solution contents and C = Free water contents

Equation 7. 28-day compressive strength of GGBS/SF mortars

$$f'c = - 3.62 + 0.59 * RSiO_2 + 3.35 * RAl_2O_3 - 0.48 * RCaO - 0.74 * d50 - 4.39 * LOI (N/mm^2)$$

Where RSiO₂ = reactive SiO₂ contents, RAl₂O₃ = reactive Al₂O₃ contents, RCaO = reactive CaO contents, d50 = median particle size, LOI = loss on ignition value

Equation 8. Diaz-Loya et al. (2013a)

$$28 \text{ day } CS = 244.3 * 0.15FA - 1.43FSO - 0.56FAO - 0.085S + 0.041SH + 0.79SS + 66.88 \left(\frac{SO}{N} \right) - 27.7 \left(\frac{H}{N} \right) - 30.6 \left(\frac{L}{B} \right) + 0.894M + 0.212TE + 0.735T + 0.428AG$$

Equation 9. Ahmed et al. (2022) LR

$$28 \text{ day } CS = 32.32 * FA^{-5.85} * FSO^{-1.9} * FAO^{0.283} * S^{-1.8} * SH^{1.145} * SS^{2.107} * \left(\frac{SO}{N} \right)^{-3.56} * \left(\frac{H}{N} \right)^{6.952} * \left(\frac{L}{B} \right)^{-3.3} * M^{0.17} * TE^{0.33} * T^{9.198} * AG^{0.181}$$

Equation 10. Ahmed et al. (2022) MLR

$$\begin{aligned}
28 \text{ day } CS = & \left(53.4 * FA^{-7.2} * FAO^{0.14} * S^{-5} * SH^{0.38} * SS^{2.13} * \left(\frac{SO}{N} \right)^{-7} * \left(\frac{H}{N} \right)^{11.8} \right. \\
& * \left(\frac{L}{B} \right)^{-2.1} * M^{0.96} * TE^{0.68} * T^{15.4} * AG^{0.24} \left. \right) \\
& + \left(7.69 * FA^{-1.1} * FSO^{-14} * FAO^{9.42} * S^{-1.7} * SH^{3.38} * SS^{4.01} \right. \\
& * \left(\frac{SO}{N} \right)^{5.23} * \left(\frac{H}{N} \right)^{-2.47} * \left(\frac{L}{B} \right)^{-7.99} * M^{1.12} * TE^{-0.29} * T^{2.07} * AG^{0.1} \left. \right)
\end{aligned}$$

Where FA = FA (kg/m³), FSO = SiO₂% of FA, FAO = Al₂O₃% of FA, S = sand (kg/m³), SH = NaOH contents (kg/m³), SS = Na₂SiO₃ (kg/m³), SO/N = SiO₂/Na₂SiO₃, H/N = H₂O/Na₂O from the silicate solution, L/B = the liquid to geopolymer solids ratio, M = NaOH molarity, TE = curing temperature, T = curing time, AG = age.

Equation 11. Ahmed et al. (2022) NLR

$$\begin{aligned}
28 \text{ day } CS &= A * B * C \\
A &= \frac{AS + SF - NH - 4.23}{NH * (GS - SF)} + 2.42 \\
B &= \sqrt{4.23 - \sqrt{\frac{SF}{AS}}} - \sqrt{NH + 10.87 + 6.65} \\
C &= \sqrt[4]{10.87 * (AS + SF + 4.23) + GS - NZ - NH}
\end{aligned}$$

Where AS = age, NH = NaOH concentration, NZ = natural zeolite (kg/m³), SF = SF contents (kg/m³), GGBS contents

Equation 12. Shahmansouri et al. (2020)

Table 7.4. Model information for primary and secondary equations

Model	Pozz. precursor	Activation	Curing	Vital criteria
100%MK	100%MK	K_2SiO_3	Ambient	1.Activator 2.Binder 3.Water
GGBS/MK	80%GGBS 20%MK	K_2SiO_3	Ambient	1.Water 2.Activator 3.Binder
GGBS/SF	80%GGBS 20%SF	Na_2SiO_3 +NaOH	Ambient	1.Water 2.Activator
Diaz-Loya et al. (2013)	100% FA	Na_2SiO_3 +NaOH	24 hours @ 60°C	1.d50 2.R Al_2O_3 3.LOI
Ahmed et al. (2022) LR	100% FA	Na_2SiO_3 +NaOH	18-24 hours @ 25-80°C	1. SiO_2/Na_2SiO_3 2.L/S 3. H_2O/Na_2O
Ahmed et al. (2022) MLR	100% FA	Na_2SiO_3 +NaOH	18-24 hours @ 25-80°C	1.L/S 2. H_2O/Na_2O 3.FA contents
Ahmed et al. (2022) NLR	100% FA	Na_2SiO_3 +NaOH	18-24 hours @ 25-80°C	1.FA contents 2. H_2O/Na_2O 3.L/S
Shahmansouri et al. (2020)	70-100% GGBS 0-30% SF 0-30% NZ	Na_2SiO_3 +NaOH	Ambient	1.SF contents 2.Age 3.NaOH conc.

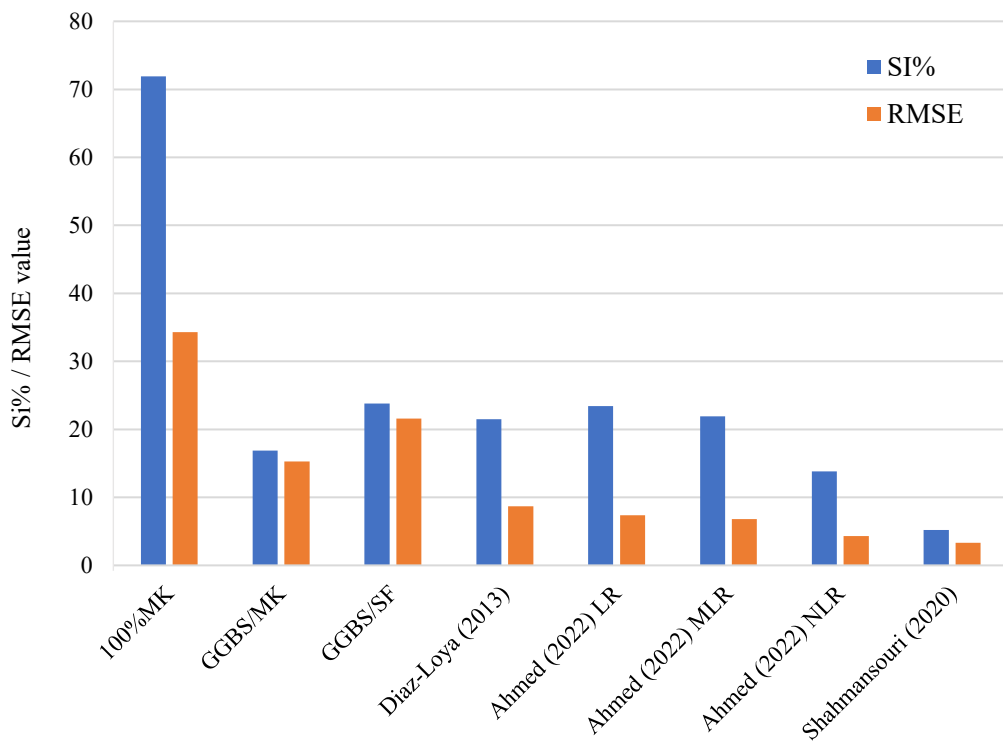


Figure 7.4. Statistical comparison of 28-day strength prediction models.

7.1.2 Basalt fibre geopolymer composite performance

The purpose of the geopolymer composites created in this research is to replace GRC in building cladding applications and reduce the carbon footprint of building construction. GRC materials are specified by their flexural strength (MOR at 28 days) as opposed to the compressive strength designations used in bulk concrete materials. Table 7.5 shows the typical flexural strength ranges for different types of GRC materials (sprayed and premix). Table 7.6 the strength requirements for each strength grade (G18, G10, G5) as per GRCA Practical design guide using limit states (GRCA, 2016-c). As illustrated in Table 7.5 sprayed GRC, containing 4-5%, 25-40mm fibres, is significantly stronger than premix GRC, which is recommended to contain 2-3.5% volume of 12-13mm glass fibres to achieve maximum flexural strength. Strength grades G5 and G10 usually designate a premix GRC with G18 only achieved by sprayed GRC's (GRCA, 2016-c). All composites were premix and these same values for fibre size and volume described in (GRCA, 2016-c) were found to provide optimal performance for basalt fibres in the MK geopolymer mortars studied. Of the four basalt fibre/geopolymer composites and the GRC control, only GP-17-A failed to meet the requirements of a G5 flexural strength class and therefore unsuitable for cladding applications.

Mix GP-17-A did have sufficient strength at 7 days for a G5 classification, but lost strength between 7- and 28-days. This indicated that the unsized fibres degraded in the alkaline MK matrix over time, and that PC specific sizing is necessary for high performance and composite durability. This finding is vital for the future design of geopolymer specific sizing formulations for basalt fibres and developing high performance basalt fibre composites.

The GRC control materials that were used in this study achieved an MOR value of 8 MPa after 1 day. Through the experimental methods employed in this research, the measured MOR value was 6.58 MPa, 17.5% lower than the control. If this strength reduction was

due to the unique test parameters and part machining methods employed in this research, flexural strength values for these materials from 3rd party testing could reasonably be predicted to increase by up to 21.6%.

The optimal composite developed in this research achieved a 28-day flexural strength of 6.3 MPa while the commercially available material currently being used for these applications achieved 7.5 MPa. As such, a GP-13-B composite would need to be increased in thickness from 13 mm up to 15.6 mm thick to provide equivalent performance. Alternatively, a reduction in L/S ratio of the highly flowable GGBS/MK mortar would also provide the required engineering performances. Even at 13 mm thickness, the composite proved to be sufficiently strong to form the structural component of building cladding panels by GRCA standards, whilst also providing the additional benefits of increased durability and reduced carbon embodiment intrinsic to geopolymeric materials.

Table 7.5. Types of GRC

GRC type	LOP (MPa)	MOR (MPa)
Sprayed	5-10	18-30
Premix	5-10	5-14

Table 7.6. GRC strength grades

GRC Grade	MOR range (MPa)
G18	18-30
G10	10-17
G5	5-10

7.1.3 Foamed geopolymer insulation performance

As described in Figures 6.4 - 6.6 and Tables 6.3 and 6.5, the foamed geopolymer materials developed a thermal conductivity of 0.09 W/mk. However, this could not compete with the conductivity of current building cladding panels, such as mineral wool (0.038 W/mk) or phenolic foam (0.018 W/mk). To achieve similar thermal performance, significant increases in panel thickness (and therefore panel mass) were required, resulting in a higher carbon footprint when panels incorporated the foamed geopolymer insulation. As a result, further reduction of thermal conductivity and density would be required before the developed materials are suitable for commercial use.

While the level of thermal performance achieved by the foamed geopolymers was disappointing, compared with results published in the literature - a thermal conductivity of 0.09 W/mk is typical based on the materials and methods used (Figure 7.5). The only study which produced foamed geopolymer using MK and H_2O_2 with thermal conductivity comparable to that of current insulation materials (0.03 W/mk) was that of Boros and Korim (2022). Their study produced foams similar to this research but at higher dosages of H_2O_2 . These foams used stabilising agents added to the mix to combat foam instability and reduce the likelihood of collapse from the high H_2O_2 contents, allowing foams of lower density to be produced. The adoption of these compounds in the H_2O_2 foamed MK materials investigated in this research could allow the density and thermal conductivity to be reduced to a similar level (0.041 W/mk). Other studies by Vaou and Panyas (2010) reported perlite-based geopolymers to produce foams with the lowest density of around 0.03 W/mk, which is even lower than that of mineral wool insulation.

products to geopolymer materials requires investment in the forms of financial capital, time and research. The construction sector will not adopt any new materials or techniques without a proven path to return on investment/profit. Any uncertainty in long term supply chains must be eliminated and any new geopolymer solutions must comply with British and European engineering performance and LCA standards.

7.2.1 Availability of pozzolanic precursor supply

In November 2016, the UK government announced the closure of all coal fired power plants by 2025. With the majority of other European countries adopting similar policies, FA production is rapidly declining. This will make the future commercial use of FA based geopolymers impractical. However, various solutions have been discussed in the literature. Due to overproduction of FA since the 1990's, approximately 50 Mt of wet FA has been stockpiled around the UK. It is considered possible, as already demonstrated in France and Germany, that this material can be recovered for use in geopolymers or PC-concrete products but will require drying and processing such that it is suitable for use, which in turn will be costly in terms of cost, energy and carbon embodiment (Alberici et al., 2017). Research by Hope et al. (2017) and McCarthy et al. (2018) has focussed on developing methodologies capable of increasing the quality of stockpiled wet FA such that it satisfies BS EN 450 standards for use in standard concrete products. Alternatively, huge stockpiles of FA exist in India and China (generated from coal-fired power plants, iron and steel manufacturing industries) and appear to have at least a medium-term security in supply due to the global demand for steel. While it may be expensive and carbon intensive to transport FA from industrial hubs to ports for shipping to the UK, it may still result in lower costs and carbon footprint given sufficient scale (Snellings et al., 2023).

While local FA production is likely to be eliminated in the next decade, alternative precursors currently being investigated by researchers could allow the continued short-

medium-term usage of FA for geopolymers, but in smaller amounts. However, given that FA is inherently variable in terms of composition and FA-based geopolymers require heat curing to achieve the highest strengths, these are major drawbacks that do not exist for other more consistent and reactive materials such as MK, GGBS or SF (Alberici et al., 2017).

Similar to FA, GGBS supplies in the UK are decreasing due to shrinkage in the steel and iron sector, specifically by 40% from 2014 to 2021 (Statista, 2020). There are currently only two major production facilities left in the UK (Port Talbot and Scunthorpe), both of which are running at half capacity. If new steel manufacturing infrastructure is to be established in the UK to support the construction sector's high demand for steel, these will likely be more efficient Electric Arc Furnaces (EAF's), which do not generate GGBS as a byproduct. Hence, the UK's short- to medium- term demand for GGBS will likely be met by importation from blast-furnaces that remain in operation in the Republic of Ireland, Continental Europe and China (Snellings et al., 2023; Vogl et al., 2021). With sufficient economies of scale, this long-distance transport could be cost effective, as illustrated by Redcar Grinding plant, set up in 2017, which will import and process 500 Mt of Chinese GGBS for use as SCM or geopolymer precursor (Alverici et al., 2017).

Over 190 Mt of legacy slags from historic steel and iron manufacture are available in the UK but will require similar processing to wet FA stockpiles (Riley et al., 2020). Comparative analysis of legacy slags against the requirements of BS EN 15167 shows that while the inorganic components are suitable, that LOI and moisture contents will be too high for use in concrete or mortars. However, if these slags are pretreated to remove accumulated moisture and carbonate contents, they could serve as a suitable replacement for GGBS production and reduce the UK's reliance on importation of GGBS (Rihner et al., 2022).

In tandem with recovery of materials from legacy stockpiles, the development of new pozzolanic precursors will be required to replace the limited FA and GGBS supplies in the UK. A wide range of natural and waste materials have therefore been investigated for use as SCM's in PC concrete and as pozzolanic precursors for geopolymerisation (Snellings et al., 2023).

The EAF's replacing blast furnaces produce a byproduct similar to GGBS called EAF steel slag, which possesses some cementitious properties. EAF slag is crystalline and composed mainly of Fe-substituted monticellite. Ozturk et al. (2019) showed that after activation with NaOH and Na₂SiO₃ it was possible to create mortars with strengths of up to 22 MPa. However, SEM analysis showed that mortars developed a porous microstructure and an irregular pore network. Although, using the correct alkali reagent solution increased C-S-H contents, densified the structure and created increased compressive strength. Muhmood et al. (2009) increased the pozzolanic and cementitious properties of EAF slag for use as an SCM in PC mortars, by remelting and quenching the material. This in turn reduced the iron oxide content, increased the basicity and therefore increased its cementitious properties. This same treatment could be used to increase the strength of EAF slag-based geopolymers, thereby highlighting the potential to partially or fully replace GGBS as an SCM in PC-based materials and as a pozzolanic precursor for geopolymerisation.

Natural (volcanic) pozzolans such as perlite and pumice also show great promise as geopolymeric precursors, due to their high amorphous contents. However, their low calcium contents would often result in performance effects similar to those of Class F FA's when used as an SCM in PC concrete or as geopolymer precursor (Snellings et al., 2023). Perlite has shown great promise for use in foamed geopolymers, due to its ability to achieve densities and thermal conductivities lower than any other precursor materials (Szabo and Mucsi, 2016). Natural pozzolans can also be blended with high calcium

materials (e.g. GGBS) to increase reactivity and allow significant strength generation with ambient curing (Snellings et al., 2023).

Another alternative precursor is ash derived from the incineration of biomass fuels. Approximately 810 Mt of ash is generated each year globally (Snellings et al., 2023). Owing to their high silica contents, these ashes could be used as an additive for controlling S/A ratio and therefore produce durable geopolymers (Chindaprasirt et al., 2022). Localised sources of materials such as bamboo leaf ash, date palm ash, sewage and paper sludge ash can also be used as they display similar properties to biomass ash. However, these ashes have irregular particle shape and rough surface textures, which will result in low workability and increased water demand in mortars (Snellings et al., 2023).

Ground recycled glass also has potential as a pozzolanic precursor. Whilst it has variable chemistry based on the types of glass present (e.g. coloured pigments), it is highly amorphous and silicious, but has a low Ca content. For full dissolution of the glass particles during geopolymerisation, the mortar pH must be maintained at ~ 10.7 . When used to form geopolymers, they will require heat curing and blending with other high-Ca precursors to produce high strength gains, as for Class F FA-based geopolymers (Siddika et al., 2021).

Whilst there are various potential alternative pozzolans to GGBS and FA for use in geopolymers, further research is needed to establish a database for these materials in addition to further investment in plant infrastructure to process and supply these materials at commercial scale. MK (or other forms of calcined clays) generally do not have the same issues concerning their future supply due to the abundance of suitable clay sources and are specifically produced for geopolymerisation or as SCMs. 37 Mt/year of MK is produced worldwide but only 10 Mt/year is currently used. 1370 Mt of MK reserves are therefore currently held which if used solely for geopolymer production could replace all

PC use for the next 7.5 years (Assi et al., 2020). Increased production would be required to meet this demand on an ongoing basis but is likely to be infeasible due to the commonality of suitable clay deposits worldwide (Davidovits, 2013). Hence, the investigations performed in this research on MK-based geopolymers may have the largest long-term impact due to their reliable supply chains.

7.2.2 Availability of activating mediums

The availability of cost effective, sustainable alkali reagent solutions is another critical factor that could limit the scale at which geopolymers are commercially used in the UK. Most geopolymers are activated using NaOH and/or Na₂SiO₃ but a wide range of other suitable materials are available (Austroads, 2016). Worldwide, NaOH production totals 72 Mt/year – whilst the demand is 120 Mt. Hence, a material deficit already exists before any additional demand arises from growth in the geopolymer market. NaOH is also the most expensive component of geopolymers, with prices varying significantly based on geographic region (US = \$770-920/t, China = \$350-450/t). Hence, limiting (or even eliminating) NaOH contents in geopolymer mix designs would be advantageous in reducing cost and reducing health and safety risks associated with handling NaOH on site (e.g. skin conditions such as skin burns, dermatitis).

Global annual production of Na silicates is ~12 Mt/year, which exceeds the current demand of 9.6 Mt/year. Hence, without major increases to production capacity, only a small proportion of PC materials could be replaced with the most studied geopolymer compositions (Assi et al., 2020). Research using alternative activating mediums is therefore vital to increase the practicality of geopolymer adoption. The use of KOH and/or K₂SiO₃ (as in this research) provides some extra availability; although production is currently 10% of that for current Na-silicates and hydroxides (ChemAnalyst, 2023).

One vital criterion for alkali reagents is high silica content, as this is required for polycondensation, structural development and therefore development of mechanical strength. Commercial alkaline silicates, such as the K-silicate used in this research (Geosil) are expensive and require significant carbon and energy to produce. Extraction of suitable activators from high silica waste could lower costs and carbon embodiment from activator production and boost global supply. One study investigated using waste glass particles dissolved in NaOH to activate Class C FA/GGBS mixtures. As waste glass contents increase (up to 20 g / 100 ml) and therefore silica contents in the activator, so does mechanical strength. Although for waste glass contents exceeding 20 g/100 ml, this increases water demand resulting in a high porosity and strength reductions (Sasiu et al., 2020). Vinai and Soutsos (2019) produced Na-silicate from waste glass using a similar process and reported similar or better compressive strengths from geopolymer mortars which contained commercially available Na_2SiO_3 and NaOH solutions.

Acid-based activating solutions have also been investigated (e.g. phosphoric acid) and successfully demonstrated to create geopolymers with strengths up to 140 MPa, increased durability and thermal stability compared with alkali reagent based geopolymers. However, further research is required to understand the implications of acidic geopolymer matrices on engineering performance and durability (Pu et al., 2022). While a significant amount of phosphoric acid is produced worldwide (83.4 Mt), approximately 85% of this is used for fertiliser. With rapidly increasing population and food demand, fertilisers are high in demand for the agriculture sector; hence acid-based geopolymers may struggle to achieve the supply required for commercial adoption (Statista, 2023). Little to no research has been performed to investigate other acid-based activation systems for potential use in geopolymers or AACMs.

7.2.3 Availability of basalt fibre reinforcement

The availability of basalt fibres for manufacturing fibre reinforced geopolymer composites (as proposed in this research) could limit the practicality of their widespread replacement of GRC if sufficient supply cannot be relied upon. Currently, global basalt fibre production is <0.1 Mt, which is significantly lower than construction sectoral demands. However, significant investment from the Chinese government (amongst other nations) has been proposed, which will result in an increase of global basalt fibre manufacture to >0.5 Mt by 2030 (IIUSE, 2020). Long-term growth of the basalt fibre production sector will certainly be achievable as basalt is one of the most abundant volcanic rocks in nature (King, 2023). The UK has large deposits of basalt in regions such as Northern Ireland and Scotland. Thus, local manufacture and supply of basalt fibres to the geopolymer composites industry will be possible, but will require infrastructure investment (Patti et al., 2022).

Whilst basalt fibres currently have a low UK technical readiness level, the development of facilities for mining basalt and manufacturing basalt fibres would assist the UK's construction sector in becoming self-sufficient in terms of access to raw materials (Ministry of Defence, 2022). For example, basalt fibres can be used to manufacture structural reinforcement bars as an alternative to steel bars, which would otherwise be energy intensive to manufacture and require importation from India and/or China. The cost and carbon embodiment associated with the use of basalt fibres could be significantly reduced by using local supplies and reduced transport distances.

7.2.4 Geopolymer production facilities

One of the major factors that increases the practicality of developing the infrastructure required for geopolymer manufacture, on a scale great enough to replace PC in the construction industry, is that geopolymers can be batched, mixed, cast and cured by using

existing PC production facilities (Ahmad and Alsaied, 2019). For instance, many PC pre-casters already have heat curing facilities for PC concretes with high SCM contents. Precursors such as MK or GGBS which are more reactive do not require heat curing and therefore post casting processes would remain identical to those previously used for PC concretes.

Whilst PC-concrete and geopolymer production processes are similar, there are some complicating factors when modifying facilities to manufacture geopolymers or hybrid PC/geopolymer materials (Tempest et al., 2015). The use of alkaline or acidic activation solutions has additional health and safety issues that are absent in PC concrete production facilities. If these reagent solutions are to be used in their current form, their delivery, storage, dosing and mixing systems must be strictly managed with significant capital investment likely required to prevent accidental contact with, and injury of, production staff. Where possible user-friendly activating solutions ($M = 1.45\text{-}1.85$) should be used to alleviate this risk (Geopolymer Institute, 2016; Davidovits, 2017).

One-part geopolymer mortars have previously been developed to eliminate or reduce health and safety risks associated with alkaline reagent solutions; comprising a powdered alkaline activator as part of the pozzolanic precursor powder. These could be supplied premixed in a similar manner to CEM-II, CEM-III and GRC-RTU materials, whereby only water is required to be added to the powders at the pre-casting facility. According to Luukkonen et al. (2018), no obstacles currently prohibit the development and use of commercially feasible “just add water” AACMs. However, further documentation and testing is required to demonstrate the suitability and long term durability of these materials, along with a better fundamental understanding of the reaction kinetics exhibited.

An additional challenge is present for pre-casters who wish to adopt geopolymers as a proportion of their production total alongside PC concrete is that the materials must not come into contact with each other in their fresh state. The Ca content of PC concrete causes a flash set in geopolymeric materials which could not only produce geopolymers with significantly reduced strength but cause severe damage to the batching plant and delivery equipment. Therefore, mixers and transport equipment must either be thoroughly cleaned before switching between them or separate batching and delivery systems used to eliminate the risk (Tempest et al, 2015).

7.3 Sustainability

This section focusses on comparing the sustainability of the fibre reinforced geopolymer cladding materials developed in this research with that of currently available GRC cladding options. Different methodologies are employed in the industry to ascertain true material sustainability with the majority focussing solely on the carbon footprint. The methodology used to calculate the carbon embodiment in this research is also compared with other methods currently used in the construction industry.

Sustainability analysis focussed solely on the structural component of the proposed cladding panels, as from the results presented in Chapter 6, it is evident that the foamed geopolymer composite has a significantly higher carbon embodiment than existing commercial insulation materials (e.g. polyurethane insulation boards). This results from the relatively high density/thermal conductivity of the foamed geopolymer and the higher mass of materials required for a given level of thermal insulation. By focussing future efforts on reducing the density and thermal conductivity properties, foamed geopolymers still have the potential to serve as low CO₂ insulation products as the embodied carbon/kg of its constituent materials is significantly lower than that of mineral wool or polyurethane boards (Kingspan, 2022; Rockwool limited, 2020).

7.3.1 LCA methodologies

Accurate calculation of the carbon embodiment for the geopolymer materials developed in this research was vital as part of their route to commercialisation. A range of methodologies exist for calculating carbon footprints, but there are significant differences regarding the factors considered, the methods used to allocate carbon from production processes and the stage(s) considered in the material life cycle. LCA's are the most commonly used and effective tool for these applications. ISO 14040 and ISO 14044 are the primary standards used for undertaking LCA, which specify principles, requirements and guidelines for the quantification and reporting of carbon footprint (ISO, 2006; ISO, 2006-b).

A range of LCA methodologies have previously been developed based on the principles presented in ISO 14040 and 14044 for different applications. ISO 14067, PAS 2050 and the GHG protocol are examples of specialised documents based on ISO 14040 and 14044, which assess factors solely related to global warming and are designed for specific niches or geographical locations. Others such as Product Environmental footprint method, generally recommended by the EU for LCA's, French standard BPX 30-323-0 and BS EN 15804 have wider scope and applicability, assessing all environmental impacts through a material lifecycle. All LCA standards aim towards strong alignment with the results of each other and the latest reports from Intergovernmental Panel on Climate change (IPCC) (Schryver and Zampori, 2022). As such, the most suitable choice will be dictated by the goal of the study, the industry or geographical location and requirements for reproducibility and width of applicability.

Existing third party, cradle-to-gate LCA's carried out according to BS EN 15804 provided the data used in this research to calculate the carbon embodiment of the geopolymer materials. BS EN 15804 was selected due to the extremely stringent and well-defined requirements, the high reproducibility and applicability of resulting carbon

embodiment values, as well as it being specifically focussed on the construction industry (BSI, 2019-b). Carbon embodiment figures are reported to be in line with those calculated through other common methodologies described; whereby the stringent control of the procedures intrinsic to this method provides high confidence in the accuracy of the results (Schryver and Zampori, 2022). Whilst this standard and other LCA's based on ISO 14040 and 14044 provide comprehensive and successful methodologies for carbon calculation of building materials, their focus is limited to the products themselves. No consideration is given to the effects these have on the carbon generated by the buildings or infrastructure which they form part of. The UK's PAS 2080 document was developed to calculate how products, goods and services integrate into buildings and infrastructure at a systems level, to fully assess the whole life carbon of the built environment and construction industry as a whole to help increase the likelihood of achieving net zero by 2050 (ICE, 2023).

7.3.2 Relative carbon embodiment of geopolymer/basalt fibre cladding materials

As the geopolymer/basalt fibre composites developed in this study were intended as a low carbon replacement for GRC, quantification of potential carbon savings must therefore be considered against the carbon footprint of GRC options available on the market today. EPD's for three GRC products carried out to BS EN 15804 were therefore identified from Reider (IBU-EPD, 2018), Telling (BRE Global, 2022) and Fiberbeton (EPD Danmark, 2021).

Figure 7.6 compares the embodied carbon contents per kg of the basalt fibre geopolymer cladding developed in this research, with those of three commercially available GRC cladding options. As previous calculations for carbon embodiment in this research only included LCA stage A-1, or the carbon attributable to the extraction and production of the raw materials, data from (EPD Danmark, 2021) was used to estimate the carbon attributable to transport of raw materials (A-2) and to the manufacturing processes used i.e. mixing and casting of panels (A-3). This data was selected due to the similar: 1)

production processes of GRC and geopolymer basalt composites, 2) geographical location and travel distances to manufacturing facilities considered, and 3) manufacturing facility in the UK. Most of the carbon embodiment exhibited by all the composites investigated was derived from the extraction and production of the raw materials, with PC and alkali reagent solution contents being the primary contributors in GRC and geopolymer/basalt composites, respectively.

Figure 7.6 illustrates that the composites developed in this research have much lower carbon embodiment than the commercially available GRC cladding options, due to the low CO₂ materials they are composed of. LCA stage A-1 contributed 91% of the total embodied carbon of the Fiberbeton GRC panel but only 72% of the geopolymer/basalt composites. The developed basalt fibre geopolymer composites have total stage A1-3 carbon embodiment of 0.228 kgCO₂/kg; just 31% that of Reider GRC, 56% of that for Telling GRC and 27% of that for Fiberbeton GRC.

If the K-silicate based reagent used in this research was replaced with an Na-silicate derived from waste glass, the embodied carbon of the geopolymer composites could be reduced significantly. Researchers have reported potential carbon savings of 31% (Bianco et al., 2021) to 50% (Scrivener et al., 2018). If a midpoint is taken between these two estimates of 40% the total kgCO₂/kg of basalt fibre geopolymer cladding could be reduced by 31% from 0.228 to 0.171 kgCO₂/kg. This would mean that the total carbon embodiment would be just 21% that of Reider GRC, 37% that of Telling GRC and 18% that of Fiberbeton GRC. These significant carbon savings highlight how successful geopolymer basalt fibre composites could be in reducing the carbon emissions of the cladding industry.

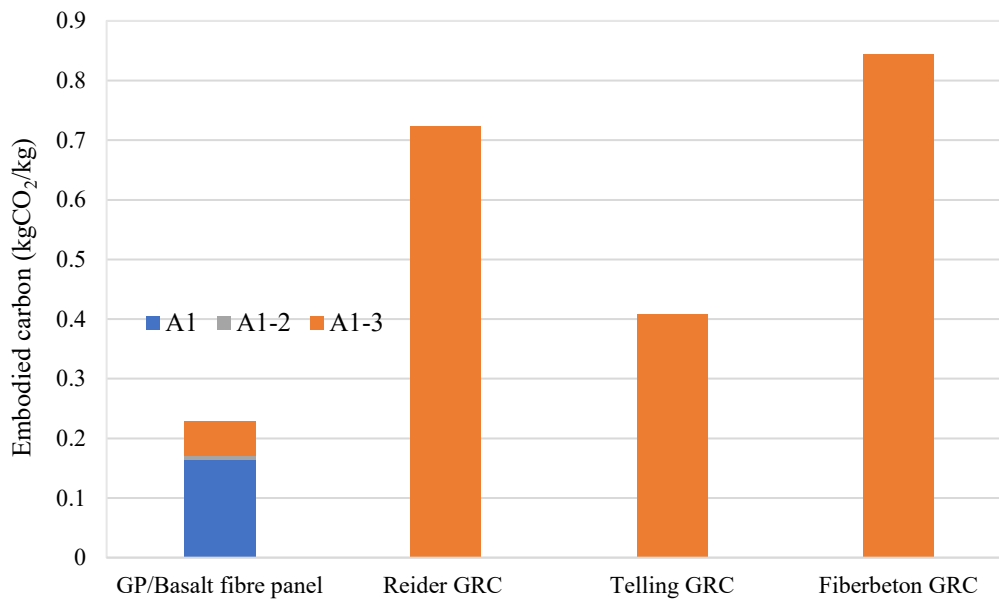


Figure 7.6. Embodied carbon of GRC and basalt fibre geopolymer cladding panels.

7.4 Financial analysis

The engineering performance of geopolymer materials developed in this research was analysed based on GRC RTU, serving as a control material sourced from Oscrete construction products. This material is an ‘all-in-one’, pre-bagged GRC material that only requires the addition of water by the end user. A price of £1,850/tonne was quoted for these materials by Oscrete in July 2023, although the additional water added comprises just over 15% of the finished product – hence the cost/tonne of GRC produced was lower at £1,567.88.

The basalt fibre geopolymer composites developed in this research could form the basis of a similar product to the one-part GRC. This new product would need to be mixed with a pre-specified mass of water and then identical manufacturing processes could be followed. This material would have a significantly reduced carbon embodiment, similar performance and an identical casting and curing process to the GRC-RTU. Therefore, any cost savings from the constituent material will be extremely significant to total reductions.

Table 7.7 shows costs for each component of the developed geopolymer composites, GRC-RTU materials and raw K-silicate. The primary factor determining the cost of basalt fibre geopolymer composites is the choice of activating solution. The commercially available K-silicate solution Geosil 15415 has increased in price over the course of this research - in 2023 the cost is £13,500/ton. As a result, when using Geosil as the activating solution the basalt fibre geopolymer composites developed in this research would cost £2,464.76; a 57% increase over the GRC-RTU product. However, as raw K-silicate costs just £1,029.35/ton in Europe (Chemanalyst, 2023) it would be possible to create a 45% by mass solution, K-silicate product identical to Geosil, for just £463.21/ton.

Alternatively raw K-silicate powder could be premixed with the precursor, basalt fibre and sand to produce a one part, basalt fibre geopolymer fibre composite solution similar to the GRC-RTU that only requires the addition of water. The activating solution used in this research was composed of 55% water, hence the mass of K-silicate in the dry mix would be 45% that specified of the solution and costs would be identical.

Figure 7.7 shows the total cost/ton of the GRC-RTU, basalt fibre geopolymer composites made with Geosil and with an activating medium produced in the lab from raw K-silicate. The production of alkali reagents in the lab would allow basalt fibre geopolymer cladding materials to be produced at a total cost/tonne of £128.10; just 8% that of the GRC-RTU. However, this price does not include costs incurred for producing, selling or marketing the product, nor does it account for elevated costs to generate profit, and as such cannot be compared with the price for GRC-RTU. However, it is evident that commercialisation of this product is economically viable and great scope exists for profitable business to be created.

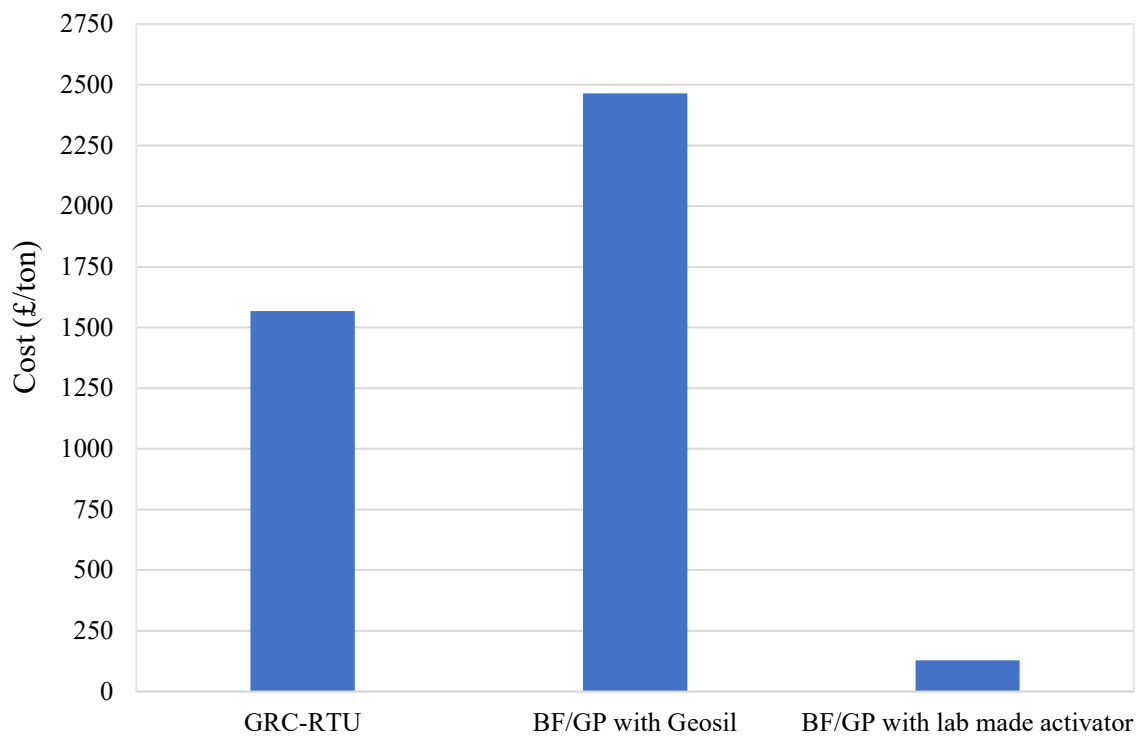


Figure 7.7. Costs of GRC and basalt fibre geopolymer cladding panels

Table 7.7. Material costs (ChemAnalyst, 2023).

Materials	Cost/ton
GRC-RTU	£1850
GGBS	£125
MK	£207
Sand	£16.50
Chopped basalt fibre	£245
Geosil 14515	£13500
Raw K-Silicate	£1029.35
45% K-Silicate solution	£463.45

7.5 The future

In 2022, over half of the world's population (7.8 billion) were concentrated in urban areas, which are expected to accommodate a further 2.5 billion by 2047. This will necessitate an increase in the construction of high rise, residential and mixed-use buildings as free land area in cities becomes increasingly scarce. High rise buildings are most often

composed of a portal frame enclosed by cladding panels, therefore the cladding industry and use of GRC-like cladding systems are also expected to grow significantly (Stouhi, 2022).

In 2023 the global GRC market was valued at £2.26 billion, but with a predicted compound annual growth rate of over 12% for the next six years the industry will grow significantly. Furthermore, the global GRC market is predicted to be valued at £4.46 billion by 2028. With the market rated as highly fragmented, highly competitive and as yet not consolidated by a small group of major players, plenty of scope exists for new companies and products to claim some of this market share.

Based on the cost/tonne of the GRC-RTU, by 2028 approximately 2,844,605 tons of GRC will need to be manufactured annually to meet market demand. If an average of the EPD results for the three GRC panels considered in section 7.3 ($0.654 \text{ kgCO}_2/\text{kg}$) is applied, this would release 1,874,594 tons of atmospheric CO_2 . Basalt fibre geopolymer composites have been shown in this research and other published studies to have the potential to significantly reduce the carbon embodiment of cementitious cladding systems, which would help towards achieving net zero carbon emissions by 2050.

If the entire GRC production of 2028 was replaced by basalt fibre geopolymer composites involving the use of Geosil K-silicate solution, approximately 1,218,487 tons of CO_2 could be saved – representing a 35% reduction in CO_2 emissions compared with predicted levels. If geopolymers were to use waste glass-based alkali silicate reagents, a further 168,713 tons of CO_2 could be saved with emissions just 26% of predicted values.

While the composites made with Geosil were more expensive than traditional GRC when lab made K-silicate solutions were used, the composite cladding panels were just 8% the cost of the GRC-RTU material. Using the cost/ton of this GRC as a basis for the

calculation, replacing all GRC predicted to be created in 2028 with basalt fibre geopolymer composites could save approximately £4.09 billion.

While these carbon and cost savings are significant, they are based on total replacement of the entire global GRC market. To achieve a fraction of this is currently unfeasible, especially without rapid development of geopolymer production infrastructure, investment and support from cladding specifiers and architects across the construction industry. The global geopolymer industry is still in its infancy compared with the well-established PC-based cement and concrete industries. With that said, similarities in manufacturing processes and materials will allow some of this existing infrastructure to be repurposed for geopolymers.

In 2023, the global geopolymer industry was worth £8.87 billion. With a predicted compound annual growth rate of over 29%, by 2028 this is anticipated to grow to £32.09 billion (Mordor Intelligence, 2023). These market statistics, the success of geopolymers in replacing PC based materials and the effects this will have on supply chains, prices and confidence for geopolymers in the construction industry will make replacement of a significant volume of worldwide GRC construction a feasible possibility. Increased widespread geopolymer use will, through economies of scale, allow precursor materials and alkaline reagents to become cheaper and more widely available, providing lower travel distances from source to manufacturing facilities and marked carbon savings.

Wagners, an Australian-based geopolymer manufacturer, have developed *Earth Friendly Concrete* (EFC) - a commercially available geopolymer concrete product composed of FA and GGBS, which offers CO₂ reductions of up to 80% compared with PC concretes; a world first. This material is batched in ordinary ready mix and precast concrete plants, delivered in trucks and placed by pump, chute or spray in a manner identical to the PC-concretes they are to replace; a major advantage as no changes are required by contractors

to specify EFC compared with PC-concrete. EFC is one of the first, fully commercialised and user-friendly products that through its ease of use, could allow rapid proliferation of geopolymer concretes in the construction industry. This concrete has been used in major projects around Australia (e.g. Global Change Institute in Queensland, Wellcamp International Airport, Pinkenba Wharf deck). This product has moved away from sole use in major civil engineering projects run by large highly skilled contractors and is now being used in small scale residential projects in Queensland (Aus) (EFC, 2023). Wagners launched EFC in the UK in 2020 and has so far been used on major projects including HS2 (e.g. floor slabs, foundations, tunnel segments and a temporary foundation of 232m³; the largest geopolymer pour ever in the UK). Wagners are the only major company marketing geopolymer concrete and its usage has been limited to flagship projects where government contracts allow for more innovation than would typically be accepted (EFC, 2023).

A primary reason for the lack of commercial use of geopolymers to date is that design engineers are reluctant to specify a material for which there are no standards – meaning that there is a high risk and little legal protection associated with using these materials. BS EN 206 and 8500, the main documents for specification of PC-concrete based materials in the UK, do not cover geopolymers or AACMs and therefore would not meet the majority of job specifications (BSI, 2019; BSI, 2021). However, positive progress has been made in recent years for standardising geopolymers and AACMs, through the release of PAS 8820 in 2016.

For geopolymer potential to be fully realised in the UK, either engineering standards for cementitious construction materials require modification to include geopolymers and AACMs, or new standards need to be developed. While the UK recognised as far back as 2011 that modifying these documents to be less prescriptive, and more performance based is vital, few significant changes have been made with no evidence that the European

Commission is following this lead. The potential for significant replacement of GRC by geopolymer composites and the cost and carbon savings predicted by this research is linked to the wider development of the geopolymer industry and the development of strong material supply chains especially for novel precursor and reagents.

In conclusion geopolymer cladding materials have great real-world potential to help the decarbonisation of the construction sector. However, significant and rapid industrial development is required, coupled with strong legislative standards on mix design and specification, to give designers and material specifiers the confidence needed to use geopolymer and AACM products in standard construction projects.

Chapter 8 – Conclusions and recommendations

This final chapter summarises the key outputs from this research, how they fulfilled the aims and objectives defined for this research, and identify possible routes for undertaking further work.

8.1 Conclusions

Geopolymers have great potential for use as a ‘greener’ replacement for GRC, provided that a well-established and understood knowledge base is in place to facilitate safe working practices involving geopolymer cement mortars in construction. The possibility of foaming geopolymers to create an insulation material that could form part of an all-in-one cladding panel solution was identified. Despite its benefits, a key challenge that must be addressed to enable the commercial use of geopolymers is the lack of recognised mix design methodologies capable of producing materials with specified values of performance properties like compressive strength and/or workability.

This research investigated five different pozzolanic precursors (MK, FA, GGBS, SF and IS) and two alkali silicate reagents (Na_2SiO_3 and K_2SiO_3). K_2SiO_3 was found to be a more successful alkaline reagent, providing higher strength and mortar flowability to the MK mortars studied. Both MK and GGBS promoted high strength, highly flowable geopolymer mortars when used to make up 100% of the pozzolanic precursor powder, whereas FA, SF and IS were only useful at lower dosages. GGBS/SF based mortars produced the highest compressive strengths of up to 108 MPa after 28-days. Two mix design methodologies have been proposed to allow easy specification of geopolymer mortars, especially to those familiar with specification of PC-based materials. The first attempted to mimic water-to-cement ratio-based specification common in PC using the analogous geopolymer L/S ratio. This made the specification easy to use for the current construction industry and was applicable to a wide range of pozzolanic precursor

materials. The second, more comprehensive, mix design method used contour plots based on empirical equations that predict performance properties. These were more accurate and could make geopolymer design recommendations for which the 7- and 28-day strength, flowability, cost and carbon embodiment could all be specified simultaneously. This process allowed the identification of a range of high performance geopolymer mortars suitable for forming the matrix component of high-strength fibre composites.

Fibre reinforced geopolymer composites were created using basalt fibres that exhibited up to 84% of the flexural strength of GRC control mixes. An optimal fibre diameter of 13 μm was identified and that the zirconia-based sizing used in GRC to protect fibres from degradation, may also be required. These composites offered additional benefits over GRC in that they have much lower embodied carbon and energy embodiment. The compositions of the reinforced geopolymer composites have scope for achieving better engineering performances through the use of suitable additives or a reduction of the matrix water to binder ratio. As such, this composition formed the structural component of the proposed cladding panels.

Four methods to increase geopolymer porosity were investigated during the development of the geopolymer insulation materials: 1) endogenous foaming using H_2O_2 , 2) surfactant-based foaming industrial surfactant, 3) the inclusion of preformed foam and 4) porous aggregates. Most of these methods promoted material properties which would exclude their use as insulation materials. Endogenous foaming with H_2O_2 produced high porosity but large, open pores unsuitable for high thermal resistance. Surfactant-based foaming of MK mortars using glucopon industrial surfactant was a suitable method to provide thermal conductivities as low as 0.0933 W/mK. Several cladding design options were developed based on these materials and a basalt fibre reinforced mortar to meet the thermal requirements required for domestic and non-domestic structures.

In summary, geopolymeric materials were found to be a successful option for the creation of building cladding and insulation materials. The performances achieved were comparable to existing cladding materials currently in use, but in a form that is fireproof and contains only a fraction of the embodied carbon. Further development in the thermal resistance of these panels would allow the creation of a low carbon claddings systems that minimise carbon usage, while the structure is in use and significantly increase the safety of its occupants.

8.2 Recommendations for further work

The materials and systems developed as part of this research are all at a preliminary development stage and have potential for further performance development and application. Suggestions for performing further work to progress this area of research include the following:

- Future research will focus on improving predictions by widening the range of mix parameters and compositions studied and increasing the data sets on which they are based. The ultimate aim would be to develop a single model suitable for accurately predicting the performance of any geopolymer binder type. The use of modern analytics techniques such as machine learning could be adopted to increase prediction accuracy and ascertain general rules applicable to wide ranges of geopolymer mortar compositions.
- SEM imaging is required to confirm the internal structures present in geopolymer mortars especially for GGBS/MK geopolymers, where understanding the interaction between the various reaction products during the geopolymerisation process and their effects on mechanical strength is vital

- The creation of a software application (or similar digital tool) that could synthesise the equations for determining performance properties in geopolymers mortars into a simple specification tool. This would allow specifiers to input required performance properties, with a range of suggested mix designs and binder compositions as outputs. This ability is already available in Design expert 12. The development of an intuitive, easy to use interface that could inform contractors of the wide range of potential geopolymer source materials would make adoption of geopolymer materials much easier.
- The exploration of alternative alkali reagents and new alumino-silicate precursor materials for geopolymer materials that are waste based and less carbon intensive than current products – thereby enhancing local, national and international circular economies.
- Additives are fundamental to modern cementitious materials. However, the efficacy of these in geopolymer materials is often undetermined. The development of a range of geopolymer-specific additives could revolutionise their engineering performances in a similar manner to the use of additives in traditional PC-based materials over the past century.
- While fibre sizings developed for cementitious materials are effective in improving the performance of basalt fibre geopolymer composites, specific sizings developed for these compositions have the potential to reduce the cost and environmental impact and improve performance. Work aimed towards the development of compounds and techniques tailored to the exact properties and requirements of geopolymer paste/basalt fibre composites is required and has potential to increase mechanical performance significantly.

- Research should be undertaken on controlling mix viscosity in surfactant-based geopolymer foams and determining its effect on the resulting pore structure. This could allow the creation of materials with increased porosity, mechanical strength and thermal resistance.
- Full scale production of cladding panels including connectors and structural and thermal field testing of the final product.
- A detailed LCA (cradle-to-cradle) is needed to ascertain the whole life carbon embodiment of geopolymer/basalt fibre composites and foamed geopolymer insulation.

References

- Mustafa Al Bakri, A. M., Kamarudin, H., Bnhussain, M., Khairul Nizar, I., Rafiza, A. R. and Izzat, A. M., 2011. Chemical reactions in the geopolymerisation process using fly ash-based geopolymer: A review. *Australian Journal of Basic and Applied Sciences*, 5(7), pp. 1199-1203.
- Adam, A. A., Ramadhan, B. R. and Maricar, S., 2019. The Effects of Water to Solid Ratio, Activator to Binder Ratio, and Lime Proportion on the Compressive Strength of Ambient-Cured Geopolymer Concrete. *Journal Of The Civil Engineering Forum*, 5(2), pp.161-167. <https://doi.org/10.22146/jcef.43878>.
- Al-Majidi, M. H., Lampropoulos, A. and Cundy, A. BM., 2017. Tensile properties of a novel fibre reinforced geopolymer composite with enhanced strain hardening characteristics. *Composite Structures*, 168(1), pp. 402-427. <https://doi.org/10.1016/j.compstruct.2017.01.085>.
- Ahmad, A. and Alsaied, A., 2019. Review on Properties, Performance, and Application of Geopolymer Concrete. *Sustainable Structure and Materials*, 2(1), pp.61-75. <https://doi.org/10.26392/SSM.2019.02.01.061>.
- Ahmed, H. U., Abdalla, A. A., Mohammed, A. S., Mohammed, A. A. and Mosavi, A. et al., 2022. Statistical methods for modeling the compressive strength of geopolymer mortar. *Materials (Basel)*, 15(5), 1868, pp.18-24. <https://doi.org/10.3390/ma15051868>.
- Alberici, S., De Beer, J., van der Hoorn, I. and Staats, M., 2017. *Fly ash and blast furnace slag for cement manufacturing: BEIS research paper no. 19*, London: Department for Business, Energy and Industrial Strategy.
- Altoubat, S., 2018. *Fibre reinforced concrete design concepts*, Dubai: Research Institute of Science and Engineering.

Alves, L., Leklou, N. and de Barros, S., 2020. A comparative study on the effect of different activating solutions and formulations on the early stage geopolymerization process. *MATEC Web of Conferences*, 322, 01039, pp. 1-5, <https://doi.org/10.1051/mateconf/202032201039>.

Anderson, B. and Kosmina, L., 2019. *Conventions for U value calculations*, London: BRE.

Assi, L. N., Carter, K., Deaver, E. and Ziehl, P., 2020. Review of availability of source materials for geopolymer/sustainable concrete. *Journal of Cleaner Production*, 263, 121477, <https://doi.org/10.1016/j.jclepro.2020.121477>.

ASTM, 1996. *ASTM C 1228 – 96 Standard Practice for Preparing Coupons for Flexural and Washout Tests on Glass Fiber Reinforced Concrete*, New York: ASTM International.

ASTM, 2016. *ASTM C947-03 Standard Test Method for Flexural Properties of Thin-Section Glass-Fiber-Reinforced Concrete (Using Simple Beam With Third-Point Loading)*, New York: ASTM International.

Aughenbaugh, K. L., Williamson, T. and Juenger, M. C. G., 2015. Critical evaluation of strength prediction methods for alkali-activated fly ash. *Materials and Structures*, 48(1), pp.607–620, <https://doi.org/10.1617/s11527-014-0496-z>.

Aurubis, 2017. *Iron silicate (Fayelite)*, Sofia: Aurubis.

Austroroads, 2016. *Technical report AP-T318-16 Specification and use of Geopolymer concrete in the manufacture of structural and non-structural components: Review of literature*, Sydney: Austroroads Ltd.

Aydın, S. and Baradan, B., 2013. The effect of fiber properties on high performance alkali-activated slag/silica fume mortars. *Composites Part B: Engineering*, 45(1), pp. 63-69, <https://doi.org/10.1016/j.compositesb.2012.09.080>.

Ball, H., 2005. *25 years of forton polymer modified GRC: reasons for its use*. GRCA 2005 Congress. Hong Kong, GRCA, pp. 72-96.

Banah, 2014. *Introduction to Geopolymer Binders*. Ballyclare: Banah UK., Ballyclare: Banah UK.

Banah, 2014. *Introduction to Geopolymer Binders*, Ballyclare: Banah UK.

BASF, 2013. *Glucopon 225 DDK Non-ionci surfactants for the detergent and cleaning industry*, Texas: BASF.

Bediako, M. and Amankwah, E. O., 2015. Analysis of Chemical Composition of Portland Cement in Ghana: A Key to Understand the Behavior of Cement. *Advances in Materials Science and Engineering*, 2015(1), pp.1-5, <https://doi.org/10.1155/2015/349401>.

Benhelal, E., Zahedi, G., Shamsaei, E., Bahadori, A., 2013. Global strategies and potentials to curb CO₂ emissions in cement industry. *Journal of Cleaner Production*, 51, pp.142-161, <https://doi.org/10.1016/j.jclepro.2012.10.049>.

Bernal, S., De Gutierrez, R., Delvasto, S., Rodriguez, E., 2010. Performance of an alkali-activated slag concrete reinforced with steel fibres. *Construction and Building Materials*, 24(2), pp.208-214, <https://doi.org/10.1016/j.conbuildmat.2007.10.027>.

Bianco, L., Bad, T., and Vinai, R. (2021). Analysis of the environmental impacts of alkali-activated concrete produced with waste glass-derived silicate activator – A LCA study. *Journal of Cleaner Production*, 316, 128383, <https://doi.org/10.1016/j.jclepro.2021.128383>.

Boros, A. and Korim, T., 2022. Development of Geopolymer Foams for Multifunctional Applications. *Crystals - Special issue: Geopolymer*, 12(3), 386, <https://doi.org/10.3390/cryst12030386>.

Branston, J., Das, S., Kenno, S. Y. and Taylor, C., 2016. Mechanical behaviour of basalt fibre reinforced concrete. *Construction and Building Materials*, 124, pp.878-886, <https://doi.org/10.1016/j.conbuildmat.2016.08.009>.

BRE Global, 2022. *Environmental product declaration for Ibstock Telling GRC Ltd Plain GRC facade panels*, London: BRE Global.

BSI, 1999. *BS EN 1015-3:1999 Methods of test for mortar for masonry - Part 3: Determination of consistence of fresh mortar (by flow table)*, London: BSI.

BSI, 2005. *BSEN 1991-1-4:2005 Eurocode 1. Actions on structures- General actions - Wind actions*, London: BSI.

BSI, 2009. *BS EN 476-10:2009. Fire tests on building materials and structures. Guide to the principles, selection, role and application of fire testing and their outputs.*, Milton Keynes: British Standards Institution BSI.

BSI, 2017. *BS 8297:2017 Design, manufacture and installation of architectural precast concrete cladding. Code of practice*, London: BSI.

BSI, 2019. *BS EN 15804:2012+A2:2019 - Sustainability of construction works. Environmental product declarations. Core rules for the product category of construction products*, London: BSI.

BSI, 2019. *BS EN 12350-5:2019 Testing fresh concrete (flow table test)*, London: BSI.

Bumrongjaroen, W., Swatekititham, S., Livingston, R., Schweitzer, J., 2007. Synthetic glass models for investigating fly ash reactivity. *ACI Spec. Publication*, 1(1), pp. 227-242.

BSI, 2019. *BS 8500:2019 Concrete - Complementary British Standard to BS EN 206*. London: BSI.

BSI, 2021. *BS EN 206:2013+A2:2021 Concrete. Specification, performance, production and conformity*. London: BSI.

Business insider India, 2021. *Business insider*. [Online]
Available at: <https://www.businessinsider.in/tech/30-giant-chinese-infrastructure-projects-that-are-reshaping-the-world/slidelist/52836152.cms#slideid=52836153>
[Accessed 2 March 2023].

Cabrera, J. and Frias Rojas, M., 2001. Mechanism of hydration of the metakaolin-lime-water system. *Cement and Concrete Research*, 31(2), pp.177-182, [https://doi.org/10.1016/S0008-8846\(00\)00456-7](https://doi.org/10.1016/S0008-8846(00)00456-7).

Callister, W., 2014. *Materials science and engineering; An introduction. 9th ed. USA: Wiley*. All.. 9 ed. New York: Wiley.

Chen, X., Kim, E., Suraneni, P. and Struble, L., 2020. Quantitative Correlation between the Degree of Reaction and Compressive Strength of Metakaolin-Based Geopolymers. *Materials (Basel)*, 13(24), 5784, <https://doi.org/10.3390/ma13245784>.

ChemAnalyst, 2023. *Global Potassium Silicate Market Analysis: Demand & Supply, End-User Demand, Distribution Channel, Regional Demand, 2015-2035*, New York: Research And Markets.

Chindaprasirt, P., Rattanasak, U. and Posi, P., 2022. Geopolymers Based on Biomass Ash and Bio-based Additives for Construction Industry. In: A. Hunt, ed. *High-Performance Materials from Bio-based Feedstocks*. New York: John Wiley & Sons Ltd, pp. pp.289-314.

Choi, W-C., Yun, H-D., Kang, J-W. and Kim, S-W., 2012. Development of recycled strain-hardening cement-based composite (SHCC) for sustainable infrastructures. *Composites Part B: Engineering*, 43(2), pp. 627-635, <https://doi.org/10.1016/j.compositesb.2011.11.060>.

CIOB, 2016. *World's biggest low carbon cement plant to open in UK*, London: Chartered Institute of Builders.

CIRIA, 2010. *RP566 Cladding fixings: Good practice*, London: CIRIA.

Clearloop, 2021. www.Cleerloop.us. [Online] Available at: <https://clearloop.us/2021/03/24/cradle-to-gate-vs-cradle-to-grave/> [Accessed 14 2023].

Cockburn, H., 2018. *Worst case climate change scenario could be more extreme than thought, scientists warn*. The Independent. [online] Last accessed 19.04.2022. Available at: <<https://www.independent.co.uk/climate-change/news/climate-change-model-scenario-rcp85-global-warming-illinois-study-a8353346.html>>

Creagh , 2020. *Structural precast brochure*, Belfast: Creagh .

Cross UK, 2020. *Structural issues with cladding Report ID 904*, London: Cross UK.

Davidovits, J., 2002. *30 years of successes and failures in geopolymer applications: market trends and potential breakthroughs*, *Geopolymer 2002: international geopolymer conference, Melbourne , Australia..* Melbourne, Geopolymer Institute.

Davidovits, J., 2013. *Geopolymer Cements: A review*. Geopolymer Science and Technics. 1 (1). pp.1-11. Geopolymer Institute Library. www.geopolymer.org.

Davidovits, J., 2015. *Environmental implications of Geopolymers*. Materials Today. [online]. Date accessed: 05.06.2022. Available at: <<https://www.materialstoday.com/polymers-soft-materials/features/environmental-implications-of-geopolymers/>>

Davidovits, J., 2016. *Reinforced geopolymer composites: A critical review*. Materials Today. [online]. Date accessed: 02.04.2019. Available at: <<https://www.materialstoday.com/polymers-soft-materials/features/reinforced-geopolymer-composites-a-critical-review/>>.

Davidovits, J., 2017. *Geopolymer webinar 2017*, Paris: Geopolymer Institute.

Deghani, A., Aslani, F. and Panah, N., 2021. Effects of initial SiO₂/Al₂O₃ molar ratio and slag on fly ash-based ambient cured geopolymer properties. *Construction and Building Materials*, 293, 123527, <https://doi.org/10.1016/j.conbuildmat.2021.123527>.

DFPNI, 2012. *Department of Finance and Personnel Northern Ireland DFPN Building Regulations 2012 (Northern Ireland) Technical booklet E Fire safety*, Belfast : DFPNI.

DFPNI , 2022. Technical booklet F1 Conservation of fuel and power in dwellings. *NI Building Regulations 2012 (Northern Ireland)*,

DFPNI, 2022-b. Technical booklet F2 Conservation of fuel and power in buildings other than dwellings. *NI Building Regulations*, p. Belfast.

Diaz-Loya, E., Allouche, E., Cahoy, D., 2013-a. Statistical based approach for predicting the mechanical properties of geopolymer concretes. In: H. J. Struble L, ed. *Geopolymer binder systems*. West Conshohocken: ASTM International, pp. 119-143.

Diaz-Loya, E., Kinney, F. and Rios, C., 2013-b. Reactivity indicators for activated high-calcium fly ash-based binders. *ACI Special Publication*, 294(1), pp. 1-22.

Donà, M. a. O. M., 2017. Fatigue Performance of a Connection for GRC Cladding Panels *In: Proceedings of the 8th International Conference on Advanced Composites in Construction (ACIC 2017)* 05-07.09.2017. Sheffield, ACIC 2017.

Downey, M. and Drzal, L. T., 2016. Toughening of carbon fibre-reinforced epoxy polymer composites utilizing fibre surface treatment and sizing. *Composites Part A: Applied Science and Manufacturing*, 90, p.687–698, <https://doi.org/10.1016/j.compositesa.2016.09.005>.

Duan, P., Song, L., Yan, C., Ren, D. and Li, Z., 2017. Novel thermal insulating and lightweight composites from metakaolin geopolymer and polystyrene particles. *Ceramics International*, 43(6), pp.5115–5120, <https://doi.org/10.1016/j.ceramint.2017.01.025>.

Duxson, P., Mallicoat, S. W., Lukey, G. C., Kriven, W. M. and van Deventer, J. S. J., 2007. The effect of alkali and Si/Al ratio on the development of mechanical properties of metakaolin-based geopolymers. *Colloids and Surfaces A: Physicochemical and Engineering Aspects*, 292(1), pp.8-20, <https://doi.org/10.1016/j.colsurfa.2006.05.044>.

Duxson, P. and Provis, J., 2008. Designing precursors for Geopolymer Cements. *Journal of the American Ceramic Society*, 91(12), pp.3864–3869, <https://doi.org/10.1111/j.1551-2916.2008.02787.x>.

Ebnesajjad, S., 2014. Chapter 12 - Adhesion Promoters. In: S. Ebnesajjad, ed. *Surface Treatment of Materials for Adhesive Bonding*. New York: William Andrew Publishing, pp. pp. 301-329.

EFC. (2023). *Earth friendly concrete*. [online]. Date accessed: 21st June 2023. Available at: <<https://earthfriendlyconcrete.com/>>.

Enfedaque, A., Sanchez Paradela, L. and Sanchez-Galvez, V., 2012. An alternative methodology to predict aging effects on the mechanical properties of glass fiber reinforced cements (GRC). *Construction and Building Materials*, 27(1), pp.425-431, <https://doi.org/10.1016/j.conbuildmat.2011.07.025>.

EPD Danmark, 2021. *VERIFIED ENVIRONMENTAL PRODUCT DECLARATION to ISO 14025 & EN 15804 for Glassfibre reinforced concrete elements*, Skensved: Danish Technological Institute.

EPD Ireland, 2019. *ENVIRONMENTAL PRODUCT DECLARATION as per ISO 14025 and EN 15804+A1 for ECOCEM products*, Dublin: Irish Green Building Council.

ESFA, 2018. *Concrete cladding - monitoring building condition*, London: Education and Skills Funding Agency.

European commission, 2014. *2030 Climate & Energy Framework.*, Brussels: European Commision.

European Commission, 2020. *research-and-innovation.ec.europa.* [Online] Available at: https://research-and-innovation.ec.europa.eu/funding/funding-opportunities/funding-programmes-and-open-calls/horizon-europe_en [Accessed 20 03 2023].

European Council, 2018. *International agreements on climate action*, Brussels : s.n.

Fauzi, A, Nuruddin, M. F., Malkawi, A., Abdullah, M. M. A. B. and Mohammed, B., 2017. Effect of Alkaline Solution to Fly Ash Ratio on Geopolymer Mortar Properties. *Key Engineering Materials*, 733, pp.85-88, <https://doi.org/10.4028/www.scientific.net/KEM.733.85>.

Fawer, G., Concannon, M. and Rieber, W., 1999. Life cycle inventories for the production of sodium silicates. *The International Journal of Life Cycle Assessment*, 4, pp.207-212, <https://doi.org/10.1007/BF02979498>.

Fibre technologies international, 2020. *GRC guide*, Bristol: FTI.

Fiore, V., Scalici, T., Di Bella, G. and Valenza, A., 2015. A review on basalt fibre and its composites. *Composites Part B: Engineering*, 74, pp.74-94, <https://doi.org/10.1016/j.compositesb.2014.12.034>.

Fletcher, R. A., MacKenzie, K. J. D., Nicholson, C. L. and Shimada, S., 2005. The composition range of aluminosilicate geopolymers. *Journal of the European Ceramic Society*, 25(9), pp.1471-1477, <https://doi.org/10.1016/j.jeurceramsoc.2004.06.001>.

Foamglas, 2022. *Foamglass downloads*. [Online] Available at: <https://www.foamglas.com/en/download> [Accessed 14 2022].

Frearson, A., 2013. *Library and Learning Centre in Vienna by Zaha Hadid Architects*, London: www.dezeen.com.

Gamonchuan, J., Grudpan, K. and Burahkam, R., 2021. A Facile Synthesized Polyaniline Coated Zerovalent Iron-Silica as an Efficient Sorbent for Magnetic Solid Phase Extraction of Phenolic Pollutants in Water Samples. *Journal of the Brazilian Chemical Society*, 32(1), pp. 194-206. <https://doi.org/10.21577/0103-5053.20200168>.

Gao, K., Lin, K-L., Wang, D., Shiu, H-S., Hwang, C-L., Cheng, T-W., 2013. Effects of Nano-SiO₂ on Setting Time and Compressive Strength of Alkali-activated Metakaolin-based Geopolymer. *The Open Civil Engineering Journal*, 7, pp.84-92.

Geopolymer Institute, 2006. *Technical Data Sheet for Geopolymeric cement type (Potassium, Calcium) – Poly(sialate-siloxo) / (K,Ca) – (Si-O-Al-O-Si-O-), Si:Al=2:1*. Last accessed 01/1, Paris: Geopolymer Institute.

Geopolymer Institute, 2016. *State of the Geopolymer R&D 2016.*, Paris: Geopolymer Institute.

Geopolymer Institute, 2009. *Geopolymer Scientific papers on exponential growth*. [online]. Date accessed: 14.07.21 Available at: <<https://www.Geopolymer.org:https://www.geopolymer.org/news/geopolymer-scientific-papers-on-exponential-growth/>>.

Glad, B. E. and Kriven, W. M., 2015. Highly Porous Geopolymers Through Templating and Surface Interactions. *Journal of the American Ceramic Society*, 98(7), pp.2052-2059, <https://doi.org/10.1111/jace.13584>.

GOV.UK, 2021. *Building safety bill (HL Bill 98)*, London: The stationary office.

GRCA, 2016-a. *Specifiers Guide to Glass fibre Reinforced Concrete*, London: GRCA. Available at : <https://www.grca.online/technical/grca-publications>.

GRCA, 2016-b. *About GRC.*, Online: GRCA. Available at : <https://www.grca.online/technical/grca-publications>.

GRCA, 2016-c. *A Practical Design Guide for GRC using Limit States*, London: GRCA. Available at : <https://www.grca.online/technical/grca-publications>.

GRCA, 2017. *Methods of Testing Glass reinforced Concrete (GRC)*, Northhampton: The International Glassfibre Reinforced Concrete Association (GRCA). Available at : <https://www.grca.online/technical/grca-publications>.

GRCA, 2021. *Specification for the Manufacture, Curing & Testing of GRC Products*, London: GRCA. Available at : <https://www.grca.online/technical/grca-publications>.

Guzmán-Aponte, L. A., de Gutierrez, R. B. and Maury-Ramirez, A., 2017. Metakaolin-Based Geopolymer with Added TiO₂ Particles: Physicomechanical Characteristics. *Coatings*, 7(12), 233, <https://doi.org/10.3390/coatings7120233>.

Habert, G., 2014. Chapter 25: Life cycle assessment (LCA) of alkali-activated cements and concretes. In: F. Pacheco-Torgal, ed. *Handbook of alkali-activated cements, mortars and concretes*. Paris: Elsevier, pp.663-686. ISBN: 9780081013953

Habert, G., d'Espinose de Lacaillerie, J. B. and Roussel, N., 2011. An environmental evaluation of geopolymer based concrete production: reviewing current research trends. *Journal of Cleaner Production*, 19(11), pp.1229-1238, <https://doi.org/10.1016/j.jclepro.2011.03.012>.

Hammell, J., Balaguru, P. and Lyon, R., 1998. Influence of Reinforcement Types on the Flexural Properties of Geopolymer Composites. *Proceedings of the 1998 43rd International SAMPE Symposium and Exhibition, Part 2 of 2 - Anaheim, CA, USA (31st May - 4th June 1998)*, pp. 1600-1608.

Hartman, D. R., Peters, L. and Antle, J. L., 2006. Sizing for high performance glass fibers and composite materials incorporating same. *US patent 20060204763*, New York: US Patent Office.

Heah, C. Y., Kamarudin, H., Mustafa Al Bakri, A. M., Bnhussian, M., Luqman, M., Khairul Nizar, I., Ruzaidi, C. M. and Liew, Y. M., 2012. Study on solids-to-liquid and alkaline activator ratios on kaolin-based geopolymers. *Construction Building Materials*, 35, pp.912-922, <https://doi.org/10.1016/j.conbuildmat.2012.04.102>.

Hope, T., McCarthy, M. and Carrol, R., 2017. *Recovery and Processing of Wet-stored Fly Ash for use in Concrete Construction*. Brno, Czech Republic, EuroCoalAsh 2017: Innovations in Power Plant Technology and CCP Utilisation.

Hyde, R. and Kinnane, O., 2016. Early Stage Development of an Ultra-High Performance Geopolymer. *Proceedings of the 36th Cement and Concrete Science Conference, Cardiff, UK*, pp. 245-255.

Hyde, R., Kinnane, O., West, R. and Nanukuttan, S, 2017-a. *Manufacture and assembly of a thin, lightweight, low impact, prototype precast geopolymer sandwich panel for the retrofit cladding of existing buildings*, Belfast: QUB Poster Presentation.

Hyde, R., Kinnane, O., West, R. and Nanukuttan, S. V., 2017-b. Design of a test hut field experiment for prototype precast geopolymer sandwich panels for the retrofit cladding of existing buildings. *Proceedings of the 3rd International Conference on Chemically Activated Materials, 8th - 11th August 2017, Gold Coast, Australia*.

IBU-EPD, 2018. *Environmental Product Declaration according to ISO 14025 AND EN 15804 for concrete skin or Oko skin GRC*, Munich: IBU-EPD.

ICE, 2023. *Guidance Document for PAS 2080 - Practical actions and examples to accelerate the decarbonisation of buildings and infrastructure*, London: ICE.

IIUSE, 2020. *iiuse.seu.edu.cn*. [Online]
Available at: https://iiuse.seu.edu.cn/iiuse_en/2022/0620/c41382a412238/page.htm
[Accessed 15 06 2023].

ISO, 1991. *ISO 8301:1991 Thermal insulation -- Determination of steady-state thermal resistance and related properties -- Heat flow meter apparatus*, Paris: ISO.

ISO, 1999. *ISO 8301:1991(en) Thermal insulation — Determination of steady-state thermal resistance and related properties — Heat flow meter apparatus*, Brussels: ISO.

ISO, 2006. *ISO 14040:2006 - Environmental management — Life cycle assessment — Principles and framework*, Geneva: ISO.

ISO, 2006-b. *ISO 14044:2006 - Environmental management — Life cycle assessment — Requirements and guidelines*, Geneva: ISO.

Ivashchenko, E. A., 2009. Sizing and finishing agents for basalt and glass fibers. *Theoretical Foundations of Chemical Engineering*, 43, pp.511-516, <https://doi.org/10.1134/S0040579509040277>.

Jan, A., Pu, Z., Khan, K. A., Ahmad, I., Shaukat, A. J., Hao, Z. and Khan, I., 2022. A Review on the Effect of Silica to Alumina Ratio, Alkaline Solution to Binder Ratio, Calcium Oxide + Ferric Oxide , Molar Concentration of Sodium Hydroxide and Sodium Silicate to Sodium Hydroxide Ratio on the Compressive Strength of Geopolymer Concrete. *Silicon*, 14, pp.3147-3162, <https://doi.org/10.1007/s12633-021-01130-3>.

Jiang, C., Fan, K., Wu, F., Chen, D., 2014. Experimental study on the mechanical properties and microstructure of chopped basalt fibre reinforced concrete. *Materials & Design*, 58, pp.187-193, <https://doi.org/10.1016/j.matdes.2014.01.056>.

Jones, C., 2019. *Inventory of Carbon and Energy (ICE) Version 3.0*, Bath: s.n.

Kaddami, A., 2017. *Elaboration and study of the functional properties of geopolymer foams (Geopolymer Camp 2017)*. Saint Quentin, Geopolymer Institute .

Khater, H., 2013. Effect of silica fume on the characterization of the geopolymer materials. *International Journal of Advanced Structural Engineering*, 5 (12), pp.5-12, <https://doi.org/10.1186/2008-6695-5-12>.

Kim, E., 2012. Understanding effects of silicon/aluminum ratio and calcium hydroxide on chemical composition, nanostructure and compressive strength for metakaolin geopolymers. Masters Thesis, University of Illinois at Urbana-Champaign, Illinois, USA.

King, H., 2023. *www.Geology.com*. [Online]
Available at: <https://geology.com/rocks/basalt.shtml>
[Accessed 05 06 2023].

Kingspan, 2022. *Kingspan.com*. [Online]
Available at: <https://www.kingspan.com/gb/en/products/insulation-boards/wall-insulation-boards/kooltherm-k108-cavity-board/?s=t>
[Accessed 1 June 2022].

Koehler, P. and Fowler, D. W., 2007. Aggregates in Self-Consolidating Concrete - Final Report ICAR Project 108. The University of Texas at Austin.

Komnitsas, K. A., 2011. Potential of geopolymer technology towards green buildings and sustainable cities. *Procedia Engineering*, 21, pp.1023-1032, <https://doi.org/10.1016/j.proeng.2011.11.2108>.

Korniejenko, K., Fraczek, E., Pytlak, E. and Adamski, M., 2016. Mechanical Properties of Geopolymer Composites Reinforced with Natural Fibers. *Procedia Engineering*, 151, pp.388-393, <https://doi.org/10.1016/j.proeng.2016.07.395>.

Kumar, R., 2015. Study on behaviour of geo polymer concrete.. *Journal of Industrial Pollution Control*, 33(2), pp. 1341-1344.

Kwasny, J., Soutsos, M., McIntosh, J. A., Cleland, D. J., 2016. *banahCEM – comparison of properties of a laterite-based geopolymer with conventional concrete. Proceedings of 9th International Concrete Conference 2016: Environment, Efficiency and Economic Challenges for Concrete*. Dundee, University of Dundee.

- Lach, M., Korniejeko, K. and Mikula, J., 2016. Thermal Insulation and Thermally Resistant Materials Made of Geopolymer Foams. *Procedia Engineering*, 151, pp.410-416, <https://doi.org/10.1016/j.proeng.2016.07.350>.
- Lahoti, M., Narang, P., Tan, K. H. and Yang, E-H., 2017. Mix design factors and strength prediction of metakaolin-based geopolymer. *Ceramics International*, 43(1), pp.11433-11441, <https://doi.org/10.1016/j.ceramint.2017.06.006>.
- Lecomte, I., Henrist, C., Liegeois, M., Maseri, F., Rulmont, A. and Cloots, R., 2006. (Micro)-structural comparison between geopolymers, alkali-activated slag cement and Portland cement. *Journal of the European Ceramic Society*, 26(16), pp.3789-3797, <https://doi.org/10.1016/j.jeurceramsoc.2005.12.021>.
- Lin, T., Jia, D., He, P., Wang, M. and Liang, D., 2008. Effects of fiber length on mechanical properties and fracture behavior of short carbon fiber reinforced geopolymer matrix composites. *Materials Science and Engineering: A*, 497(1-2), pp.181-185, <https://doi.org/10.1016/j.msea.2008.06.040>.
- Lin, Z. and Li, V. C., 1997. Crack bridging in fiber reinforced cementitious composites with slip-hardening interfaces. *Journal of the Mechanics and Physics of Solids*, 45(5), pp.763-787, [https://doi.org/10.1016/S0022-5096\(96\)00095-6](https://doi.org/10.1016/S0022-5096(96)00095-6).
- Lin, Z., Kanda, T. and Li, V. C., 1999. On Interface Property Characterization and Performance of Fibre Reinforced Cementitious Composites. *Journal of Concrete Science and Engineering, RILEM*, 1, pp.173-184, <https://hdl.handle.net/2027.42/84718>.
- Li, V. C. and Wu, H-C., 1992. Conditions for Pseudo Strain-Hardening in Fiber Reinforced Brittle Matrix Composites. *Applied Mechanics Reviews*, 45(8), pp.390-398, <https://doi.org/10.1115/1.3119767>.

Lizcano, M., Gonzalez, A., Basu, S., Lozano, K. and Radovic, M., 2012. Effects of Water Content and Chemical Composition on Structural Properties of Alkaline Activated Metakaolin-Based Geopolymers. *Journal of the American Ceramic Society*, 95(7), pp.2169-2177, <https://doi.org/10.1111/j.1551-2916.2012.05184.x>.

Luukkonen, T., Abdollahnejad, Z., Yliniemi, J., Kinnunen, P. and Illikainen, M., 2018. One-part alkali-activated materials: A review. *Cement and Concrete Research*, 103, pp.21-34, <https://doi.org/10.1016/j.cemconres.2017.10.001>.

MacKenzie, K. J. D., 2003. What are These Things Called Geopolymers? A Physicochemical Perspective. In *Advances in Ceramic Matrix Composites IX*, 153, Eds N. P. Bansal, J. P. Singh, W. M. Kriven and H. Schneider, pp.175-186, <https://doi.org/10.1002/9781118406892.ch12>.

Mannock, 2021. *Mannock aircrete super*. [Online] Available at: <https://www.mannokbuild.com/aircrete-thermal-blocks/mannok-aircrete-super/> [Accessed 8 may 2022].

Masi, G., Rickard, W. D. A., Vickers, L., Bignozzi, M. C. and van Riessen, A., 2014. A comparison between different foaming methods for the synthesis of light weight geopolymers. *Ceramics International*, 40(9A), pp.13891-13902, <https://doi.org/10.1016/j.ceramint.2014.05.108>.

Mason, K., 2006. *Sizing Up Fiber Sizings*, London: Composites World Articles.

McCarthy, M., Jones, M. & Zheng, L. a. D. R., 2008. *New Approach to Fly Ash Processing and Applications to Minimise Wastage to Landfill WR0401*, Dundee: Defra.

Matsimbe, J., Dinka, M., Olukanni, D., and Musonda, I., 2022. A Bibliometric Analysis of Research Trends in Geopolymer. *Materials (Basel)*, 15(19), 6979, <https://doi.org/10.3390/ma15196979>.

McCarthy, M. J., Zheng, L., Dhir, R. K. and Tella, G., 2018. Dry-processing of long-term wet-stored fly ash for use as an addition in concrete. *Cement and Concrete Composites*, 92, pp.205-215, <https://doi.org/10.1016/j.cemconcomp.2017.10.004>.

McIntosh, J., 2021. The development of a geopolymer binder from the interbasaltic laterites of Northern Ireland. *PhD thesis, Queens University Belfast, UK*.

McLellan, B. C., Williams, R. P., Lay, J. and van Riessen, A. and Corder, G. D., 2011. Costs and carbon emissions for geopolymer pastes in comparison to ordinary portland cement. *Journal of Cleaner Production*, 19(9-10), pp.1080-1090, <https://doi.org/10.1016/j.jclepro.2011.02.010>.

McMican, R., 2012. Sizing stability is a key element for glass fibre manufacturing. *Reinforced Plastics*, 56(5), pp.29-32, [https://doi.org/10.1016/S0034-3617\(12\)70110-8](https://doi.org/10.1016/S0034-3617(12)70110-8).

Mindess, S., 2008. Chapter 7 - Fibrous concrete reinforcement. In: Mindess, S., ed. *Developments in the Formulation and Reinforcement of Concrete* (1 ed.). London: Woodhead Publishing. pp. 154-166. ISBN 9781845692636. <https://doi.org/10.1533/9781845694685.154>.

Mordor Intelligence. (2023). *GEOPOLYMER MARKET SIZE & SHARE ANALYSIS - GROWTH TRENDS & FORECASTS (2023 - 2028)*. Hyderabad: Mordor Intelligence.

Muhmood, L., Vitta, S. and Venkateswaran, D., 2009. Cementitious and pozzolanic behavior of electric arc furnace steel slags. *Cement and Concrete Research*, 39(2), pp.102-109, <https://doi.org/10.1016/j.cemconres.2008.11.002>.

Mustofa, A. and Pinotowantoro, S., 2016. The Effect of Si/Al Ratio to Compressive Strength and Water Absorption of Ferronickel Slag-based Geopolymer. *The 2nd International Seminar on Science and Technology, 2nd August 2016, Surabaya, Indonesia*.

Ministry of Defence, 2022. *Technology Readiness Levels (TRLs) in the Project Lifecycle*, London: Ministry of Defence.

Nagendra, V., Sashidhar, C. and Kumar, S. M. P., 2018. Ground Granulated Blast Furnace Slag (GGBS): Effect of Particle Size and Dosage on Compressive Strength with Microstructural Analysis of Concrete. *International Journal for Research in Applied Science & Engineering Technology*, 6(5), pp. 2467-2474. ISSN: 2321-9653.

Nambiar, E. K. K. and Ramamurthy, K., 2007. Air-void characterisation of foam concrete. *Cement and Concrete Research*, 37(2), pp.221–230, <https://doi.org/10.1016/j.cemconres.2006.10.009>.

Narayanan, N. and Ramamurthy, K., 2000. Structure and properties of aerated concrete: a review. *Cement and Concrete Composites*, 22(5), pp.321-329, [https://doi.org/10.1016/S0958-9465\(00\)00016-0](https://doi.org/10.1016/S0958-9465(00)00016-0).

Nematollahi, B. and Sanjayan, J., 2014. Effect of different superplasticizers and activator combinations on workability and strength of fly ash based geopolymer. *Materials & Design*, 57, pp.667-672, <https://doi.org/10.1016/j.matdes.2014.01.064>.

Oh, J. E., Moon, J., Oh, S-G., Clark, S. M. and Monteiro, P. J. M., 2012. Microstructural and compositional change of NaOH-activated high calcium fly ash by incorporating Na-aluminate and co-existence of geopolymeric gel and C-S-H(I). *Cement and Concrete Research*, 42(5), pp.673-685, <https://doi.org/10.1016/j.cemconres.2012.02.002>.

Oh, J. E., Jun, Y., Jeong, Y. and Monteiro, P. J. M., 2015. The importance of the network-modifying element content in fly ash as a simple measure to predict its strength potential for alkali-activation. *Cement and Concrete Composites*, 57, pp.44-54, <https://doi.org/10.1016/j.cemconcomp.2014.12.001>.

Oscrete, 2016. *GRC-RTU: Ready to use GRC composite material PDS 7897* , Bradford: Oscrete Construction Products.

Ozturk, M., Bankir, M. B., Bolukbasi, O. S. and Sevim, U. K., 2019. Alkali activation of electric arc furnace slag: Mechanical properties and micro analyzes. *Journal of Building Engineering*, 21, pp.97-105, <https://doi.org/10.1016/j.jobbe.2018.10.005>.

Palmieri, A., Matthys, S. and Tierens, M., 2009. Basalt fibres: Mechanical properties and applications for concrete structures. *In Concrete Solutions, Eds: Grantham, Majorana and Salomoni*. Taylor and Francis Group, London, ISBN 978-0-415-55082-6.

Park, S., Yu, J., Oh, J. E. and Pyo, S., 2020. Effect of Silica Fume on the Volume Expansion of Metakaolin-Based Geopolymer Considering the Silicon-to-Aluminum Molar Ratio. *International Journal of Concrete Structures and Materials*, 16(20), <https://doi.org/10.1186/s40069-022-00510-2>.

Pillay, D. L., Olalusi, O. B., Awoyera, P. O., Rondon, C., Echeverria, A. M. and Kolawole, J. T., 2020. A Review of the Engineering Properties of Metakaolin Based Concrete: Towards Combatting Chloride Attack in Coastal/ Marine Structures. *Advances in Civil Engineering*, 8880974. <https://doi.org/10.1155/2020/8880974>.

Piret, W., Masson, N. and Peters, L., 2013. *Glass fibre sizing composition*. *European patent EP2540683 A1.*, Brussels: European Patent Register.

Patti, A, Acierno, S, Nele, L, Graziosi, L, and Acierno, D., 2022. Sustainable Basalt Fibers vs. Traditional Glass Fibers: Comparative Study on Thermal Properties and Flow Behavior of Polyamide 66-Based Composites. *ChemEngineering* , 6(6), 86, <https://doi.org/10.3390/chemengineering6060086>.

Pu, S., Zhu, Z., Song, W., Huo, W. and Zhang, C., 2022. A eco-friendly acid fly ash geopolymer with a higher strength. *Construction and Building Materials*, 335, <https://doi.org/10.1016/j.conbuildmat.2022.127450>.

Provis, J. L. and van Deventer, J. S. J., 2009. Geopolymers: Structures, Processing, Properties and Industrial Applications. Woodhead Publishing Ltd and CRC Press LLC. ISBN 978-1-84569-449-4.

Provis, J. L., Palomo, A. and Shi, C., 2015. Advances in understanding alkali-activated materials. *Cement and Concrete Research*, 78 (Part A), pp.110-125, <https://doi.org/10.1016/j.cemconres.2015.04.013>.

Ralph, C., Lemoine, P., Boyd, A., Archer, E. and McIlhagger, A., 2019. The effect of fibre sizing on the modification of basalt fibre surface in preparation for bonding to polypropylene. *Applied Surface Science*, 475(1), pp.435-445, <https://doi.org/10.1016/j.apsusc.2019.01.001>.

Ranjbar, N., Telebian, S., Mehrali, M., Kuenzel, C., Metselaar, H. S. C. and Jumaat, M. Z., 2016. Mechanisms of interfacial bond in steel and polypropylene fiber reinforced geopolymer composites. *Composites Science and Technology*, 122, pp.73-81, <https://doi.org/10.1016/j.compscitech.2015.11.009>.

RIBA, 2020. *GFRC M4 Cladding System (Telling Architectural)* , London: RIBA.

Rieder, 2020. *Facades guide*, Vienna: Rieder.

Rienhardt, H. W., Parra-Montesinos, G. J. and Garrecht, H., 2015. *Proceedings pro094: Seventh International RILEM Workshop on High Performance Fiber Reinforced Cement Composites (HPFRCC7)*. London, RILEM, ISBN 978-2-35158-145-2.

Rihner, M. C. S., Marsh, A. T. M., Provis, J. L., Koh, L. S. C., Walkley, B. and Bernal, S., 2022. Legacy slags - a solution to the future shortages of GGBFS in the UK. *In: 41st Cement and Concrete Science Conference*, 12-13 September 2022, Leeds, UK.)

Riley, A. L., MacDonald, J. M., Burke, I. T., Renforth, P., Jarvis, A. P., Hudson-Edwards, K. A., McKie, J. and Mayes, W. M., 2020. Legacy iron and steel wastes in the UK: Extent, resource potential, and management futures. *Journal of Geochemical Exploration*, 219, 106630, <https://doi.org/10.1016/j.gexplo.2020.106630>.

Rockwool limited, 2020. *HP Partial fill cavity slab tds*, London: Rockwool.

Rowles, M. R. and O'Connor, B. H., 2009. Chemical and Structural Microanalysis of Aluminosilicate Geopolymers Synthesized by Sodium Silicate Activation of Metakaolinite. *Journal of the American Ceramic Society*, 92(10), pp.2354-2361, <https://doi.org/10.1111/j.1551-2916.2009.03191.x>.)

Ruiz-Santaquiteria, C., Skibsted, J., Fernandez-Jimenez, A. and Palomo, A., 2012. Alkaline solution/binder ratio as a determining factor in the alkaline activation of aluminosilicates. *Cement and Concrete Research*, 42(9), pp.1242–1251, <https://doi.org/10.1016/j.cemconres.2012.05.019>.

Sasui, S., Kim, G., Nam, J., van Riessen, A., Eu, H., Chansomsak, S., Alam, S. F. and Cho, C. H., 2020. Incorporation of Waste Glass as an Activator in Class-C Fly Ash/GGBS Based Alkali Activated Material. *Materials (Special Issue: Research of Mechanical Behavior of Cement and Concrete Composites)*, 13(17), 3906, <https://doi.org/10.3390/ma13173906>.

Schryver, A. and Zampori, L., 2022. *Product Carbon Footprint standards: which one to choose?* [Online] Available at: <https://pre-sustainability.com/articles/product-carbon-footprint-standards-which-standard-to-choose/>. [Accessed 18 07 2023].

Scrivener, K. L., John, V. M., Gartner, E. M. and UN Environment. (2018). Eco-efficient cements: Potential economically viable solutions for a low-CO₂ cement-based materials industry. *Cement and Concrete Research*, 114, pp.2-26, <https://doi.org/10.1016/j.cemconres.2018.03.015>.

Shahmansouri, A. A., Bengar, H. A. and Ghanbari, S., 2020. Compressive strength prediction of eco-efficient GGBS-based geopolymer concrete using GEP method. *Journal of Building Engineering*, 31, 101326, <https://doi.org/10.1016/j.jobe.2020.101326>.

Shivaranjan, N. S., Shiva Kumar, K. S., Venkatesh Babu, D. L. and Nagaraj, V. K., 2016. A study on self compacting geopolymer concrete with various water to gepolymer solids ratios. *International Research Journal of Engineering and Technology*, 3(7), pp. 2064-2069, e-ISSN: 2395-0056.

Siddika, A., Hajimohammadi, A., Al Mamun, M. A., Alyousef, R. and Ferdous, W., 2021. Waste Glass in Cement and Geopolymer Concretes: A Review on Durability and Challenges. *Polymers (Basel) (Special Issue: Geopolymers - Design, Preparation, Applications)*, 13(13), 2071, <https://doi.org/10.3390/polym13132071>.

De Silva, P., Sagoe-Crenstil, K. and Sirivivatnanon, V., 2007. Kinetics of geopolymerization: Role of Al₂O₃ and SiO₂. *Cement and Concrete Research*, 37(4), pp.512-518, <https://doi.org/10.1016/j.cemconres.2007.01.003>.

Sim, J., Park, C. and Moon, D. Y., 2005. Characteristics of basalt fiber as a strengthening material for concrete structures. *Composites Part B: Engineering*, 36(6-7), pp.504-512, <https://doi.org/10.1016/j.compositesb.2005.02.002>.

Skidmore, C., 2023. *Mission Zero : Independent review of Net Zero*, London: Department of Energy, Security and Net Zero and Department for Business, Energy and Industrial Strategy.

Snellings, R., Suraneni, P. and Skibsted, J., 2023. Future and emerging supplementary cementitious materials. *Cement and Concrete Research*, 171, 107199, <https://doi.org/10.1016/j.cemconres.2023.107199>.

Srinath, S. S. V. and Prabha, S. L., 2016. Evaluation of Wall Panels Using Geopolymer Concrete. *International Journal of Innovative Research in Science, Engineering and Technology*, 5(6), pp.10435-10441, <https://doi.org/10.15680/IJIRSET.2015.0506170>.

Staniford, S., 2012. *Cement production, China and elsewhere: Early Warning, Rational analysis of global warming risk*, New York: Earlywarn.

Start2see , 2012. *LCA of geopolymer concrete (E-crete) Final Report* , Melbourne: Start2see.

Statista, 2020. *Chinese cement consumption*. [Online] Available at: <https://www.statista.com/statistics/1042516/chinese-cement-consumption/> [Accessed 23 2023].

Statista, 2023. *Global Phosphoric Acid Production by Region*. [Online] Available at: <https://www.statista.com/statistics/1289301/global-phosphoric-acid-productionbyregion/#:~:text=The%20global%20production%20of%20phosphoric,million%20metric%20tons%20in%202021.> [Accessed 29 June 2023].

Steel Construction Info, 2016. *Corrosion of structural steel*, s.l.: s.n.

Stouhi, D., 2022. *What is the Future of High Rise Buildings?* [online] Available at: <https://www.archdaily.com/972401/what-is-the-future-of-high-rise-buildings>. Date accessed: 04.06.2023.

Szabo, R. and Mucsi, G., 2015. Generally about geopolymers. *In: Proceedings from MultiScience - XXIX. microCAD International Multidisciplinary Scientific Conference*, Hungary 21st-24th April 2016. Miskolc, University of Miskolc, <https://doi.org/10.26649/musci.2015.014>.

Telling Architectural, 2019. *Excellence in glass fibre reinforced concrete*, London: The NBS.

Tempest, B., Snell, C., Gentry, T., Trejo, M. and Isherwood, K., 2015. Manufacture of full-scale geopolymer cement concrete components: A case study to highlight opportunities and challenges. *PCI Journal*, 60(6), pp.39-50, <https://doi.org/10.15554/pcij.11012015.39.50>.

Terzano, R., Spagnuolo, M., Medici, L., Tateo, F. and Ruggiero, P., 2005. Characterisation of Different Coal Fly Ashes For Their Application in the Synthesis of Zeolite X as a Cation Exchanger for Soil Remediation. *Fresenius Environmental Bulletin*. 14(4), pp263-267.

Thomason, J. L. and Adzima, L. J., 2001. Sizing up the interface: an insider's guide to the science of sizing. *Composites Part A: Applied Science and Manufacturing*, 32(3-4), pp.313-321, [https://doi.org/10.1016/S1359-835X\(00\)00124-X](https://doi.org/10.1016/S1359-835X(00)00124-X).

Timakul, P., Thanaphatwetphisit, K. and Aungkavattana, P., 2015. Effect of Silica to Alumina Ratio on the Compressive Strength of Class C Fly Ash-Based Geopolymers. *Key Engineering Materials*, 659, pp.80-84, <https://doi.org/10.4028/www.scientific.net/KEM.659.80>.

Tiwari, S. and Bijwe, J., 2014. Surface Treatment of Carbon Fibres - A Review. *Procedia Technology*, 14, pp.505-512, <https://doi.org/10.1016/j.protcy.2014.08.064>.

Turner, L. K. and Collins, F. G., 2013. Carbon dioxide equivalent (CO₂-e) emissions: A comparison between geopolymer and OPC cement concrete. *Construction and Building Materials*, 43, pp.125-130, <https://doi.org/10.1016/j.conbuildmat.2013.01.023>.

UNEP SBCI, 2009. *Buildings and Climate Change Summary for Decision Makers*, Brussels:: United Nations Environment Programme Sustainable Buildings & Climate Initiative.

Vinai, R. and Soutsos, M., 2019. Production of sodium silicate powder from waste glass cullet for alkali activation of alternative binders. *Cement and Concrete Research*, 116, pp.45-56, <https://doi.org/10.1016/j.cemconres.2018.11.008>.

van Deventer, J. S. J., Provis, J. L., Duxson, P. and Lukey, G. C., 2007. Reaction mechanisms in the geopolymeric conversion of inorganic waste to useful products. *Journal of Hazardous Materials*, 139(3), pp.506-513, <https://doi.org/10.1016/j.jhazmat.2006.02.044>.

Vaou, V and Panias, D., 2010. Thermal insulating foamy geopolymers from perlite. *Minerals Engineering*, 23(14), pp.1146-1151, <https://doi.org/10.1016/j.mineng.2010.07.015>.

Visintin, P. and Oehlers, D. J., 2018. Fundamental mechanics that govern the flexural behaviour of reinforced concrete beams with fibre-reinforced concrete. *Advances in Structural Engineering*, 21(7), pp.1088–1102, <https://doi.org/10.1177/1369433217739705>.

Vogl, V., Olsson, O. and Nykvist, B., 2021. Phasing out the blast furnace to meet global climate targets. *Joule*, 5(10), pp.2646-2662, <https://doi.org/10.1016/j.joule.2021.09.007>.

- Wan, Q., Rao, F. and Song, S., 2017. Reexamining calcination of kaolinite for the synthesis of metakaolin geopolymers - roles of dehydroxylation and recrystallization. *Journal of Non-Crystalline Solids*, 460, pp.74-80, <https://doi.org/10.1016/j.jnoncrysol.2017.01.024>.
- Wang, H., Wu, H., Xing, Z., Wang, R. and Dai, S. ~~et al.~~, 2021. The Effect of Various Si/Al, Na/Al Molar Ratios and Free Water on Micromorphology and Macro-Strength of Metakaolin-Based Geopolymer. *Materials*, 14(14), 3845, <https://doi.org/10.3390/ma14143845>.
- White, I., 2015. *The application of GRC in the Middle East*, Dubai: Middle East Concrete, Fibre technologies international, Powersprays.
- Wilkinson, A., 2018. The use of geopolymer cement for road. *PhD thesis, Ulster University, UK*.
- Wilson, A. P., 2015. Establishing a mix design procedure for geopolymer concrete. *BEng dissertation, University of Southern Queensland, Australia*.
- Woellner, 2014. *Geosil 14515 Alkaline activator based on potassium silicate*, Berlin: Woellner.
- World Cement Assosiation, 2019. *World cement production 2018 and forecast 2030*, London: WCA.
- World Green Building Council, 2019. *Bringing Embodied Carbon Upfront*, London: World Green Building Council.
- World Resource Institue (WRI), 2019. World greenhouse gas emissions. [Online] Available at: <https://www.wri.org/data/world-greenhouse-gas-emissions-2018> [Accessed 19 04 2020].

Xu, H. and van Deventer. J. S. J., 2000. The geopolymerisation of alumino-silicate minerals. *International Journal of Mineral Processing*, 59(3), pp.247-266, [https://doi.org/10.1016/S0301-7516\(99\)00074-5](https://doi.org/10.1016/S0301-7516(99)00074-5).

Bernal, S. A., Mejía de Gutiérrez, R. and Provis, J. L., 2012. Engineering and durability properties of concretes based on alkali-activated granulated blast furnace slag/metakaolin blends. *Construction and Building Materials*, 33, pp.99-108, <https://doi.org/10.1016/j.conbuildmat.2012.01.017>.

Yan, L., Kasal, B. and Huang, L., 2016. A review of recent research on the use of cellulosic fibres, their fibre fabric reinforced cementitious, geo-polymer and polymer composites in civil engineering. *Composites Part B: Engineering*, 92, pp.94-132, <https://doi.org/10.1016/j.compositesb.2016.02.002>.

Yunsheng, Z., Yantao, J., Wei, S. and Zongjin, L., 2009. Study of ion cluster reorientation process of geopolymerisation reaction using semi-empirical AM1 calculations. *Cement and Concrete Research*, 39(12), pp.1174-1179, <https://doi.org/10.1016/j.cemconres.2009.07.022>.

Zeobond, 2012. *The geopolymer solution*, s.l.: The Zeobond group.

Zhang, F., Zhang, L., Liu, M., Mu, C., Liang, Y. N. and Hu, X., 2017. Role of alkali cation in compressive strength of metakaolin based geopolymers. *Ceramics International*, 43(4), pp.3811-3817, <https://doi.org/10.1016/j.ceramint.2016.12.034>.

Zhang, X., Fan, X., Yan, C., Li, H., Zhu, Y., Li, X. and Yu, L., 2012. Interfacial Microstructure and Properties of Carbon Fiber Composites Modified with Graphene Oxide. *ACS Applied Material Interfaces*, 4(3), pp.1543–1552, <https://doi.org/10.1021/am201757v>.

Zhang, Z. and Wang, H., 2016. The Pore Characteristics of Geopolymer Foam Concrete and Their Impact on the Compressive Strength and Modulus. *Frontiers in Materials*, 3(38), <https://doi.org/10.3389/fmats.2016.00038>.

Zibouche, F., Kerdjoudj, H., d'Espinose de Lacaillerie, J-B. and Van Damme, H., 2009. Geopolymers from Algerian metakaolin. Influence of secondary minerals. *Applied Clay Science*, 43(3-4), pp.453-458, <https://doi.org/10.1016/j.clay.2008.11.001>.

Zuhua, Z., Xiao, Y., Huajun, Z. and Yue, C., 2009. Role of water in the synthesis of calcined kaolin-based geopolymer. *Applied Clay Science*, 43(2), pp.218-223, <https://doi.org/10.1016/j.clay.2008.09.003>.

Appendices

Appendix 1 – Conference paper from ICCAC 2018 Florida

PRELIMINARY MIX DESIGN PROCEDURE FOR ALKALI ACTIVATED CEMENT
MORTARS BASED ON METAKAOLIN AND INDUSTRIAL WASTE PRODUCTS
ACTIVATED WITH POTASSIUM SILICATE

Luke Oakes, Allistair Wilkinson, Bryan Magee

School of the Built environment, Ulster University, Shore road, Newtownabbey, UK

Oakes-L1@email.ulster.ac.uk

ABSTRACT

This research investigates a mix design methodology for performance specification of metakaolin, GGBS and hybrid alkali activated (AA) binders to enable their widespread adoption as an alternative to Portland cement (PC) in glass reinforced concrete cladding systems. Binder powders investigated include metakaolin, GGBS, fly ash, silica fume and iron silicate, activated by potassium silicate. The effects of binder composition on mechanical and environmental performance is studied with ternary contour maps created for each blend showing performance levels for easy selection. The liquid/solid ratio and the effect this has on mechanical properties is quantified for selected binders allowing further strength gains. This work is considered to be novel as few studies exist based on ambient curing, potassium silicate activation or novel industrial waste products analysing this effect. High performance mixes were developed, with 28-day compressive strength exceeding 100 N/mm² with high flow. A preliminary mix design and selection methodology based on binder composition and liquid to solid ratios is presented, that could be used to predict strength, flow or embodied emissions. This preliminary mix

design process is suitable for the materials studied allowing easy selection of alkali activated cements by non-experts, especially those familiar with performance specification of PC. Further research expanding the range of materials and mix compositions is ongoing to advance this innovative methodology further.

1. INTRODUCTION

In modern architecture, cladding systems are widely used as the outer skin of new and retrofitted buildings providing design flexibility through a huge range of possible forms to allow interesting and striking aesthetics to be created ⁽¹⁾. Cladding systems are designed to efficiently outline multi-layered building elements by creating a controlled internal environment protected from external conditions sufficiently to provide privacy, security, fire protection and comfort for occupants ⁽²⁾.

Established cement-based cladding solutions include precast reinforced concrete and glass reinforced concrete (GRC) panels, both of which can be designed to incorporate insulation as required. Precast reinforced concrete cladding offers many benefits such as intrinsic durability, robustness and the fact that it can create precise architectural features with an enormous range of potential surface finishes. Precast concrete panels can be supported by the structural frame of a building, or self-supporting and restrained. Cladding panels can also be designed to be load bearing to support floors. Alternatively, GRC offers a solution for creating architectural cladding comprising high strength panels moulded using a hand-spray manufacturing technique. GRC allows design of thin, lightweight, non-structural cladding elements with a wide range of surface finishes and shapes. In recent years, GRC use for structural applications, such as industrial floors and roofs is also emerging ^(3,4).

A significant drawback of both precast reinforced concrete and GRC cladding panels is the high environmental footprint of their constituent parts owing, primarily, to their

reliance on Portland cement (PC) use. PC manufacture is responsible for 5-7% of global CO₂ emissions ⁽⁵⁾ with the average concrete mix in the UK releasing 0.73kgCO₂/kg of material produced and using 4.5MJ of energy ⁽⁶⁾. The environmental impact of GRC panels is heightened further as requirements for robustness and high quality surface finishes necessitate the use of low water/cement ratios, high cement to aggregate ratios and more expensive white cement and silica sand ⁽⁷⁾.

To help address this issue, the underlying focus of this research is to investigate and advance the application of geopolymer or AA cement binder systems in cladding solutions. These cements offer potential as a replacement for PC as they have been shown to have improved strength (4-hour and 28-day compressive strengths over 20 and 100 N/mm² respectively), increased fire and chemical resistance and emission footprints up to 90% lower than for PC; many with a 100% recycled binder component ⁽⁸⁻¹⁰⁾. Geopolymer or AA cement concrete can be formed at room temperature by combining user-friendly alkaline reagents, water and alumina/silicate-based source materials such as kaolin or industrial waste products to form a solid matrix similar to PC ⁽¹¹⁾. As such, their usage in cladding panel systems offers technical, economic and environmental benefits to the construction industry. Work in this area to date includes one research group which have begun to create geopolymer cladding panels using a hybrid ambient cured binder system with potassium silicate activation that is reinforced with steel and polyvinyl alcohol fibres. These are designed for retrofitting existing buildings to improve aesthetics and, through the use phenolic foam and vacuum insulation, the thermal performance of the envelope ⁽¹²⁾. Two, 20 mm thick high-strength geopolymer face sections enable U-values of 0.1135 at a total thickness of 120mm. Compressive strengths of geopolymer mortar of 40 and 84 N/mm² at 24 hours and 90 days respectively are reported ^(13,14).

Despite these benefits, however, a key barrier to the widespread industrial adoption of geopolymer and AA cement as a replacement for PC is the lack of recognised mix design methodologies capable of producing material with specified values of compressive strength. While many papers exist in the literature regarding geopolymer cement concrete design, the importance of mix parameters on compressive strength has not been fully quantified as previous work is limited and with many shortcomings ⁽¹⁵⁾. Design of these mixes depends on mixing a suitable activator with an alumina-silicate powder. However, deciding this is not straight forward. The literature shows several methods; some based on constituent oxide ratios or factors such as liquid/solid ratio with oxide ratios fixed ⁽¹⁶⁾. The most important and well known of these oxide ratios is the silica (SiO₂) to alumina (Al₂O₃) ratio; known to directly affect geopolymer concrete mechanical strength and microstructure. Other common ratios used are Na₂O or K₂O (activators)/Al₂O₃, H₂O/Na₂O and Na₂O/SiO₂.

Most papers about geopolymer mix design focus on specific binders and mixture compositions. However, with the wide range of both binder source materials and alternative activators available, the applicability of this to mix design as a whole is low. Studies most often focus on fly ash systems that tend to be heat cured and as such are of limited use in the design of ambient cured systems which provide the greatest potential for embodied CO₂ reductions ^(16,17). The vast majority of current geopolymer or AA cement studies use sodium based activating solutions, with very few papers using only potassium silicate activation and even less that focus on the specific mix design of these materials⁽¹⁸⁾.

Attempts have been made to understand the relative effects of the many mix design parameters of fly ash geopolymers in order to enable an accurate prediction of the compressive strength achieved by specific mixes. Methods employed include using single

2.2 Mix designs

From an earlier phase of research, a suite of MK-based geopolymer mortar mixes was investigated to identify appropriate mix composition designs. From this work, an appropriate mix design - with liquid/solids (L/S) and paste/sand ratios of 0.51 and 0.84 respectively - was selected for use as a base mix in the current study (see Table 2). As shown in Table 2, this base mix was held constant and replicated multiple times with only the binder composition varying to allow a comprehensive range of material combinations to be investigated. Binder combinations were categorised as MK/GGBS/FA, MK/GGBS/SF and MK/GGBS/IS, with a range of unary, binary and ternary binders considered for each. By adopting this approach, it was recognised that performance levels were likely to vary considerably and potentially beyond limits of suitability. MK-based mixes, for instance, are reported to require significantly more liquids and activator than fly ash or slag based geopolymer to ensure monomer transport and full dissolution and reorganisation to take place ⁽¹⁵⁾.

2.3 Sample preparation and testing sequence

All samples for compressive strength testing were cast in 50 mm cubes for 24 hours, covered with plastic to ensure uniform drying conditions then stored in a sealed container until testing at 7 and 28 days in accordance with BS EN 1015-11:1999. Ambient laboratory temperatures of approximately 20°C were provided over this casting and curing period. Rheological behaviour was determined using flow table testing in accordance with BS EN 1015-3:1999 to ensure sufficient workability and minimal void creation when casting.

from ECOCEM Ireland under the commercial product name ECOCEM GGBS. Silica fume was sourced from Elkem in Norway under the commercial name Elkem Micro Silica. Low-level calcium fly ash was sourced from Kilroot power station, Northern Ireland. Iron silicate, a waste product from copper manufacturing processes, was sourced from Aurubis Bulgaria. Measured chemical compositions and published embodied CO₂ values for the various binder materials considered are given in Table 1; compared against Portland cement (PC) for comparative purposes. Clear from this table are significant variations in major oxide contents, suggesting ability to achieve a wide range of performance levels. Also apparent are significantly lower embodied CO₂ values for potential binders sourced as industrial wastes. Many of the hybrid mixes created are no longer technically considered geopolymers but instead AA mortars.

Geosil activator with a potassium silicate solids content of 45% by mass was sourced from Woellner GMBH in Ludwigshafen, Germany. Potassium, rather than sodium, silicate activator was used owing to its reactivity and emergence as a cost-effective solution for geopolymer production ⁽²⁶⁾. Mortar mixes were studied in this work, with the lough sand fine aggregate component sourced from Stanley Emerson & Sons Ltd in Northern Ireland.

Table 1: Composition and environmental impact of source materials used in this study

Material	Chemical composition (% by mass)				Embodied carbon (kgCO ₂ /kg)
	SiO ₂	Al ₂ O ₃	CaO	Fe ₂ O ₃	
OPC ⁺	20	4.6	64.6	3.8	0.73 ⁽⁶⁾
MK	55	40	0.3	1.4	0.33 ⁽⁶⁾
GGBS	36.5	10.4	42.4	0	0.083 ⁽⁶⁾
SF	96	0.8	0.5	0.8	0.064 ⁺⁺
FA	57	24	3.9	6	0.008 ⁽⁶⁾
IS	27	3.2	1.8	46	0.057 ⁺⁺

oxide ratios, with the $\text{SiO}_2/\text{Al}_2\text{O}_3$ ratio found to be the most effective ⁽¹⁶⁾. Creation of empirical models based on the factors such as the vitreous content of fly ashes, their loss on ignition and mean particle size which have been determined to strongly affect reactivity ^(18,19). Another study created a neural network based on factors such as recorded strength developments over time, the liquid to solid ratio and the activator to binder ratio using this to predict resulting strengths with relative success ⁽²⁰⁾. Many of these systems would be more suited for use analysing consistent source materials like metakaolin or GGBS, as the inherent variability in composition of fly ash complicates the process ⁽¹⁶⁾.

Against this background, the overall aim of this study is to propose a simplistic methodology enabling predictions of fresh properties and mechanical performance for a wide range of alkali activated binder combinations, in order to drive forward their adoption as high-performing, low CO_2 alternatives to PC in cladding panels. More specifically, the focus is to quantify the effect of varying both the binder composition and the liquid to solid ratio on mechanical and environmental properties of metakaolin-based hybrid ambient cured binders activated using potassium silicate.

2. EXPERIMENTAL METHODOLOGY

2.1: Materials

In terms of binder materials, metakaolin (MK) was used as a base binder material for all mixes considered in this study owing to its highly amorphous nature and rapid participation in geopolymerization compared to other potential precursor options like fly ash ⁽²⁵⁾. Sourced from Imerys UK, the commercially available product Metastar 501 was used. In addition, commonly available industrial by-product materials were investigated as binders to maximise potential environmental benefits and geographic applicability of the research. Materials investigated in

3. RESULTS AND DISCUSSION

3.1 Flow and compressive strength results

All compressive strength and flow test results for the mix designs investigated in this study (see Table 2) are presented in Table 3. For 7- and 28-day strength, results are also plotted on contoured ternary graphs in Figure 2, which designates equivalent ranges of strength in 10 N/mm^2 increments. It is reported ⁽¹⁸⁾ that changes to binder composition cause significant variation in the compressive strength and flow of the mortars created. While designing ternary binder blends allowed use of higher percentages of industrial waste, which in turn reduces the cost, emissions and embodied energy of the samples produced, selective mixes performed poorly. Indeed, some mixes exhibited strength losses after 7 days and were generally weaker than binary mix designs created.

The results indicate that GGBS has great potential for replacing MK in the creation of high strength mortars, with all percentage additions to binary mixes improving both 7- and 28-day compressive strengths up to a maximum of 86.0 N/mm^2 at 80% replacement. All mix designs achieving 28-day strengths greater than 50 N/mm^2 contained at least 20% GGBS, indicating that CASH gel formation is vital to gaining high strength ⁽²⁵⁾ and highlighting this waste material's huge potential as an AA cement or geopolymer precursor. The mix with 20% MK had higher strength than the 100% GGBS mix, suggesting that the two form separate reaction products in CASH and geopolymer gels simultaneously without detriment to each other. The high strength of the resultant sample suggests that these two gels bond well together to provide a homogenous structure due to their gel pores and the expansion of CASH during formation.

While reducing strength at 7 days, SF has been found to offer significant strength gains at 28 days for both MK- and GGBS-based mortars. Both the 80% MK/SF and 80% GGBS/SF binary mixes had strength improvements greater than 100% from 19 to 45

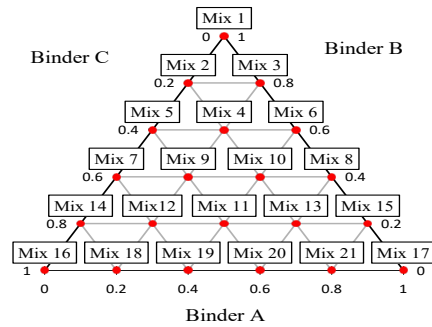
N/mm² and 45 to 106 N/mm² respectively; the latter result being the highest strength achieved in this study. This is likely due to the high silica content in this material changing the SiO₂/Al₂O₃ ratio and suggests future studies may be more successful at higher ratios.

Table 2 – Mix design methodology

Material quantities (kg/m ³)				L/S ratio	Paste/sand ratio
Binder	Activator	Water	Sand		
542	453	134	1340	0.514	0.843



Mix no.	Binder composition (% by mass)		
	Binder A	Binder B	Binder C
1	0	100	0
2	0	80	20
3	20	80	0
4	20	60	20
5	0	60	40
6	40	60	0
7	0	40	60
8	60	40	0
9	20	40	40
10	40	40	20
11	40	20	40
12	20	20	60
13	60	20	20
14	0	20	80
15	80	20	0
16	0	0	100
17	100	0	0
18	20	0	80
19	40	0	0
20	60	0	40
21	80	0	20



Binder combinations considered		
A	B	C
Fly ash	MK	GGBS
Silica Fume	MK	GGBS
Iron Silicate	MK	GGBS

Iron silicate has been found to increase both 7- and 28-day strengths of GGBS and MK binders at a 20% inclusion level, with strengths recorded for binary mixes dropping off after this point. The strongest mix design created with IS was the binary mix with 80% GGBS/IS. The ternary blend 40% IS/20% MK/40% GGBS achieved comparable strength of over 50 N/mm². While all mixes containing FA exhibited 7-day strengths less than the 100% MK base mix, ternary blend FA 20%/MK 20%/GGBS 60% exhibited significant strength gain between 7 and 28 days. This mix had a compressive strength increase of over 98% from 38 to 76 N/mm², far exceeding the figures for the 100% MK (increase of just over 10% from 41.5 to 46 N/mm²). While these mixes may have lower strength than the 100% MK base mix, they also have the lowest embodied CO₂ values owing to the low impact of FA. However, it is recognised that non-uniformity of FA potentially makes widespread adoption more challenging.

The inclusion of industrial waste materials in MK geopolymer has been shown to increase the flow of resultant mixes at all increments of addition, indicating that their use is well suited to high flow requirements of fibre reinforced geopolymer cement mortar. However, flows measured in this research were generally higher than the 255 mm limit of the BS EN 1015-3:1999 test method. As such, comparison of flow levels above this point was not possible. Moving forward, lower liquid contents or a new flow methodology needs to be developed; possibly involving a dynamic shear rheometer, a larger flow table or a smaller amount of material.

Table 3 – Fresh and hardened properties

Mix no.	MK/GGBS/SF			MK/GGBS/FA			MK/GGBS/IS		
	Compressive strength (N/mm ²)*		Flow (mm)	Compressive strength (N/mm ²)		Flow (mm)	Compressive strength (N/mm ²)		Flow (mm)
	7-day	28-day		7-day	28-day		7-day	28-day	
1	41.5	46.0	195	41.5	46.0	195	41.5	46.0	195
2	41.5	51.5	255	41.5	51.5	255	41.5	51.5	255
3	19.0	45.0	255	40.0	42.0	220	47.0	51.0	255
4	38.0	41.5	195	36.0	39.5	255	36.5	37.0	255
5	43.5	54.5	255	43.5	54.5	255	43.5	54.5	255
6	4.2	5.0	165	24.0	30.5	255	36.5	43.0	255
7	47.0	66.0	255	47.0	66.0	255	47.0	66.0	255
8	0	0	165	17.5	32.0	255	0	0	255
9	44.0	53.0	225	31.0	55.0	255	45.0	33.5	255
10	40.0	36.5	185	17.0	31.0	255	31.5	41.5	255
11	27.0	42.0	190	33.5	28.5	255	34.0	51.0	255
12	41.0	70.0	255	38.0	76.0	255	35.0	45.0	255
13	26.0	32.0	135	19.5	23.0	255	18.0	19.0	255
14	69.5	86.0	255	69.5	86.0	255	69.5	86.0	255
15	0	0	105	0	0	255	0	0	255
16	50.0	68.0	255	50.0	68.0	255	50.0	68.0	255
17	0	0	110	0	0	255	0	0	255
18	45.0	106.5	255	33.0	52.0	255	46.5	52.0	255
19	21.5	24.0	210	26.0	46.5	255	27.5	41.5	255
20	21.0	30.0	120	15.0	28.0	255	18.5	19.0	255
21	17.5	25.5	110	7.0	9.0	255	5.5	5.0	255

*1N/mm²=1mpa=0.145ksi=1454psi

3.2 Investigation of performance relative to L/S ratio

While the work presented to this point has demonstrated effects of binder composition on performance, all of the mortar mixes used for the work were prepared at a constant L/S ratio of 0.51. Just as water/cement ratio is the most significant factor determining compressive strength development of PC-based materials, it is recognised that liquid/solid ratio acts in the same way for geopolymer or AA cement-based materials ⁽²¹⁾.

While relationships of strength versus L/S ratio exist in the literature, studies are limited to specific sets of mainly FA and MK-based mixes ⁽¹⁵⁻¹⁷⁾.

Against this background, work was undertaken to investigate and develop generic relationships of performance versus L/S ratio with applicability to a wide range of geopolymer or AA binder types. To this end, laboratory work was undertaken to assess the flow and compressive strength performance of selected representative binder types across a range of L/S ratios (0.35-0.61). Binder combinations considered in this way included: 100% MK; 100% GGBS; 80% GGBS/20% MK and 60% GGBS/20% MK/20% SF. Primary data collected was supplemented by performance versus L/S ratios published in the literature ^(15,24,27-29).

The findings of this work with respect to compressive strength are presented in Figure 2. From Figure 2(a) it is evident that while clearly distinctive and somewhat inconsistent relationships exist for individual mix types (determined by differences in binder types, associated geopolymerisation reactions, testing times, experimental variables, etc. used) families of generic relationships are identifiable. A proposed normalisation of this observation is presented in Figure 2(b) for use in future mix design scenarios. Similar normalised relationships for flow versus L/S ratio are presented in Figure 3.

4. MIX DESIGN METHODOLOGY

Combining the results presented to this point, a simplistic mix design procedure is proposed for geopolymer and AA mortar mixes comprising any binder combination of MK/GGBS/FA (see Figure 4). This methodology is obviously reproducible for the other material combinations considered. Included in Figure 4 are values of embodied CO₂ and 7-day compressive strength for mixes with a L/S ratio of 0.51, as well as generic relationships linking both 7-day compressive strength and flow with L/S ratio in the range

0.30-0.65. In this way, the figure enables estimations of approximate mixture proportions for specified values of compressive strength and/or flow.

In the example presented, initial mix design requirements include a maximum value of embodied CO₂ content (0.15 kgCO₂/kg) and 7-day strength (50 N/mm²). Using Figures 4(a) and (b), the 7-day strength can be estimated for geopolymer cement mortar comprising a suitable binder combination and L/S ratio of 0.51. In the example shown, a value of 35 N/mm² is predicted for a 30% MK/50% GGBS/20% FA binder combination. This value can then be transposed onto Figure 4(c) to enable an estimation of the required L/S ratio to achieve the required 7-day strength of 50 N/mm². In the example shown a L/S value of 0.38 is estimated, leading to an approximate flow value of 260 mm.

It is recognised that by not accounting for other mix design criteria, such as aggregate size/type/properties and paste/aggregate ratio, this mix design procedure is by no means the finished article for geopolymer cement mortar/concrete. With that said, provided is a simplistic provisional methodology enabling rapid estimation of performance for a wide range of low impact binder material options.

5. CONCLUSIONS AND FURTHER RESEARCH

In this study we have presented a simplistic mix design methodology capable of enabling initial performance predictions of geopolymer and AA cement mortars incorporating a wide range of primary and recycled binder components. In so doing, the aim of this research is to help facilitate an increasing use of high performance, low impact cement mixes in cladding panels worldwide. Global GRC production totalled approximately 136,500 metric tonnes in 2015. With a compound growth rate identified as 20.5%, this is predicted to rise to 346,800 metric tonnes by 2020 ⁽²²⁾. Production of PC-based materials to meet this demand would involve the

exists to reduce this by approximately 3330 tonnes per year ^(4,6,23). As such, this research is timely and has the potential to beneficially impact the environmental footprint of cladding-related construction activities.

Moving forward, further research is ongoing to increase the range of source materials and mix designs investigated. Central composite experimental designs are being employed to study a broader range of mix design variables and to increase the accuracy of the methodology. Work will involve studies of setting times; a critical production property pertaining to precast applications. Investigations to determine why some ternary mixes lose strength with time will be carried out and further improvements of compressive strength will be explored via reduced L/S ratios and admixture use. As the mortars produced in this study are intended to act as a matrix for a fibre reinforced composite, work will also focus on bond characteristics and bulk behaviour of various binders with a range of fibre types. As such, research will progress to efficient product designs and trial- and full-scale cladding panel construction.

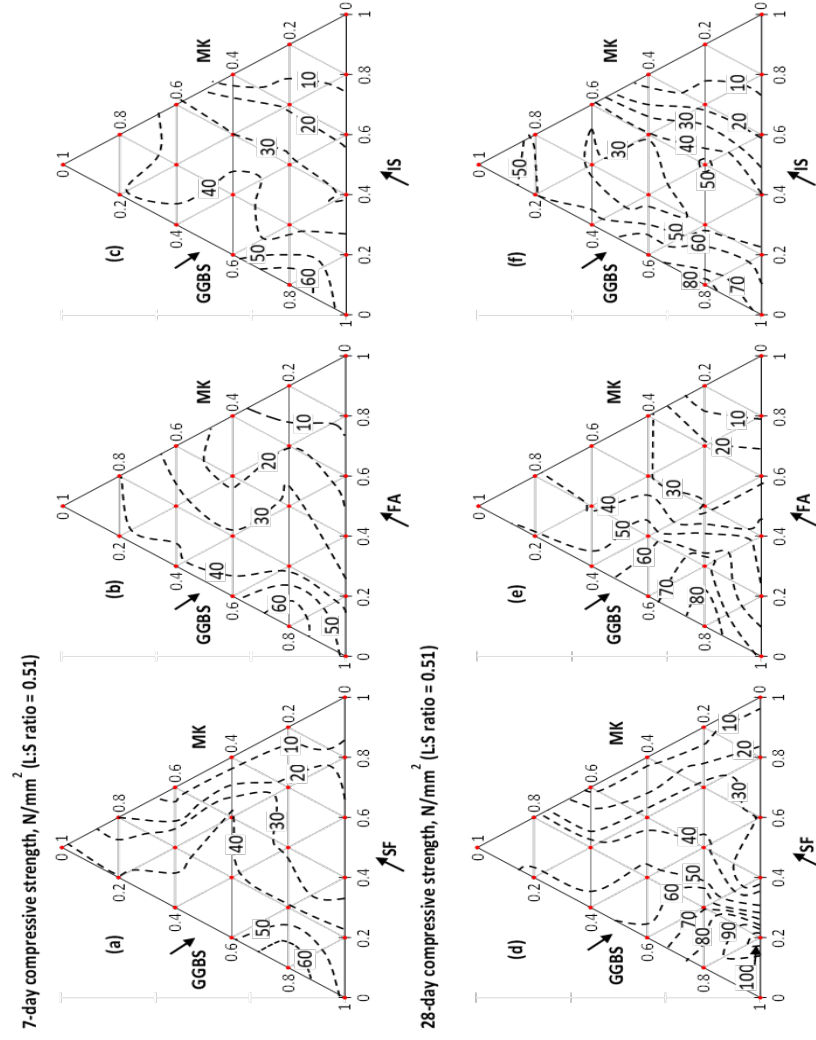


Figure 1. Ternary plots of 7- and 28-day compressive strength results

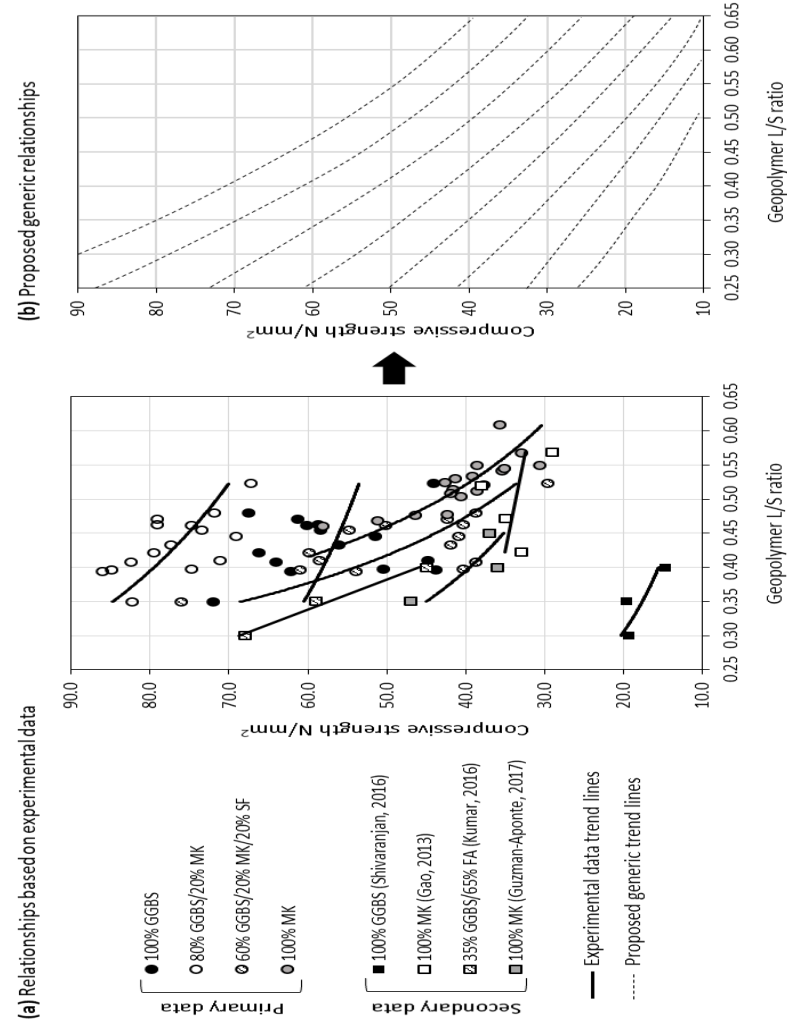


Figure 2. Relationships between 7-day compressive strength and L/S ratio for a range of geopolymmer cement binder groups

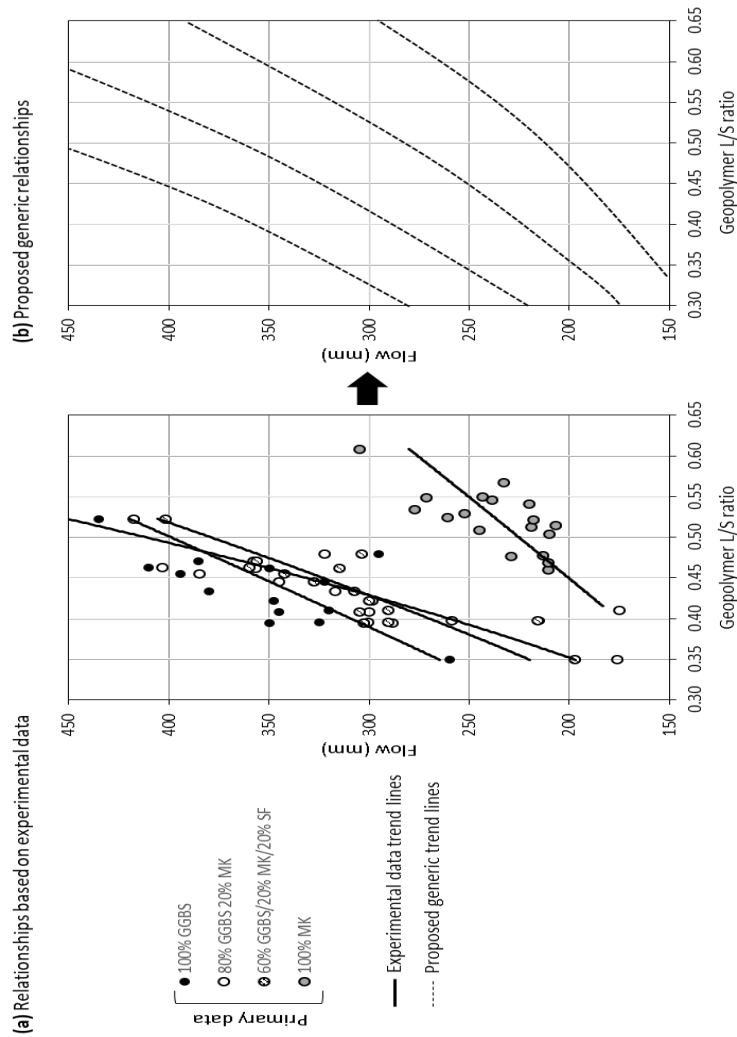
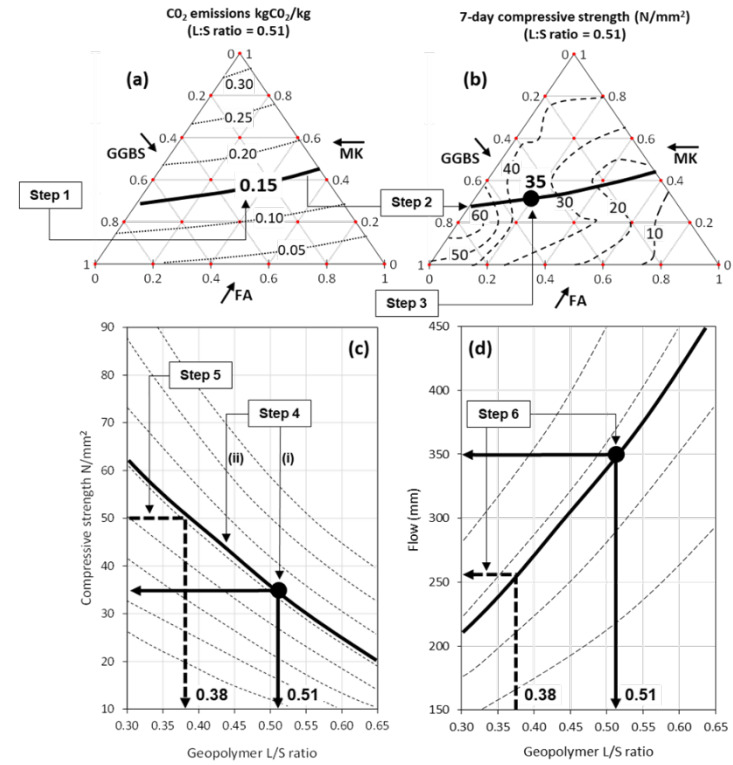


Figure 3. Relationships between flow and L/S ratio for a range of geopolymer cement binder groups



Example mix design requirements: 1) Max. embodied CO₂ content = 0.15 kgCO₂/kg; 2) 7-day strength = 50 N/mm²

- Step 1:** Highlight required embodied CO₂ equivalence line on ternary plot (0.15 kgCO₂/kg in example shown);
- Step 2:** Transpose embodied CO₂ equivalence line on to compressive strength ternary plot;
- Step 3:** Select appropriate binder combination (30% MK/50% GGBS/20% FA in example shown) and note corresponding 7-day compressive strength at L/S ratio of 0.51 (35 N/mm² in example shown);
- Step 4:** (i) Transpose performance level of chosen binder combination at L/S ratio 0.51 onto generic strength versus L/S ratio chart; (ii) Plot corresponding strength versus L/S ratio relationship curve for binder combination chosen;
- Step 5:** Use plotted curve to identify approximate L/S ratio required to achieve target strength (0.38 in example shown);
- Step 6:** Repeat steps 4 and 5 to predict approximate flow levels (260 mm in example shown);
- Step 7:** Undertake trial mixes and adjust proportions accordingly (not shown on figure).

Figure 4. Indicative mix design worked example

6. REFERENCES

1. Theodosiou, T. (2015). Thermal bridging analysis on cladding systems for building facades. *Energy and Buildings*. 109. pp.377–384.
2. Designing Buildings Wiki. (2017). Cladding for buildings. Available: https://www.designingbuildings.co.uk/wiki/Cladding_for_buildings. Last accessed 24/11/17.
3. Enfedaque, A. (2012). An alternative methodology to predict aging effects on the mechanical properties of glass fiber reinforced cements (GRC). *Construction and Building Materials*. 27 (1), pp.425-431
4. GRCA (2016b). *Specifiers Guide to Glass fibre Reinforced Concrete*. London: GRCA.
5. Benhelal, E, Zahedi, G., Shamsaei, E. and Bahadori, A, (2013). Global strategies and potentials to curb CO2 emissions in cement industry. *Journal of Cleaner Production*, 51, pp.142–161.
6. Jones, C. (2011). *Inventory of Carbon and Energy (ICE) Version 2.0*. Available: http://www.circularecology.com/embodied-energy-and-carbon-footprint-database.html#.Wltaet9l_IU. Last accessed 15/12/17.
7. GRCA Glass Reinforced Concrete Association (2016c). *A Practical Design Guide for GRC using Limit States*. London: GRCA.
8. Davidovits, J. (2013). *Geopolymer Cement. A review*. Geopolymer Institute, Technical papers, 21, pp.1-11.
9. Banah UK, 2014. *Introduction to Geopolymer Binders*. Ballyclare: Banah UK.
1. Geopolymer Institute. (2016). *State of the Geopolymer R&D 2016*. Available: <https://www.geopolymer.org/conference/gpcamp/gpcamp-2016/>. Last accessed 06/12/2016.
2. The Zeobond group. (2012). *The geopolymer solution*. Available: <http://www.zeobond.com/geopolymer-solution.html>. Last accessed 23/02/2016
3. Hyde, R., Kinnane, O., West, R., Nanukuttan, S. and Davis, G (2017, October), *Manufacture and assembly of a thin, lightweight, low impact, prototype precast geopolymer sandwich panel for the retrofit cladding of existing buildings*. Paper presented at the 12th Conference on Advanced Building Skins. Bern, Switzerland. Retrieved from: https://www.researchgate.net/publication/320183067_Manufacture_and_assembly_of_a_thin_lightweight_low_impact_prototype_precast_geopolymer_sandwich_panel_for_the_retrofit_cladding_of_existing_buildings
4. Hyde, R., Kinnane, O., West, R. and Nanukuttan, S., (2017, August) *Design of a test hut field experiment for prototype precast geopolymer sandwich panels for the retrofit cladding of existing buildings*. Paper presented at the 3rd International Conference on Chemically Activated Materials. Gold Coast, Australia. Retrieved from: https://www.researchgate.net/publication/319207486_Design_of_a_test_hut_field_experiment_for_prototype_precast_geopolymer_sandwich_panels_for_the_retrofit_cladding_of_existing_buildings

1. https://www.researchgate.net/publication/310572116_Early_Stage_Development_of_an_Ultra-High_Performance_Geopolymer
2. Lahoti, M. Narang, P. Tan, K. Yang, E. (2017). Mix design factors and strength prediction of metakaolin-based geopolymer. *Ceramics International*. 43 (14), pp.11433-11441.
3. Aughenbaugh, K. (2015). Critical evaluation of strength prediction methods for alkali-activated fly ash. *Materials and Structures*. 48 (3), pp.607–620.
4. Timakul, P. (2015). Effect of silica to alumina ratio on the compressive strength of Class C Fly ash geopolymers. *Key Engineering Materials*. 659, pp.80-84.
5. Austroads (2016). Technical report AP-T318-16 Specification and use of Geopolymer concrete in the manufacture of structural and non-structural components: Review of literature. Sydney NSW: Austroads Ltd.
6. Diaz-Loya EI, Allouche EN, Cahoy D (2013a) Statistical based approach for predicting the mechanical properties of geopolymer concretes. In: Struble L, Hicks JK (eds) **Geopolymer binder systems**. West Conshohocken, Pennsylvania. ASTM International, **Appendix 2: Conference paper from YRF 2018 in Newcastle, England** pp.119–143
7. Diaz-Loya EI, Kinney F, Rios CAO (2013b) Reactivity indicators for activated high-calcium fly ash-based binders. *ACI Special Publication*, 294. Farmington, pp.1–22
8. Wilson, A (2015). Establishing a mix design procedure for geopolymer concrete. Queensland: University of South Queensland. Ph.D. thesis.

1. <https://www.businesswire.com/news/home/20170914005694/en/Global-Glass-Fiber-Reinforced-Concrete-Market-->. Last accessed 15/12/2017.
2. Aurora Construction Materials, 2012. LCA of Geopolymer Concrete (E-Crete). Melbourne: Start2See
3. Gao, K et al. (2013). Effects of Nano-SiO₂ on Setting Time and Compressive Strength of Alkali-activated Metakaolin-based Geopolymer. *The Open Civil Engineering Journal*. 7, pp.84-92.
4. Provis, L. Palomo, A. Shi, C. (2015). Advances in understanding alkali-activated materials. *Cement and Concrete Research*. 78, pp.110–125.
5. Davidovits, J (2017). Geopolymer webinar 2017. Paris. Geopolymer Institute.
6. Kumar, R. (2015). Study on behaviour of geopolymer concrete. *International Journal of Civil and Structural Engineering Research*. 3 (1), pp.384-388.
7. Guzmán-Aponte, L. (2017). Metakaolin-Based Geopolymer with Added TiO₂ Particles: Physicomechanical Characteristics. *Coatings*. 7 (12), pp.1-12.
8. Shivanranjan, N. (2016). Study on self-compacting geopolymer concrete with various water to geopolymer solids ratio. *International Research Journal of Engineering and Technology*. 3 (7), pp 2064-2068.

Appendix 2: Conference paper from YRF 2018 in Newcastle

A critical evaluation of the influence of the liquid to solid (L/S) ratio on the mechanical properties of novel geopolymer cements developed to create structural insulated panels

Luke Oakes, Department of the built environment, Ulster University
Dr Bryan Magee, Department of the built environment, Ulster University

ABSTRACT: This project exploits the high strength and fire resistance of geopolymers to create innovative, cladding systems with integral foamed geopolymer insulation that provide a building's envelope, thermal performance and finish; eliminating fire tragedies like Grenfell tower with a lower environmental impact than current cementitious options. Mortars created will need to provide high strength at low weight to create thin, lightweight panels that maximise the potential applications and structural forms. Central composite experimental design (CCD) is used to identify the optimal L/S ratio for compressive strength development in novel geopolymer cements based on mixes of metakaolin, GGBS and silica fume activated by only potassium silicate and will be presented here for the first time. The optimal ratio varied with source material; metakaolin mixes required significantly higher than GGBS or hybrid mixes. Results confirm a low L/S ratio as vital to high strength development but this ratio must be high enough to provide sufficient fluidity to allow full binder dissolution, monomer transport and geopolymer formation to take place. Geopolymer cement is reported to be highly suitable for precast cladding with 7-day compressive strength of up to 86N/mm² at an L/S ratio of 0.394; many using 100% recycled binders. All mixes tested showed their highest strength when the L/S ratio is lowest and binder content is highest and its similarity to the water/cement ratio in OPC is confirmed for this data set. Strength prediction from regression analysis was relatively successful and promising for the future.

1. INTRODUCTION

Modern construction often uses structural steel or concrete portal frames to hold up the floor, transfer structural loads to the foundation and provide the building with rigidity and support. Cladding then forms the outer skin creating a protected internal environment with privacy, security, fire protection and comfort for occupants with massive design flexibility and a huge range of possible forms allowing unique, striking aesthetics to be created^(1,2). Precast concrete cladding is common due to the intrinsic durability, robustness, high strength and low cost of its products and the fact that it can create precise architectural features with an enormous range of potential surface finishes. Systems can be structural and load bearing like with reinforced concrete panels or more commonly self-supporting and restrained to the frame like glass reinforced concrete (GRC). Specifying GRC allows design of thin, lightweight, non-structural cladding elements with a wide range of surface finishes and shapes. Structural GRC floors and roofs are also emerging as problems of static fatigue are mitigated^(3,4). Current systems however have significant drawbacks such as the extremely high environmental impact of its component parts. The building materials sector is the 3rd largest in terms of carbon emissions providing 10% of the global total⁽⁵⁾ with 50-70% of this from concrete⁽⁶⁾. The average UK concrete mix has embodied emissions of 0.73kgCO₂/kg using 4.5MJ of energy⁽⁷⁾ but with GRC this is further increased as the need for robustness and high-quality surface finishes necessitate the use of low water/cement ratios, high cement to aggregate ratios and more expensive white cement and silica sand⁽⁸⁾. 95 % of concrete emissions are from production, only 5% is from transportation of raw materials and final products with 85% of the total from the Portland cement (PC)

component⁽⁵⁾. This shows the huge impact that low impact cements as a replacement for PC could have. Per Kominitsas (2011) the best way for the concrete industry to meet its current goal to reduce 1990 CO₂ emissions by a factor of four by 2050 would be to produce geopolymer concrete from industrial waste materials without emissions to be allocated. As such, geopolymer cladding panel systems offer technical, economic and environmental benefits to the construction industry. Geopolymer cements can replace the PC in GRC and improve performance allowing use of thinner, lighter members due to increased strength (4-hour and 28-day compressive strength (CS) over 20 and 100 N/mm² respectively), fire protection and chemical resistance coupled with an up to 90% reduction in carbon emissions and the use of a 100% recycled waste binder. These mortars which form, cure and gain their strength rapidly in ambient temperatures by combining user-friendly alkaline reagents and alumina/silicate based source materials such as metakaolin or industrial waste products and water to form a strong, solid matrix like PC⁽⁹⁾. Novel research has attempted to create geopolymer cladding for building retrofits to improve aesthetics and thermal performance using phenolic foam and vacuum insulation,⁽¹⁰⁾ Mortar CS's of 40 and 84 N/mm² at 24 hours and 90 days respectively are reported and these are used to create 20 mm thick high-strength geopolymer face sections that enable U-values of 0.1135 at a total thickness of 120mm^(11,12). A key barrier to adoption of geopolymers is the lack of a recognised, performance based mix design methodology that can produce materials with a specified strength and workability⁽¹³⁾. Many papers discuss mix design but most study heat cured fly ash or ambient systems with sodium activation; as such these are of little relevance to the ambient cured systems activated with potassium silicate reported on here which

^(11,12). A key barrier to adoption of geopolymers is the lack of a recognised, performance based mix design methodology that can produce materials with a specified strength and workability⁽¹³⁾. Many papers discuss mix design but most study heat cured fly ash or ambient systems with sodium activation; as such these are of little relevance to the ambient cured systems activated with potassium silicate reported on here which provide the greatest potential for embodied CO₂ reductions. Studies often focus on specific binder materials and mixture compositions however the wide range of both binder source materials and alternative activators available make the applicability of this to geopolymer mix design as a whole is low^(14,15,16).⁽¹⁴⁾. Attempts to understand the relative effects of mix design parameters to predict strength include using single oxide ratios with the S/A ratio being the most effective⁽¹⁴⁾ or empirical models based on factors like the vitreous content of fly ashes or their mean particle size⁽¹⁶⁾. One used neural networks based on factors like strength development over time, the L/S ratio and the activator to binder ratio to predict resulting strengths with relative success⁽²⁰⁾. This report aims to ascertain the exact effect of altering the liquid to solid ratio on selected geopolymer cement mortars allowing some prediction of their strength and to find an optimal level for strength development while still preserving sufficient flow for future fibre additions, a smooth, high quality surface finish and easy compaction to prevent excessive void area in created products.

2. Experimental methodology

2.1 Materials

Metakaolin (MK) sourced from Imerys UK under the product name Metastar 501 was selected as the primary binder due to ease of availability, its consistent and highly amorphous nature and its rapid dissolution and geopolymerization at ambient temperatures⁽¹⁷⁾. MK is mined and fired and while it has a low environmental impact compared to PC partially or fully replacing this with industrial waste products has been shown to significantly reduce this and provide reduced set times, greater strength or higher flow. Industrial waste materials used include GGBS from ECOPEM Ireland under the product name ECOPEM GGBS and silica fume (SF) sourced from Elkem under the name Elkem micro silica. GGBS geopolymers require a much smaller amount of activator solids, the highest impact component of a geopolymer mix, and therefore have lower environmental impact than metakaolin systems whose lower Si:Al ratio necessitates a greater amount to be used for full dissolution to occur⁽⁵⁾. SF has been shown in the literature and in this project to increase the Si:Al of the binder and provide increased strength development between 7 and 28 days especially at around 20% binder mass. Geosil activating solution with a potassium silicate solids content of 45% by mass was sourced from Woellner and used in all mix designs. Potassium, rather than sodium, silicate activator was chosen

due to its reactivity and emergence as a cost-effective solution for geopolymer production⁽²⁶⁾. Mortar mixes were studied in this work, with the lough sand fine aggregate component sourced from Stanley Emerson & Sons Ltd in Northern Ireland. Measured chemical compositions and published embodied CO₂ values for the binder materials considered are given in Table 1 with Portland cement (PC) for comparative purposes. It is evident that there are significant variations in major oxide contents which suggests the ability to garner a wide range of performance levels and that there are lower embodied CO₂ values for potential binders sourced as industrial waste.

Table 1: Composition and environmental impact of source materials used in this study.

Material	Chemical composition (% by mass)				Embodied carbon (kgCO ₂ /kg)
	SiO ₂	Al ₂ O ₃	CaO	Fe ₂ O ₃	
PC+	20	4.6	64.6	3.8	0.73 (7)
MK	55	40	0.3	1.4	0.33(7)
GGBS	36.5	10.4	42.4	0	0.083(7)
SF	96	0.8	0.5	0.8	0.064++

+ Included for comparative purposes ++Provided by Elkem

2.2 Sample preparation and testing sequence

Samples for CS tests were cast in 50 mm cubes for 24 hours, covered with plastic to ensure uniform drying conditions then stored in a sealed container until testing at 7 days in accordance with BS EN 1015-11:1999. Ambient temperatures of 20°C were provided over this casting and curing period. Rheology was tested by flow table to BS EN 1015-3:1999 to ensure sufficient workability and limited void areas. This specifies a 250mm wide flow table but this was too small for comparing high flow mixes and a modified methodology was created using the same volume of material but a 700mm flow table as specified in BS EN 12350-5:2000.

2.3 Mix design methodology

A MK-based mortar from earlier research activated by potassium silicate and shown in table 2 is used as a base for the study. This base mix was held constant and replicated with only the binder composition varied to allow a comprehensive range of binder combinations to be investigated and a range of unary, binary and ternary binder blends created to ascertain the effects of varied binder composition through partial or total replacement by mass of the mined, fired and costly metakaolin with industrial waste materials GGBS, SF, iron silicate and fly ash. This has been shown to increase compressive strength and workability of mortars⁽¹⁶⁾ while also reducing the environmental impact as shown by the CO₂ emissions data in table 1.

Table 2 – Base MK mix design

Material quantities (kg/m ³)					L/S ratio	Paste to sand ratio
Binder	Activator	Water	Sand			
542	453	134	1340	0.514	0.843	

Binder	Activator	Water	Sand	L/S ratio	Paste to sand ratio
542	453	134	1340	0.514	0.843

Samples showed 7-day CS improvements from the base mortars 41.6 N/mm² but at nearly all replacement levels the flow was extremely high. The L/S ratio of 0.51 resulted in a large flow variation across binder types; MK-based mixes required significantly more water and activating liquids than fly ash or slag geopolymers for monomer transport and full dissolution and reorganisation to take place (13). Four high performing mixes were selected to identify if some of this excess liquidity could be traded for increased compressive strength like in PC based materials. L/S ratio is reported analogous to the water/cement ratio in PC mix designs and the most significant factor determining compressive strength development and flow (16). Data describing the relationship of geopolymer strength to L/S ratio exists in the literature but studies are limited to specific sets of mainly FA and MK-based mixes and are unlikely to use only potassium silicate activation (13,14,19). As such this project attempts to determine relationships of performance versus L/S ratio with applicability to a wide range of geopolymer mix compositions and binder types especially those from waste sources activated with potassium silicate.

Face centred CCD mapped the effects on compressive strength and flow caused by varied L/S ratios in the fifteen mixes representing all combinations of three mortar component variables (binder powder, activator and free water content) across three levels (-1,0, +1) for each selected binder blend. Table 3 shows the mass of the components at each level. Table 4 shows the levels of each component for the fifteen mix designs. Correlation analysis of mix variables to 7 -day CS dictated optimal independent variables for regression analysis. Parameters considered include the binder mass, activator solution mass, water mass, sand mass, activator solids mass, total water content, activator to binder (A/B) ratio, free water to activating solution (FW/A) ratio, the free water to binder (FW/B) ratio, L/S ratio and silica to alumina ratio. The most deterministic were selected to optimise the predictive ability given by the regression output coefficients then comparing variables such as the adjusted r square, f values, p values and the significance f allowed the most accurate prediction of the strength possible from the data set. Table 4 shows the average error in the predictive models created for each of the four binder blends.

Level	-1	0	1
Binder	490	540	590
Activator	400	450	500
Water	100	130	160

Binder	550	600	650
--------	-----	-----	-----

Binder	550	600	650
--------	-----	-----	-----

Binder	550	600	650
--------	-----	-----	-----

Binder	550	600	650
--------	-----	-----	-----

Binder	550	600	650
--------	-----	-----	-----

Binder	550	600	650
--------	-----	-----	-----

Binder	550	600	650
--------	-----	-----	-----

Binder	550	600	650
--------	-----	-----	-----

Binder	550	600	650
--------	-----	-----	-----

Binder	550	600	650
--------	-----	-----	-----

Binder	550	600	650
--------	-----	-----	-----

Binder	550	600	650
--------	-----	-----	-----

Binder	550	600	650
--------	-----	-----	-----

Binder	550	600	650
--------	-----	-----	-----

Binder	550	600	650
--------	-----	-----	-----

Binder	550	600	650
--------	-----	-----	-----

Binder	550	600	650
--------	-----	-----	-----

Binder	550	600	650
--------	-----	-----	-----

Binder	550	600	650
--------	-----	-----	-----

Binder	550	600	650
--------	-----	-----	-----

Binder	550	600	650
--------	-----	-----	-----

Binder	550	600	650
--------	-----	-----	-----

Binder	550	600	650
--------	-----	-----	-----

Binder	550	600	650
--------	-----	-----	-----

Binder	550	600	650
--------	-----	-----	-----

Binder	550	600	650
--------	-----	-----	-----

Binder	550	600	650
--------	-----	-----	-----

Binder	550	600	650
--------	-----	-----	-----

Binder	550	600	650
--------	-----	-----	-----

Binder	550	600	650
--------	-----	-----	-----

Binder	550	600	650
--------	-----	-----	-----

Binder	550	600	650
--------	-----	-----	-----

Binder	550	600	650
--------	-----	-----	-----

Binder	550	600	650
--------	-----	-----	-----

Binder	550	600	650
--------	-----	-----	-----

Binder	550	600	650
--------	-----	-----	-----

Binder	550	600	650
--------	-----	-----	-----

Binder	550	600	650
--------	-----	-----	-----

Binder	550	600	650
--------	-----	-----	-----

Binder	550	600	650
--------	-----	-----	-----

Binder	550	600	650
--------	-----	-----	-----

Binder	550	600	650
--------	-----	-----	-----

Binder	550	600	650
--------	-----	-----	-----

Binder	550	600	650
--------	-----	-----	-----

Binder	550	600	650
--------	-----	-----	-----

Binder	550	600	650
--------	-----	-----	-----

Binder	550	600	650
--------	-----	-----	-----

Binder	550	600	650
--------	-----	-----	-----

Binder	550	600	650
--------	-----	-----	-----

Binder	550	600	650
--------	-----	-----	-----

Binder	550	600	650
--------	-----	-----	-----

Binder	550	600	650
--------	-----	-----	-----

Binder	550	600	650
--------	-----	-----	-----

Binder	550	600	650
--------	-----	-----	-----

Binder	550	600	650
--------	-----	-----	-----

Binder	550	600	650
--------	-----	-----	-----

Binder	550	600	650
--------	-----	-----	-----

Binder	550	600	650
--------	-----	-----	-----

Binder	550	600	650
--------	-----	-----	-----

Binder	550	600	650
--------	-----	-----	-----

Binder	550	600	650
--------	-----	-----	-----

Binder	550	600	650
--------	-----	-----	-----

Binder	550	600	650
--------	-----	-----	-----

Binder	550	600	650
--------	-----	-----	-----

Binder	550	600	650
--------	-----	-----	-----

Binder	550	600	650
--------	-----	-----	-----

Binder	550	600	650
--------	-----	-----	-----

Binder	550	600	650
--------	-----	-----	-----

Binder	550	600	650
--------	-----	-----	-----

Binder	550	600	650
--------	-----	-----	-----

Binder	550	600	650
--------	-----	-----	-----

Binder	550	600	650
--------	-----	-----	-----

Binder	550	600	650
--------	-----	-----	-----

Binder	550	600	650
--------	-----	-----	-----

Binder	550	600	650
--------	-----	-----	-----

Binder	550	600	650
--------	-----	-----	-----

Binder	550	600	650
--------	-----	-----	-----

Binder	550	600	650
--------	-----	-----	-----

Binder	550	600	650
--------	-----	-----	-----

Binder	550	600	650
--------	-----	-----	-----

Binder	550	600	650
--------	-----	-----	-----

Binder	550	600	650
--------	-----	-----	-----

Binder	550	600	650
--------	-----	-----	-----

Binder	550	600	650
--------	-----	-----	-----

Binder	550	600	650
--------	-----	-----	-----

Binder	550	600	650
--------	-----	-----	-----

Binder	550	600	650
--------	-----	-----	-----

Binder	550	600	650
--------	-----	-----	-----

Binder	550	600	650
--------	-----	-----	-----

Binder	550	600	650
--------	-----	-----	-----

Binder	550	600	650
--------	-----	-----	-----

Binder	550	600	650
--------	-----	-----	-----

Binder	550	600	650
--------	-----	-----	-----

Binder	550	600	650
--------	-----	-----	-----

Binder	550	600	650
--------	-----	-----	-----

Binder	550	600	650
--------	-----	-----	-----

Binder	550	600	650
--------	-----	-----	-----

Binder	550	600	650
--------	-----	-----	-----

Binder	550	600	650
--------	-----	-----	-----

Binder	550	600	650
--------	-----	-----	-----

Binder	550	600	650
--------	-----	-----	-----

Binder	550	600	650
--------	-----	-----	-----

Binder	550	600	650
--------	-----	-----	-----

Binder	550	600	650
--------	-----	-----	-----

Binder	550	600	650
--------	-----	-----	-----

Binder	550	600	650
--------	-----	-----	-----

Binder	550	600	650
--------	-----	-----	-----

Binder	550	600	650
--------	-----	-----	-----

Binder	550	600	650
--------	-----	-----	-----

Binder	550	600	650
--------	-----	-----	-----

Binder	550	600	650
--------	-----	-----	-----

Binder	550	600	650
--------	-----	-----	-----

Binder	550	600	650
--------	-----	-----	-----

Binder	550	600	650
--------	-----	-----	-----

Binder	550	600	650
--------	-----	-----	-----

Binder	550	600	650
--------	-----	-----	-----

Binder	550	600	650
--------	-----	-----	-----

Binder	550	600	650
--------	-----	-----	-----

Binder	550	600	650
--------	-----	-----	-----

Binder	550	600	650
--------	-----	-----	-----

Binder	550	600	650
--------	-----	-----	-----

Binder	550	600	650
--------	-----	-----	-----

Binder	550	600	650
--------	-----	-----	-----

Binder	550	600	650
--------	-----	-----	-----

Binder	550	600	650
--------	-----	-----	-----

Binder	550	600	650
--------	-----	-----	-----

Binder	550	600	650
--------	-----	-----	-----

Binder	550	600	650
--------	-----	-----	-----

Binder	550	600	650
--------	-----	-----	-----

Binder	550	600	650
--------	-----	-----	-----

Binder	550	600	650
--------	-----	-----	-----

Binder	550	600	650
--------	-----	-----	-----

Binder	550	600	650
--------	-----	-----	-----

Binder	550	600	650
--------	-----	-----	-----

Binder	550	600	650
--------	-----	-----	-----

Binder	550	600	650
--------	-----	-----	-----

Binder	550	600	650
--------	-----	-----	-----

Binder	550	600	650
--------	-----	-----	-----

Binder	550	600	650
--------	-----	-----	-----

Binder	550	600	650
--------	-----	-----	-----

Binder	550	600	650
--------	-----	-----	-----

Binder	550	600	650
--------	-----	-----	-----

Binder	550	600	650
--------	-----	-----	-----

Binder	550	600	650
--------	-----	-----	-----

Binder	550	600	650
--------	-----	-----	-----

Binder	550	600	650
--------	-----	-----	-----

Binder	550	600	650
--------	-----	-----	-----

Binder	550	600	650
--------	-----	-----	-----

Binder	550	600	650
--------	-----	-----	-----

Binder	550	600	650
--------	-----	-----	-----

Binder	550	600	650
--------	-----	-----	-----

Binder	550	600	650
--------	-----	-----	-----

Binder	550	600	650
--------	-----	-----	-----

Binder	550	600	650
--------	-----	-----	-----

Binder	550	600	650
--------	-----	-----	-----

Binder	550	600	650
--------	-----	-----	-----

Binder	550	600	650
--------	-----	-----	-----

Binder	550	600	650
--------	-----	-----	-----

Binder	550	600	650
--------	-----	-----	-----

Binder	550	600	650
--------	-----	-----	-----

Binder	550	600	650
--------	-----	-----	-----

Binder	550	600	650
--------	-----	-----	-----

Binder

Appendix 3: Conference paper from CERi 2018 in Dublin, Ireland

Appendix 3: Conference paper from CERi 2018 in Dublin, Ireland

A simplified mix design procedure for geopolymer cement mortars based on metakaolin and industrial waste products activated with potassium silicate

Luke Oakes, Bryan Magee, Philip Millar, Alistair McIlhagger and Mark McCartney

Faculty of Computing, Engineering and the Built Environment, Ulster University, Shore Road, Newtownabbey, N. Ireland
email: oakes-11@ulster.ac.uk, b.magee@ulster.ac.uk

ABSTRACT: This paper presents a mix design methodology for geopolymer mortars based on metakaolin and industrial waste products activated using potassium silicate. The work is aimed at enabling performance-based specification and compressive strength prediction to drive forward their adoption as an alternative to Portland cement-based mortars used in fibre reinforced cladding systems. Few studies currently quantify the effects of mix parameters on broad families of geopolymer materials and no standard mix design methodology exists. Resultant mortars must have high strength to create light, thin panels, have high flow to enable effective dispersal of reinforcement fibres and as low an environmental impact as possible to maximise the impact of replacement. For a standard geopolymer mix, the effect of binder composition on mechanical performance and environmental impact is initially studied using ternary contour maps for a range of material blends. Next, the effects of altering mixture parameters such as the liquid/solid, silica/alumina and activator/binder ratios are quantified for three binder compositions identified as having high performance. Finally, correlation analysis is used to identify mix variables strongly correlating with compressive strength and regression analysis of the most deterministic to create a prediction models. Geopolymer mortars have been developed with compressive strengths over 80 and 100 N/mm² at 7 and 28 days respectively and the methodology presented allows design of such mortars by non-experts. Model predictions of compressive strength is shown to be relatively accurate, with average errors across binder compositions ranging from 2.3-5.8%. Further research expanding the range of materials and mix compositions is ongoing to advance this innovative methodology further.

KEY WORDS: Geopolymer; Mortar; Metakaolin; Industrial waste; Potassium silicate; Liquid to solid ratio; Mix design; Compressive strength, Prediction.

1. INTRODUCTION

There is a significant need for change in the way we design, build and use energy in our buildings. The materials currently used are struggling to keep up with demands for increasingly high levels of thermal performance, fire safety and finish to be achieved with increasingly limited environmental impact, greenhouse gases and energy allowances. The EU recognise this and plan to invest around €40 billion a year through schemes like the €5.9 billion horizon 2020 project by renovating existing buildings, making construction projects more sustainable and making all new builds require no energy from the grid by 2020 [1].

Geopolymer-based materials have the potential to form the next generation of cladding panel systems with improved performance over current alternatives such as glass reinforced concrete (GRC). Geopolymers form, cure and gain strength rapidly in ambient temperatures by combining water, user friendly alkaline reagents and alumina/silicate source materials that are either commercially produced, such as metakaolin, or industrial wastes, such as slags and ashes. The result are materials with a strong, durable, solid matrix that behaves like Portland cement (PC)-based concrete [2]. In comparison to GRC, geopolymers offer increased strength (over 20 and 100 N/mm² at 4-hours and 28-days respectively), and improved fire protection and chemical resistance. This is coupled with up to 90% reductions in embodied carbon and the use of a 100% recycled waste binder [3-5]. In this way, the material has the potential to offer the construction industry

with a novel approach to producing high performance, lightweight cladding panel systems for buildings.

However, the lack of recognised, performance based mix design methodologies for geopolymer binder systems enabling attainment of specified strength and/or workability presents a major stumbling block to its widespread adoption [6]. Previous related research focusing on mix design methods has focussed on single proportioning ratios such as silica/alumina (S/A), activating solution to binder powder (A/B) or liquid to solid (L/S); an approach analogous to the water/cement ratio in Portland cement-based concrete [7]. While other studies have used multiple parameters synergistically to create empirical formulas and neural networks to predict strength [8], existing work describing generic relationships between geopolymer strength and key mix design parameters is limited; typically focusing on specific materials such as fly ash-based systems requiring curing at high temperature and/or sodium based activating solutions. As such, these methods are of little relevance to wider groups of geopolymer binder systems and potassium silicate activation.

Against this background, the aim of this study is to produce a methodology enabling strength prediction for potassium silicate activated geopolymer mortars comprising a wide range of binder combinations and mix parameters. In this way, the intention is to drive forward the adoption of these systems as a high performance, low impact alternative to PC-based materials such as GRC in building cladding components.

EXPERIMENTAL METHODOLOGY

2.1 Materials

Metastar 501 metakaolin (MK) from Imerys UK was used as the primary binder due to its commercial availability, consistent and highly amorphous nature and its rapid dissolution and geopolymerization at ambient temperatures [9]. While MK has a low environmental impact compared to Portland cement (PC), partially or fully replacing it with industrial waste products has been shown to significantly reduce this impact and provide reduced set times, greater strength or higher flow [7]. The industrial waste materials used in this study included GGBS from ECOCEM Ireland, silica fume (SF) from Elkem, fly ash (FA) from Kilroot power station in Northern Ireland and iron silicate fines from Aurubis Bulgaria. Iron silicate is a low impact by-product of copper production and novel in its usage as a geopolymer source material. GGBS geopolymers require a much smaller amount of activator solids and, therefore, have lower environmental impact than metakaolin systems which have a lower Si:Al ratio necessitating a greater amount to be used for full dissolution to occur [10]. SF has been shown in the literature and in this project to increase the Si:Al of the binder to help with this and provide increased strength development between 7 and 28 days, especially at around 20% binder mass. Geosil activating solution with a potassium silicate solids content of 45% by mass was sourced from Woellner and used in all mix designs. Potassium, rather than sodium, silicate activator was chosen due to its reactivity and emergence as a cost-effective solution for geopolymer production [11]. Mortar mixes were studied in this work, with the lough sand fine aggregate component sourced from Stanley Emerson & Sons Ltd. Measured chemical compositions and published embodied CO₂ values for the binder materials considered are given in Table 1 with PC for comparative purposes.

2.2 Sample preparation and testing sequence

All samples for compressive strength testing were cast in 50 mm cubes, covered with plastic for 24 hours to ensure uniform drying conditions, then stored in a sealed container until testing at 7 and 28 days in accordance with BS EN 1015-11:1999. Ambient laboratory temperatures of approximately 20°C were provided over this casting and curing period. Rheological behaviour was determined using flow table testing in accordance with BS EN 1015-3:1999 to ensure sufficient workability and minimal void creation when casting. While this method specifies a 250 mm-wide flow table, this was identified as too small for comparing high flows created during the binder variation studies. As such, the flow exhibited by many of the mixes produced in Phase 1 could not be compared accurately.

3 PHASE I – INFLUENCE OF BINDER COMPOSITION

3.1 Mix designs

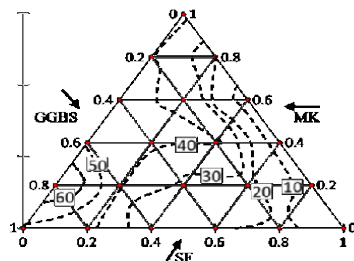
From Table 1 it is evident that significant variation exists in the major oxide contents of the various binder materials considered, suggesting potential to achieve geopolymer mixes with a wide range of performance and embodied CO₂ levels. To investigate the impact of binder composition in this regard, a base MK only geopolymer mix with L/S and paste/sand ratios of 0.51 and 0.84 respectively was initially developed as part of a preliminary research phase (see Figure 1-a). This mix design was then held constant and replicated with the principal variation being binder powder composition, enabling investigation of effects on mortar compressive strength, flow and environmental impact. Binder combinations considered included MK/GGBS/FA, MK/GGBS/SF and MK/GGBS/IS, with a wide range of unary, binary and ternary binders considered for each by considering respective binder increments of 20% in the range 0-100% by mass. By adopting this approach, it was recognised that performance levels were likely to vary considerably and potentially beyond limits of suitability. MK-based mixes, for instance, are reported to require more liquids than fly ash or slag geopolymers to ensure monomer transport, full dissolution and reorganisation [6].

3.2 Phase I results and discussion

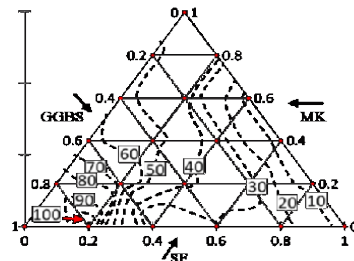
Plotted in Figure 1 for the MK/GGBS/SF mixes are contoured ternary graphs illustrating the significant influence binder powder composition has on geopolymer mortar strength at 7 and 28 days (Figures 1(b) and (c)). Plotted at the pinnacle of the ternary plots in Figure 1, the 100% MK mix attained 7 and 28 day strengths of 41.5 and 46 N/mm² respectively. Relative to this, performance levels ranging from 4-69.5 N/mm² at 7 days and 5-106 N/mm² at 28 days were attained by the various alternative binder combinations considered. GGBS has been shown to be a successful replacement for MK in high strength geopolymers, producing improved strength in binary blends at all increments of addition to maximums of 85 and 105 N/mm² at 7 and 28 days respectively. All binders exhibiting strengths over 50 N/mm² comprised at least 20%GGBS, suggesting the formation of CASH gel as vital to achieving high strength [9]. Binder blend 20%MK/80%GGBS was stronger than the 100% GGBS mortar, suggesting that geopolymer gels and CASH hydration products formed simultaneously and bonded well together as the latter expanded into the pores of the former to create a homogenous microstructure. SF offered significant strength increases to both MK and GGBS mortars at 28 days, despite reducing the 7-day strength of these unary blends. From 7 to 28 days the 80%MK/SF and 80%GGBS/SF binary mixes more than doubled in strength from 19 to 45 N/mm² and 45 to 106 N/mm² respectively, producing the highest compressive strength measured in the study. As suggested previously this is likely due to an increase in the amount of Si-O-Si bonds present in the mix caused by the increasing silica to alumina ratio.

Material quantities (kg/m ³)				L/S ratio	Paste to sand ratio
Binder	Activator	Water	Sand		
540	455	135	1340	0.51	0.84

(b) 7-Day compressive strength, N/mm² (L/S ratio = 0.51)



(c) 28-Day compressive strength, N/mm² (L/S ratio = 0.51)



(d) Embodied carbon emissions (kg CO₂/kg)

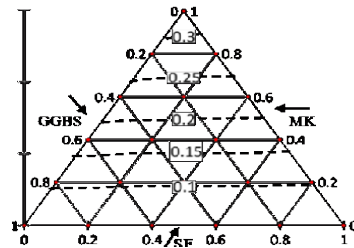


Figure 1: (a) Phase I mix design; (b) and (c) 7 and 28-day compressive strength results, and (d) embodied CO₂ contents, for unary, binary and ternary binder combinations considered

Also illustrated in Figure 1 is the embodied CO₂ content of each MK/GGBS/SF binder combination, with values generally reducing with corresponding reductions of MK reflecting the fact that it is commercially mined and calcined, as opposed to a by-product from other industrial activities. Of particular significance from the plots presented in Figure 1 is the fact that, for the geopolymer mortars considered, the improving levels of compressive strength corresponded with reducing levels of environmental impact (in terms of embodied CO₂). This is contrary to trends typical of conventional PC-based concrete mixes. In terms of mortar flow, results varied significantly and at almost all increments of MK replacement were in excess of 250 mm and, therefore, too high for accurate measurement and comparison. While this high range was clearly influenced by the L/S ratio of the base mix used (0.51), the ability of industrial waste materials to increase flow is a positive finding in terms of industrial-scale cladding panel production using highly-flowable, high-strength, low-impact geopolymer materials.

4 PHASE II – INFLUENCE OF MIX PARAMETERS

4.1 Mix designs

While Phase I clearly identified the influence of binder composition on geopolymer mortar performance, this was established for one mix design only, with other important and inter-relating key mix parameters not considered. As such, three high-performing binder powder blends were selected for further investigation in Phase II. This included: 100% MK base mix; 80%GGBS/20%MK and 80% GGBS/20% SF. The latter two blends were chosen as they achieved the highest strength at 7 and 28 days respectively from Phase I. As shown in Table 2, a face centred central composite mix design approach was used to consider three mortar component variables (binder powder, activator and free water content) across three levels (-1, 0, +1) for each selected binder blend.

In Phase I, the L/S solid of 0.51 used provided a wide range of flow across the different binder types with pure MK geopolymers exhibiting significantly lower values than hybrid or GGBS-based blends. This is due to the fact that the MK geopolymers require higher L/S and A/B ratios than fly ash or slag geopolymers for full dissolution, monomer transport and reorganisation to take place. This trend was addressed in Phase II by lowering the binder mass and increasing water mass for the 100%MK mixes in order to maximise the potential of forming homogenous geopolymers. Ranges of binder powder, activator and free water content considered for the MK mixes were 490-590, 400-500 and 100-160 kg/m³ respectively, while for the GGBS/MK and GGBS/SF mixes these were 550-650, 400-500 and 70-130 kg/m³. In this way, the intention was to further investigate the influence of key relationships presented in the literature [6-9,12] as significant for geopolymers, such as S/A, L/S and A/B. For instance, via the variables and ranges considered as part of the central composite design, values of A/B and L/S ranged from 0.76-1.02 and 0.46-0.57 respectively for the 15 MK mixes. Corresponding ratio ranges for the GGBS/MK and GGBS/SF mixes were 0.62-0.91, 0.35-0.52.

Table 2. Experimental design, 7-day compressive strength results and model prediction errors

Mix	Central composite design variables			7-day compressive strength (N/mm ²)									Modeling errors (%)		
	A	B	C	Measured			Predicted			1*	2*	3*	1*	2*	3*
				1*	2*	3*	1*	2*	3*						
1	-1	-1	-1	42.5	75	48	42	73.5	50	1.1	1.6	4.5			
2	-1	1	-1	42	69	53.5	42.5	70	53.5	0.1	1.5	0.2			
3	1	1	-1	58	86	60	57.5	86.5	67.5	1	0.5	7.7			
4	1	-1	-1	-	82.5	68.5	-	82.5	61.5	-	0.4	10.1			
5	-1	1	1	38	67.5	38.5	34.5	66.5	42	3.4	1.2	10.4			
6	1	1	1	39	79	51	39	79.5	53.5	1.6	0.4	4.9			
7	-1	-1	1	33	72	34.5	33.5	73.5	36	1.3	2.4	4.7			
8	1	-1	1	-	79.5	44.5	-	77	47.5	-	3.5	6.1			
9	0	0	0	42	77.5	55.5	42	78.5	51.5	0.7	1.2	7.4			
10	0	1	0	41.5	73.5	54.5	42.5	76	53.5	3.3	3.3	2.2			
11	0	-1	0	-	71	52.5	-	76	49	-	7.1	7.4			
12	-1	0	0	35	75	50.5	38	73.5	45.5	8.7	1.8	9.6			
13	1	0	0	46.5	82.5	57	48	83.5	57	3.9	1.4	0.1			
14	0	0	-1	51	85	52.5	49	80	57.5	4.3	5.4	9.5			
15	0	0	1	39	79	47	35.5	76.5	45	8.1	3.4	3.6			
Average:													3.1	2.3	5.8

* 1: 100% MK; 2: 80% GGBS/20% MK; 3: 80%GGBS/20% SF

4.2 Phase II compressive strength results

The 7-day compressive strength results achieved by the geopolymer mortar mixes considered as part of Phase II are presented in Table 2. As expected, and reflecting the mix constituent ranges introduced as part of the experimental design, broad ranges of strength were recorded for each binder combination investigated. For the MK, GGBS/MK and GGBS/SF combinations, these were 33.0-58.0, 67.5-86.0 and 34.5-68.5 N/mm² respectively.

Of the 15 mix compositions considered for each binder blend, mix 4 was perhaps expected to produce the greatest compressive strength as it had the lowest L/S ratio, highest mass of binder powder and the lowest amount of activating solution and free water. This was provided, of course, that sufficient activating solids existed in the mix for full dissolution to occur without leaving unreacted binder to act as microdefects. Indeed for 100%MK mix 4 (as well as for mixes 8 and 11), this proved not to be the case, with the material failing to set and gain any appreciable strength.

Alternatively, all of the GGBS/MK and GGBS/SF mixes successfully broke down the binder powder and had sufficient liquidity for monomer transport and reorganisation, allowing homogeneous hardened geopolymer mortar to form in all 15 mix iterations irrespective of the lower ratio values considered. This suggests that the amount of activator solids required for geopolymers based on these industrial waste materials is significantly lower; as this is the most expensive portion of a geopolymer mixture from both economic and environmental standpoints the benefits of partially replacing the MK with these is obvious.

4.3 Relationships between singular mixture proportioning ratios and compressive strength

As illustrated in Figure 2, work progressed to explore if clear relationships existed between the strength results obtained and the aforementioned ratios reported as being significant for geopolymer mix design (i.e. S/A, L/S and A/B). Figure 2 plots these ratios against the 7-day compressive strength measured for all 15 mixes considered for the three binder combinations under investigation.

The S/A ratio of source materials used to create geopolymers dictates molecular- and nano-scale structures formed, and theoretically there should be a direct correlation between silica content and strength due to increasing stronger Si-O-Si bonds. With that said, owing to other impacting mixture proportioning parameters optimum levels of S/A reported by researchers vary [7,12]. In this study however, the influence of S/A ratio on 7-day strength was not as significant as previously reported, with R² values of 0.06, 0.28 and 0.07 noted for the MK, GGBS/MK and GGBS/SF mixes respectively (Figure 2(a)).

L/S in geopolymeric materials (calculated by dividing the mass of solid materials in the binder and activator by that of the liquid portion of the activator and free water) is reported to be analogous to the water/cement (W/C) ratio in PC mix designs in terms of its impact on properties such as flow and compressive strength. In PC-based materials, compressive strength is negatively proportional to W/C. Similar, albeit varying and diminished relationships were noted for the three geopolymer binder blends considered (Figure 2(b)) reflecting the probable influence of other key mix variables not present in PC concrete. The R² values noted in this case ranged from 0.41-0.72, indicating a more significant correlation between L/S and strength.

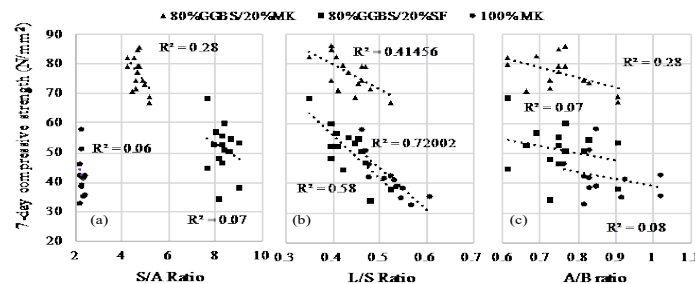


Figure 2. Geopolymer proportioning ratios vs 7-day compressive strength

Finally, A/B is reported to be one of the most important factors in the successful design of geopolymer mixes, enabling full dissolution and reorganisation of the mortar without defects from unreacted binder powder [8]. As mentioned previously, three of the 100%MK mortar mixes (4, 8 and 11) were unable to form geopolymer products owing to insufficient activator solids in the mix to break down the binder powder. With no release of silica and alumina monomers and chemically bound water, dry, sandy mortars lacking any cohesion or liquidity were formed. All MK mixes with an A/B ratio less than 0.75, or an activator solid to binder ratio of 0.34 reacted in this way. While vital to geopolymer formation, this ratio was found to be of little relevance in trying to predict strength, with low R^2 values ranging from 0.07 to 0.28 (Figure 2(c)).

In conclusion from Figure 2, it can be noted that when the all principal mix proportioning ratios are varied, none can be considered in isolation to accurately predict 7-day compressive strength. Out of the three considered, L/S emerged as the most significant, albeit with differing relationships apparent for the different binder compositions considered.

4.4 Correlation and regression analysis

As the ratios studied above in isolation were found to be poor predictors for compressive strength, work proceeded to ascertain if combinations of several mix parameters could be used synergistically with more success. Firstly, correlation analysis was carried out to determine which mix parameters were most closely linked to compressive strength. Parameters considered include the binder mass (B), activator solution mass (A), water mass (W), sand mass (S), activator solids mass (AS), total water content (TW), A/B ratio, free water to activating solution (FW/A) ratio, the free water to binder (FW/B) ratio, L/S ratio, and S/A ratio. Independent variables were then selected from this list to undergo regression analysis to produce a compressive strength predicting equation from the intercept and slope coefficients

Table 3. Regression model outputs and parameters

Binder	Mix parameters used by model						Model outputs		
	X1	X2	X3	X4	X5	X6	Adj. R ²	Sig. f	Average error %
100%MK	B	W	FW/A	FW/B	--	--	0.91	1.9×10^{-4}	3.1
80%GGBS/20%MK	B	FW/A	FW/B	TW	S/A	L/S	0.70	9.5×10^{-3}	2.3
80%GGBS/20%SF	B	FW/A	--	--	--	--	0.77	5.8×10^{-3}	5.9

provided for geopolymers mortars at 7 days. Predicted compressive strength results for the 15 mixes for each binder blend were then compared to corresponding experimental results to quantify the success of this methodology. Comparing outputs such as: adjusted R^2 ; significance f ; p values, allowed the most accurate prediction of strength possible from the data set. The equation used for compressive strength prediction is shown below in equation 1, with X1, X2, etc. representing the various mix parameters.

$$7\text{-day strength} = \text{Intercept} + (X1 * \text{slopeX1}) + (X2 * \text{slopeX2}) \dots (1)$$

Table 3 shows the regression outputs and the predictions the models made for the 15 mix designs created for each of the three binder blends, and shows the average error in these as a method of analysing the success of the models. The mix parameters used for the equation relating to the MK mixes were binder mass (B), free water mass (W), FW/B and FW/A and in this way the model was capable of predicting 7-day compressive strength with an average error of 3.12%, an adjusted R^2 value of 0.91 and a statistical significance f of 1.9×10^{-4} .

$$7\text{-day strength} = \text{Intercept} + (X1 * \text{slopeX1}) + (X2 * \text{slopeX2}) \dots (1)$$

Table 3 shows the regression outputs and the predictions the models made for the 15 mix designs created for each of the three binder blends, and shows the average error in these as a method of analysing the success of the models. The mix parameters used for the equation relating to the MK mixes were binder mass (B), free water mass (W), FW/B and FW/A and in this way the model was capable of predicting 7-day compressive strength with an average error of 3.12%, an adjusted R^2 value of 0.91 and a statistical significance f of 1.9×10^{-4} .

As stated previously, the equation described in Equation 1 and Table 3 is only valid for mixes with an activator to binder ratio high enough to ensure geopolymerisation occurs, and should not be used at lower ratios. For the GGBS/MK mixes, independent variables used were binder mass, total water mass, FW/A, FW/B, S/A and L/S ratios, leading to an average modelling error of 2.34% and adjusted R^2 and significance, f , values of 0.7 and 9.5×10^{-3} respectively. For the GGBS/SF mixes, the singular modelling variable FW/A ratio produced the most accurate strength predictions (average error = 5.8%; adjusted R^2 = 0.77; significance, f = 5.8×10^{-5}).

Prediction of strength using multiple mix parameters for regression analysis has been relatively successful and shows promise for future development to improve the accuracy and significance of the model in the future by expanding the range of compositions analysed to provide increased data describing the relationships present.

5 CONCLUSIONS

The goal of the work reported in this paper was to develop performance-based mix design methodologies capable of reliably producing potassium silicate-activated geopolymer mortars – based on MK and a range of industrial by-products – with specified levels of strength, flow and/or embodied carbon content. In this way, the broader aim of the work is to drive forward the adoption of geopolymers as a lower impact replacement for conventional PC-based building components such as those manufactured using GRC.

For a given geopolymer mix design (i.e. constant binder, water and activator contents), the influence of binder composition on the resulting reactions and corresponding values of strength gain were found to be significant. High performance geopolymer mortars were developed, exhibiting high flow and 7 and 28-day strengths of up to 87 and 106 N/mm² respectively; the latter using a binder system comprising 100% by-product materials. Indeed, many of the highest performing mortars investigated had embodied CO₂ binder levels around 30% lower than corresponding PC-based mixes. This is deemed to be a major benefit of geopolymers, where a broad range of structural performance levels can be attained using various combinations of, ideally, locally available, low impact binder materials. Further improvements to performance are possible for geopolymer mixes via further adjustments to mixture proportioning parameters, such as mass of activating solids, as these are the costly component and levels are unnecessarily high in binders without MK. While the CO₂ savings reported in this paper are modest compared to some published in the literature, if geopolymer systems were used to replace all PC-based materials, the theoretical reduction in total global carbon emission would be approximately 2.1% [13,14].

This study found that the use of single proportioning ratios was insufficient for accurate strength prediction and that a wide range of mix parameters have bearing on performance.

Of the single ratios studied, L/S ratio appeared to show the greatest correlation with strength, albeit that mixes with low L/S values did not consistently provide the greatest strength in the mix designs studied. Those with the lowest L/S ratios often also had the lowest A/B ratio, causing samples to be unable break down the binder powder sufficiently to form a homogenous geopolymer without unreacted materials acting as a microdefect. In MK based mortars, A/B ratios below 0.75 produced dry, sandy mortars with no cohesion due to the lack of activating solids present causing incomplete dissolution.

For the various sets of MK-, GGBS/MK- and GGBS/SF-based geopolymers mixes studied, a suite of regression models was developed to predict compressive strength at 7 days. With an average prediction error across the binder combinations considered all below 5.8%, the methods developed were relatively successful and indicate potential for future improvements. Future research will attempt to improve predictions by widening the range of mix parameters and compositions studied to increase the data sets from which they are made, and seek to develop a single model suitable for accurately predicting the performance of any geopolymer binder type.

6 REFERENCES

- [1] European commission. (2014). 2030 climate & energy framework. Available: https://ec.europa.eu/clima/policies/strategies/2030_en#tab-0-0. Last accessed 29/4/2018.
- [2] The Zeobond group. (2012). The geopolymer solution. Available: <http://www.zeobond.com/geopolymer-solution.html>. Last accessed 23/02/2016.
- [3] Davidovits, J (2013). Geopolymer cements: A review. Paris: Geopolymer Institute. all
- [4] Banah UK, 2014. Introduction to Geopolymer Binders. Ballyclare: Banah UK.
- [5] Geopolymer Institute. (2016). State of the Geopolymer R&D 2016. Available: <https://www.geopolymer.org/conference/gpcamp/gpcamp-2016/>. Last accessed 06/12/2016.
- [6] Lahoti, M. Narang, P. Tan, K. Yang, E. (2017). Mix design factors and strength prediction of metakaolin-based geopolymer. Ceramics International. 43 (.), 11433-1.
- [7] Austroads (2016). Technical report AP-T318-16 Specification and use of Geopolymer concrete in the manufacture of structural and non-structural components: Review of literature. Sydney NSW: Austroads Ltd. all.
- [8] Wilson, A (2015). Establishing a mix design procedure for geopolymer concrete. Queensland: University of South Queensland. Phd thesis.
- [9] Provis, L. Palomo, A. Shi, C. (2015). Advances in understanding alkali-activated materials. Cement and Concrete Research. 78, p 110-125.
- [10] K. Komnitsas. (2011). Potential of geopolymer technology towards green buildings and sustainable cities. Procedia engineering. 21 (.), p1023-1032.
- [11] Davidovits, J (2017). Geopolymer webinar 2017. Paris: Geopolymer Institute.
- [12] Kim, E. (2012). Understanding effects of silicon/aluminum ratio and calcium hydroxide on chemical composition, nanostructure and compressive strength for metakaolin geopolymers. PHD Thesis. 1 (.), all.
- [13] Jones, C. (2011). Inventory of Carbon & Energy (ICE) Version 2.0. Available: http://www.circularecology.com/embodied-energy-and-carbon-footprint-database.html#Wtaet9L_UU_15/12/17.

Appendix 4: Journal paper in JSIM 2018

Strength prediction and mix design procedures for geopolymer and alkali
activated cement mortars comprising a wide range of environmentally
responsible binder systems

Appendix 4: Journal paper in JSIM 2018

L. Oakes⁺, B. Magee, A. McIlhagger and M. McCartney

*Faculty of Computing, Engineering and the Built Environment, Ulster University, Belfast,
Northern Ireland*

⁺Oakes-L1@ulster.ac.uk

Strength prediction and mix design procedures for geopolymer and alkali
activated cement mortars comprising a wide range of environmentally
responsible binder systems

This research presents a mix design methodology for geopolymer (GP) and alkali activated (AA) mortars based on metakaolin and industrial waste products activated using potassium silicate. The aim is to enable a wide range of mix designs to be specified to given compressive strength, consistency and environmental footprints to facilitate their adoption as a Portland cement (PC) alternatives in the construction industry in applications such as fibre reinforced building cladding systems. The impact of the work is timely as literature quantifying effects of mix parameters on broad families of GP and AA materials is limited, and no standardised performance-based methodology exists. Initially, effects of binder composition on mechanical and environmental properties is presented for a standard GP mix design using contoured ternary plots for a range of material blends. Next, effects of altering mixture parameters such as liquid/solid, silica/alumina and activator/binder ratios are quantified for three selected binder compositions before a preliminary mix design methodology is presented allowing initial selection of mixture proportions. Finally, correlation analysis is used to identify multiple mix variables strongly correlating with strength, and regression modelling used to present predictive tools with average errors <6%.

Keywords: Geopolymer; alkali activated, metakaolin; industrial wastes; mixture design; performance prediction

Introduction

There is a significant need for change in the way buildings are designed, constructed and consume energy. The materials currently used are increasingly unable to meet demands for levels of thermal performance, fire safety and finish to be achieved with increasingly limited environmental impact, greenhouse gases and energy allowances (Jones, 2011; Benhelal et al, 2013). In recognition of this, the EU plan to invest around €40 billion a year through schemes like the €5.9 billion horizon 2020 project focused on renovating existing buildings, making construction projects more sustainable and making all new builds energy independent by 2020 (European commission, 2014).

To help address this issue, the underlying focus of this research is to investigate and advance the application of geopolymer (GP)- and alkali activated (AA) cement solutions; families of materials offering innovative, high-performance and low environmental impact construction solutions relative to, for instance, existing Portland cement (PC)-based alternatives. GPs and AAs can be designed to form, cure and gain strength rapidly in ambient temperatures by combining water, user friendly alkaline reagents and alumina/silicate source materials that are either commercially produced, such as metakaolin, or industrial wastes, such as slags and ashes. The result are strong, durable, solid matrices that behave similar to PC concrete (Zeobond group, 2012). Geopolymers offer the potential for high strength (over 20 and 100 N/mm² at 4-hours and 28-days respectively), fire protection and chemical resistance. Crucially, this is coupled with up to 90% reductions in embodied carbon relative to PC-based materials via the use of 100% recycled waste-based binders (Davidovits, 2013; Banah UK, 2014; Geopolymer Institute, 2016).

Despite these benefits, a key barrier to the widespread industrial adoption of geopolymer as a replacement for PC is the lack of recognised mixture proportioning methodologies capable of producing materials with specified performance levels (Lahoti et al., 2017). Manufacturing geopolymer systems depends on mixing a suitable activator with one or more alumina-silicate powders. However, deciding the proportions required is not straight forward. While literature regarding geopolymer cement concrete design exists, the importance of various mixture parameters on compressive strength has not been fully quantified, with previous work limited in terms of scope (Lahoti et al., 2017). Previous related research has focussed on exclusive binder types or combinations and/or single proportioning ratios such as silica/alumina (S/A), activating solution to binder powder (A/B) or liquid to solid (L/S); an approach analogous to the

water/cement ratio in PC-based concrete (Aughenbaugh, 2015; Austroads, 2016). The ratio most commonly reported to directly affect geopolymer concrete mechanical strength and microstructure is S/A. Other common ratios reported are sodium or potassium to alumina, water to sodium and sodium to silica. In the majority of cases, existing studies focus on specific materials such as fly ash-based systems, with empirical models reported to strongly relate to reactivity, based on the fly ash vitreous content, loss on ignition and mean particle size (Diaz-Loya et al, 2013; Austroads, 2016). As fly ash systems typically require curing at elevated temperatures, these methods are of limited relevance to wider groups of ambient-cured GP/AA binder systems that provide the greatest potential for embodied CO₂ reduction (Aughenbaugh, 2015; Timakul, 2015). The vast majority of existing geopolymer studies use sodium based activating solutions, with very few papers considering potassium silicate activation (Austroads, 2016). No previous papers considering the use of iron silicate in geopolymer systems and associated mixture design procedures exist. While selective existing studies have investigated multiple parameters synergistically to create empirical formulas and neural networks to predict strength (e.g. Wilson, 2015), existing work describing generic relationships between strength and key mix design parameters for various binder types is limited.

Against this background, the aim of this study is to produce simplified, preliminary mix design methods allowing preliminary proportioning of GP and AA materials. The unique feature of this work is a methodology enabling strength prediction for potassium silicate activated mortars comprising a wide range of binder combinations and mix parameters. In this way, the intention is to facilitate adoption of these systems as a high performance, low impact alternative to PC-based materials in buildings. The work is presented in three phases. In the first, the effect of a wide range of binder composition on performance is initially investigated by holding all other components of a control mix constant. The second phase of work proceeds to investigate the influence of additional key mixture variables and proposes a preliminary mix design method based on liquid/solid ratio for a wide range of binder compositions. In the final phase, the synergistic effects of a more comprehensive suite of mixture variables is investigated for selective binder compositions and a more robust mixture proportioning model based on regression analysis, albeit for selective binder compositions, is presented.

Experimental methodology

Materials

A range of binder materials was investigated as part of this research to facilitate widespread national/international adoption of the methodologies presented and beneficial reuse of prevalent local waste streams. Metastar 501 metakaolin (MK) from Imerys UK was used as the primary binder due its commercial availability, consistent and highly amorphous nature and its rapid dissolution and geopolymerization at ambient temperatures (Provis, 2015). While MK has a low environmental impact compared to PC, partially or fully replacing it with industrial waste products has been shown to both significantly reduce this impact and provide reduced setting times and increased strength and flow values (Austroads, 2016). As such, the industrial waste materials used in this study included: ground granulated blastfurnace slag (GGBS) from ECOCEM Ireland; silica fume (SF) from Elkem; fly ash (FA) from Kilroot power station in Northern Ireland; and iron silicate (IS) fines from Aurubis Bulgaria. Iron silicate is a low impact by-product of copper production and novel in its usage as a geopolymer source material. GGBS geopolymers require a much smaller amount of activator solids and, therefore, have lower environmental impact than metakaolin systems, which have a lower Si:Al ratio necessitating a greater amount to be used for full dissolution to occur (Komnitsas, 2011). SF has been shown in the literature (Austroads, 2016) to increase the Si:Al of the binder and thereby provide increased strength development between 7 and 28 days, especially at around 20% binder mass. Measured chemical compositions and published embodied CO₂ values for the binder materials considered are presented in Table 1, together with typical values for PC for comparative purposes.

Geosil, a commercially available activating solution with a potassium silicate solids content of 45% by mass was sourced from Woellner and used in all mix designs. Potassium, rather than sodium, silicate activator was chosen due to its reactivity and emergence as a cost-effective solution for geopolymer production (Davidovits, 2017). Mortar mixes were studied in this work, with locally sourced lough-dredged sand from Stanley Emerson & Sons Ltd. used as fine aggregate.

Sample preparation and testing sequence

All samples for compressive strength testing were cast in 50 mm cubes, covered with plastic for 24 hours to ensure uniform drying conditions and then stored in sealed containers until testing at 7 and 28 days in accordance with BS EN 1015-11:1999. Ambient laboratory temperatures of approximately 20°C were provided over this casting and curing period. Relative workability was determined using flow table testing in accordance with BS EN 1015-3:1999 to ensure minimal void creation when casting. While this method specifies a 250 mm-wide flow table, this was identified as too small for comparing high flows created during the binder variation studies. As such, the flow exhibited by many of the mixes produced in Phase I could not be compared accurately.

Results and discussion

Phase I: Influence of binder composition

From Table 1, it is evident that significant variation existed in the major oxide contents of the various binder materials considered, suggesting potential to achieve geopolymer mixes with a wide range of performance and embodied CO₂ levels. To investigate the impact of binder composition in this regard, a base MK only GP control mix with liquid/solid (L/S) and paste/sand ratios of 0.51 and 0.84 respectively was initially developed as part of a preliminary research phase. This mix was then held constant and replicated with the exclusive variation being binder powder composition, enabling investigation of effects on mortar compressive strength, flow and environmental impact (see Figure 1). Binder combinations considered in this way included MK/GGBS/FA, MK/GGBS/SF and MK/GGBS/IS, with full ranges of unary, binary and ternary binders considered for each by considering respective binder increments of 20% in the range 0-100% by mass. By adopting this approach, it was recognised that performance levels were likely to vary considerably and potentially beyond limits of suitability. MK-based mixes, for instance, are reported to require more liquids than fly ash or slag geopolymers to ensure monomer transport, full dissolution and reorganisation (Lahoti, 2017).

In terms of mortar flow, results varied significantly for the binder combinations considered and, at almost all increments of MK replacement, were in excess of 250 mm. As such, flow rates were generally too high for accurate measurement and meaningful comparison. While this high range was clearly influenced by the L/S ratio of the base

mix used (0.51), the ability of industrial waste materials to increase flow was considered a positive finding in terms of industrial-scale cladding panel production, for example; a factory-based precast production process demanding high-flow and high-strength materials.

Based on the mixes considered, Figure 2 presents contoured ternary plots illustrating the significant influence of binder powder composition on both 7- and 28-day mortar strength. Represented at the pinnacle of each ternary plot in Figure 2, the 100% MK mix attained 7 and 28-day strengths of 41.5 and 46 N/mm² respectively. At both 7 and 28 days, GGBS was proven to be a successful replacement for MK, with respective strengths of 69.5 and 85 N/mm² recorded for the binary 20%MK/80%GGBS combination. Indeed, this binder blend outperformed the 100%GGBS mortar, suggesting that in these mixes geopolymer gels and CASH hydration products formed simultaneously, bonding well together as the latter expanded into the pores of the former to create a homogenous microstructure. While at 7 days (Figures 2a-c), the 20%MK/80%GGBS combination delivered the highest strength of all combinations considered (69.5 N/mm²), at 28 days this was achieved by the 20%SF/80%GGBS binary blend (106 N/mm²). As suggested previously these performance levels reflect increasing quantities of Si-O-Si bonds present due to associated increasing silica to alumina ratios.

In comparison to these maximum binary combinations, similar general trends were noted from the three ternary plots considered at both 7 and 28 days (MK/GGBS/SF, MK/GGBS/FA and MK/GGBS/IS), with strengths steadily decreasing as levels of MK and GGBS were replaced with increasing levels of either SF, FA or IS. While this was perhaps unexpected given the significant disparity of the chemical compositions of these binders, it confirmed the dominance of GGBS and MK in resultant geopolymerisation reactions and performance levels. Overall from Figure 2, it can be seen that compressive strength values ranged from 4-69.5 and 5-106 N/mm² at 7 and 28 days respectively across the range of binder combination considered, offering significant performance and mix design flexibility moving forward.

Overlaid on the 28-day strength ternary plots (Figures 2d-f) are embodied CO₂ contents for each binder combination based on published values, enabling both environmental- and performance-informed decision making. Clearly from these plots, embodied CO₂ values generally decrease with corresponding reductions of MK; reflecting the fact that it is commercially mined and calcined, as opposed to a by-

product from other industrial activities. Of particular significance from these combined plots in Figure 2(d-f) is the fact that, for the binder combinations considered, improving levels of compressive strength generally correspond with reducing levels of embodied CO₂. This is contrary to trends typical of conventional PC-based concrete mixes.

Phase II: Influence of singular mixture proportioning ratios

Mix designs

While Phase I was effective in identifying the influence of binder composition on geopolymer mortar performance, this was established for one mix design only, with other important and inter-relating mix parameters not considered. As such, the following three binder powder blends were selected for further investigation in Phase II: 100% MK base mix; 80%GGBS/20%MK and 80% GGBS/20% SF. The latter two were chosen as they achieved the highest strength at 7 and 28 days respectively from Phase I. As shown in Table 2, a face centred central composite mix design approach was used to consider three mortar component variables (binder powder, activator and free water content) across three levels (-1, 0, +1) for each selected binder blend.

In Phase I, the L/S solid of 0.51 used provided a wide range of flow across the different binder types considered, with pure MK geopolymers exhibiting significantly lower values than hybrid or GGBS-based blends. This is due to the fact that the MK geopolymers require higher L/S and A/B ratios than fly ash or slag geopolymers for full dissolution, monomer transport and reorganisation to take place. This trend was addressed in Phase II by lowering the binder mass and increasing water mass for the 100%MK mixes in order to maximise the potential of forming homogenous geopolymers. Ranges of binder powder, activator and free water content considered for the MK mixes were 490-590, 400-500 and 100-160 kg/m³ respectively, while for the GGBS/MK and GGBS/SF mixes corresponding ranges were 550-650, 400-500 and 70-130 kg/m³. In this way, the intention was to further investigate influences of the following key relationships presented in the literature (Kim, 2012; Wilson, 2015; Provis, 2015; Austroads, 2016; Lahoti, 2017) as significant for geopolymers: S/A, L/S and A/B. Via the variables and ranges considered as part of the central composite design adopted, values of A/B and L/S ranged from 0.76-1.02 and 0.46-0.57 respectively for the 15 MK mixes. Corresponding ratio ranges for the GGBS/MK and GGBS/SF mixes were 0.62-0.91, 0.35-0.52.

Compressive strength results

The 7-day compressive strength results achieved by the geopolymer mortar mixes considered as part of Phase II are presented in Table 2. As expected and reflecting the mix constituent ranges introduced as part of the experimental design, broad ranges of strength were recorded for each binder combination investigated. For the 100%MK, 80%GGBS/20%MK and 80%GGBS/20%SF combinations, these were 33.0-58.0, 67.5-86.0 and 34.5-68.5 N/mm² respectively. Of the 15 mix compositions considered for each binder blend, mix 4 was perhaps expected to produce the greatest compressive strength as it had the lowest L/S ratio, highest mass of binder powder and the lowest amount of activating solution and free water. This was provided, of course, that sufficient activating solids existed in the mix for full dissolution to occur without leaving unreacted binder to act as microdefects. Indeed, for the 100%MK mix 4 (as well as for mixes 8 and 11) this proved not to be the case, with the material failing to set and gain any appreciable strength.

Alternatively, all of the GGBS/MK and GGBS/SF mixes successfully broke down the binder powder and had sufficient liquidity for monomer transport and reorganisation, allowing homogeneous hardened geopolymer mortar to form in all 15 mix iterations irrespective of the lower ratio values considered. This suggests that the amount of activator solids required for geopolymers based on these industrial waste materials is significantly lower. As this is likely to be the most significant portion of these geopolymer mixtures from both an economic and environmental standpoint, the benefits of partially replacing the MK with these is obvious.

Relationships between singular mixture proportioning ratios and strength

As illustrated in Figure 3, work progressed to explore if clear relationships existed between the strength results obtained and the aforementioned ratios reported as being significant for geopolymer mix design (i.e. S/A, L/S and A/B). Figure 3 plots these ratios versus 7-day compressive strength for all 15 mixes considered for the three binder combinations under investigation. The S/A ratio of source materials used to create geopolymers dictates molecular- and nano-scale structures formed and, theoretically, there should be a direct correlation between silica content and strength due to increasing quantities of stronger Si-O-Si bonds. With that said, owing to other impacting mixture proportioning parameters such as L/S or activating solution composition, optimum levels of S/A reported by researchers vary (Kim, 2012; Austroads, 2016;). In this study,

however, the influence of S/A ratio on 7-day strength was not as significant as previously reported, with insignificant R² values of 0.06, 0.28 and 0.07 noted for the MK, GGBS/MK and GGBS/SF mixes respectively.

A/B ratio is reported to be one of the most important factors in the successful design of geopolymer mixes, enabling full dissolution and reorganisation of the mortar without defects from unreacted binder powder (Wilson, 2015). As mentioned previously, three of the 100%MK mortar mixes (4, 8 and 11) were unable to form geopolymer products owing to insufficient activator solids in the mix to break down the binder powder. With no release of silica and alumina monomers and chemically bound water, dry, sandy mortars lacking any cohesion or liquidity were formed. All MK mixes with an A/B ratio less than 0.75, or an activator solid to binder ratio of 0.34 reacted in this way. While vital to geopolymer formation, this ratio was found to be of little relevance in trying to predict strength, with R² values ranging from 0.07 to 0.28.

L/S ratio in geopolymer materials (calculated by dividing the mass of solid materials in the binder and activator by that of the liquid portion of the activator and free water) is reported to be analogous to the water/cement (W/C) ratio in PC concrete mix designs in terms of its impact on properties such as flow and compressive strength. In PC-based materials, compressive strength is negatively proportional to W/C. Similar, albeit varying and diminished relationships were noted for the three geopolymer binder blends considered, reflecting the probable influence of other key mix variables not present in PC concrete. The R² values noted in this case ranged from 0.41-0.72, indicating a more significant correlation between L/S ratio and strength.

In conclusion from Figure 3, it appears that no principal mix proportioning ratio can be considered in isolation to accurately predict 7-day compressive strength. With that said, of the three considered, L/S emerged as the most significant; albeit with differing relationships apparent for the different binder compositions investigated. Against this background, the data presented in Figure 3 was manipulated further in an attempt to investigate and develop generic relationships of performance versus L/S ratio and to explore its applicability to a wide range of geopolymer binder types. To this end, further laboratory work was undertaken to assess flow and compressive strength performance of additional selected representative binder types across a range of L/S ratios (0.35-0.61). Binder combinations considered in this way included: 100% MK; 100%GGBS; 80%GGBS/20%MK; and 60%GGBS/20%MK/20%SF. Primary data was additionally supplemented by performance versus L/S ratios published in the literature

(Gao et al. 2013; Kumar, 2015; Shivanjan, 2016; Lahoti, 2017; Guzman-Aponte, 2017). The findings of this work with respect to compressive strength are presented in Figure 4. From Figure 4(a), it is evident that while clearly distinctive and somewhat inconsistent relationships exist for individual mix types (determined by differences in binder types, associated geopolymerisation reactions, testing times, experimental variables, etc. used), families of generic relationships are identifiable. While recognised not to closely fit all primary and secondary data sets compiled in Figure 4(a), a proposed normalisation of this observation is presented in Figure 4(b) for use within a preliminary mixture proportioning methodology. Similar normalised relationships for flow versus L/S ratio are presented in Figure 5(a&b).

Simplified preliminary mix design methodology

Combining the results presented to this point, a simplistic mix design procedure is proposed for geopolymer mortar mixes comprising any binder combination of MK/GGBS/FA (see Figure 6). This methodology is intended to be reproducible for the other material combinations considered. Included in Figure 6 are values of embodied CO₂ and 7-day compressive strength for mixes with L/S ratio of 0.51, as well as generic relationships linking both 7-day compressive strength and flow with L/S ratio in the range 0.30-0.65. In this way, the figure enables estimations of approximate mixture proportions for specified values of compressive strength and/or flow.

In the example presented, initial mix design requirements include a maximum value of embodied CO₂ content (0.15 kgCO₂/kg) and 7-day strength (50 N/mm²). Using Figures 6(a) and (b), the 7-day strength can be estimated for geopolymer cement mortar comprising a suitable binder combination and L/S ratio of 0.51. In the example shown, a value of 35 N/mm² is predicted for a 30%MK/50%GGBS/20%FA binder combination. This value can then be transposed onto Figure 6(c) to enable an estimation of the required L/S ratio to achieve the required 7-day strength of 50 N/mm². In the example shown, a L/S value of 0.38 is estimated, leading to an approximate flow value of 260 mm. It is recognised that by not accounting for other mix design criteria, such as aggregate size/type/properties and paste/aggregate ratio, this mix design procedure is by no means the finished article for geopolymer cement mortar/concrete. With that said, provided is a simplistic provisional methodology enabling rapid estimation of performance for a wide range of low impact binder material options.

Phase III: Synergistic influence of multiple mixture proportioning ratios

While the mixture proportioning method presented in Phase II was capable of providing preliminary mixture proportions for a variety of GP/AA materials, its limitations were recognised given the method's sole reliance on L/S ratio as a predictor of performance. As such, work in this phase proceeded to ascertain if combinations of several mix parameters could be used synergistically with more success. Based on the 7-day compressive strength results presented in Table 2, correlation analysis was initially carried out to determine mix parameters most closely linked with performance. Parameters considered included binder mass (B), activator solution mass (A), free water mass (FW), sand mass (S), activator solids mass (AS), total water content (TW), A/B ratio, free water to activating solution (FW/A) ratio, free water to binder (FW/B) ratio, L/S ratio and S/A ratio. While the aim at the outset was to generate a generic model capable of predicting the performance of any binder combination, this was found not to be possible within acceptable limits of accuracy. As a result, independent variables were identified from the above list for each binder combination considered (100%MK; 80%GGBS/20%MK; and 80%GGBS/20%SF) separately. Strength prediction models were then generated for each based on intercept and slope coefficients generated from related regression analysis. Predicted compressive strength results for the 15 mixes for each binder blend were compared to corresponding experimental results to quantify the modelling accuracy. Comparing outputs such as adjusted R², significance, f and p values, allowed the most accurate prediction of strength possible from the data sets available.

Results from this analysis are presented in Table 3, which shows modelling parameters and predictions for each of the three binder blends. For the 100%MK-based model, for instance, the key mix parameters identified included binder mass (B), free water mass (FW), FW/B and FW/A. Based on these, 7-day compressive strength predictions were possible with an average error of 3.12%, adjusted R² value of 0.91 and statistical significance, f of 1.9×10^{-4} . In comparison, for mixes comprising 100%GGBS/20%MK, modelling parameters used included binder mass, free water mass, FW/A, FW/B, S/A and L/S ratios, with an average modelling error, adjusted R² and significance, f, value of 2.34%, 0.7 and 9.5×10^{-3} respectively. For the 100%GGBS/20%SF mixes, the singular modelling variable FW/A ratio produced the most accurate strength predictions with average error, adjusted R² and significance, f values of 5.8%, 0.77 and 5.8×10^{-5} respectively.

Based on these findings, regression analysis of multiple mix parameters has provided a novel approach for AA/GP strength predictions; albeit that the models presented in Table 3 are only valid for mixes with activator to binder ratios appropriate to ensure full geopolymerisation. Moving forward, future development is clearly required, however, to improve model accuracy and significance by expanding their remit to encompass broader ranges of binder compositions.

Conclusions

The goal of the work reported in this paper was to develop mix design methodologies capable of reliably producing potassium silicate-activated geopolymer mortars – based on MK and a range of industrial by-products – with specified levels of strength, flow and/or embodied carbon content. In this way, the broader aim of the work was to facilitate adoption of alkali-activated and geopolymer cement systems as low impact replacements for conventional PC-based building components.

For a given geopolymer mix design (i.e. constant binder, water and activator contents), the influence of binder composition on the resulting reactions and corresponding values of strength gain has been shown to be significant. High performance AA and GP mortars were developed, exhibiting high flow and 7 and 28-day strengths of up to 87 and 106 N/mm² respectively; the latter using a binder system comprising 100% by-product materials. Indeed, many of the highest performing mortars investigated had embodied CO₂ binder levels around 30% lower than corresponding PC-based mixes when the activating solution is taken into account. This is deemed to be a major benefit of geopolymers, where a broad range of structural performance levels can be attained using various combinations of, ideally, locally available, low impact binders. Further improvements to performance are possible for geopolymer mixes via further adjustments to mixture proportioning parameters, such as the mass of activating solids, as these are the costly component and levels are unnecessarily high in binders without MK. While the CO₂ savings reported in this paper are modest compared to some published in the literature (Davidovits, J (b) 2013), if geopolymer systems were used to replace all PC-based materials, the theoretical reduction in total global carbon emission would be approximately 2.1% (Jones, 2011; Benhelal, 2013).

This study confirmed that the use of single proportioning ratios is not the optimum approach for accurate strength prediction and that combinations of mixture design parameters can have a bearing on performance. Of the single ratios studied, L/S

ratio appeared to show the greatest correlation with strength, albeit that mixes with low L/S values did not consistently provide the greatest strength in the mix designs studied. Those with the lowest L/S ratios often also had the lowest A/B ratio, causing samples to be unable break down the binder powder sufficiently to form a homogenous geopolymer without unreacted materials acting as a microdefect. In MK based mortars, A/B ratios below 0.75 produced dry, sandy mortars with no cohesion due to the lack of activating solids present causing incomplete dissolution.

For the various sets of MK-, GGBS/MK- and GGBS/SF-based mortar mixes studied, a suite of regression models was developed to predict compressive strength at 7 days. With average prediction errors across the binder combinations considered below 5.8%, the methods developed were relatively successful and indicate potential for future improvements. Future research will focus on improving predictions by widening the range of mix parameters and compositions studied and increasing the data sets on which they are based. The ultimate aim is to develop a single model suitable for accurately predicting the performance of any geopolymer binder type.

References

- Aughenbaugh, K. (2015). Critical evaluation of strength prediction methods for alkali-activated fly ash. *Materials and Structures*. 48 (.), p 607–620.
- Austrroads (2016). Technical report AP-T318-16 Specification and use of Geopolymer concrete in the manufacture of structural and non-structural components: Review of literature. Sydney NSW: Austrroads Ltd. all.
- Banah UK, 2014. Introduction to Geopolymer Binders. Ballyclare: Banah UK.
- Benhelal, E., Zahedi, G., Shamsaei, E. and Bahadori, A., 2013. Global strategies and potentials to curb CO₂ emissions in cement industry. *Journal of cleaner production*, 51, pp. 142–161.
- BS EN 1015-3:1999, Methods of test for mortar for masonry. Determination of consistence of fresh mortar (by flow table), British Standards Institute, 1999.
- BS EN 1015-11:1999, Methods of test for mortar for masonry. Determination of flexural and compressive strength of hardened mortar, British Standards Institute, 1999.
- Davidovits, J (2017). Geopolymer webinar 2017. Paris: Geopolymer Institute.

Davidovits, J (b)(2013). Geopolymer cements: A review. Paris: Geopolymer Institute. All European commission. (2014). 2030 climate & energy framework. Retrieved from: https://ec.europa.eu/clima/policies/strategies/2030_en#tab-0-0.

Diaz-Loya EI, Allouche EN, Cahoy D (2013a) Statisticalbased approach for predicting the mechanical properties of geopolymer concretes. In: Struble L, Hicks JK (eds)

Gao, K et al. (2013). Effects of Nano-SiO₂ on Setting Time and Compressive Strength of Alkaliactivated Metakaolin-based Geopolymer . The Open Civil Engineering Journal, 7 (.), 84-92.

Geopolymer binder systems (pp. 119–143). ASTM International, West Conshohocken. Accessed from http://www.astm.org/digital_library/stp/pages/STP156620120080.htm

Geopolymer Institute. (2016). State of the Geopolymer R&D 2016. Retrieved from: <https://www.geopolymer.org/conference/gpcamp/gpcamp-2016/>.

Guzmán-Aponte, L. (2017). Coatings. Metakaolin-Based Geopolymer with Added TiO₂ Particles: Physicomechanical Characteristics. 7 (.), p1-12.

Jones, C. (2011). Inventory of Carbon and Energy (ICE) Version 2.0. Available: http://www.circularecology.com/embodied-energy-and-carbon-footprint-database.html#_IU. Last accessed 15/12/17.

Kim, E. (2012). Understanding effects of silicon/aluminum ratio and calcium hydroxide on chemical composition, nanostructure and compressive strength for metakaolin geopolymers. PHD Thesis. 1 (.), all.

Kumar, R. (2015). Study on behaviour of geo polymer concrete. International Journal of Civil and Structural Engineering Research. 3.1(.), p384-388.

Lahoti, M. Narang, P. Tan, K. Yang, E. (2017). Mix design factors and strength prediction of metakaolin-based geopolymer. Ceramics International. 43, 11433-1.

Provis, L. Palomo, A. Shi, C. (2015). Advances in understanding alkali-activated materials. Cement and Concrete Research. 78, p 110–125.

Shivaranjan, N. (2016). Study on self compacting geopolymer concrete with various water to gepolymer solids ratio. International Research Journal of Engineering and Technology. 3.7 (.), p2064-2068.

Timakul, P . (2015). Effect of silica to alumina ratio on the compressive strength of Class C Fly ash geopolymers. Key Engineering Materials. Vol. 659 (.), pp 80-84.

Wilson, A (2015). Establishing a mix design procedure for geopolymer concrete. Queensland: University of South Queensland. Phd thesis.

Table 1. Composition and environmental impact of source materials used in this study

Material	Chemical composition (% by mass)				Embodied carbon (kgCO ₂ /kg)
	SiO ₂	Al ₂ O ₃	CaO	Fe ₂ O ₃	
PC	20	4.6	64.6	3.8	0.73 ⁺
MK	55	40	0.3	1.4	0.33 ⁺
GGBS	36.5	10.4	42.4	0	0.083 ⁺
SF	96	0.8	0.5	0.8	0.064 ⁺⁺
FA	57	24	3.9	6	0.008 ⁺
IS	27	3.2	1.8	46	0.057 ⁺⁺

⁺ Jones, C. (2011); ⁺⁺Values provided by Elkem and Aurubis

Table 2. Phase II experimental design methodology and resultant 7-day strength results

Mix	Central composite design variables			7-day compressive strength (N/mm ²)		
	A	B	C	Binder combination: ⁺		
1	-1	-1	-1	1	2	3
2	-1	1	-1	42.5	75	48
3	1	1	-1	42	69	53.5
4	1	-1	-1	58	86	60
5	-1	1	1	-	82.5	68.5
6	1	1	1	38	67.5	38.5
7	-1	-1	1	39	79	51
8	1	-1	1	33	72	34.5
9	0	0	0	-	79.5	44.5
10	0	1	0	42	77.5	55.5
11	0	-1	0	41.5	73.5	54.5
12	-1	0	0	-	71	52.5
13	1	0	0	35	75	50.5
14	0	0	-1	46.5	82.5	57
15	0	0	1	51	85	52.5
				39	79	47

⁺1: 100%MK; 2: 80%GGBS/20%MK; 3: 80%GGBS/20%SF

Table 3. Regression statistics and formulas

Key modelling equation parameters identified	Coefficients	t Stat	P-value
Binder 1: 100%MK			
Intercept	-94.36	-2.31	5.413x10 ⁻²
Binder	0.3073	3.981	5.317x10 ⁻³
Free water (FW)	-1.046	-3.26	1.385x10 ⁻²
Free water/ Binder (FW/B)	459.03	2.738	2.899x10 ⁻²
Free water/Activator (FW/A)	-13.51	-0.48	6.466x10 ⁻¹
7-day strength = -94.36 + (Binder*0.3173) + (FW*-1.046) + (FW/A*-13.51) + (FW/B*459.03)		Adjusted R ² = 0.91 Significance, f = 1.9x10 ⁻³ Average error = 3.1%	
Binder 2: 80%GGBS/20%MK			
Intercept	-33.88	-0.15	8.844x10 ⁻¹
Binder	0.4905	1.717	1.244x10 ⁻¹
Total water (TW)	-280.4	-2.11	6.823x10 ⁻²
Free water/Binder (FW/B)	-1153	-2.23	5.631x10 ⁻²
Free water/ Activator (FW/A)	-0.7	-1.42	1.927x10 ⁻¹
S/A ratio	-168.8	-2.6	3.156x10 ⁻²
L/S ratio	2554	-2.412	4.235x10 ⁻²
7-day strength = -33.88 + (Binder*0.4905) + (TW*-280.4) + (FW/B*-1153) + (FW/A*-0.7) + (S/A*-168.8) + (L/S*2554)		Adjusted R ² = 0.70 Significance, f = 9.5x10 ⁻³ Average error = 2.3%	
Binder 3: 80%GGBS/20%SF			
Intercept	5.3752	0.343	7.373x10 ⁻¹
Binder	0.1117	4.431	8.195x10 ⁻³
Free water/Activator (FW/A)	-94.54	-5.41	1.572x10 ⁻³
7-day strength = 5.38 + (Binder*0.1117) + (FW/A*-94.54)		Adjusted R ² = 0.77 Significance, f = 5.8x10 ⁻⁵ Average error = 5.9%	

Material quantities (kg/m ³)				L/S ratio	Paste/sand ratio
Binder	Activator	Water	Sand		
542	453	134	1340	0.514	0.843

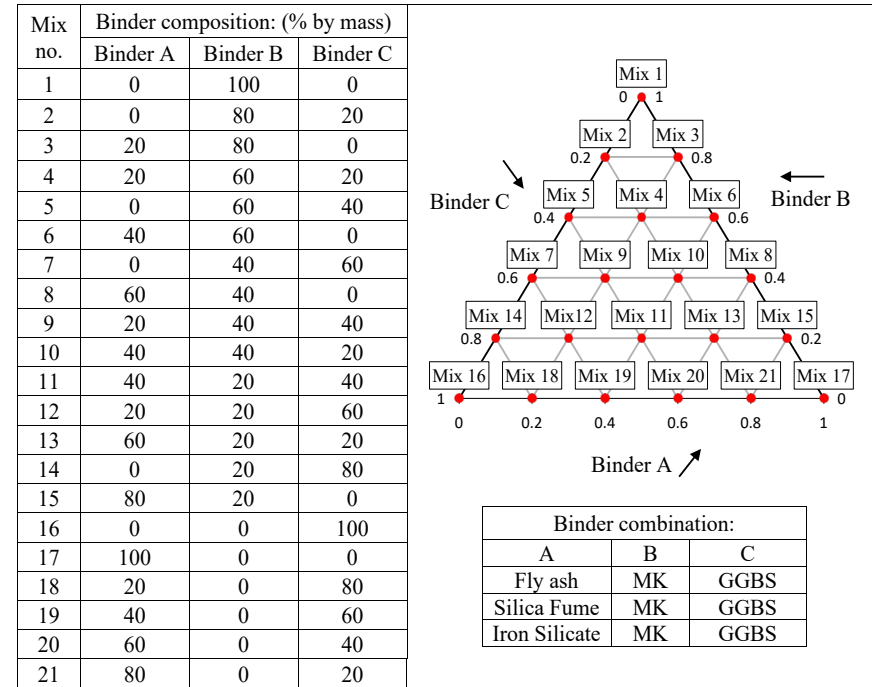


Figure1. Phase I mix design methodology

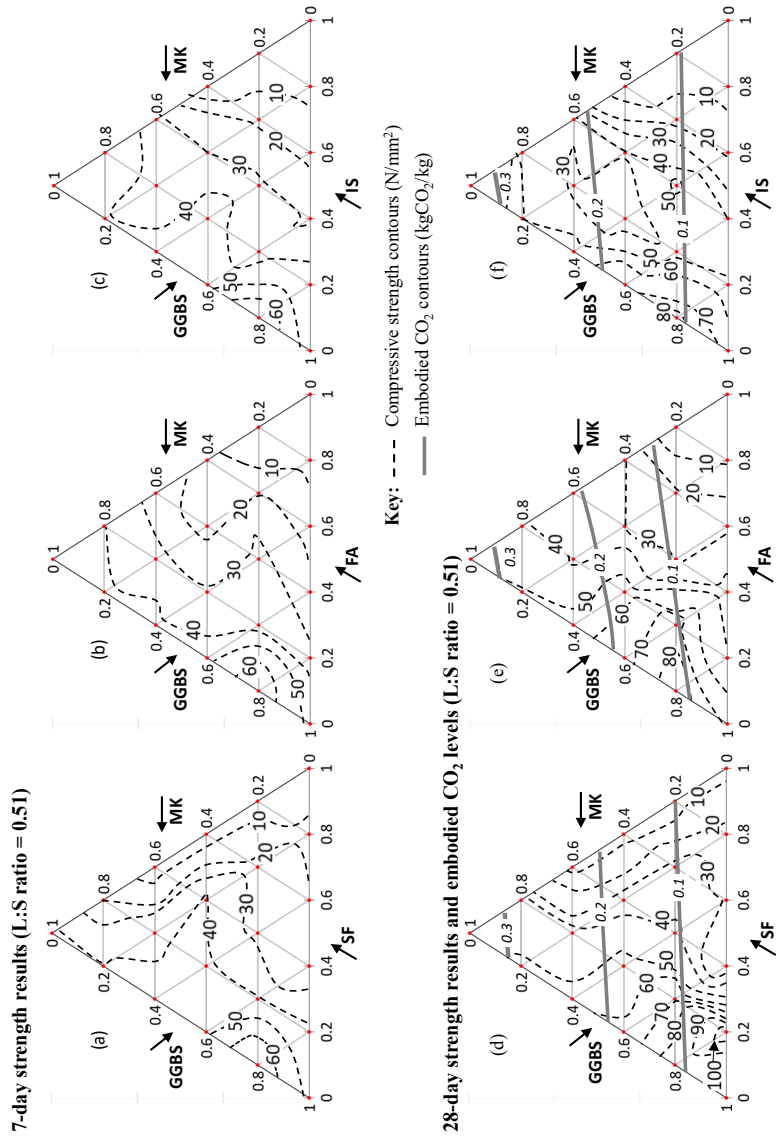


Figure 2. Ternary plots of 7-day strength (a-c) and combined ternary plots of 28-day strength and embodied CO₂ (d-f)

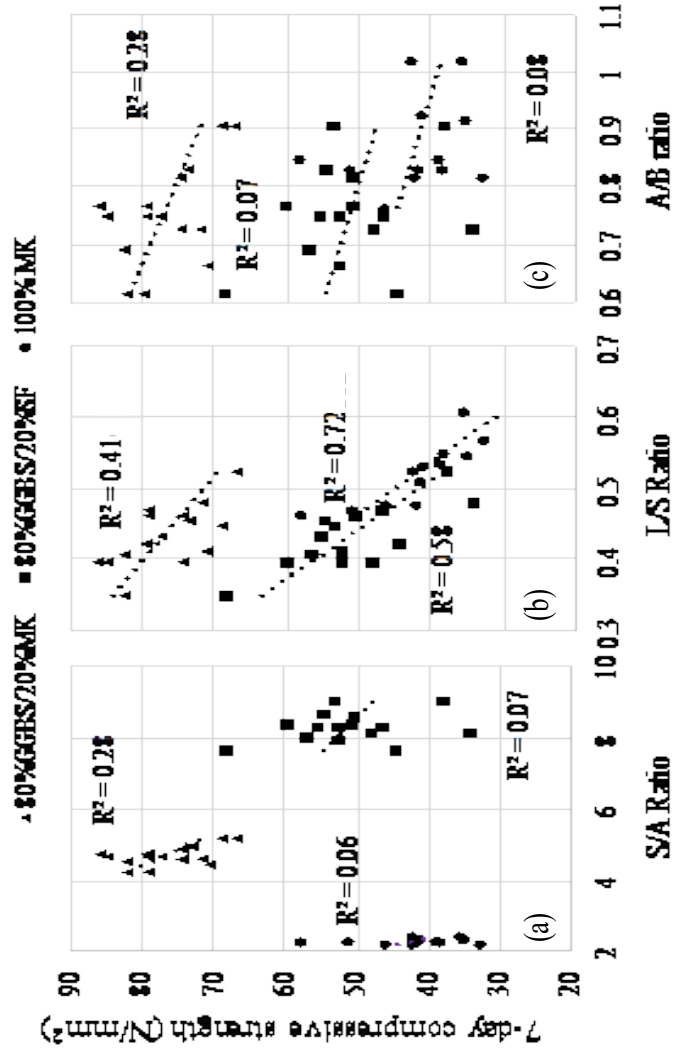


Figure 3. Silica/Alumina, Liquid/Solid and Activating solution to Binder powder ratios vs 7-day compressive strength

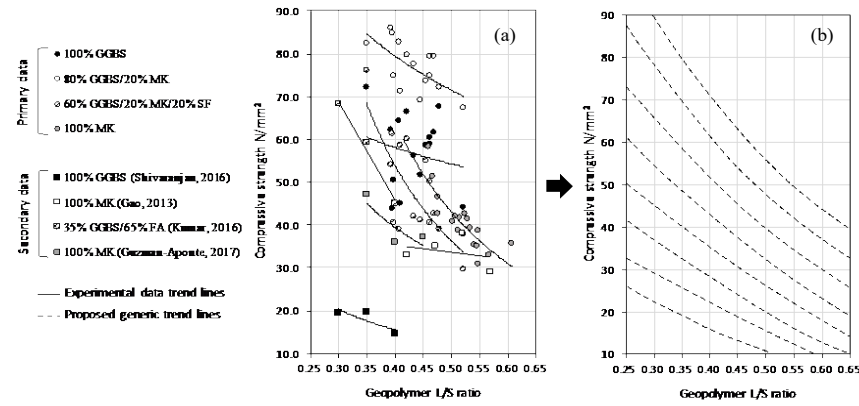


Figure 4. Relationships between 7-day strength and L/S ratio for various binder combinations

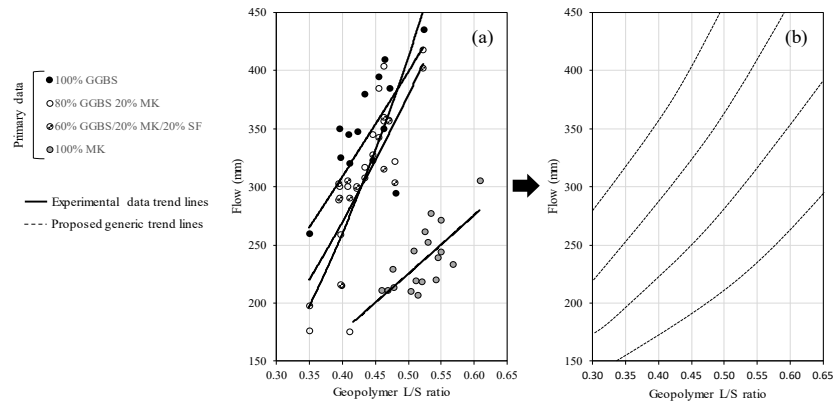


Figure 5. Relationships between flow and L/S ratio for various binder combination

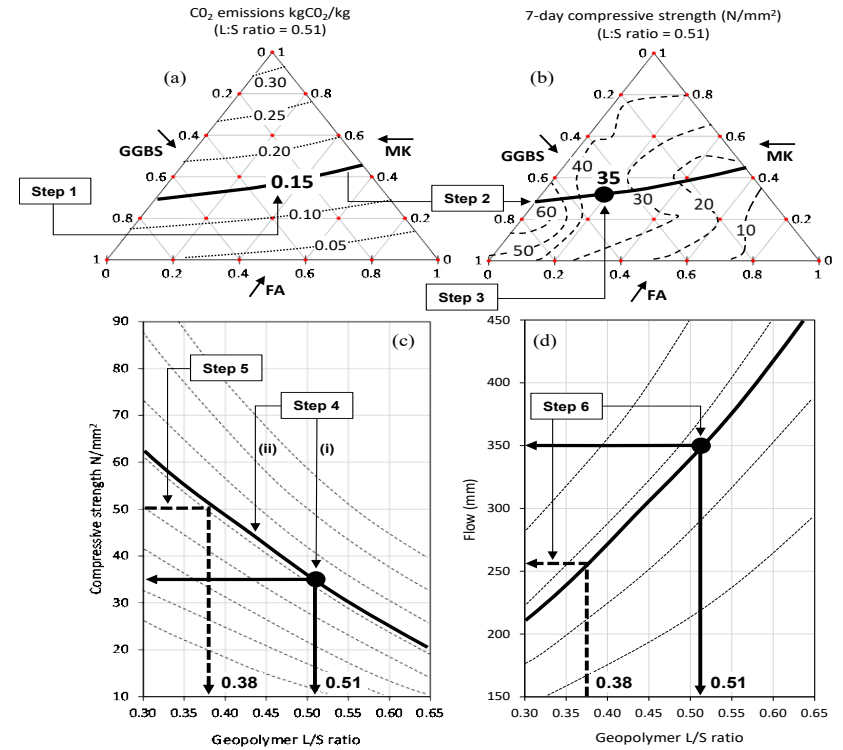


Figure 6. Indicative mix design worked example

Appendix 5: Declaration

I hereby declare that this thesis represents my own work which has been done after registration for the degree of Doctor of Philosophy following all academic and ethical policies of Ulster University. All references or data used from other research has been referenced and credit given to the applicable parties. No materials subject to copyright protection has been used in any part of this document.

Signed

Luke Oakes